

Effects of Electron-Electron and Electron-Phonon Interactions on the One-Electron States of Solids

LARS HEDIN AND STIG LUNDQVIST

Chalmers University of Technology, Göteborg, Sweden

I.	Introduction	2
II.	The Independent Particle Model	5
1.	Introduction	5
2.	The Hartree-Fock Equations	6
3.	The Total Energy and the Single Particle Excitation Energies	8
4.	Unrestricted Hartree-Fock Theory	10
5.	Time-Dependent Hartree Theory and the Lindhard Dielectric Function	12
III.	Summary of Key Concepts and Formulas in Green Function Theory	19
6.	Introduction	19
7.	Operators and States in Second Quantization	20
8.	Equation of Motion for the Field Operator	22
9.	The One-Electron Green Function at Zero Temperature	25
10.	Spectral Representation of the One-Electron Green Function	26
11.	The Structure of the Spectral Function. Elementary Excitations and Quasi Particles	28
12.	The Two-Particle Green Function. Formulas for the Total Energy	31
IV.	Equation of Motion for the Electron Green Function	33
13.	Electrons in a Rigid Lattice	34
14.	Physical Interpretation of the Electron Self-Energy	38
15.	Electrons in a Vibrating Lattice	43
16.	The Phonon Contribution to the Electron Self-Energy	48
17.	Remarks on Temperature Green Functions	51
V.	The Landau Fermi Liquid Theory	54
18.	Introductory Remarks	54
19.	The Kinetic Equation and Wavelike Excitations	59
VI.	Wave-Packet States in Many-Particle Systems	65
20.	Introductory Remarks on Wave Packets	65
21.	The Optical Potential. Scattering on Atoms and Surfaces	68
22.	Motion of Wave Packets in an Extended Medium	69
VII.	Properties of an Electron Gas	73
23.	Introduction	73
24.	The Total Energy and the Compressibility	75
25.	The Electron Self-Energy	80
26.	The Fermi Liquid Parameters	96
27.	The Dielectric Function	103

VIII.	Phonon Contributions to the Electron Self-Energy.....	108
28.	Some General Results and Formulas.....	108
29.	Early Calculations of the Effective Mass. The Work of Engelsberg and Schrieffer.....	111
30.	Calculations with Realistic Phonon Spectra and Including Band-Structure Effects.....	113
31.	Self-Energy and the Spectral Function from Tunneling Data. Density of Levels.....	118
32.	Temperature Effects in Specific Heat and Cyclotron Resonance.....	120
IX	The One-Electron Spectrum in a Real Solid.....	122
33.	Introductory Remarks about the Self-Energy and the Energy Spectrum	122
34.	The Dielectric Properties.....	124
35.	The Valence Bands.....	129
36.	The Core Electrons.....	135
37.	The Effective Crystal Potential.....	140
38.	Local Density Approximations.....	146
X.	Discussion of Various Metallic Properties.....	151
39.	Soft X-Ray Emission Spectra.....	151
40.	Photoemission and Photoabsorption Spectra.....	157
41.	Positron Annihilation in Metals.....	162
42.	Cohesive Energy.....	168
	43. Fermi Liquid Parameters.....	171
Appendix A:	Linear Response Theory.....	173
Appendix B:	Equations of Motion for Green Functions.....	175
Appendix C:	Spectral Resolutions.....	180

I. Introduction

We shall attempt in this review to interrelate two major developments that have taken place over the last decade. On one hand, we have the enormous wealth of *energy band calculations* which have had tremendous success in explaining the properties of specific solids, but in which the connection with first principles is not always apparent. On the other hand, we have seen the spectacular progress of *many-body theory* applied to the solid state, which has given a number of new results, although often of a rather general and formal nature, such as to provide the justification and a formal basis for a one-electron theory.

We would like to emphasize that even though a large number of energy bands have been determined, little is known about e.g. matrix elements. We thus do not know how far a one-particle model can go in explaining say optical properties. With this in mind it seems somewhat premature to develop a very sophisticated many-body theory associated with the concept of band structure. We have therefore chosen to pay particular attention to one more limited although essential aspect of the theory, namely, the concept of an *exchange-correlation potential* that includes important dynamical effects not described by an independent particle theory.

The electron gas problem is treated in some detail. This does not mean that we regard the solid as an inhomogeneous electron gas. On the contrary, we consider the *ions* as the basic components in the solid, components that are fairly well described by Hartree-Fock theory. The electron gas results serve as a guide for a discussion of the valence electrons, taking due account of their Bloch wave character.

The problem of the *crystal potential* is given due attention. We discuss the potential from the ion cores as well as from the valence electrons, and suggest schemes that incorporate essential exchange and correlation effects for the valence electrons. The various methods and techniques for calculating energy bands will, however, not be reviewed; there are several excellent recent expositions dealing with such aspects.

An energy band calculation which properly includes the effects of exchange and correlation describes the elementary excitations called *quasi particles*. Quasi-particle properties are usually discussed using the remarkable Landau theory of the Fermi liquid. We shall give a brief presentation of the theory and review the present status of calculations of the Fermi liquid parameters and how they are determined from experiments.

An even more important concept than the quasi particle is the *spectral weight function* of the system. The analysis of the structure of the spectral function provides justification for the concept of quasi particles and clarifies their meaning. It is usually emphasized that quasi-particle states only have a well-defined meaning in a narrow region around the Fermi surface. *It is certainly true that the damping of one-electron states is small in absolute numbers only in the immediate neighborhood of the Fermi surface.* However, the problem of defining acceptable quasi-particle states seems partly to be a question of semantics and partly a question about the nature of the physical situation under study. Indeed, calculations of the spectral function for an interacting electron gas show clearly the existence of a strong well-defined peak with an approximately parabolic dispersion law for all momenta. In this sense we can extend the notion and state that quasi particles in a simple metal have a meaning for all energies, over a broad range from bound core electrons to fast keV electrons injected externally into the system. The energy band theory describes these quasi-particle states, provided that the effects of exchange and correlation have been properly included.

In the same sense as the spectral function clarifies the meaning of quasi particles, it also points out the limitations. Indeed, the quasi-particle peak constitutes only part of the spectrum. Also, there is not only a smooth background out of which a quasi-particle peak rises, as is sometimes indicated in the literature, but there is often *additional characteristic structure in the spectrum* having a direct physical interest and significance.

Such effects occur due to both electron-electron and electron-phonon interactions although on different energy scales. This is a clear indication that the quasi-particle description is insufficient for many purposes and that many-body theory and calculations have to be carried beyond the quasi-particle approximation. Ample numerical examples of such effects will be given and we shall mention some experiments where such effects could be observed.

The next step in complication beyond the one-particle spectral function would be to discuss problems in terms of *two-particle functions*. These functions are indeed necessary to describe "final state" interactions involved in, say, exciton effects. Consideration of these questions falls however, essentially outside the scope of this review.

We shall concentrate the discussion on normal solids and indeed mostly on simple metals. Many of the results have obvious extensions to more complicated solids, but the limit for the simple type of theory presented here is not well understood. One may question e.g. its application to magnetic materials. We shall not at all discuss the specific methods developed for narrow bands and their consequences for the challenging problem of magnetism.

We discuss the exchange-correlation potential or *the self-energy* using the lowest order approximation in the screened dynamical interaction. The screening properties are described by the Lindhard dielectric function or modifications thereof. Technically, this means that so-called "vertex corrections" are neglected. Although this approximation cannot be justified at metallic densities using formal criteria of smallness of higher order terms, we feel that there is a reasonably physical justification for this approach. One must have in mind that we are looking for improvements in the real world of energy band theory, where one-electron theories of Hartree and Hartree-Fock type are being used, without ever asking for their regimes of validity. We feel that the extension from a static theory of correlations to a dynamical description of the interactions is a major step forward, which already in lowest order brings in new physical effects. The higher-order effects will certainly give numerical changes, and may of course also give rise to interesting structures in the experimental spectra.

The last part of this article will be concerned with various properties of metals, in which effects of the interactions on the electron spectrum is of importance. Each of these sections could be the topic for a separate review and we have limited the discussion to a few points of interest seen in the light of this review. The X-ray photoemission spectroscopy (XPS) seems to be the ideal method to study in detail the complete spectrum of both conduction and core electrons. Soft X-ray emission and absorption, uv

photoemission and absorption may reflect some of the structure in the one-electron spectrum. However, in discussing these experiments we have really transcended beyond the realms of one-electron theory and entered a field where the study of many-body interactions, exciton resonances, etc. forms a new exciting area of theoretical research.

II. The Independent Particle Model

1. INTRODUCTION

The concept of a band structure is usually discussed in a one-electron approximation. The range of validity of this approximation will be discussed later. In this part we shall discuss the independent particle model from the standpoint of the Hartree-Fock theory.

The Hartree-Fock theory (HF) has been applied with great success to atomic problems, and recently also to molecular problems. Very accurate numerical solutions are now available for most atoms.¹ Quite naturally the HF approximation has been put forward as a goal in band calculations in solids as well. However, it is well known² that an exact solution of the HF equations would, because of the exchange terms, lead to a most unsatisfactory theory for conduction electrons in a metal and (probably) also for valence electrons in a semiconductor. In actual band calculations the exchange terms are replaced by an ordinary potential using e.g. the Slater approximation,³ and there are good reasons to believe such a procedure to be much better in most cases than an actual solution of the HF equations.

In spite of such shortcomings, the HF theory plays an important role in the band structure problem for the following reasons. In the first place, it provides a quite adequate description of the basic constituents in the solid, the ions. Secondly, from a didactic point of view it provides a convenient basis to introduce some important concepts needed later. Thirdly, it will be convenient to have the properties and results of the HF theory well listed as a reference level. Since many detailed expositions of the HF theory can be found in the literature, we will present only a condensed outline, and refer particularly to Seitz⁴ and Slater⁵ for a complete discussion.

¹ E. Clementi, *IBM J. Res. Develop.* **9**, 2 (1965); C. Froese, Tech. Rept., Dept. of Math., Univ. of Br. Columbia, Vancouver 8, B.C., March 1966, *Can. J. Phys.* **46**, 2336 (1968).

² E. P. Wigner, *Trans. Faraday Soc.* **34**, 678 (1938).

³ J. C. Slater, *Phys. Rev.* **81**, 385 (1951).

⁴ F. Seitz, "The Modern Theory of Solids." McGraw-Hill, New York, 1940.

⁵ J. C. Slater, "Quantum Theory of Atomic Structure," Vol. II. McGraw-Hill, New York, 1960.

We shall discuss excitation energies and ground state properties, and we shall comment on the so called unrestricted HF method. The extension of the self-consistent approximation to time-dependent solutions has been of great importance in the developments of the last decade, and we shall discuss the time-dependent Hartree and HF theories and the Lindhard dielectric function in detail.

2. THE HARTREE-FOCK EQUATIONS

We shall in this section define the HF approximation, write down the HF equations, and give a brief discussion of their significance. Consider a Hamiltonian for N electrons of the form

$$H = \sum_{i=1}^N h(\mathbf{x}_i) + \frac{1}{2} \sum'_{i,j} v(\mathbf{r}_i, \mathbf{r}_j) + V_{\text{nuc}}. \quad (2.1)$$

The coordinate \mathbf{x} denotes both space and spin $\mathbf{x} = (\mathbf{r}, \xi)$. The one-electron part h of the Hamiltonian is

$$h(\mathbf{x}) = -(\hbar^2/2m) \nabla^2 - \sum_n Z_n v(\mathbf{r}, \mathbf{R}_n), \quad (2.2)$$

where \mathbf{R}_n denotes the position of the nucleus n and v is the Coulomb interaction

$$v(\mathbf{r}, \mathbf{r}') = e^2/|\mathbf{r} - \mathbf{r}'|. \quad (2.3)$$

V_{nuc} , finally, is the nuclear Coulomb repulsion

$$V_{\text{nuc}} = \frac{1}{2} \sum'_{nn'} Z_n Z_{n'} v(\mathbf{R}_n, \mathbf{R}_{n'}). \quad (2.4)$$

In the present context we consider the nuclear coordinates \mathbf{R}_n as parameters and discuss only the dynamics of the electrons. The spin-orbit term will not be considered explicitly.

The HF theory is obtained by considering a wave function in the form of a single Slater determinant,

$$|\Psi\rangle = (N!)^{-1/2} \det \{u_i(\mathbf{x}_k)\}, \quad (2.5)$$

and minimizing the energy $E = \langle \Psi | H | \Psi \rangle$ under the subsidiary condition $\int u_i^*(\mathbf{x}) u_j(\mathbf{x}) d\mathbf{x} = \delta_{ij}$. This procedure results in the HF equations for u_k ,

$$(h + V_{\text{HF}}) u_k = \sum_{l=1}^N \lambda_{kl} u_l; \quad k = 1, 2, \dots, N, \quad (2.6)$$

where V_{HF} is the sum of the average Coulomb potential, the Hartree potential V_H , and a nonlocal exchange potential V_{ex} :

$$V_{HF} = V_H + V_{ex}$$

$$V_H(\mathbf{x}) = \int v(\mathbf{r}, \mathbf{r}') \rho(\mathbf{x}') d\mathbf{x}' \quad (2.7)$$

$$V_{ex}(\mathbf{x}, \mathbf{x}') = -v(\mathbf{r}, \mathbf{r}') \rho(\mathbf{x}, \mathbf{x}')$$

$$\rho(\mathbf{x}) = \sum_{k=1}^N |u_k(\mathbf{x})|^2; \quad \rho(\mathbf{x}, \mathbf{x}') = \sum_{k=1}^N u_k(\mathbf{x}) u_k^*(\mathbf{x}').$$

In many cases we can write the one-electron functions as a product of a space and a spin part in the following way:

$$\begin{aligned} u_{k\sigma}(\mathbf{x}) &= \phi_{k\sigma}(\mathbf{r}) \chi_\sigma(\xi) = \phi_{k\uparrow}(\mathbf{r}) \alpha(\xi), & \sigma = \uparrow \\ &= \phi_{k\downarrow}(\mathbf{r}) \beta(\xi), & \sigma = \downarrow. \end{aligned} \quad (2.8)$$

In this case the exchange potential becomes

$$V_{ex}(\mathbf{x}, \mathbf{x}') = V_{ex\uparrow}(\mathbf{r}, \mathbf{r}') \alpha(\xi) \alpha^*(\xi') + V_{ex\downarrow}(\mathbf{r}, \mathbf{r}') \beta(\xi) \beta^*(\xi')$$

and we have e.g.

$$V_{ex} u_{k\uparrow} = \alpha(\xi) \int V_{ex\uparrow}(\mathbf{r}, \mathbf{r}') \phi_{k\uparrow}(\mathbf{r}') d\mathbf{r}'. \quad (2.9)$$

In the general case, e.g. to discuss Overhauser's spin density waves, we must write

$$u_k(\mathbf{x}) = \sum_\sigma \phi_{k\sigma} \chi_\sigma(\xi) = \phi_{k\uparrow}(\mathbf{r}) \alpha(\xi) + \phi_{k\downarrow}(\mathbf{r}) \beta(\xi). \quad (2.10)$$

From Eqs. (2.5) and (2.7) it follows that a unitary transformation of the functions u_k leaves the Hermitian operator V_{HF} unchanged and changes $|\Psi\rangle$ only by a phase factor. One can therefore also transform Eqs. (2.6) into their canonical form where the λ 's form a diagonal matrix ($\lambda_{kk} = \epsilon_k$), thus

$$(h + V_{HF}) u_k = \epsilon_k u_k. \quad (2.11)$$

In atomic calculations for open shells one usually introduces some simplifying restrictions on the form of the solutions and as a result some off-diagonal elements λ_{kl} must be kept. Equation (2.11) is referred to as the

unrestricted HF approximation. We refer to Nesbet⁶ for a discussion of various procedures used in simplified treatments of the HF problem.

The HF approximation reduces the N -body problem to N one-body problems as in Eq. (2.11), however, with a self-consistency requirement due to the dependence of V_{HF} on the solutions u_k as expressed by Eq. (2.7).

The HF theory is of course far from exact, because the wave function of the system cannot be written as a single Slater determinant. Indeed, the overlap between the exact wave function and the HF wave function goes to zero exponentially with the number of electrons,⁷

$$|\langle \Psi_{\text{exact}} | \Psi_{\text{HF}} \rangle| \sim \exp(-\alpha N). \quad (2.12)$$

Fortunately, one needs only the "local" properties of the system in order to calculate matrix elements of one- and two-particle operators,⁸ and some of these are predicted fairly well by the HF approximation even though the full HF wave function is essentially orthogonal to the true wave function.

The HF theory serves as a model example of self-consistent theories, and by replacing V_{HF} by better choices in which the dynamical effects of the interactions are included, various important improvements can be obtained, such as e.g. the Brueckner theory. Indeed, with the proper replacement of V_{HF} , the equations will give *exact* results for excitation energies, one-electron properties in the ground state, and also the ground state energy.

3. THE TOTAL ENERGY AND THE SINGLE PARTICLE EXCITATION ENERGIES

We return to the HF approximation where the total energy is given by

$$E = \sum_k^{\infty} h_{kk} + \frac{1}{2} \sum_{k,l}^{\infty} [\langle kl | v | kl \rangle - \langle kl | v | lk \rangle] + V_{\text{nuc}}, \quad (3.1)$$

and the one-electron energies by

$$\epsilon_k = \langle k | h + V_{\text{H}} + V_{\text{ex}} | k \rangle = h_{kk} + \sum_l^{\infty} [\langle kl | v | kl \rangle - \langle kl | v | lk \rangle], \quad (3.2)$$

where

$$\langle ij | v | kl \rangle = \int u_i^*(\mathbf{x}) u_j^*(\mathbf{x}') v(\mathbf{r}, \mathbf{r}') u_k(\mathbf{x}) u_l(\mathbf{x}') d\mathbf{x} d\mathbf{x}'.$$

⁶ R. K. Nesbet, *Advan. Chem. Phys.* **9**, 321 (1965).

⁷ N. M. Hugenholtz, *Physica* **23**, 481 (1957).

⁸ K. A. Brueckner, in "The Many Body Problem" (C. DeWitt, ed.), p. 81. Methuen, London, 1959.

Combining the two equations above we obtain the alternative forms

$$\begin{aligned} E &= \sum_k^{\infty} \epsilon_k - \frac{1}{2} \sum_{kl}^{\infty} [\langle kl | v | kl \rangle - \langle kl | v | lk \rangle] + V_{\text{nuc}} \\ &= \frac{1}{2} \sum_k^{\infty} (h_{kk} + \epsilon_k) + V_{\text{nuc}}. \end{aligned} \quad (3.3)$$

Applications of these formulas lead to reasonable agreement with experiment, the error in percent is quite small, but in absolute numbers (e.g. electron volts per atom) usually larger than one would like.

The significance of the ϵ_k as one-electron energies has been discussed particularly by Koopmans.⁹ Considering the energy difference between the ground state and a state with an electron in the one-electron state k missing, we have from Eqs. (3.1) and (3.2) that

$$\begin{aligned} E_k &\equiv E(N) - E(N-1, k \text{ empty}) \\ &\simeq h_{kk} + \sum_l^{\infty} \{ \langle kl | v | kl \rangle - \langle kl | v | lk \rangle \} = \epsilon_k. \end{aligned} \quad (3.4)$$

ϵ_k represents the energy required to ionize the system leaving a hole in state k , if we assume that the wave functions u_k in the N - and $(N-1)$ -particle states are the same, i.e. if we neglect the relaxation of the system. A better procedure should be to perform the self-consistent calculation for the $(N-1)$ th particle state as well and subtract the total energies to find E_k . When the one-electron wave function is extended over a large system (like a Bloch wave), this procedure gives the same result as Koopmans, while for a small system the difference can be significant, as shown for core levels in atoms by, e.g., Sureau and Berthier,^{9a} Bagus¹⁰ and Lindgren.¹¹

To proceed beyond simple procedures like that of Koopmans and the comparison between two HF calculations, one needs a more general and systematic approach. Perturbation theory could be used to obtain formulas for the ionization energies by subtracting the expansions for the N and $(N-1)$ systems. However, for valence electrons in solids one would have to perform infinite summations or equivalent procedures to obtain accurate results. One convenient procedure is to use the Green function method, which gives an equation of a similar structure as the HF equation, but with V_{ex} replaced by an exchange correlation kernel called the *self-energy operator* Σ , and with energy eigenvalues *exactly* equal to the quantities E_k .

⁹ T. Koopmans, *Physica* **1**, 104 (1934).

^{9a} A. Sureau and G. Berthier, *J. Phys. (Paris)* **24**, 672 (1963).

¹⁰ P. Bagus, *Phys. Rev.* **139**, A619 (1965).

¹¹ I. Lindgren, *Arkiv Fysik* **31**, 59 (1966).

Approximation procedures in this scheme reduce to approximating the self-energy, which is a quantity of the same order of magnitude as the excitation energy rather than the total energy.

4. UNRESTRICTED HARTREE-FOCK THEORY

As pointed out in Section 2, one often introduces simplifying restrictions about the form of the orbitals in the HF equations. An illustrating example is that conventionally the ground state of Li is calculated assuming the configuration to be $1s^22s$, whereas the true HF equations demand a more general choice of configuration, e.g. $1s^+1s^-2s^+$, which permits the exchange interaction to make the radial parts of the $1s^+$ and $1s^-$ functions to be different. We say that the outer $2s$ electron *spin-polarizes the ion core*.¹² A calculation¹³ for Li shows that the polarization of the core has a large effect on the hyperfine splitting, which depends only on the spin density of electrons at the nucleus. However, unrestricted HF calculations in other cases have sometimes given better results than the conventional HF, but in other cases the results have been even worse.^{13a}

The problem of restricted versus unrestricted HF theory has interesting implications for the case of conduction electrons also, here illustrated by the electron gas problem. The conventional HF solution for the uniform electron gas in a box of volume Ω consists of doubly occupied plane waves, with \mathbf{k} vectors filling the Fermi sphere. In 1962 Overhauser¹⁴ showed that a different type of state has a lower energy than the paramagnetic ground state. Instead of plane waves with spin up and spin down,

$$\varphi_{\mathbf{k}\uparrow}(\mathbf{x}) = \Omega^{-\frac{1}{3}} \exp(i\mathbf{k}\cdot\mathbf{r})\alpha(\xi), \quad \varphi_{\mathbf{k}\downarrow}(\mathbf{x}) = \Omega^{-\frac{1}{3}} \exp(i\mathbf{k}\cdot\mathbf{r})\beta(\xi), \quad (4.1)$$

Overhauser considered superpositions of e.g. the form

$$\begin{aligned} \varphi_{\mathbf{k}}^{(+)} &= \varphi_{\mathbf{k}\uparrow} \cos \theta(\mathbf{k}) + \varphi_{\mathbf{k}+\mathbf{Q}\downarrow} \sin \theta(\mathbf{k}) \\ \varphi_{\mathbf{k}}^{(-)} &= -\varphi_{\mathbf{k}-\mathbf{Q}\uparrow} \sin \theta(\mathbf{k}) + \varphi_{\mathbf{k}\downarrow} \cos \theta(\mathbf{k}), \end{aligned} \quad (4.2)$$

where $\theta(\mathbf{k})$ is a periodic function of \mathbf{k} with the period \mathbf{Q} ,

$$\theta(\mathbf{k}) = \theta(\mathbf{k} + \mathbf{Q}).$$

These functions form a complete orthonormal set which reduces to the conventional set of plane waves for $\theta(\mathbf{k}) = 0$. Choosing $\theta(\mathbf{k})$ to be zero for all \mathbf{k} except in small regions around $-\frac{1}{2}\mathbf{Q}$ and $\frac{1}{2}\mathbf{Q}$ (and $-\frac{3}{2}\mathbf{Q}, \frac{3}{2}\mathbf{Q}, \dots$) and \mathbf{Q} approximately equal to the diameter of the Fermi sea, Overhauser

¹² G. W. Pratt, *Phys. Rev.* **102**, 1303 (1956).

¹³ L. M. Sachs, *Phys. Rev.* **117**, 1504 (1960).

^{13a} D. A. Goodings, *Phys. Rev.* **123**, 1706 (1961).

¹⁴ A. W. Overhauser, *Phys. Rev.* **128**, 1437 (1962).

obtained an energy slightly lower than for the paramagnetic solution. The Overhauser functions were called *spin density waves* (SDW), since the spin density for, e.g., $\varphi_{\mathbf{k}}^{(+)}$ is given by

$$\begin{aligned} \mathbf{P}(\mathbf{r}) &= \int \varphi_{\mathbf{k}}^{(+)*}(\mathbf{x}) \mathbf{S} \varphi_{\mathbf{k}}^{(+)}(\mathbf{x}) d\xi \\ &= \Omega^{-1} \{ \cos^2 \theta \langle \alpha | \mathbf{S} | \alpha \rangle + \sin^2 \theta \langle \beta | \mathbf{S} | \beta \rangle \\ &\quad + \sin \theta \cos \theta [\exp(i\mathbf{Q} \cdot \mathbf{r}) \langle \alpha | \mathbf{S} | \beta \rangle + \exp(-i\mathbf{Q} \cdot \mathbf{r}) \langle \beta | \mathbf{S} | \alpha \rangle] \} \\ &= \Omega^{-1} (\hbar/2) \{ \cos 2\theta \hat{x} + \sin 2\theta [\cos(\mathbf{Q} \cdot \mathbf{r}) \hat{x} + \sin(\mathbf{Q} \cdot \mathbf{r}) \hat{y}] \}, \end{aligned} \quad (4.3)$$

which forms a spiral wave.

Overhauser's results demonstrate the instability of the paramagnetic ground state against formation of spin density waves *within the framework of the HF theory*. The result derives from the strong effect due to the un-screened HF exchange potential, which is replaced in more accurate formulations by a screened interaction. Model calculations with a screened Coulomb interaction do not seem to give any stable SDW solution¹⁶⁻¹⁷ and the present status of the theory seems to give preference to the paramagnetic ground state, at least over the region of metallic densities. However, there is theoretical evidence¹⁷ that band-structure effects may act to stabilize SDW's, as seems to be the case for chromium.^{17a}

Another HF-type approach, developed by Löwdin and others,¹⁸ is "different orbitals for different spins" (DODS), which has been used mainly to obtain a lower total energy. In the case in which the lattice can be divided into two equivalent sublattices, all spin up functions are mainly localized on one sublattice and all spin down functions mainly on the other. This relaxation of the usual restriction of double occupancy lowers the energy considerably.

The different methods briefly mentioned here are all of the self-consistent field type, and we wish to emphasize the variety and flexibility but also the limitations of these methods. All the approaches that are based on the simple HF theory finally lead into a dead end street, and one needs a systematic method to improve the theory and if possible estimate the errors. The Green function approach, to be discussed later, has the flexibility of the self-consistent method, and also has a firm conceptual and mathematical basis that permits a systematic expansion and improvement.

¹⁶ A. K. Rajagopal, *Phys. Rev.* **142**, 152 (1966).

¹⁷ D. R. Hamann and A. W. Overhauser, *Phys. Rev.* **143**, 183 (1966).

^{17a} P. A. Fedders and P. C. Martin, *Phys. Rev.* **143**, 245 (1966).

^{17a} W. M. Lomer, *Proc. Phys. Soc.* **80**, 489 (1962).

¹⁸ P. O. Löwdin, *Phys. Rev.* **97**, 1509 (1955); K. F. Berggren and B. Johansson, *Int. Journ. Quant. Chem.* **2**, 483 (1968).

5. TIME-DEPENDENT HARTREE THEORY AND THE LINDHARD DIELECTRIC FUNCTION

The HF equation derived in Section 2,

$$(h + V_{HF}) u_k = \epsilon_k u_k, \quad (5.1)$$

has the obvious time-dependent generalization

$$[h(\mathbf{x}) + V_{HF}(\mathbf{x}, t)] u_k(\mathbf{x}, t) = i\hbar(\partial/\partial t) u_k(\mathbf{x}, t). \quad (5.2)$$

$V_{HF}(\mathbf{x}, t)$ depends on time through the functions $u_k(\mathbf{x}, t)$. These equations can be derived from the variational principle

$$\langle \delta\Psi(t) | \{H - i\hbar(\partial/\partial t)\} | \Psi(t) \rangle = 0, \quad (5.3)$$

restricting Ψ to be a single Slater determinant.

A particular solution of Eq. (5.2) is

$$\Psi_k(\mathbf{x}, t) = \Psi_k^0(\mathbf{x}, t) = \Psi_k^0(\mathbf{x}) \exp(-i\epsilon_k t), \quad (5.4)$$

which gives the ordinary HF theory. We may also find solutions in which each orbital function $\Psi_k(\mathbf{x}, t)$ differs but little from the ordinary HF solution $\Psi_k^0(\mathbf{x}, t)$. Such a solution can be described by an ansatz of the form

$$\begin{aligned} \Psi_i(\mathbf{x}, t) = & \Psi_i^0(\mathbf{x}) \exp(-i\epsilon_i t) + \sum_m x_{mi} \Psi_m^0(\mathbf{x}) \exp(-i\omega t - i\epsilon_i t) \\ & + \sum_m y_{mi}^* \Psi_m^0(\mathbf{x}) \exp(i\omega t - i\epsilon_i t), \end{aligned} \quad (5.5)$$

where m denotes particle states, i.e. states outside the configuration considered.

We consider the Hartree approximation, i.e. we neglect the exchange potential V_{ex} . Assuming the solution to be close to the ordinary solution, which means that x_{mi} and y_{mi}^* should be small, we need retain only terms linear in these amplitudes. Equating separately coefficients of negative and positive frequencies one obtains, after multiplying the equations by $\Psi_m^0(\mathbf{x})$ and integrating, the *linearized time-dependent Hartree* (LTH) approximation for determining the frequency ω and amplitudes x_{mi}, y_{mi}^* :

$$\begin{aligned} (\epsilon_m - \epsilon_i - \omega) x_{mi} + \sum_{n,j} (jm | v | ni) x_{nj} + \sum_{n,j} (mn | v | ij) y_{nj} &= 0; \\ (\epsilon_m - \epsilon_i + \omega) y_{mi}^* + \sum_{n,j} (mn | v | ij) x_{nj}^* + \sum_{n,j} (jm | v | ni) y_{nj}^* &= 0. \end{aligned} \quad (5.6)$$

Equation (5.6) describes the excitation as the eigensolutions corresponding to free oscillations around the time-independent solution.¹⁹

¹⁹ D. J. Thouless, "The Quantum Mechanics of Many-Body Systems," pp. 88. Academic Press, 1961.

We shall later consider the case in which one applies a time-varying external field and studies the forced oscillations, or *linear response*, of the system. The ansatz for the solution will be the same for this case and the equations are the same as Eqs. (5.6) except that we have to add the driving terms in the right-hand side. The physical interpretation of the forced oscillations is again simple: the particle moves in the external field plus the added induced field from the rest of the system; the latter gives rise to important screening effects. Indeed, this physically natural and simple extension of the self-consistent field approximation which we shall refer to as LTH is equivalent to a number of approximations obtained in different ways by summing diagrams, by using equation of motion methods, etc. It should be mentioned that the LTH approximation has contributed essentially to a number of important problems. Equations (5.6) give the dispersion relation for plasmons in a uniform electron gas and the corresponding equations for forced oscillations give the dielectric function first derived by Lindhard.²⁰ Applying the theory to a system which is completely different, the case of weakly interacting atoms in a van der Waals' crystal, the same approximation describes well the excitations corresponding to waves of electronic polarization and gives the polarizability of the system.²¹ The theory has also been applied with success to atoms and molecules, and last but not least important we should mention a number of successful applications in nuclear theory, particularly the study of vibrational levels. The approximation is often referred to as the random phase approximation or RPA, alluding to the arguments used by Bohm and Pines in their pioneering work on plasma properties of metals.²² The term RPA is in many cases misleading, and has no physical relevance in the applications mentioned above, except for uniform systems, and we are therefore going to refer to this theory as the linearized time-dependent Hartree theory (LTH).

We are now going to apply the theory to study the effect of a small external potential $V_{\text{ext}}(\mathbf{r}, t)$ on the system. In the linear approximation one obtains for the induced charge density the formula

$$\rho_{\text{ind}}(\mathbf{r}, t) = \int R(\mathbf{r}, \mathbf{r}', t - t') V_{\text{ext}}(\mathbf{r}', t') d\mathbf{r}' dt', \quad (5.7)$$

in which the *response function* $R(\mathbf{r}, \mathbf{r}', t - t')$ is nonzero only for $t > t'$ because of causality requirements. From $\rho_{\text{ind}}(\mathbf{r}, t)$ we can calculate the

²⁰ J. Lindhard, *Dan. Math. Phys. Medd.* **28**, No. 8 (1954).

²¹ S. Lundqvist and A. Sjölander, *Arkiv Fysik* **26**, 17 (1964).

²² D. Pines, *Solid State Phys.* **1**, 367 (1955).

effective potential

$$\delta V(\mathbf{r}, t) = \int v(\mathbf{r}, \mathbf{r}') \rho_{\text{ind}}(\mathbf{r}', t') d\mathbf{r}' + V_{\text{ext}}(\mathbf{r}, t). \quad (5.8)$$

$\delta V(\mathbf{r}, t)$ is also linearly related to V_{ext}

$$\delta V(\mathbf{r}, t) = \int \epsilon^{-1}(\mathbf{r}, \mathbf{r}', t - t') V_{\text{ext}}(\mathbf{r}', t') d\mathbf{r}' dt'. \quad (5.9)$$

This relation defines the *inverse dielectric function* of the system. In deriving the explicit formula for the dielectric function in the LTH approximation, we follow closely the work by Ehrenreich and Cohen,²³ who formulated the theory in terms of the *density matrix*

$$\rho(\mathbf{x}, \mathbf{x}', t) = \sum_k^{\infty} u_k(\mathbf{x}, t) u_k^*(\mathbf{x}', t), \quad (5.10)$$

which satisfies the equation of motion [obtained from Eq. (5.2)]

$$i(\partial/\partial t)\rho(\mathbf{x}, \mathbf{x}', t) = [H(\mathbf{x}, t) - H(\mathbf{x}', t)]\rho(\mathbf{x}, \mathbf{x}', t), \quad (5.11)$$

with

$$H(\mathbf{x}, t) = h(\mathbf{x}) + V_H(\mathbf{x}, t) + V_{\text{ext}}(\mathbf{r}, t). \quad (5.12)$$

We consider a matrix representation

$$\rho(\mathbf{x}, \mathbf{x}', t) = \sum_{k,k'} u_k(\mathbf{x}) u_{k'}^*(\mathbf{x}') \rho_{kk'}(t), \quad (5.13)$$

where u_k are solutions of the unperturbed problem

$$[h(\mathbf{x}) + V_H^{(0)}(\mathbf{x})]u_k(\mathbf{x}) = \epsilon_k u_k(\mathbf{x}). \quad (5.14)$$

This transformation replaces Eq. (5.11) by

$$i(\partial/\partial t)\rho_{kk'} = \sum_l (H_{kl}\rho_{lk'} - \rho_{kl}H_{lk'}) = [H, \rho]_{kk'}, \quad (5.15)$$

where

$$H_{kl}(t) = \int u_k^*(\mathbf{x}) H(\mathbf{x}, t) u_l(\mathbf{x}) d\mathbf{x}.$$

We split H and ρ into perturbed and unperturbed parts according to $\delta V = V_{\text{ind}} + V_{\text{ext}}$ [see Eq. (5.8)]:

$$\begin{aligned} H(\mathbf{x}, t) &= h(\mathbf{x}) + V_H^{(0)}(\mathbf{x}) + \delta V(\mathbf{x}, t), \\ \rho(\mathbf{x}, \mathbf{x}', t) &= \rho^{(0)}(\mathbf{x}, \mathbf{x}') + \rho^{(1)}(\mathbf{x}, \mathbf{x}', t). \end{aligned} \quad (5.16)$$

²³ H. Ehrenreich and M. H. Cohen, *Phys. Rev.* **115**, 786 (1959).

Note that $(h + V_{\text{H}}^{(0)})_{kk'} = \epsilon_k \delta_{kk'}$ and $\rho_{kk'}^{(0)} = n_k \delta_{kk'}$, where $n_k = 1$ for occupied and 0 for unoccupied states. In the linear approximation Eq. (5.15) becomes

$$i(\partial/\partial t)\rho_{kk'}^{(1)}(t) = (\epsilon_k - \epsilon_{k'})\rho_{kk'}^{(1)}(t) + (n_{k'} - n_k) \delta V_{kk'}(t). \quad (5.17)$$

We are interested in the response to a field of given frequency and therefore write δV and $\rho^{(1)}$ in a form that explicitly shows that they were zero in a remote past:

$$\begin{aligned} \delta V_{kk'}(t) &= (2\pi)^{-1} \int \delta V_{kk'}(\omega) \exp[-i(\omega + i\delta)t] d\omega \\ \rho_{kk'}^{(1)}(t) &= (2\pi)^{-1} \int \rho_{kk'}^{(1)}(\omega) \exp[-i(\omega + i\delta)t] d\omega. \end{aligned} \quad (5.18)$$

For the Fourier transforms $\delta V(\omega)$ and $\rho^{(1)}(\omega)$ we obtain

$$\rho_{kk'}^{(1)}(\omega) = \frac{n_k - n_{k'}}{\epsilon_k - \epsilon_{k'} - \omega - i\delta} \delta V_{kk'}(\omega). \quad (5.19)$$

We now define a *response function* P which relates ρ_{ind} to the *effective field* δV , rather than to V_{ext} :

$$\rho_{\text{ind}}(\mathbf{r}, \omega) \equiv \int \rho^{(1)}(\mathbf{x}, \mathbf{x}, \omega) d\xi = \int P(\mathbf{r}, \mathbf{r}', \omega) \delta V(\mathbf{r}', \omega) d\mathbf{r}'. \quad (5.20)$$

Using Eqs. (5.13) and (5.19) we have

$$\begin{aligned} \rho_{\text{ind}}(\mathbf{r}, \omega) &= \sum_{kk'} \int d\xi u_k(\mathbf{x}) u_{k'}^*(\mathbf{x}) \frac{n_k - n_{k'}}{\epsilon_k - \epsilon_{k'} - \omega - i\delta} \\ &\quad \times u_k^*(\mathbf{x}') u_{k'}(\mathbf{x}') \delta V(\mathbf{r}', \omega) d\mathbf{x}', \end{aligned}$$

and thus

$$P(\mathbf{r}, \mathbf{r}', \omega) = \sum_{kk'} \frac{n_k - n_{k'}}{\epsilon_k - \epsilon_{k'} - \omega - i\delta} f_{kk'}(\mathbf{r}) f_{kk'}^*(\mathbf{r}'), \quad (5.21)$$

where

$$f_{kk'}(\mathbf{r}) = \int u_k(\mathbf{x}) u_{k'}^*(\mathbf{x}) d\xi. \quad (5.22)$$

It remains to relate P to the dielectric function. We can simplify the notation by considering the equations as matrices in the continuous labels \mathbf{r} , and \mathbf{r}' . From Eqs. (5.20) and (5.8) we then have

$$\begin{aligned} \rho_{\text{ind}} &= P \delta V = P(v\rho_{\text{ind}} + V_{\text{ext}}) \\ \rho_{\text{ind}} &= (1 - Pv)^{-1} PV_{\text{ext}} \\ \delta V &= [1 + v(1 - Pv)^{-1}P]V_{\text{ext}}. \end{aligned} \quad (5.23)$$

Comparing with Eq. (5.9) we have

$$\epsilon^{-1} = 1 + v(1 - Pv)^{-1}P = (1 - vP)^{-1}, \quad (5.24)$$

and thus, finally

$$\epsilon(\mathbf{r}, \mathbf{r}', \omega) = \delta(\mathbf{r}, \mathbf{r}') - \int v(\mathbf{r}, \mathbf{r}'') P(\mathbf{r}'', \mathbf{r}'; \omega) d\mathbf{r}''. \quad (5.25)$$

We now specialize to the case of a uniform electron gas. P and ϵ then depend only on the difference between the coordinates, e.g. $P(\mathbf{r}, \mathbf{r}', \omega) = P(\mathbf{r} - \mathbf{r}', \omega)$. It is convenient to go over to momentum variables, thus

$$\begin{aligned} P(\mathbf{q}, \omega) &= \int P(\mathbf{r}, \omega) \exp(i\mathbf{q} \cdot \mathbf{r}) d\mathbf{r} \\ \epsilon(\mathbf{q}, \omega) &= \int \epsilon(\mathbf{r}, \omega) \exp(i\mathbf{q} \cdot \mathbf{r}) d\mathbf{r} \\ &= 1 - v(\mathbf{q}) P(\mathbf{q}, \omega), \end{aligned} \quad (5.26)$$

with

$$v(\mathbf{q}) = 4\pi e^2/q^2. \quad (5.27)$$

The wave functions are plane waves (normalized in a box of volume Ω) and we obtain from Eq. (5.22)

$$\begin{aligned} f_{\mathbf{k}\mathbf{k}'}(\mathbf{r}) &= \Omega^{-1} \exp[i(\mathbf{k} - \mathbf{k}') \cdot \mathbf{r}], & \mathbf{k} \text{ and } \mathbf{k}' \text{ have parallel spins,} \\ &= 0, & \text{otherwise,} \end{aligned} \quad (5.28)$$

which gives for P

$$P(\mathbf{q}, \omega) = \sum_{\mathbf{k}\mathbf{k}'} \frac{n_{\mathbf{k}} - n_{\mathbf{k}'}}{\epsilon_{\mathbf{k}} - \epsilon_{\mathbf{k}'} - \omega - i\delta} \Omega^{-2} \int \exp[i(\mathbf{q} + \mathbf{k} - \mathbf{k}') \cdot \mathbf{r}] d\mathbf{r} \quad (5.29)$$

with

$$\epsilon(\mathbf{k}) = \dot{\hbar}^2 k^2 / 2m. \quad (5.30)$$

Making the replacement

$$\sum_{\mathbf{k}} \rightarrow \Omega (2\pi)^{-3} \int d\mathbf{k}, \quad (5.31)$$

we obtain after performing the integrations and spin summations

$$P(\mathbf{q}, \omega) = 2(2\pi)^{-3} \int \frac{n_{\mathbf{k}} - n_{\mathbf{k}+\mathbf{q}}}{\epsilon_{\mathbf{k}} - \epsilon_{\mathbf{k}+\mathbf{q}} - \omega - i\delta} d\mathbf{k}. \quad (5.32)$$

The integration of P can be made analytically and so we obtain the Lindhard formula²⁰

$$\epsilon(q, \omega) = 1 + \frac{\alpha r_s}{\pi} \frac{1}{q^3} \left[2q + f\left(q + \frac{\omega + i\delta}{q}\right) + f\left(q - \frac{\omega + i\delta}{q}\right) \right] \quad (5.33)$$

with

$$f(z) = (1 - \frac{1}{4}z^2) \ln[(z + 2)/(z - 2)], \quad \alpha = (4/9\pi)^{1/3} = 0.521.$$

We have expressed q in units of the Fermi momentum k_F , ω in units of the Fermi energy, $\epsilon_F = (\hbar^2 k_F^2)/(2m)$, and r_s ²⁴ in units of the Bohr radius $a_0 = 0.529 \text{ \AA}$. The logarithms in the function $f(z)$ should be taken from the principal branch. The imaginary part of ϵ is different from zero only in the regions marked I and II in Fig. 1. We need only consider $\omega > 0$, since $\epsilon(q, -\omega) = \epsilon(q, \omega)^*$.

The explicit formula for $\text{Im } \epsilon(q, \omega)$ is

$$\text{Im } \epsilon(q, \omega) = \begin{cases} \frac{\alpha r_s}{q^3} \omega & \text{region I} \\ 1 - \frac{1}{4}[q - (\omega/q)]^2 & \text{region II.} \end{cases} \quad (5.34)$$

If the condition $\epsilon(q, \omega) = 0$ is fulfilled, we can according to Eq. (5.9) have a charge oscillation in the system even in the absence of an external field. This is the condition for a plasma oscillation in the system²⁰ which has been discussed extensively by Pines and collaborators.²² The dispersion curve for plasmons is plotted in Fig. 1. It starts at the classical plasma frequency ω_p , corresponding to the long-wavelength limit where the classical Drude formula applies:

$$\lim_{q \rightarrow 0} \epsilon(q, \omega) = 1 - (\omega_p^2/\omega^2), \quad (5.35)$$

$$\omega_p = 4(\alpha r_s/3\pi)^{1/2} \epsilon_F = (12/r_s^3)^{1/2} \text{ Ry.}$$

The dielectric function is an important quantity in discussing the dynamical properties of the electron gas. One can also calculate the total energy of the system, using a formula derived by Hubbard.²⁵ The Lindhard formula produces for small r_s the same result as that obtained by Gell-Mann and Brueckner.²⁶ The Gell-Mann and Brueckner result is obtained as a series expansion in r_s , which is clearly doubtful for $r_s \gtrsim 1$, whereas the Lindhard formula is based on the self-consistent treatment of the response as we have just described, and shows no indication of breakdown over the region of metallic densities.

The Lindhard formula describes quite well the gross properties of the system but fails to describe some details correctly, particularly in the limit of short wavelengths. This is to be expected because we cannot expect the Hartree approximation to describe things well at distances much shorter

²⁴ The quantity r_s is the conventional electron gas parameter defined by $N4\pi r_s^3/3 = \Omega$.

²⁵ J. Hubbard, *Proc. Roy. Soc. A240*, 539 (1957).

²⁶ M. Gell-Mann and K. Brueckner, *Phys. Rev. 106*, 364 (1957).

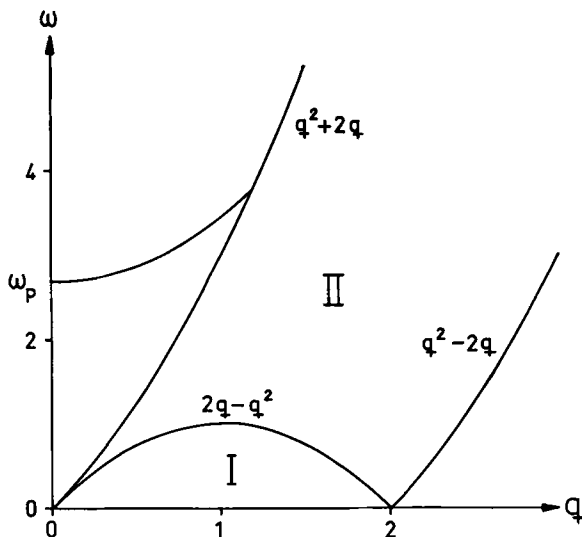


FIG. 1. Regions in the $q\omega$ plane where the imaginary part of the LTH approximation for the dielectric constant is nonzero.

than the average distance between particles. Quantities such as the correlation energy, pair correlation function, and phonon dispersion curves depend strongly on details of the dielectric functions, whereas single particle properties are generally less sensitive.

A first step to obtain a better approximation for the dielectric function is to consider the linearized form of the time-dependent HF equations rather than the Hartree equation. The total effective field will then be

$$\delta V = V^{\text{ext}} + \delta V_H + \delta V_{\text{ex}}. \quad (5.36)$$

This gives an integral equation for $\rho_{kk'}^{(1)}$,

$$\begin{aligned} \rho_{kk'}^{(1)} = & \frac{n_k - n_{k'}}{\epsilon_k - \epsilon_{k'} - \omega - i\delta} \left\{ V_{kk'}^{\text{ext}} + \sum_{qq'} [\langle kq' | v | k'q \rangle \right. \\ & \left. - \langle kq' | v | qk' \rangle] \rho_{qq'}^{(1)} \right\}, \end{aligned} \quad (5.37)$$

which in the special case of a uniform electron gas becomes

$$\begin{aligned} \rho_{k,k+q}^{(1)} = & \Omega^{-1} \frac{n_k - n_{k+q}}{\epsilon_k - \epsilon_{k+q} - \omega - i\delta} \left\{ V^{\text{ext}}(q) \right. \\ & \left. + 2v(q) \sum_{k'} \rho_{k',k'+q} - \sum_{k'} v(k - k') \rho_{k',k'+q}^{(1)} \right\}. \end{aligned} \quad (5.38)$$

If we replace the Coulomb potential in the exchange term by an average value, thus

$$\sum_{\mathbf{k}'} v(\mathbf{k} - \mathbf{k}') \rho_{\mathbf{k}', \mathbf{k}' + \mathbf{q}}^{(1)} = v_s(\mathbf{q}) \sum_{\mathbf{k}'} \rho_{\mathbf{k}', \mathbf{k}' + \mathbf{q}}^{(1)}, \quad (5.39)$$

we can solve for the density Fourier component $\rho^{(1)}(\mathbf{q}, \omega)$,

$$\rho^{(1)}(\mathbf{q}, \omega) = \frac{P(\mathbf{q}, \omega) V^{\text{ext}}(\mathbf{q}, \omega)}{1 - P(\mathbf{q}, \omega)[v(\mathbf{q}) - \frac{1}{2}v_s(\mathbf{q})]}, \quad (5.40)$$

and obtain

$$\epsilon^{-1}(\mathbf{q}, \omega) = 1 + \frac{v(\mathbf{q}) P(\mathbf{q}, \omega)}{1 - P(\mathbf{q}, \omega)[v(\mathbf{q}) - \frac{1}{2}v_s(\mathbf{q})]}. \quad (5.41)$$

Choosing $v_s(\mathbf{q})$ as a *screened potential*,

$$v_s(\mathbf{q}) = 4\pi e^2/(q^2 + k_F^2), \quad (5.42)$$

Eq. (5.41) gives the *Hubbard* modification of the dielectric function.²⁷ Further improvements beyond this approximation have recently been developed by Singwi *et al.*²⁸ (cf. also Hubbard²⁹). The basic formulas for P and ϵ in Eqs. (5.21) and (5.25) are of course general and apply to any system: atom, molecule, or solid.

III. Summary of Key Concepts and Formulas in the Green Function Theory

6. INTRODUCTION

A number of methods have been developed in the past to deal with various aspects of the many-body problem in solids: canonical transformation methods, equation of motion methods, density matrix formulations, and time-independent and time-dependent perturbation methods often systematized by diagram methods. The key tools, however, are the Green function methods. The Green functions used in many-body problems are extremely useful generalizations of the original Green functions, well known from the theory of ordinary differential and integral equations. They form basic elements in the field theoretical approach to the many-body problem and provide a direct way to calculate physical properties.

We would like to emphasize, before giving even a single definition, the close relation between Green functions and experiments. Let us as an example consider the case of inelastic scattering in the Born approximation.

²⁷ J. Hubbard, *Proc. Roy. Soc. A* **243**, 336 (1957).

²⁸ K. S. Singwi, M. P. Tosi, R. H. Land, and A. Sjölander, *Phys. Rev.* **176**, 589 (1968).

²⁹ J. Hubbard, *Phys. Letters* **25A**, 709 (1967).

It was shown by Van Hove³⁰ in the special case of neutron scattering that the scattering cross section can be expressed by means of a certain time correlation function of the form $\langle A(t)A(0) \rangle$, where the brackets indicate a statistical average over the system. Van Hove's result is quite general and applies to all scattering phenomena in the Born approximation. The nature of the probe and its interaction with the system determines the type of correlation function in each case. Examples of such correlation functions are the density-density correlation, the current-current correlation, and the spin-spin correlation. The time correlations are themselves not Green functions, but are closely related to them, and can easily be calculated if the corresponding Green function is known.

Another example is the case in which we apply a steady or a time-varying external field to a system and measure the response in the linear approximation. The external field acts on the system via some dynamical variable A and one measures the average response in the variable B . First order perturbation theory gives the response of the system expressed as the statistical average for the unperturbed system of the retarded commutator of A and B , i.e. one can define a response function of the form $\theta(t - t') \langle [B(t), A(t')] \rangle$. This response function is itself a Green function, satisfying the requirement of causality, and is therefore referred to as a *retarded Green function*. By considering other boundary conditions with respect to time, one obtains other kinds of Green functions, e.g. *advanced Green functions*. Of particular importance in the theory are the *time-ordered Green functions*, which are statistical averages of the form $\langle T\{A(t)B(t')C(t'')\dots\} \rangle$. The time-ordering symbol T indicates that the variables should be ordered from the right to the left after increasing time arguments and a minus sign should be included for every interchange of fermion operators needed to obtain the right order. The properties of these functions will be summarized in this part of the article.

7. OPERATORS AND STATES IN SECOND QUANTIZATION

There is a one-to-one correspondence between normal quantum mechanics in configuration space and the method of second quantization. The reason why the second quantization scheme has been rapidly out-phasing the conventional approach is the ease with which one handles problems of statistics, etc. in a many-body system. It is simply the practical question of providing an economical language and simple rules for calculations that gives a strong preference for second quantization. We summarize a number of definitions and formulas which we shall use and refer the reader to any standard text for a more extensive discussion.

³⁰ L. Van Hove, *Phys. Rev.* **95**, 249 (1954).

The set of all Slater determinants based on any complete set of single particle functions $u_k(\mathbf{x})$ form a complete set for the N -body problem. We introduce a notation in which the state is specified by listing the quantum labels k_1, k_2, \dots, k_N as follows:

$$(N!)^{-1/2} \det \{u_k(\mathbf{x}_i)\} = |k_1, k_2, \dots, k_N\rangle. \quad (7.1)$$

We define a "creation" operator a_k^+ by

$$a_k^+ |k_1, k_2, \dots, k_N\rangle = |k, k_1, k_2, \dots, k_N\rangle. \quad (7.2)$$

If the state k is already occupied, i.e. if $k = k_i$ for some i , then

$$a_k^+ |k_1, k_2, \dots, k_N\rangle = 0.$$

Next we define an annihilation operator a_k as the Hermitian adjoint of a_k^+ . It then follows that

$$a_k |k, k_1, k_2, \dots, k_N\rangle = |k_1, k_2, \dots, k_N\rangle, \quad (7.3)$$

and also that

$$a_k |k_1, k_2, \dots, k_N\rangle = 0,$$

if $k \neq k_i$ for all i . From the definitions of a_k and a_k^+ follow the commutation relations

$$[a_k, a_{k'}^+]_+ \equiv a_k a_{k'}^+ + a_{k'}^+ a_k = \delta_{kk'}; \quad [a_k, a_{k'}]_+ = [a_k^+, a_{k'}^+]_+ = 0. \quad (7.4)$$

The formula for a general operator in second quantization is obtained for example from the requirement that the matrices of the operator between states in second quantization should be the same as those in the configuration space approach between the corresponding Slater determinants. In particular, the Hamiltonian in Eq. (2.1) takes the form

$$H = \sum_{k,l} h_{kl} a_k^+ a_l + \frac{1}{2} \sum_{k_1 k_2 k_3 k_4} \langle k_1 k_2 | v | k_4 k_3 \rangle a_{k_1}^+ a_{k_2}^+ a_{k_3} a_{k_4} + V_{\text{nuc}}, \quad (7.5)$$

with

$$h_{kl} = \int u_k^*(\mathbf{x}) h(\mathbf{x}) u_l(\mathbf{x}) d\mathbf{x}$$

$$\langle k_1 k_2 | v | k_3 k_4 \rangle = \int u_{k_1}^*(\mathbf{x}) u_{k_2}^*(\mathbf{x}') v(\mathbf{r}, \mathbf{r}') u_{k_3}(\mathbf{x}) u_{k_4}(\mathbf{x}') d\mathbf{x} d\mathbf{x}'. \quad (7.6)$$

Instead of using operators a_k and a_k^+ acting on particular one-electron states, one often uses wave field operators $\psi(\mathbf{x})$ and $\psi^+(\mathbf{x})$ acting in space, and defined by

$$\psi(\mathbf{x}) = \sum_k a_k u_k(\mathbf{x}). \quad (7.7)$$

From Eq. (7.4) it follows that

$$[\psi(\mathbf{x}), \psi^+(\mathbf{x}')]_+ = \delta(\mathbf{x}, \mathbf{x}'), \quad [\psi(\mathbf{x}), \psi(\mathbf{x}')]_+ = [\psi^+(\mathbf{x}), \psi^+(\mathbf{x}')]_+ = 0. \quad (7.8)$$

The Hamiltonian now takes the form

$$\begin{aligned} H = & \int \psi^+(\mathbf{x}) h(\mathbf{x}) \psi(\mathbf{x}) d\mathbf{x} \\ & + \frac{1}{2} \int \psi^+(\mathbf{x}) \psi^+(\mathbf{x}') v(\mathbf{r}, \mathbf{r}') \psi(\mathbf{x}') \psi(\mathbf{x}) d\mathbf{x} d\mathbf{x}' + V_{\text{nuc}}. \end{aligned} \quad (7.9)$$

The particle density is represented by the operator

$$\rho(\mathbf{r}) = \sum_i \delta(\mathbf{r} - \mathbf{r}_i) = \int \psi^+(\mathbf{x}) \psi(\mathbf{x}) d\xi \quad (7.10)$$

and the operator for the total number of particles is

$$N = \int \rho(\mathbf{r}) d\mathbf{r} = \int \psi^+(\mathbf{x}) \psi(\mathbf{x}) d\mathbf{x} = \sum_k a_k^+ a_k. \quad (7.11)$$

The *average charge density* in a state $|N\rangle$ is

$$\rho(\mathbf{r}) = \langle N | \int \psi^+(\mathbf{x}) \psi(\mathbf{x}) d\xi | N \rangle \quad (7.12)$$

and the *density matrix* of that state is given by

$$\rho(\mathbf{x}, \mathbf{x}') = \langle N | \psi^+(\mathbf{x}') \psi(\mathbf{x}) | N \rangle. \quad (7.13)$$

In a single-particle theory we have that

$$\langle N | a_{k_1}^+ a_{k_2} | N \rangle = \delta_{k_1 k_2} n_{k_2}, \quad (7.14)$$

where n_k equals 0 or 1 depending on whether the state is empty or occupied. The density and the density matrix then reduce to (cf. Eq. (2.7))

$$\rho(\mathbf{r}) = \sum_k^{\text{occ}} \int |u_k(\mathbf{x})|^2 d\xi \quad (7.15)$$

$$\rho(\mathbf{x}, \mathbf{x}') = \sum_k^{\text{occ}} u_k(\mathbf{x}) u_k^*(\mathbf{x}'). \quad (7.16)$$

8. EQUATION OF MOTION FOR THE FIELD OPERATOR

In the last section we introduced the field operator $\psi(\mathbf{x})$ in Eq. (7.7). One usually works in the Heisenberg picture and we therefore introduce the time-dependent operator

$$\psi(\mathbf{x}, t) = e^{iHt} \psi(\mathbf{x}) e^{-iHt}. \quad (8.1)$$

The Heisenberg equation of motion gives $i(\partial/\partial t)\psi(\mathbf{x}, t) = [\psi(\mathbf{x}, t), H]$, and using the commutation relations and the form of the Hamiltonian in Eq. (7.9), we obtain

$$i(\partial/\partial t)\psi(\mathbf{x}, t) = \left[h(\mathbf{x}) + \int v(\mathbf{r}, \mathbf{r}')\psi^+(\mathbf{x}', t)\psi(\mathbf{x}', t) d\mathbf{x}' \right] \psi(\mathbf{x}, t). \quad (8.2)$$

This is the fundamental dynamical equation of motion in the theory. It has a simple structure closely resembling Eq. (5.2) in the time-dependent Hartree theory. However, Eq. (8.2) is a complicated nonlinear equation in the field *operators* and the techniques to solve single-particle equations do not apply at all.

We wish to make some introductory remarks about the meaning of a single-particle wave function and equation in an interacting system. Let us form the matrix element of $\psi(\mathbf{x}, t)$ between the two states

$$\begin{aligned} |N\rangle &\quad \text{ground state of } N \text{ electrons} \\ |N-1, s\rangle &\quad \text{some eigenstate } s \text{ of } (N-1) \text{ electrons.} \end{aligned}$$

We obtain

$$\langle N-1, s | \psi(\mathbf{x}, t) | N \rangle = f_s(\mathbf{x}) \exp(-i\epsilon_s t) \quad (8.3)$$

with

$$\epsilon_s = E(N) - E(N-1, s), \quad f_s(\mathbf{x}) = \langle N-1, s | \psi(\mathbf{x}) | N \rangle. \quad (8.4)$$

Taking matrix elements of Eq. (8.2), we have³¹

$$\epsilon_s f_s(\mathbf{x}) = h(\mathbf{x})f_s(\mathbf{x}) + \int v(\mathbf{r}, \mathbf{r}') \langle N-1, s | \psi^*(\mathbf{x}')\psi(\mathbf{x}')\psi(\mathbf{x}) | N \rangle d\mathbf{x}'. \quad (8.5)$$

We may also take matrix elements with respect to the ground state $|N\rangle$ and the state $|N+1, s\rangle$ which is equal to some eigenstates of $(N+1)$ electrons. We then obtain

$$\langle N | \psi(\mathbf{x}, t) | N+1, s \rangle = \exp(-i\epsilon_s t)f_s(\mathbf{x}), \quad (8.6)$$

with

$$\epsilon_s = E(N+1, s) - E(N), \quad f_s(\mathbf{x}) = \langle N | \psi(\mathbf{x}) | N+1, s \rangle. \quad (8.7)$$

³¹ We shall not at this point enter into a discussion of how to make approximations of the interaction term, but only remark that the Hartree theory is obtained as a first approximation by the decoupling

$$\langle N-1, s | \psi^+(\mathbf{x}')\psi(\mathbf{x}')\psi(\mathbf{x}) | N \rangle = \langle N-1, s | \psi^+(\mathbf{x}')\psi(\mathbf{x}') | N-1, s \rangle f_s(\mathbf{x}),$$

which obviously neglects fluctuations in the density.

We also obtain the equation

$$\epsilon_s f_s(\mathbf{x}) = h(\mathbf{x})f_s(\mathbf{x}) + \int v(\mathbf{r}, \mathbf{r}') \langle N | \psi^*(\mathbf{x}') \psi(\mathbf{x}') \psi(\mathbf{x}) | N + 1, s \rangle d\mathbf{x}'. \quad (8.8)$$

As a simple illustration we consider a system of noninteracting particles where $|N\rangle$ corresponds to a single Slater determinant. The label s can now be identified with the single-particle label and thus we obtain

$$|N - 1, s\rangle = a_s |N\rangle, \quad |N + 1, s\rangle = a_s^+ |N\rangle. \quad (8.9)$$

Straightforward application of the rules gives the expected results:

$$\begin{aligned} f_s(\mathbf{x}) &= \langle N - 1, s | \psi(\mathbf{x}) | N \rangle = u_s(\mathbf{x}) && \text{if } s \text{ occupied} \\ &= \langle N | \psi(\mathbf{x}) | N + 1, s \rangle = u_s(\mathbf{x}) && \text{if } s \text{ unoccupied.} \end{aligned} \quad (8.10)$$

The second term in the rhs of Eqs. (8.5) and (8.8) now reduces to

$$\begin{aligned} \int v(\mathbf{r}, \mathbf{r}') \sum_k^{\text{occ}} [u_k^*(\mathbf{x}') u_k(\mathbf{x}') u_s(\mathbf{x}) - u_k^*(\mathbf{x}') u_k(\mathbf{x}) u_s(\mathbf{x}')] d\mathbf{x}' \\ = V_H(\mathbf{r}) u_s(\mathbf{x}) + \int V_{ex}(\mathbf{x}, \mathbf{x}') u_s(\mathbf{x}') d\mathbf{x}'. \end{aligned} \quad (8.11)$$

We have thus retrieved the HF equation discussed in Section 2.

In an interacting system we lose the simple one-to-one relation between states $|N + 1, s\rangle$ and one-particle states. To illustrate this point we take the case of Li and consider the following states:

$$\begin{aligned} |N\rangle &= |\text{Li}^+, 1s^2\rangle = \text{Li}^+ \text{ ion in its ground state} \\ |N + 1, 1\rangle &= |\text{Li}, 1s^22s\rangle = \text{Li atom in its ground state} \\ |N + 1, 2\rangle &= |\text{Li}, 1s2s3s\rangle = \text{particular excited state of Li atom.} \end{aligned}$$

The corresponding functions $f_s(\mathbf{x})$ are

$$\begin{aligned} f_1(\mathbf{x}) &= \sum_k u_k(\mathbf{x}) \langle \text{Li}^+, 1s^2 | a_k | \text{Li}, 1s^22s \rangle \\ f_2(\mathbf{x}) &= \sum_k u_k(\mathbf{x}) \langle \text{Li}^+, 1s^2 | a_k | \text{Li}, 1s2s3s \rangle. \end{aligned} \quad (8.12)$$

The function $f_1(\mathbf{x})$ will be dominated by the contribution from the HF function $u_{2s}(\mathbf{x})$ but there are additional small components of $u_{1s}(\mathbf{x})$, $u_{3s}(\mathbf{x})$, etc. The function $f_2(\mathbf{x})$ will not be zero as for a noninteracting system but will have small components of many functions u_{1s} , u_{2s} , u_{3s} , etc. The problem about the nature of single-particle states and equations will be left in this incomplete state for the moment. We shall return to the problem later on and derive and discuss at length an equation that represents an essential

step beyond the one-particle Schrödinger-type wave equations characteristic of independent particle models.

9. THE ONE-ELECTRON GREEN FUNCTION AT ZERO TEMPERATURE

We consider a system of N electrons in its ground state and define the one-electron Green function in coordinate space:

$$\begin{aligned} G(\mathbf{x}t, \mathbf{x}'t') &= -i\langle N | T[\psi(\mathbf{x}, t)\psi^+(\mathbf{x}', t')] | N \rangle \\ &= -i\langle N | \psi(\mathbf{x}) \exp[-i(H - E_N)(t - t')] \psi^+(\mathbf{x}') | N \rangle \Theta(t - t') \\ &\quad + i\langle N | \psi^+(\mathbf{x}') \exp[i(H - E_N)(t - t')] \psi(\mathbf{x}) | N \rangle \Theta(t' - t), \\ \Theta(t) &= 1, \quad t > 0 \\ &= 0, \quad t < 0. \end{aligned} \quad (9.1)$$

Here \mathbf{x} stands for both space and spin coordinates, $\mathbf{x} = (\mathbf{r}, \xi)$, $|N\rangle$ denotes the ground state, and $\psi^+(\mathbf{x}, t)$ and $\psi(\mathbf{x}, t)$ are the Heisenberg operators for creation and annihilation, respectively. For $t > t'$ the Green function describes the propagation of an additional electron injected at time t' , whereas for $t < t'$ it describes the propagation of a hole (extraction of an electron).

Next we introduce in Eq. (9.1) the complete set of eigenstates of H for the $(N+1)$ or $(N-1)$ particles. The quantum labels of these states are denoted by s . By writing $\tau = t - t'$ and remembering that the limiting energy for injection of electrons or holes is the chemical potential μ , we obtain

$$\begin{aligned} G(\mathbf{x}, \mathbf{x}', \tau) &= -i \sum_s f_s(\mathbf{x}) f_{s*}(\mathbf{x}') \exp(-i\epsilon_s \tau) \\ &\quad \times \{\Theta(\tau) \Theta(\epsilon_s - \mu) - \Theta(-\tau) \Theta(\mu - \epsilon_s)\}, \end{aligned} \quad (9.2)$$

with

$$\begin{aligned} f_s(\mathbf{x}) &= \langle N | \psi(\mathbf{x}) | N+1, s \rangle, \quad \epsilon_s = E_{N+1,s} - E_N \quad \text{for } \epsilon_s \geq \mu \\ f_s(\mathbf{x}) &= \langle N-1, s | \psi(\mathbf{x}) | N \rangle, \quad \epsilon_s = E_N - E_{N-1,s} \quad \text{for } \epsilon_s < \mu. \end{aligned} \quad (9.3)$$

We proceed to transform Eq. (9.2) to energy space and obtain

$$\begin{aligned} G(\mathbf{x}, \mathbf{x}', \epsilon) &= \int_{-\infty}^{\infty} G(\mathbf{x}, \mathbf{x}', \tau) e^{i\epsilon\tau} d\tau \\ &= \sum_s f_s(\mathbf{x}) f_{s*}(\mathbf{x}') \left\{ -i\Theta(\epsilon_s - \mu) \int_0^{\infty} \exp[i(\epsilon - \epsilon_s)\tau] d\tau \right. \\ &\quad \left. + i\Theta(\mu - \epsilon_s) \int_{-\infty}^0 \exp[i(\epsilon - \epsilon_s)\tau] d\tau \right\}. \end{aligned}$$

Adding infinitesimal convergence factors

$$\begin{aligned}\epsilon_s &\rightarrow \epsilon_s + i\delta \quad \text{for } \epsilon_s < \mu, \\ &\qquad\qquad\qquad \delta > 0, \\ \epsilon_s &\rightarrow \epsilon_s - i\delta \quad \text{for } \epsilon_s > \mu,\end{aligned}$$

we obtain

$$G(\mathbf{x}, \mathbf{x}', \epsilon) = \sum_s [f_s(\mathbf{x})f_s^*(\mathbf{x}')/(\epsilon - \epsilon_s)], \quad (9.4)$$

where we understand that the proper infinitesimals are included in ϵ_s .

Although Eq. (9.4) is identical in form with the corresponding expression for the ordinary Green function,³² there are fundamental differences. In our case the functions $f_s(\mathbf{x})$ are not normalized to unity and they are not linearly independent. They do, however, fulfill the completeness relation

$$\sum_s f_s(\mathbf{x})f_s^*(\mathbf{x}') = \langle N | \psi(\mathbf{x})\psi(\mathbf{x}')^* + \psi^*(\mathbf{x}')\psi(\mathbf{x}) | N \rangle = \delta(\mathbf{x} - \mathbf{x}'). \quad (9.5)$$

10. SPECTRAL REPRESENTATION OF THE ONE-ELECTRON GREEN FUNCTION

Spectral representations and spectral weight functions are extremely useful in the development of the theory as well as for the physical interpretations of results. We define the *spectral weight function* $A(\mathbf{x}, \mathbf{x}'; \epsilon)$ as follows:

$$A(\mathbf{x}, \mathbf{x}'; \epsilon) = \sum_s f_s(\mathbf{x})f_s(\mathbf{x}') \delta(\epsilon - \epsilon_s). \quad (10.1)$$

Combining Eq. (10.1) with Eq. (9.4) we obtain the *spectral representation* of $G(\mathbf{x}, \mathbf{x}', \epsilon)$:

$$G(\mathbf{x}, \mathbf{x}'; \epsilon) = \int_C \frac{A(\mathbf{x}, \mathbf{x}'; \epsilon')}{\epsilon - \epsilon'} d\epsilon', \quad (10.2)$$

where the integral should be taken along the path C in Fig. 2. From Eqs. (10.1) and (9.5) follows the *sum rule*,

$$\int_{-\infty}^{\infty} A(\mathbf{x}, \mathbf{x}'; \epsilon) d\epsilon = \delta(\mathbf{x} - \mathbf{x}'). \quad (10.3)$$

The spectral weight function A can be chosen as a real function except for some problems involving magnetic fields.

In applications of the theory one often prefers to represent the Green

³² See e. g. P. M. Morse and H. Feshbach, "Methods of Theoretical Physics," Part I, p. 832. McGraw-Hill, New York, 1953.

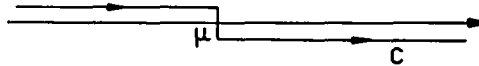


FIG. 2. Contour C to be used in the spectral resolutions of G and Σ .

function as a matrix in a space spanned by some suitable complete orthonormal set of single-particle states $u_k(\mathbf{x})$. One then obtains

$$\begin{aligned} G_{kk'}(\epsilon) &= \int u_k^*(\mathbf{x}) G(\mathbf{x}, \mathbf{x}'; \epsilon) u_{k'}(\mathbf{x}') d\mathbf{x} d\mathbf{x}' \\ &= -i \int_{-\infty}^{\infty} e^{i\epsilon\tau} \langle N | T[a_k(\tau) a_{k'}^+(0)] | N \rangle d\tau, \end{aligned} \quad (10.4)$$

where a_k and a_k^+ are creation and annihilation operators referring to the chosen set $\{k\}$.

The spectral weight function takes the form

$$A_{kk'}(\epsilon) = \int u_k^*(\mathbf{x}) A(\mathbf{x}, \mathbf{x}'; \epsilon) u_{k'}(\mathbf{x}') d\mathbf{x} d\mathbf{x}'. \quad (10.5)$$

The spectral representation will be unchanged in form, thus

$$G_{kk'}(\epsilon) = \int_C d\epsilon' \frac{A_{kk'}(\epsilon')}{\epsilon - \epsilon'}, \quad (10.6)$$

and the sum rule takes the form

$$\int_{-\infty}^{\infty} d\epsilon A_{kk'}(\epsilon) = \delta_{kk'}. \quad (10.7)$$

According to its definition, $A(\epsilon)$ is a Hermitian matrix, and can often be chosen as a real matrix. It can be brought to diagonal form for any given value of ϵ . This property is, however, of limited usefulness since the matrix of transformation will depend on the value of ϵ .

The spectral function is closely related to the imaginary part of the Green function. Using the formula

$$(x \pm i\epsilon)^{-1} = P(x^{-1}) \mp i\pi \delta(x), \quad (10.8)$$

we find from Eq. (10.2) or Eq. (10.6) that, when A is real,

$$A(\epsilon) = \pi^{-1} | \text{Im } G(\epsilon) | \quad (10.9)$$

(the coordinates \mathbf{x} , \mathbf{x}' or labels k , k' have been suppressed).

As the simplest illustration let us consider the case of independent fermions with quantum labels k . The Green function matrix, Eq. (10.6)

will then be diagonal. The time-dependent Green function becomes

$$\begin{aligned} G_k(t) &= -i(1 - n_k) \exp(-i\epsilon_k t), & t > 0 \\ &= i n_k \exp(-i\epsilon_k t), & t < 0, \end{aligned} \quad (10.10)$$

where $n_k = \langle a_k^\dagger a_k \rangle$ is the occupation number of the one-particle state k in the ground state of the system. Equation (10.10) shows that $G_k(t)$ describes particles outside the Fermi sea for positive times and holes in the Fermi sea for negative times. In energy space we obtain

$$G_k(\epsilon) = [\epsilon - \epsilon_k + i \operatorname{sgn}(\epsilon_k - \mu) \delta]^{-1}. \quad (10.11)$$

Equation (10.11) shows that the excitations corresponding to injected electrons or holes appear as poles in the Green function. The excitations are sharp and the spectral weight function according to Eq. (10.9) is simply $A_k(\epsilon) = \delta(\epsilon - \epsilon_k)$.

As another simple illustration we consider the case of a *decaying particle*, having a width Γ , and obtain

$$\begin{aligned} G_k(\epsilon) &= -i \exp(-i\epsilon_k t) \exp(-\Gamma t), & t > 0 \\ &= 0, & t < 0. \end{aligned} \quad (10.12)$$

The Fourier transform is

$$G_k(\epsilon) = (\epsilon - \epsilon_k + i\Gamma)^{-1} \quad (10.13)$$

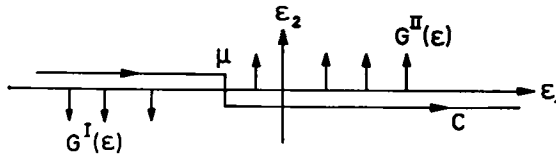
and from the imaginary part we obtain the expected Lorentzian form for the spectral function,

$$A_k(\epsilon) = \pi^{-1} \Gamma / [(\epsilon - \epsilon_k)^2 + \Gamma^2]. \quad (10.14)$$

This description of decaying states is indeed an oversimplification and we shall discuss the properties of wave-packet states and decay of quasi particles at length in Part VI.

11. THE STRUCTURE OF THE SPECTRAL FUNCTION. ELEMENTARY EXCITATIONS AND QUASI PARTICLES

The spectrum of interacting fermions is by far more complicated than the simple examples just mentioned indicate. Because of the many-body interactions, the spectral function will in its energy dependence extend over a wide energy range and will show more or less pronounced structure. In cases in which an appreciable fraction of the total spectral strength goes into a strong and narrow peak, we usually talk about a *quasi-particle* state or an *elementary excitation*. In order to discuss such features we should make some remarks about the analytical properties of the Green function, regarding the energy ϵ as a complex variable. For simplicity we assume the Green function to be diagonal in the label k . From the spectral representa-

FIG. 3. Analytical continuations of G that have no poles and no zeros.

tion of $G(\epsilon)$ according to Eq. (10.6), we can obtain analytical continuations in some regions of the complex ϵ plane by simply replacing the real ϵ by a complex value as indicated in Fig. 3.

These analytical continuations have no poles and no zeros off the real axis,³³ as is evident from writing out the explicit formulas, e.g.

$$G^I(\epsilon) = \int_{-\infty}^{\infty} \frac{A(\epsilon') d\epsilon'}{\epsilon_1 - i\epsilon_2 - \epsilon'} = \int_{-\infty}^{\infty} \frac{\epsilon_1 - \epsilon' + i\epsilon_2}{(\epsilon_1 - \epsilon')^2 + \epsilon_2^2} A(\epsilon') d\epsilon', \quad \epsilon_2 > 0. \quad (11.1)$$

If, however, we make analytic continuations across the contour as in Fig. 4, the resulting functions can and will in general have poles. In the vicinity of a pole at $\epsilon = \epsilon^*$, we have

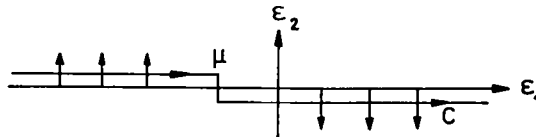
$$G(\epsilon) = [Z/(\epsilon - \epsilon^*)] + \varphi(\epsilon), \quad (11.2)$$

where $\varphi(\epsilon)$ is a smooth function. If the pole is close enough to the real axis, this gives for the spectral function $A(\epsilon)$, writing

$$\epsilon^* = \tilde{\epsilon} + i\Gamma \quad \text{and} \quad Z = Z_1 + iZ_2,$$

$$A(\epsilon) = \pi^{-1} |\operatorname{Im} G(\epsilon)| = \pi^{-1} \left| \frac{Z_1 \Gamma + Z_2(\epsilon - \tilde{\epsilon})}{(\epsilon - \tilde{\epsilon})^2 + \Gamma^2} + \operatorname{Im} \varphi(\epsilon) \right|. \quad (11.3)$$

Equation (11.3) shows that the shape of the peak in $A(\epsilon)$ associated with the pole in the complex plane may have the symmetric Lorentzian form as a limiting case if $Z_2 = 0$ but in general we obtain the asymmetric Breit-Wigner form. Since $A(\epsilon)$ is positive definite and obeys the sum rule, the

FIG. 4. Analytical continuations of G that generally have poles.

* In the general case when $G_{kk}' \neq 0$ and complex this statement may be true only for the diagonal element G_{kk} .

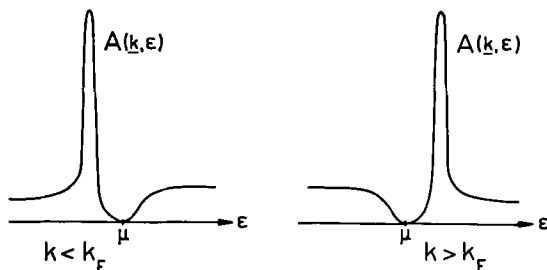


FIG. 5. Qualitative behavior of the spectral function close to the Fermi surface.

strength Z_1 of the pole must be smaller than 1. For values of k such that $\Gamma_k \ll \epsilon_k$ and for ϵ close to ϵ_k , the contribution from the pole in $G(\epsilon)$ will dominate the structure of the spectrum and we have the same formula as for a particle in a state with a linewidth Γ_k and of Breit-Wigner shape, and we then talk about a *quasi-particle state* or an *elementary excitation*.

In metals the condition $\Gamma_k \ll \epsilon_k$ is best fulfilled for particles and holes close to the Fermi surface. Consider an electron with momentum \mathbf{k} and energy $\epsilon(\mathbf{k})$ outside the Fermi sea. The state decays because the electron can make Auger transitions to other states having the same total energy and momentum. The lowest order process is one in which the quasi particle decays into a new state closer to the Fermi sea with excitation of another electron out of the Fermi sea, i.e. creation of an electron-hole pair. This process can be calculated using the Golden rule. The important thing is that the decay rate is proportional to the density of final states, which decreases rapidly as the particle approaches the Fermi surface. This is found by looking at the phase space available for the transition and an elementary calculation gives that $\Gamma_k \sim (\epsilon - \mu)^2$. Thus quasi particles close to the Fermi surface (if it exists) are stable excitations. For \mathbf{k} close to the Fermi surface the spectral function has the form indicated in Fig. 5. As a consequence the distribution function

$$n_{\mathbf{k}} \equiv \langle N | a_{\mathbf{k}}^+ a_{\mathbf{k}} | N \rangle = \int_{-\infty}^{\mu} A(k, \epsilon) d\epsilon \quad (11.4)$$

must have a discontinuity at the Fermi surface, because the quasi-particle peak comes outside the region of integration for $k > k_F$. The magnitude of the discontinuity equals the strength Z of the quasi-particle pole [Eq. (11.2)] at $k = k_F$. Thus, the distribution function has the form indicated in Fig. 6.

As just indicated, the spectral function contains the full information about the average occupation of single-particle states. It also contains the

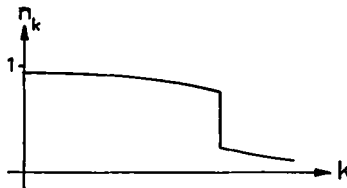


FIG. 6. Momentum distribution function n_k in an interacting system.

information about the energy distribution of one-particle states and we define the one-particle *density of states* as

$$N(\omega) = \text{tr } A(\omega) = \sum_s ||f_s||^2 \delta(\omega - \epsilon_s). \quad (11.5)$$

Here $||f_s||^2$ is a measure of the “oscillator strength” for the process of removing or adding a particle.

12. THE TWO-PARTICLE GREEN FUNCTION. FORMULAS FOR THE TOTAL ENERGY

For the forthcoming discussions we need to introduce the two-particle Green function, defined by

$$G(1, 2, 1', 2') = (-i)^2 \langle N | T\{\psi(1)\psi(2)\psi^+(2')\psi^+(1') | N \rangle \quad (12.1)$$

where 1 stands for $(\mathbf{r}_1, \xi_1, t_1)$, etc.

Expectation values of one-particle and two-particle operators can be calculated in a straightforward way from the corresponding Green function by taking the appropriate limit for equal times. In particular, the ground state energy can be calculated from the formula

$$\begin{aligned} E = & -i \int d\mathbf{x} \{h(\mathbf{x})G(\mathbf{x}t, \mathbf{x}_1t^+) \}_{\mathbf{x}_1 \rightarrow \mathbf{x}} \\ & - \frac{i}{2} \int d\mathbf{x} d\mathbf{x}' v(\mathbf{r}, \mathbf{r}') G(\mathbf{x}t, \mathbf{x}_1t, \mathbf{x}t^+, \mathbf{x}_1t^+) \\ & + \frac{i}{2} \sum_{nm} Z_n Z_m v(\mathbf{R}_n, \mathbf{R}_m), \end{aligned} \quad (12.2)$$

using the notation of Eqs. (2.1)–(2.4). With t^+ we mean $t^+ = t + \delta$ where δ is a positive infinitesimal. Several alternative formulas for the ground state energy can be written down. In particular, one can calculate the total energy in terms of the one-particle Green function alone, if use is made of the equation of motion (8.2) for the field operator $\psi(\mathbf{x}, t)$:

$$i \frac{\partial \psi(\mathbf{x}, t)}{\partial t} = h(\mathbf{x})\psi(\mathbf{x}, t) + \int d\mathbf{x}' v(\mathbf{r}, \mathbf{r}') \psi^+(\mathbf{x}', t) \psi(\mathbf{x}', t) \psi(\mathbf{x}, t). \quad (12.3)$$

If we multiply this equation by $\frac{1}{2}\psi^+(\mathbf{x}, t)$, integrate over \mathbf{x} , and finally take the ground state expectation value, we obtain a relation between the Coulomb energy and the one-particle Green function as follows:

$$\begin{aligned} \frac{1}{2} \int d\mathbf{x} d\mathbf{x}' v(\mathbf{r}, \mathbf{r}') \langle N | \psi^+(\mathbf{x}t) \psi^+(\mathbf{x}'t') \psi(\mathbf{x}'t) \psi(\mathbf{x}t) | N \rangle \\ = \frac{1}{2} \int d\mathbf{x} \langle N | \psi^+(\mathbf{x}t) [i(\partial/\partial t) - h(\mathbf{x})] \psi(\mathbf{x}t) | N \rangle \\ = -\frac{i}{2} \int d\mathbf{x} [i(\partial/\partial t) - h(\mathbf{x})] G(\mathbf{x}t, \mathbf{x}'t'); \quad \mathbf{x}' \rightarrow \mathbf{x}, \quad t' \rightarrow t^+. \end{aligned} \quad (12.4)$$

This gives for the total energy in Eq. (12.2)

$$E = -\frac{i}{2} \int d\mathbf{x} [i(\partial/\partial t) + h(\mathbf{x})] G(\mathbf{x}t, \mathbf{x}'t')_{\mathbf{x}' \rightarrow \mathbf{x}, t' \rightarrow t^+} + V_{\text{nuc}}. \quad (12.5)$$

Introducing the spectral representation according to Eq. (10.2), we obtain

$$E = \frac{1}{2} \int_{-\infty}^{\mu} d\epsilon d\mathbf{x} [\epsilon + h(\mathbf{x})] A(\mathbf{x}, \mathbf{x}'; \epsilon)_{\mathbf{x}' \rightarrow \mathbf{x}} + V_{\text{nuc}}, \quad (12.6)$$

or, in matrix form,

$$E = \frac{1}{2} \sum_{kk'} \int_{-\infty}^{\mu} d\epsilon [\epsilon \delta_{kk'} + h_{kk'}] A_{k'k}(\epsilon) + V_{\text{nuc}}. \quad (12.7)$$

These formulas are immediate generalizations of results first derived by Galitskii and Migdal.³⁴ The $h_{kk'}$ term in Eq. (12.7) has a simple meaning in configuration space, being just the expectation value of the one-electron part of the total Hamiltonian, thus

$$\int_{-\infty}^{\mu} \sum_{kk'} h_{kk'} A_{k'k}(\omega) d\omega = \langle N | \sum_{i=1}^N h(\mathbf{x}_i) | N \rangle. \quad (12.8)$$

In a HF approximation we have that $A_{kk'} = \delta_{kk'} \delta(\epsilon - \epsilon_k)$, giving the well-known HF formula for the total energy [Eq. (3.3)]:

$$E = \frac{1}{2} \sum_k^{\text{occ}} (\epsilon_k + h_{kk}) + V_{\text{nuc}}. \quad (12.9)$$

In problems in which the two-particle Green function is needed, one hardly finds use for the full four space-time point function, but only certain degenerate forms of it. Of particular importance is the (time-ordered)

³⁴ V. M. Galitskii and A. B. Migdal, *Soviet Phys. JETP (English Transl.)* **7**, 96 (1958).

dielectric function, defined by

$$\epsilon^{-1}(1, 2) = \delta(1, 2) - (i/\hbar) \int d(3) \langle N | T[\rho'(3)\rho'(2)] | N \rangle v(1, 3), \quad (12.10)$$

where $\rho'(1) = \rho(1) - \langle \rho(1) \rangle$ is the density fluctuation operator for the system ($\rho(1) = \psi^+(1)\psi(1)$ is the density operator). When calculating the response of the system to an external charge, one encounters the *retarded dielectric* function, which is related to the retarded commutator according to the formula

$$\epsilon_r^{-1}(1, 2) = \delta(1, 2) - (i/\hbar) \Theta(t_1 - t_2) \int d(3) \langle N | [\rho(3), \rho(2)] | N \rangle v(1, 3). \quad (12.11)$$

The time-dependent Hartree approximation for ϵ_r^{-1} was discussed in Section 5.

The two dielectric functions are closely related and differ only as a consequence of their different causality properties. Their Fourier transforms are equal for positive energies. ϵ^{-1} is an even function of the energy, whereas for ϵ_r^{-1} the real part is even and the imaginary part is odd. The properties of the dielectric functions will be discussed in detail in later sections.

IV. Equation of Motion for the Electron Green Function

In this part we list a number of definitions and results that will be needed in subsequent sections. The significance of these results are discussed but not their derivations. Derivations of the key formulas are given in Appendix B.³⁵

³⁵ For a more complete discussion we refer to e.g. the following textbooks (in order of increasing complexity). T. D. Schultz, "Quantum Field Theory and the Many Body Problem," Gordon & Breach, New York, 1964. J. M. Ziman, "Elements of Advanced Quantum Theory," Cambridge Univ. Press, London, 1969. N. H. March, W. H. Young, and S. Sampanthar, "The Many Body Problem in Quantum Mechanics," Cambridge Univ. Press, London and New York, 1967. D. A. Kirzhnits, "Field Theoretical Methods in Many-Body Systems," Pergamon Press, Oxford, 1967. J. R. Schrieffer, "Theory of Superconductivity," Benjamin, New York, 1964. P. Nozières, "Theory of Interacting Fermi Systems," Benjamin, New York, 1964. A. A. Abrikosov, L. P. Gorkov, and I. E. Dzyaloshinski "Methods of Quantum Field Theory in Statistical Physics," Prentice-Hall, Englewood Cliffs, New Jersey, 1963. The line of approach used here is a simplified zero temperature version of the Martin and Schwinger method, see P. C. Martin and J. Schwinger, *Phys. Rev.* **115**, 1342 (1959); and L. P. Kadanoff and G. Baym, "Quantum Statistical Mechanics," Benjamin, New York, 1962.

13. ELECTRONS IN A RIGID LATTICE

The full complications of the many-body problem with electrons interacting with phonons as well as with each other will be considered in next section, and we will first treat the case of interacting electrons moving in the field of fixed nuclei. We also consider a small external potential $\phi(\mathbf{x}, t)$ which is put equal to zero at the end. Thus we consider the Hamiltonian [cf. Eqs. (2.1)–(2.4)],

$$\begin{aligned} H &= H_0 + H_1 \\ H_0 &= \int \psi^+(\mathbf{x}) h(\mathbf{x}) \psi(\mathbf{x}) d\mathbf{x} \\ &\quad + \frac{1}{2} \int \psi^+(\mathbf{x}) \psi^+(\mathbf{x}') v(\mathbf{r}, \mathbf{r}') \psi(\mathbf{x}') \psi(\mathbf{x}) d\mathbf{x} d\mathbf{x}' \\ H_1 &= \int \psi^+(\mathbf{x}) \psi(\mathbf{x}) \phi(\mathbf{x}, t) d\mathbf{x}. \end{aligned} \tag{13.1}$$

The annihilation operator $\psi(\mathbf{x}, t)$ satisfies the equation of motion [cf. Eq. (8.2)],

$$\begin{aligned} i \frac{\partial \psi(\mathbf{x}, t)}{\partial t} &= [h(\mathbf{x}) + \phi(\mathbf{x}, t)] \psi(\mathbf{x}, t) \\ &\quad + \int v(\mathbf{r}, \mathbf{r}') \psi^+(\mathbf{x}', t) \psi(\mathbf{x}', t) \psi(\mathbf{x}, t) d\mathbf{x}'. \end{aligned} \tag{13.2}$$

Using the relation $d\Theta(t)/dt = \delta(t)$ and the commutation rules at equal times for $\psi(\mathbf{x}, t)$ and $\psi^+(\mathbf{x}, t)$, we obtain for the one-electron Green function

$$\begin{aligned} &[i(\partial/\partial t) - h(\mathbf{x}) - \phi(\mathbf{x}, t)] G(\mathbf{x}t, \mathbf{x}'t') \\ &\quad + i \int v(\mathbf{r}, \mathbf{r}'') d\mathbf{x}'' \langle N | T\{\psi^+(\mathbf{x}'', t) \psi(\mathbf{x}'', t) \psi(\mathbf{x}, t) \psi^+(\mathbf{x}', t')\} | N \rangle \\ &= \delta(\mathbf{x}, \mathbf{x}') \delta(t, t'). \end{aligned} \tag{13.3}$$

The term with four field operators contains a two-particle Green function (see Section 12) and describes the two-body correlations in the system. Equation (13.3) can be taken as the starting point for generating an infinite chain of equations introducing successively more complicated correlations. Such a chain can be terminated using a suitable assumption about *decoupling*. Instead of proceeding in such a way, however, we shall introduce a set of nonlinear equations following the standard procedure in field theory.

In order to account for the interaction between a particle and the rest of the system, one has to generalize the notion of a local potential and introduce a nonlocal time- (or energy-) dependent quantity, called the

self-energy operator Σ , which is defined in comparison with Eq. (13.3) by
 $[i(\partial/\partial t) - h(\mathbf{x}) - V(\mathbf{x}, t)]G(\mathbf{xt}, \mathbf{x}'t')$

$$- \int \Sigma(\mathbf{xt}, \mathbf{x}''t'')G(\mathbf{x}''t'', \mathbf{x}'t') d\mathbf{x}'' dt'' = \delta(\mathbf{x}, \mathbf{x}') \delta(t, t'). \quad (13.4)$$

The quantity $V(\mathbf{x}, t)$ is the *total average potential* in the system:

$$V(\mathbf{x}, t) = \phi(\mathbf{x}, t) + \int v(\mathbf{r}, \mathbf{r}') \langle N | \psi^+(\mathbf{x}'t) \psi(\mathbf{x}', t) | N \rangle d\mathbf{x}'. \quad (13.5)$$

From this implicit definition of \sum the more explicit form given in Eq. (13.19) can be derived. We will, however, not present the derivation here; this is done in Appendix B.

We will mostly work with the Fourier transforms, e.g.

$$G(\mathbf{x}, \mathbf{x}'; \omega) = \int G(\mathbf{xt}, \mathbf{x}'t') \exp[i\omega(t - t')] d(t - t'). \quad (13.6)$$

Equation (13.6) is not valid unless G is a function only of the difference between the time arguments, i.e. when the external perturbing potential $\phi(\mathbf{x}, t)$ is zero (or time independent). The Fourier transform of Eq. (13.4) then is

$$[\omega - h(\mathbf{x}) - V(\mathbf{x})]G(\mathbf{x}, \mathbf{x}'; \omega) - \int \Sigma(\mathbf{x}, \mathbf{x}''; \omega)G(\mathbf{x}'', \mathbf{x}'; \omega) = \delta(\mathbf{x}, \mathbf{x}'). \quad (13.7)$$

The complicated many-body character of G is due to the energy dependence in the self-energy Σ . If Σ did not depend on ω , we could solve for a complete and orthonormal set of eigenfunctions u_k ,

$$[h(\mathbf{x}) + V(\mathbf{x})]u_k(\mathbf{x}) + \int \Sigma(\mathbf{x}, \mathbf{x}')u_k(\mathbf{x}') d\mathbf{x}' = \epsilon_k u_k(\mathbf{x}), \quad (13.8)$$

and express G in the standard form³⁶

$$G(\mathbf{x}, \mathbf{x}'; \omega) = \sum_k [u_k(\mathbf{x})u_k^*(\mathbf{x}')/(\omega - \epsilon_k)]. \quad (13.9)$$

The solutions of the homogeneous equation

$$[E_k - h(\mathbf{x}) - V(\mathbf{x})]\varphi_k(\mathbf{x}) - \int \Sigma(\mathbf{x}, \mathbf{x}'; E_k)\varphi_k(\mathbf{x}') d\mathbf{x}' = 0 \quad (13.10)$$

³⁶ The exact G can also be written on this form [see Eq. (9.4)], but the amplitudes f , and energies ϵ , in that equation are of a much more complicated nature than the quantities generated by Eq. (13.8).

have the meaning of quasi-particle states. The energy E_k is in general complex and gives the decay time for the quasi particle. A more precise discussion of quasi particles is given in Part VI.

Two simple approximations in which Σ is independent of energy are provided by the Hartree and HF treatments:

$$\Sigma^H = 0; \quad \Sigma^{HF}(\mathbf{x}t, \mathbf{x}'t') = iv(\mathbf{x}, \mathbf{x}')G(\mathbf{x}t, \mathbf{x}'t')\delta(t - t' + \delta).$$

The Fourier transform of $\Sigma^{HF}(t - t')$ is

$$\Sigma^{HF}(\mathbf{x}, \mathbf{x}'; \omega) = -v(\mathbf{x}, \mathbf{x}')\langle N | \psi^+(\mathbf{x}')\psi(\mathbf{x}) | N \rangle = V_{ex}(\mathbf{x}, \mathbf{x}'). \quad (13.11)$$

The HF theory involves a self-consistency requirement with regard to the density matrix of the system. When effects of the dynamical interaction are included, the self-consistency requirement has to be augmented to include the full Green function rather than the particular equal time limit that gives the density matrix. Therefore, in theories beyond the HF approximation, the self-energy should be regarded as a functional of G , i.e. $\Sigma = \Sigma(G)$. The functionals may be expressed formally as a series expansion in a dynamically screened interaction W :

$$W(12) = \int v(13)\epsilon^{-1}(32) d(3). \quad (13.12)$$

Here we have used an abbreviated notation

$$(1) = (\mathbf{x}_1, t_1), \quad v(12) = v(\mathbf{r}_1, \mathbf{r}_2) \delta(t_1 - t_2). \quad (13.13)$$

The inverse dielectric function ϵ^{-1} has been discussed in Sections 5 and 12. It measures the screening in the system and is obtained as in classical theory by considering the change δV in the average potential in Eq. (13.5) due to a small variation $\delta\phi$ in the external potential

$$\epsilon^{-1}(1, 2) = \frac{\delta V(1)}{\delta\phi(2)} = \delta(12) + \int v(13) \frac{\delta\langle\rho(3)\rangle}{\delta\phi(2)} d(3). \quad (13.14)$$

Functional derivatives such as $\delta V/\delta\phi$ are very useful tools in deriving Green function relations.

The key quantity needed to calculate the dielectric function is the irreducible polarization propagator P , which is related to ϵ by

$$\epsilon(12) = \delta(12) - \int P(32)v(13) d(3) \quad (13.15)$$

and thus to W by

$$W(12) = v(12) + \int W(13)P(34)v(42) d(34). \quad (13.16)$$

The self-energy Σ and the polarization propagator P can be expressed as functional derivatives:

$$\begin{aligned}\Sigma(12) &= -i \int v(1+3)G(14) \frac{\delta G^{-1}(42)}{\delta \phi(3)} d(34) \\ P(12) &= i \int G(23)G(42) \frac{\delta G^{-1}(34)}{\delta V(1)} d(34).\end{aligned}\quad (13.17)$$

Finally we define the *vertex function* Γ by

$$\Gamma(12; 3) = -\frac{\delta G^{-1}(12)}{\delta V(3)} = \delta(12) \delta(13) + \frac{\delta \Sigma(12)}{\delta V(3)}. \quad (13.18)$$

We have now introduced all the quantities appearing in the set of equations defining Σ :

$$\Sigma(12) = i \int W(1+3)G(14)\Gamma(42; 3) d(34) \quad (13.19a)$$

$$W(12) = v(12) + \int W(13)P(34)v(42) d(34) \quad (13.19b)$$

$$P(12) = -i \int G(23)G(42)\Gamma(34; 1) d(34) \quad (13.19c)$$

$$\Gamma(12; 3) = \delta(12) \delta(13) + \int \frac{\delta \Sigma(12)}{\delta G(45)} G(46)G(75)\Gamma(67; 3) d(4567). \quad (13.19d)$$

Equation (13.19) can be used to generate expressions for Σ as functionals of G by an iteration process. We start with $\Sigma = 0$ in (13.19d), which gives the simple expression for Γ :

$$\Gamma(12; 3) = \delta(12) \delta(13). \quad (13.20)$$

The functional expression for Σ is then given by (13.19a–c) as

$$\begin{aligned}\Sigma(12) &= iW(1+2)G(12) \\ W(12) &= v(12) + \int W(13)P(34)v(42) d(34) \\ P(12) &= -iG(12)G(21).\end{aligned}\quad (13.21)$$

From Eq. (13.21) we can calculate $\delta \Sigma / \delta G$ to use in (13.19d). We then have an improved vertex function Γ and through (13.19a–c) an improved expression for Σ as a functional of G . The expressions we obtain in this way, however, become very complicated since the integral equation for Γ in general has no explicit solution. To obtain explicit results we can resort to

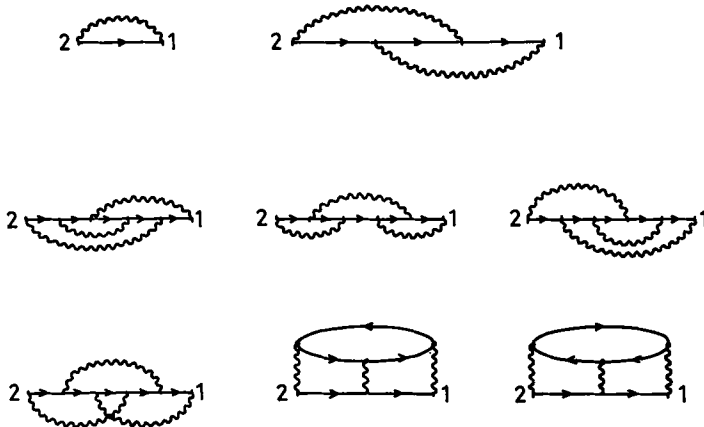


FIG. 7. Diagrams representing the expansion of the self-energy $\Sigma(12)$ in a rigid lattice. The Green function $G(12)$ is represented by an arrow from 2 to 1, and the screened potential $W(12)$ by a wiggly line between 1 and 2.

an expansion after powers of the screened interaction W . For the first few terms of Σ and P we have the result shown in Figs. 7 and 8.

We could go one step further expanding W and Γ as power series in v , $W = v + vPv + \dots$, $\Gamma = 1 + GGv + \dots$, thus obtaining also Σ as a power series in the bare potential v . This is advantageous when the polarizability P is small, as for an ion core. For valence electrons in metals and semiconductors, however, the polarizability is not small and the dielectric function is very different from unity. It then seems a much more reasonable procedure to expand in the screened potential W rather than the bare potential v .

Just as the first term of the expression for Σ in v , which gives the HF approximation, provides a reasonable description of a system with small polarizability, so does the first term of the expansion in W for a system with large polarizability. We will thus mainly discuss the properties of the approximation in Eq. (13.21). This approximation can also be considered as obtained by neglecting "vertex corrections," e.g. by using the simple expression in Eq. (13.20) for Γ . We thus neglect the influence on the self-energy of any variations in the average potential, cf. Eq. (13.18).

14. PHYSICAL INTERPRETATION OF THE ELECTRON SELF-ENERGY

We Fourier transform Σ in Eq. (13.21) from time to energy variables

$$\Sigma(\mathbf{x}, \mathbf{x}'; \omega) = (i/2\pi) \int W(\mathbf{x}, \mathbf{x}'; \omega') G(\mathbf{x}, \mathbf{x}'; \omega + \omega') e^{i\omega' d\omega'} d\omega'. \quad (14.1)$$

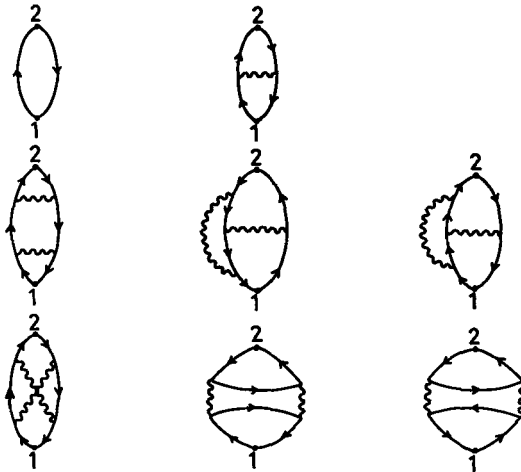


FIG. 8. Diagrams representing the expansion of the electron polarization propagator $P(12)$.

If we neglect the energy dependence in W , the ω integration can be performed by closing the contour in a semicircle in the upper half plane. We obtain contributions from all the poles in G corresponding to occupied states and find

$$\Sigma(\mathbf{x}, \mathbf{x}'; \omega) = \Sigma(\mathbf{x}, \mathbf{x}') = -W(\mathbf{x}, \mathbf{x}') \langle N | \psi^+(\mathbf{x}') \psi(\mathbf{x}) | N \rangle. \quad (14.2)$$

This is of exactly the same form as the HF exchange potential except that we have a screened interaction $W = v\epsilon^{-1}$ instead of a bare Coulomb interaction v . The screening of the Coulomb interaction has a large influence on the dispersion relations of quasi particles, particularly in metals. We illustrate this with the case of an electron gas. As will be shown in Part VI, the energy of the quasi particle is given by Dyson's equation

$$E_{\mathbf{k}} = \epsilon_{\mathbf{k}} + \Sigma(\mathbf{k}, E_{\mathbf{k}}), \quad (14.3)$$

where $\epsilon_{\mathbf{k}}$ is the energy of a free particle

$$\epsilon_{\mathbf{k}} = \hbar^2 k^2 / 2m.$$

From Eq. (14.2) we have for Σ in the momentum representation

$$\begin{aligned} \Sigma(\mathbf{k}; \omega) &= \Sigma(\mathbf{k}) = \int \exp(i\mathbf{k} \cdot (\mathbf{r} - \mathbf{r}')) \Sigma(\mathbf{x}, \mathbf{x}') d\mathbf{r} \\ &= -(2\pi)^{-3} \int W(\mathbf{k} - \mathbf{q}) n_{\mathbf{q}} d\mathbf{q}. \end{aligned} \quad (14.4)$$

The appearance of a screened interaction $W(\mathbf{q})$ of the form $4\pi e^2(q^2 + \lambda^2)^{-1}$ at small q , rather than the bare Coulomb interaction $v(q) = 4\pi e^2/q^2$ as in the HF theory, causes a dramatic change in the momentum dependence of $\Sigma(\mathbf{k})$. With a bare interaction a large part of the contributions from the \mathbf{q} integration in Eq. (14.4) comes from regions around \mathbf{k} . When \mathbf{k} passes out through the Fermi surface, this integration region is no longer allowed due to the occupation number $n_{\mathbf{q}}$. Thus the singular momentum transform $v(q)$ associated with the long-range Coulomb interaction gives rise to a singular variation of the quasi-particle energy at the Fermi surface which totally disappears when we have a screened interaction. The fact that HF exchange gives a completely unrealistic contribution to the excitation spectrum while the sum of exchange and correlation terms give only a small deviation from the Sommerfeld result, has been, of course, well known since the 1930's,² but it was not until the work by Bohm and Pines²² that a more quantitative theory developed.

The approximation we have discussed, in which the energy dependence of the screened interaction $W = ve^{-1}$ was neglected, is actually a gross oversimplification. If we do the energy integration in Eq. (14.1) properly, we will pick up contributions both from the poles in the Green function, which give rise to a *dynamic screened exchange*, and from the poles of the inverse dielectric function, which can be associated with a *Coulomb hole*. The latter is numerically the larger. Both contributions have a rather small effect on the dispersion of the quasi-particle energies.

We make a simple but rough argument which produces not just the screened exchange term but also a Coulomb hole term.²⁷ In the expression for Σ ,

$$\Sigma(\mathbf{x}, \mathbf{x}'; \tau) = iG(\mathbf{x}, \mathbf{x}'; \tau)W(\mathbf{x}, \mathbf{x}'; \tau + \delta), \quad (14.5)$$

of Eq. (13.21), we assume that W is a rather sharply peaked function of τ . From general principles we know that the peak is symmetric (see Appendix C). If the peak was a mathematical δ function, we would just obtain the screened exchange expression in Eq. (14.2). Instead we split W as $v + W_p$, and approximate Σ with

$$\begin{aligned} \Sigma(\mathbf{x}, \mathbf{x}'; \tau) &\cong [\langle N | \psi(\mathbf{x})\psi^+(\mathbf{x}') | N \rangle \Theta(\tau) - \langle N | \psi^+(\mathbf{x}')\psi(\mathbf{x}) | N \rangle \Theta(-\tau)] \\ &\times \left[v(\mathbf{x}, \mathbf{x}') \delta(\tau + \delta) + \int_{-\infty}^{\infty} W_p(\mathbf{x}, \mathbf{x}'; \tau') d\tau' \delta(\tau) \right]. \end{aligned} \quad (14.6)$$

We thus replace the part W_p in W which has no δ function contribution in time by its integrated value times a δ function that is placed symmetrically

²⁷ L. Hedin, *Phys. Rev.* **139**, A796 (1965).

with respect to the Θ functions, so that $\Theta(\tau) \delta(\tau) = \Theta(-\tau) \delta(\tau) = \frac{1}{2} \delta(\tau)$. Taking the Fourier transform of Eq. (14.6) we have

$$\begin{aligned}\Sigma(\mathbf{x}, \mathbf{x}'; \omega) &= -\langle N | \psi^+(\mathbf{x}') \psi(\mathbf{x}) | N \rangle v(\mathbf{x}, \mathbf{x}') + \frac{1}{2} [\langle N | \psi(\mathbf{x}) \psi^+(\mathbf{x}') | N \rangle \\ &\quad - \langle N | \psi^+(\mathbf{x}') \psi(\mathbf{x}) | N \rangle] W_p(\mathbf{x}, \mathbf{x}'; \omega = 0) \\ &= -\langle N | \psi^+(\mathbf{x}') \psi(\mathbf{x}) | N \rangle W(\mathbf{x}, \mathbf{x}'; \omega = 0) + \frac{1}{2} \delta(\mathbf{x}, \mathbf{x}') W_p(\mathbf{x}, \mathbf{x}'; \omega = 0).\end{aligned}\tag{14.7}$$

The Coulomb hole term $\frac{1}{2}W_p = \frac{1}{2}v(\epsilon^{-1} - 1)$ is the potential from the "Coulomb hole" in the charge density around a given electron. The factor $\frac{1}{2}$ can be associated with an adiabatic building up of the interactions.

The problem involved in obtaining the fully self-consistent solution of Eq. (13.7) for G with Σ defined by Eq. (13.21) is very difficult. To simplify the problem and obtain an expression which can be handled more easily, we replace G in Eq. (13.21) by the result from a calculation with a suitable energy independent Σ . For many purposes the simple choice $\Sigma = \text{constant}$ seems to be good enough. G then has the form given in Eq. (13.9) and the integrations to obtain P can be made analytically by closing the contour in the upper half plane (say):

$$\begin{aligned}P(\mathbf{x}, \mathbf{x}'; \omega) &= -\frac{i}{2\pi} \int G(\mathbf{x}, \mathbf{x}'; \omega') G(\mathbf{x}', \mathbf{x}; \omega' - \omega) d\omega' \\ &= -\frac{i}{2\pi} \sum_{kk'} \int \frac{u_k(\mathbf{x}) u_{k'}^*(\mathbf{x}')}{\omega' - \epsilon_k} \frac{u_{k'}(\mathbf{x}') u_{k'}^*(\mathbf{x})}{\omega' - \omega - \epsilon_{k'}} d\omega' \\ &= \sum_{kk'} \frac{n_k - n_{k'}}{\epsilon_k - \epsilon_{k'} - \omega} u_k(\mathbf{x}) u_{k'}^*(\mathbf{x}') u_{k'}^*(\mathbf{x}) u_{k'}(\mathbf{x}').\end{aligned}\tag{14.8}$$

This is the same result for P as obtained in Eq. (5.21) by the time-dependent Hartree method, except for the infinitesimal imaginary parts in the denominator. The differences are those of a time-ordered and a retarded dielectric function as mentioned in Section 12 (see also Appendix C).

To make a proper analysis of Σ and also pick up the contributions from the poles of the dielectric function, we write W as a spectral resolution:

$$W(\mathbf{x}, \mathbf{x}'; \omega) = v(\mathbf{x}, \mathbf{x}') + \int_0^\infty \frac{2\omega' B(\mathbf{x}, \mathbf{x}'; \omega')}{\omega^2 - \omega'^2} d\omega'.\tag{14.9}$$

Here ω' has a slightly negative imaginary part (see Appendix C). Per-

forming the energy integration in Eq. (14.1), we have

$$\begin{aligned}\Sigma(\mathbf{x}, \mathbf{x}'; \omega) &= \frac{i}{2\pi} \int W(\mathbf{x}, \mathbf{x}'; \omega') \sum_k \frac{u_k(\mathbf{x}) u_k^*(\mathbf{x}')}{\omega + \omega' - \epsilon_k} e^{i\omega'\delta} d\omega' \\ &= - \sum_k^{\text{occ}} W(\mathbf{x}, \mathbf{x}'; \epsilon_k - \omega) u_k(\mathbf{x}) u_k^*(\mathbf{x}') \\ &\quad + \sum_k u_k(\mathbf{x}) u_k^*(\mathbf{x}') \int_0^\infty \frac{B(\mathbf{x}, \mathbf{x}'; \omega')}{\epsilon_k - \omega - \omega'} d\omega'.\end{aligned}\quad (14.10)$$

If we put $(\epsilon_k - \omega) = 0$, we obtain Eq. (14.7). This is of course not a meaningful approximation in general, but for the purpose of calculating quasi-particle energies it works qualitatively and sometimes quantitatively. The contribution from Σ to the quasi-particle energy is

$$\begin{aligned}\Delta\epsilon_k &= \int u_k^*(\mathbf{x}) \Sigma(\mathbf{x}, \mathbf{x}'; \epsilon_k) u_k(\mathbf{x}') d\mathbf{x} d\mathbf{x}' \\ &= - \sum_{k'} \langle kk' | W(\epsilon_{k'} - \epsilon_k) | k'k \rangle + \sum_{k'} \int_0^\infty \frac{\langle kk' | B(\omega) | k'k \rangle}{\epsilon_{k'} - \epsilon_k - \omega} d\omega.\end{aligned}\quad (14.11)$$

The requirement for Eq. (14.7) to be valid is that for the most important terms in the sum over k' , the energy difference $\epsilon_{k'} - \epsilon_k$ should be small compared to the characteristic energies in the dielectric function. A clearcut example is provided by the case of a valence electron outside a closed shell ion. The characteristic energy is then the excitation energy of the ion [cf. Eq. (14.8)], which is large compared to the valence electron energy. In this case Eq. (14.7) is valid and $\Delta\epsilon_k$ reduces to the Born–Heisenberg polarization correction, (cf. Section 37).

If we consider the self-energy and damping of a fast electron we can simplify Eq. (14.11). Taking the case of an electron gas as an example and neglecting the exchange term, we have

$$\Delta\epsilon_k = \frac{1}{(2\pi)^3} \int_0^\infty \frac{B(\mathbf{q}, \omega)}{\epsilon_{\mathbf{k}+\mathbf{q}} - \epsilon_k - \omega} d\omega d\mathbf{q}. \quad (14.12)$$

For a fast electron, \mathbf{k} is large compared to \mathbf{q} values of interest and we can write

$$\epsilon_{\mathbf{k}+\mathbf{q}} - \epsilon_k = \mathbf{q} \cdot \mathbf{v}; \quad \mathbf{v} = \mathbf{k}/m. \quad (14.13)$$

Using $B(\mathbf{q}, \omega) = B(-\mathbf{q}, \omega)$, we can replace $(\mathbf{q} \cdot \mathbf{v} - \omega)^{-1}$ in Eq. (14.12) by $\omega/[(\mathbf{q} \cdot \mathbf{v})^2 - \omega^2]$, and from Eq. (14.9) we then have

$$\Delta\epsilon_k = \frac{1}{2} (2\pi)^{-3} \int W_p(\mathbf{q}, \mathbf{q} \cdot \mathbf{v}) d\mathbf{q}. \quad (14.14)$$

This is the standard expression obtained by considering the fast electron as equivalent to an external charge density

$$\rho^{\text{ext}}(\mathbf{r}, t) = \delta(\mathbf{r} - \mathbf{v}t), \quad (14.15)$$

and using linear response theory to calculate *the potential from the polarization cloud*²⁰:

$$\phi(\mathbf{r}, t) = \frac{1}{2} \int [v(\epsilon^{-1} - 1)](\mathbf{r} - \mathbf{r}', t - t') \rho^{\text{ext}}(\mathbf{r}', t') d\mathbf{r}' dt'. \quad (14.16)$$

The factor $\frac{1}{2}$ comes from adiabatically switching on the interactions. Straightforward evaluation of Eq. (14.16) shows that $\phi(vt, t)$ equals $\Delta\epsilon_k$ in Eq. (14.14). The damping of the electron is given by the imaginary part of $\Delta\epsilon_k$ as will be discussed in Part VI.

15. ELECTRONS IN A VIBRATING LATTICE

We shall in this section enter the discussion how the motion of the nuclei will affect the properties of the electrons. An early classic on the subject is Bardeen's paper^{21a} from 1937 on the conductivity of monovalent metals, in which he used the self-consistent Hartree approach. The electron-phonon problem was taken up for further consideration by Fröhlich²² in connection with his study of superconductivity, and the Fröhlich Hamiltonian is still in use. Fröhlich used a method of canonical transformations, and Nakajima²³ later extended the discussions to include electron-electron interactions. In a well-known paper by Bardeen and Pines²⁴ the Fröhlich-Nakajima results were rederived and extended by first using the Bohm-Pines collective coordinates and then making a series of canonical transformations.

These theories gave some very useful results but also ran into considerable difficulties, particularly in the description of inelastic electron-phonon processes. To appreciate these difficulties we shall sketch the basic ideas involved. The starting Hamiltonian is, in an obvious notation,

$$H = T_e + V_{ee} + V_{en} + V_{nn} + T_n. \quad (15.1)$$

A natural splitting of this Hamiltonian is

$$H = \underbrace{T_e + V_e + V_{en}^0 + V_{nn}^0}_{H_e} + \underbrace{T_n + V_{nn} - V_{nn}^0}_{H_n} + \underbrace{V_{en} - V_{en}^0}_{H_{en}^{(1)}} + \underbrace{V_{ee} - V_e}_{H_{ee}^{(1)}}, \quad (15.2)$$

^{21a} J. Bardeen, *Phys. Rev.* **52**, 688 (1937).

²² H. Fröhlich, *Proc. Roy. Soc. A* **215**, 291 (1952).

²³ S. Nakajima, *Buss. Kenkyu* **65**, 116 (1953).

²⁴ J. Bardeen and D. Pines, *Phys. Rev.* **99**, 1140 (1955).

with an unperturbed part $H_e + H_n$. The superscript zero indicates that equilibrium positions for the nuclei are considered. The electron part H_e defines realistic one-electron states provided the electron potential V_e is appropriately chosen. The phonon Hamiltonian H_n , on the other hand, is completely unrealistic and gives very strange dispersion curves for the phonons. The perturbation $H_{en}^{(1)} + H_{ee}^{(1)}$ is far too strong to be treated in low order and requires infinite summations if perturbation theory is used. With the canonical transformation method one tries to remove the interaction terms as accurately as possible. The transformed Hamiltonian will contain effective electrons dressed with phonons and effective phonons dressed with electrons plus some residual interactions which are weaker than in the original Hamiltonian. This approach, however, becomes very complex and there are no physical principles guiding in the choice of transformations. At one stage of the Nakajima transformation it was so successful that there was no electron-phonon coupling left in low order and the theory thus predicted zero electrical resistance. In all cases it was found difficult to obtain useful results for the electron-phonon interaction term off the energy shell. Similar difficulties were encountered by Ziman⁴¹ starting from the adiabatic approximation.

In retrospect it is easy to see the reason for these early difficulties: The problem was not sufficiently well defined. In principle one was looking for good and well-dressed electrons and phonons with a reasonable interaction, however, without a good criterion for how to define them properly. With the use of Green function methods, at least problems of definition have disappeared. The Green functions are indeed well defined and they contain precisely the relevant physical information. The problem still looks a bit messy, but the structure of the equations is very simple, and reasonable approximations can easily be found.

In a well-known paper by Migdal,⁴² important new results for the electron-phonon problem were obtained by Green function methods. Migdal started from the Fröhlich Hamiltonian

$$H = \sum_p \epsilon_p^0 a_p^+ a_p + \sum_q \omega_q^0 b_q^+ b_q + \sum_{p,q} \alpha_q a_{p+q}^+ a_p (b_q + b_{-q}^+), \quad (15.3)$$

which has an electron, a phonon, and an electron-phonon interaction part. The electron-electron interactions are not included explicitly but are accounted for by using a screened electron-phonon matrix element (α_q) and by choosing phonon energies having the correct type of behavior at small q , i.e. $\omega_s = c_s q$. Migdal obtained a solution for the electron and phonon Green functions, exact to order $(m/M)^{1/2}$ (m is the electron mass and M the

⁴¹ J. Ziman, *Proc. Cambridge Phil. Soc.* **51**, 707 (1955).

⁴² A. B. Migdal, *Soviet Phys. JETP (English Transl.)* **7**, 996 (1958).

ion mass). The energy spectrum of the electrons was found to be altered only close to the Fermi surface while the total phonon dispersion curve was substantially changed.

The Migdal result is very important but it remains to justify the use of the Fröhlich model Hamiltonian, since it does not explicitly take the electron-electron interactions into account. The usual argument is that since the electrons are influenced by the phonons only at the Fermi surface where the electrons in a rigid lattice have an excellent quasi-particle behavior, we may think of the a_p operators as referring to quasi particles rather than bare electrons. While this argument seems intuitively correct, a more complete discussion is certainly warranted, and we also need to define properly the basic quantities ϵ_p^0 , ω_q^0 , and α_q .

We shall discuss the complete electron and phonon Green functions in a way closely analogous to that used in Section 14. In particular, we find it convenient to work in ordinary space rather than momentum space. We shall treat all electrons, including the core electrons, on an equal basis in order to simplify the structure of the exposition. The model problem with ions and conduction electrons can be treated along similar lines, but entails a more elaborate notation. For simplicity we consider a system having only one atomic species. We write the basic many-body Hamiltonian as

$$H = T_e + T_n + \frac{1}{2} \int \psi^+(\mathbf{x}) \psi^+(\mathbf{x}') v(\mathbf{r}, \mathbf{r}') \psi(\mathbf{x}') \psi(\mathbf{x}) d\mathbf{x} d\mathbf{x}' \\ + \int [\rho_e(\mathbf{r}) + \frac{1}{2}\rho_n(\mathbf{r})] v(\mathbf{r}, \mathbf{r}') \rho_n(\mathbf{r}') d\mathbf{r} d\mathbf{r}' + \int \rho(\mathbf{r}) \phi(\mathbf{r}, t) d\mathbf{r}, \quad (15.4)$$

where T_e and T_n are the kinetic energies of electrons and nuclei and

$$\rho_e(\mathbf{r}) = \int \psi^+(\mathbf{x}) \psi(\mathbf{x}) d\xi, \\ \rho_n(\mathbf{r}) = -Z \sum_{\mu} \delta(\mathbf{r} - \mathbf{R}_{\mu}), \\ \rho(\mathbf{r}) = \rho_e(\mathbf{r}) + \rho_n(\mathbf{r}). \quad (15.5)$$

The external potential $\phi(\mathbf{r}, t)$ is put equal to zero at the end. The annihilation operator $\psi(\mathbf{x}, t)$ satisfies the equation of motion

$$i(\partial/\partial t)\psi(\mathbf{x}, t) = [T(\mathbf{r}) + \phi(\mathbf{r}, t) + V_{op}(\mathbf{r}, t)]\psi(\mathbf{x}, t), \quad (15.6)$$

where

$$V_{op}(\mathbf{r}, t) = \int v(\mathbf{r}, \mathbf{r}') \rho(\mathbf{r}', t) d\mathbf{r}', \quad T(\mathbf{r}) = -(\hbar^2/2m) \nabla^2.$$

The equation of motion for the one-electron Green function is [cf. Eq. (13.3)]

$$[i(\partial/\partial t) - T(\mathbf{r}) - \phi(\mathbf{r}, t)]G(\mathbf{x}t, \mathbf{x}'t') + i\langle N | TV_{op}(\mathbf{r}, t)\psi(\mathbf{x}, t)\psi^+(\mathbf{x}', t') | N \rangle = \delta(\mathbf{x}t, \mathbf{x}'t'). \quad (15.7)$$

In analogy with Eqs. (13.4) and (13.5), we define a self-energy Σ by

$$[i(\partial/\partial \mathbf{r}) - T(\mathbf{r}) - V(\mathbf{r}, t)]G(\mathbf{x}t, \mathbf{x}'t') - \int \Sigma(\mathbf{x}t, \mathbf{x}''t'')G(\mathbf{x}''t'', \mathbf{x}'t') d\mathbf{x}'' dt'' = \delta(\mathbf{x}t, \mathbf{x}'t') \quad (15.8)$$

and a total average potential V by

$$V(\mathbf{r}, t) = \phi(\mathbf{r}, t) + \int v(\mathbf{r}, \mathbf{r}') \langle N | \rho(\mathbf{r}', t) | N \rangle d\mathbf{r}'. \quad (15.9)$$

Note that we have defined the functions $\phi(\mathbf{r}, t)$ and $V(\mathbf{r}, t)$ to be independent of spin as we could have done also in Section 14. We define a dielectric function and a screened potential by

$$\epsilon^{-1}(\mathbf{r}t, \mathbf{r}'t') = \frac{\delta V(\mathbf{r}, t)}{\delta \phi(\mathbf{r}', t')} = \delta(\mathbf{r}t, \mathbf{r}'t') + \int v(\mathbf{r}, \mathbf{r}'') \frac{\delta \langle \rho(\mathbf{r}'', t) \rangle}{\delta \phi(\mathbf{r}', t')} d\mathbf{r}''$$

$$W(\mathbf{r}t, \mathbf{r}'t') = \int v(\mathbf{r}'', \mathbf{r}') \epsilon^{-1}(\mathbf{r}t, \mathbf{r}'t') d\mathbf{r}''. \quad (15.10)$$

Since $\rho = \rho_e + \rho_n$, the screened potential will now have contributions both from the polarization of the electrons and from the displacements of the nuclei. We introduce a polarization part P_e associated with the electrons:

$$P_e(\mathbf{r}t, \mathbf{r}'t') = \delta \langle \rho_e(\mathbf{r}, t) \rangle / \delta V(\mathbf{r}', t'). \quad (15.11)$$

The corresponding screened potential is defined by

$$W_e(\mathbf{r}t, \mathbf{r}'t') = v(\mathbf{r}, \mathbf{r}') \delta(t, t')$$

$$+ \int W_e(\mathbf{r}t, \mathbf{r}_1t_1) P_e(\mathbf{r}_1t_1, \mathbf{r}_2t'') v(\mathbf{r}_2, \mathbf{r}') d\mathbf{r}_1 d\mathbf{r}_2 dt_1, \quad (15.12)$$

or in an abbreviated notation

$$W_e = v(1 - P_e)^{-1}. \quad (15.13)$$

We also introduce a density-density correlation function for the nuclei

$$D(\mathbf{r}t, \mathbf{r}'t') = -i\langle N | T[\rho_n'(\mathbf{r}, t)\rho_n'(\mathbf{r}', t')] | N \rangle, \quad (15.14)$$

where

$$\rho_n'(\mathbf{r}, t) = \rho_n(\mathbf{r}, t) - \langle N | \rho_n(\mathbf{r}, t) | N \rangle. \quad (15.15)$$

As shown in Appendix B, W can be written in the simple form

$$W(\mathbf{r}t, \mathbf{r}'t') = W_e(\mathbf{r}t, \mathbf{r}'t')$$

$$+ \int W_e(\mathbf{r}t, \mathbf{r}_1t_1) D(\mathbf{r}_1t_1, \mathbf{r}_2t_2) W_e(\mathbf{r}_2t_2, \mathbf{r}'t') d\mathbf{r}_1 d\mathbf{r}_2 dt_1 dt_2, \quad (15.16)$$

or in an abbreviated notation

$$W = W_e + W_e D W_e. \quad (15.17)$$

To simplify the notation we shall use as before the symbol (1) for $(\mathbf{r}_1, \xi_1, t_1)$, but to indicate when the spin variable is left out we write $(1) = (\mathbf{r}_1, t_1)$ and $d(1) = d\mathbf{r}_1 dt_1$. We next define a vertex function Γ in analogy with Eq. (13.18):

$$\Gamma(12; 3) = -\delta G^{-1}(12)/\delta V(3) = \delta(12) \delta(13) + \delta\Sigma(12)/\delta V(3). \quad (15.18)$$

As shown in Appendix B, Σ is given through the following relations:

$$\begin{aligned} \Sigma(12) &= i \int G(13) W(1^+4) \Gamma(32; 4) d(34) \\ W(12) &= W_e(12) + \int W_e(13) D(34) W_e(42) d(34) \\ W_e &= v(1 - P_e v)^{-1} \\ P_e(12) &= -i \int G(13) G(41) \Gamma(34; 2) d(34) d\xi_1 \\ \Gamma(12; 3) &= \delta(12) \delta(13) + \int \frac{\delta\Sigma(12)}{\delta G(45)} G(46) G(75) \Gamma(67; 3) d(4567). \end{aligned} \quad (15.19)$$

If we neglect the effect of the lattice vibrations and put $D = 0$, the relations reduce to those obtained for a rigid lattice, Eq. (13.19). Approximations to Σ can be generated in the same way as discussed in Section 13 remembering, however, that W is a functional of G not only through W_e but also through D . The functional dependence of D on G has to be determined from the equation of motion for D .

The lowest order approximation for Γ is obtained as in Section 13 by neglecting the influence on the self-energy Σ of variations in the average potential V . We then have

$$\Gamma(12; 3) = \delta(12) \delta(13), \quad (15.20)$$

and

$$\begin{aligned}\Sigma(12) &= iG(12)W(1^+, 2) \\ W &= W_e + W_e DW_e \\ W_e &= v(1 - P_e v)^{-1} \\ P_e(12) &= -i \int G(12)G(21) d\xi_1 d\xi_2.\end{aligned}\tag{15.21}$$

Higher approximations for Σ and P_e can be obtained as series expansions in W_e and $W_e DW_e$ (Figs. 9 and 10). The technical term for the approximation in Eq. (15.21) is that "vertex corrections are neglected." As shown by Migdal the vertex corrections due to phonons (diagrams containing two or more phonon propagators) are expected to be only of order $(m/M)^{1/2}$. Neglecting all vertex corrections, the self-energy Σ is a sum of an electron part and a phonon part

$$\Sigma^{el} = iGW_e, \quad \Sigma^{ph} = iGW_e DW_e.\tag{15.22}$$

The phonon frequencies which appear in the spectral resolution of D are small compared to the characteristic frequencies in W_e and we have to a good approximation

$$W_e(\omega)D(\omega)W_e(\omega) = W_e(0)D(\omega)W_e(0).\tag{15.23}$$

W_e thus plays no dynamical role in Σ^{ph} and may be absorbed in the definition of D .

In this section we have given a number of definitions and key general formulas, without immediate physical applications. We next turn to the special problem of the electron self-energy.

16. THE PHONON CONTRIBUTION TO THE ELECTRON SELF-ENERGY

In this section we will discuss the approximation for Σ^{ph} given in Eq. (15.22) and summarize some basic results. In a more explicit notation, cf. Eq. (15.22) and (14.1), we have

$$\Sigma^{ph}(\mathbf{x}, \mathbf{x}'; \omega) = (i/2\pi) \int G(\mathbf{x}, \mathbf{x}'; \omega + \omega') W_{ph}(\mathbf{r}, \mathbf{r}'; \omega') e^{i\omega' \delta} d\omega', \tag{16.1}$$

where

$$W_{ph}(\mathbf{r}, \mathbf{r}'; \omega) = \int W_e(\mathbf{r}, \mathbf{r}_1; 0) D(\mathbf{r}_1, \mathbf{r}_2; \omega) W_e(\mathbf{r}_2, \mathbf{r}'; 0) d\mathbf{r}_1 d\mathbf{r}_2. \tag{16.2}$$



FIG. 9. Diagrams representing the expansion of the self-energy $\Sigma(12)$ in a vibrating lattice. The wiggly line represents the screened potential W_e (e for electron) and the bubble line the screened potential W_eDW_e , where D is a phonon correlation function.

$W_e(\mathbf{r}, \mathbf{r}'; 0)$ gives the potential at \mathbf{r} from a point charge at \mathbf{r}' , screened by the response of all (including core) electrons. In the phonon part W_{ph} of the effective interaction W , we may look at the Green function $D(\mathbf{r}_1, \mathbf{r}_2)$ [see Eq. (15.14)] as the source of screened potentials at \mathbf{r} and \mathbf{r}' . The source charges in the present context are thus the strong nuclear charges Z , but it is actually not the response to the point charges themselves, but only to their displacements that enters. For most purposes the core electrons can be considered to follow their nuclei exactly adiabatically. We can then calculate W_eDW_e by considering only valence electron contributions to W_e and introduce in D the charge density of ions rather than the density of nuclei as in Eq. (15.5):

$$D(\mathbf{r}t, \mathbf{r}'t') = (-i) \sum_{\mu\nu} \langle T\{\rho^i[\mathbf{r} - \mathbf{R}_\mu(t)] - \rho^i(\mathbf{r} - \mathbf{R}_\mu^0)\} \\ \times \{\rho^i[\mathbf{r}' - \mathbf{R}_\nu(t')] - \rho^i(\mathbf{r}' - \mathbf{R}_\nu^0)\} \rangle. \quad (16.3)$$

We then have for $W_{ph} = W_eDW_e = \epsilon^{-1}vDv\epsilon^{-1}$

$$W_{ph}(\mathbf{r}, \mathbf{r}'; t - t') = \int \epsilon^{-1}(\mathbf{r}, \mathbf{r}_1) \epsilon^{-1}(\mathbf{r}', \mathbf{r}_2) d\mathbf{r}_1 d\mathbf{r}_2 (-i) \\ \times \sum_{\mu\nu} \langle T\{V^i[\mathbf{r}_1 - \mathbf{R}_\mu(t)] - V^i(\mathbf{r}_1 - \mathbf{R}_\mu^0)\} \\ \times \{V^i[\mathbf{r}_2 - \mathbf{R}_\nu(t')] - V^i(\mathbf{r}_2 - \mathbf{R}_\nu^0)\} \rangle, \quad (16.4)$$

where we have introduced the ionic potential

$$V^i(\mathbf{r} - \mathbf{R}_\mu) = \int v(\mathbf{r} - \mathbf{r}') \rho^i(\mathbf{r}' - \mathbf{R}_\mu) d\mathbf{r}'. \quad (16.5)$$

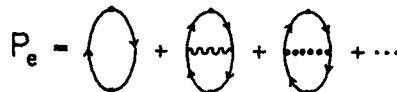


FIG. 10. Diagrams representing the expansion of the polarization propagator P_e .

Expanding in powers of the displacements

$$\mathbf{u}_\mu = \mathbf{R}_\mu - \mathbf{R}_\mu^0, \quad (16.6)$$

we have in the harmonic approximation

$$W_{ph}(\mathbf{r}\mathbf{r}'; t - t') = \int \epsilon^{-1}(\mathbf{r}, \mathbf{r}_1) \epsilon^{-1}(\mathbf{r}', \mathbf{r}_2) \sum_{\mu, \nu} \nabla V^i(\mathbf{r}_1 - \mathbf{R}_\mu^0) \\ \times D_{\mu\nu}(t - t') \nabla V^i(\mathbf{r}_2 - \mathbf{R}_\nu^0) d\mathbf{r}_1 d\mathbf{r}_2, \quad (16.7)$$

where $D_{\mu\nu}$ is the phonon Green function

$$D_{\mu\nu}(t - t') = (-i) \langle T[\mathbf{u}_\mu(t) \mathbf{u}_\nu(t')] \rangle. \quad (16.8)$$

Introducing normal coordinates we obtain⁴³

$$D_{\mu\nu}(\omega) = \sum_{q\lambda} \frac{D_{q\lambda}(\omega)}{2NM\omega_{q\lambda}} \mathbf{e}_{q\lambda} \mathbf{e}_{q\lambda}^* \exp[i\mathbf{q} \cdot (\mathbf{R}_\mu^0 - \mathbf{R}_\nu^0)], \quad (16.9)$$

where (at zero temperature)

$$D_{q\lambda}(\omega) = 2\omega_{q\lambda} [\omega^2 - (\omega_{q\lambda} - i\delta)^2]^{-1}. \quad (16.10)$$

The $\omega_{q\lambda}$ are phonon energies, $\mathbf{e}_{q\lambda}$ the polarization vectors, M the ionic mass, and N the number of unit cells. Collecting our formulas we obtain the relatively simple result

$$W_{ph}(\mathbf{r}, \mathbf{r}'; \omega) = \Omega^{-1} \sum_{q\lambda} D_{q\lambda}(\omega) g_{q\lambda}(\mathbf{r}) g_{q\lambda}^*(\mathbf{r}'), \quad (16.11)$$

where

$$g_{q\lambda}(\mathbf{r}) = (\Omega_0/2M\omega_{q\lambda})^{1/2} \sum_\mu \int \epsilon^{-1}(\mathbf{r}, \mathbf{r}_1) (\mathbf{e}_{q\lambda} \cdot \nabla) V^i(\mathbf{r}_1 - \mathbf{R}_\mu) \exp(i\mathbf{q} \cdot \mathbf{R}_\mu^0) d\mathbf{r}_1. \quad (16.12)$$

Here Ω is the total volume of the solid and Ω_0 the volume of the unit cell.

To evaluate the effect of Σ^{ph} on the quasi-particle energies we need the diagonal part

$$\Sigma^{ph}(k, \omega) = \int \varphi_k^*(\mathbf{x}) \Sigma^{ph}(\mathbf{x}, \mathbf{x}'; \omega) \varphi_k(\mathbf{x}') d\mathbf{x} d\mathbf{x}'. \quad (16.13)$$

To obtain some feeling for the phonon self-energy Σ^{ph} we evaluate the expressions replacing the Bloch functions φ_k by plane waves and the

⁴³ R. E. Peierls, "Quantum Theory of Solids," Oxford Univ. Press, London and New York, 1955.

inverse dielectric function by a translationally invariant approximation $\epsilon^{-1}(\mathbf{r} - \mathbf{r}'; 0)$. We then have

$$\begin{aligned}\Sigma^{\text{ph}}(\mathbf{k}, \omega) &= \frac{i}{(2\pi)^4} \int \sum_{q\lambda} D_{q\lambda}(\omega') \frac{|\Omega^{-1} \int \exp[i(\mathbf{k}' - \mathbf{k}) \cdot \mathbf{r}] g_{q\lambda}(\mathbf{r}) d\mathbf{r}|^2}{\omega + \omega' - \epsilon_{\mathbf{k}'}} d\mathbf{k}' d\omega' \\ &= \frac{i}{(2\pi)^4} \int \sum_{\lambda} \frac{D_{q\lambda}(\omega')}{2M\Omega_0\omega_{q\lambda}} \left| \frac{\mathbf{q} \cdot \mathbf{e}_{q\lambda} V^i(\mathbf{q})}{\epsilon(\mathbf{q}, 0)} \right|^2 \frac{1}{\omega + \omega' - \epsilon_{\mathbf{k}-\mathbf{q}}} d\omega' d\mathbf{q},\end{aligned}\quad (16.14)$$

where $V^i(\mathbf{q})$ is the Fourier transform of the ion potential. The \mathbf{q} vectors associated with the phonons are understood to be restricted to the first Brillouin zone. The effective potential due to the phonons,

$$\begin{aligned}W_{\text{ph}}(\mathbf{q}, \omega) &= \sum_{\lambda} \frac{D_{q\lambda}(\omega)}{2M\Omega_0\omega_{q\lambda}} \left| \frac{\mathbf{q} \cdot \mathbf{e}_{q\lambda} V^i(\mathbf{q})}{\epsilon(\mathbf{q}, 0)} \right|^2 \\ &= \frac{m}{M} \sum_{\lambda} \frac{|\mathbf{q} \cdot \mathbf{e}_{q\lambda}|^2}{m} \left| \frac{V^i(\mathbf{q})}{\Omega_0\epsilon(\mathbf{q}, 0)} \right| \frac{1}{\omega^2 - \omega_{q\lambda}^2} \frac{V^i(\mathbf{q})}{\epsilon(\mathbf{q}, 0)},\end{aligned}\quad (16.15)$$

may be compared with that due to the electrons, $W_e(\mathbf{q}, \omega) = v(\mathbf{q})/\epsilon(\mathbf{q}, \omega)$. W_{ph} is of the order of magnitude

$$(m/M)\epsilon_F\epsilon_F(\omega^2 - \omega_D^2)^{-1}v(q) = \omega_D^2(\omega^2 - \omega_D^2)^{-1}v(q),$$

where ω_D is the Debye frequency. The two potentials W_e and W_{ph} are thus of comparable magnitude for ω of the order of ω_D ; for larger frequencies $W_{\text{ph}} \ll W_e$. The magnitude of Σ^{ph} is hence of the order ω_D/ϵ_F as compared to Σ^{el} , and the phonons can therefore influence the dispersion curves for the quasi particles only close to the Fermi surface, where the excitation energies are of order ω_D . For a further discussion of the expression (16.13) we refer to Migdal's paper.⁴²

In our formulas we have the Fourier transform of the ionic potential, whereas instead we expect a matrix element of V^i between Bloch functions. This is due to the schematic handling of the dielectric response function. The screened electron-ion potential $V^i(\mathbf{q})/\epsilon(\mathbf{q}, 0)$ plays a central role in the electron-phonon problem. We refer to the article by Sham and Ziman in Volume 15 of this series for methods to estimate that quantity.

17. REMARKS ON TEMPERATURE GREEN FUNCTIONS

So far we have discussed only the case of zero temperature. The extension of the definitions to finite temperatures is straightforward—we just

use an ensemble average instead of a ground state expectation value, thus

$$G(\mathbf{x}t, \mathbf{x}'t') = -i \frac{\text{Tr}\{\exp[-\beta(H - \mu N)]T[\psi(\mathbf{x}, t)\psi^+(\mathbf{x}', t')]\}}{\text{Tr}\{\exp[-\beta(H - \mu N)]\}}, \quad (17.1)$$

where $\beta = (k_B T)^{-1}$. Spectral resolutions follow directly from the definitions just as in the zero temperature case,⁴⁴

$$G(\mathbf{x}, \mathbf{x}'; \omega) = \int A(\mathbf{x}, \mathbf{x}'; \omega) \left\{ \frac{1 - f(\omega')}{\omega - \omega' + i\delta} + \frac{f(\omega')}{\omega - \omega' - i\delta} \right\} d\omega', \quad (17.2)$$

where $f(\omega) = \{\exp[\beta(\omega - \mu)] + 1\}$, and the spectral function A satisfies the sum rule

$$\int A(\mathbf{x}, \mathbf{x}'; \omega) d\omega = \delta(\mathbf{x}, \mathbf{x}'). \quad (17.3)$$

The generation of approximations for Σ is, however, more complicated in the finite temperature case. To see what happens we consider the electron gas. At zero temperature we have (suppressing the variable \mathbf{k})

$$[\omega - \epsilon - \Sigma(\omega)]G(\omega) = 1. \quad (17.4)$$

G and Σ have the spectral resolutions

$$\begin{aligned} G(\omega) &= \int_C \frac{A(\omega')}{\omega - \omega'} d\omega'; & \text{Im } G(\omega) &= \pi A(\omega) \operatorname{sgn}(\mu - \omega) \\ \Sigma(\omega) &= \Sigma_0 + \int_C \frac{B(\omega')}{\omega - \omega'} d\omega'; & \text{Im } \Sigma(\omega) &= \pi B(\omega) \operatorname{sgn}(\mu - \omega), \end{aligned} \quad (17.5)$$

where C is the contour given in Fig. 2. From Eqs. (17.4) and (17.5) we find that

$$A(\omega) = \frac{B(\omega)}{[\omega - \epsilon - \operatorname{Re} \Sigma(\omega)]^2 + \pi^2 B^2(\omega)}. \quad (17.6)$$

At finite temperatures we have for G

$$\begin{aligned} G(\omega) &= \int_{-\infty}^{\infty} A(\omega') \left[\frac{f(\omega')}{\omega - \omega' - i\delta} + \frac{1 - f(\omega')}{\omega - \omega' + i\delta} \right] d\omega' \\ \text{Im } G(\omega) &= \pi[2f(\omega) - 1]A(\omega) = \pi A(\omega) \tanh[\beta(\mu - \omega)/2] \end{aligned} \quad (17.7)$$

$$\int_{-\infty}^{\infty} A(\omega) d\omega = 1.$$

So far everything is fine, but when we define Σ we have to be careful.

⁴⁴ See e.g. Schrieffer,³⁵ p. 193.

Suppose that we adopt Eq. (17.4) and a spectral resolution for Σ as in Eq. (17.7). This, however, results in the following expression for A :

$$A(\omega) = \frac{B(\omega)}{[\omega - \epsilon - \text{Re } \Sigma(\omega)]^2 + \pi^2 B^2(\omega) \tanh[(\mu - \omega)\beta/2]}, \quad (17.8)$$

which does not have the proper limit $\delta(\omega - \epsilon)$ in the independent particle case, $\text{Re } \Sigma = 0$, $B \rightarrow 0$. To obtain the relation between A and B given in Eq. (17.6) we must define Σ by

$$(\omega - \epsilon - \Sigma)G + (2\pi)^2 f(1 - f)AB = 1 \quad (17.9)$$

rather than by Eq. (17.4).

The rather messy definition of Σ in Eq. (17.9) shows that it is better if, at finite temperature, we can work with concepts other than the straightforward generalization in Eq. (17.1) of the zero temperature Green function. One possibility is to use the Matsubara technique⁴⁵ with *temperature Green functions*, or the closely related Martin and Schwinger technique⁴⁶ with *complex times Green functions*. These Green functions are closely related but not the same as in Eq. (17.1), and they have simpler properties at finite temperatures.

We illustrate a finite temperature result by a simplified derivation for the electron-phonon case, which gives the correct result but involves a slight bit of fudging. From Eq. (16.14) we have, neglecting polarization indices,

$$\Sigma(\mathbf{k}, \omega) = \frac{i}{(2\pi)^4} \int |g_{\mathbf{q}}|^2 D_{\mathbf{q}}(\omega') G(\mathbf{k} + \mathbf{q}, \omega + \omega') d\mathbf{q} d\omega'. \quad (17.10)$$

Substituting the correct zero order temperature-dependent quantities

$$G(\mathbf{k}, \omega) = \frac{f_{\mathbf{k}}}{\omega - \epsilon_{\mathbf{k}} - i\delta} + \frac{1 - f_{\mathbf{k}}}{\omega - \epsilon_{\mathbf{k}} + i\delta}$$

$$D_{\mathbf{q}}(\omega) = 2\omega_{\mathbf{q}} \left[\frac{1 + N_{\mathbf{q}}}{\omega^2 - (\omega_{\mathbf{q}} - i\delta)^2} - \frac{N_{\mathbf{q}}}{\omega^2 - (\omega_{\mathbf{q}} + i\delta)^2} \right], \quad (17.11)$$

and performing the integrations, we have

$$\Sigma(\mathbf{k}, \omega) = \frac{1}{(2\pi)^3} \int |g_{\mathbf{q}}|^2 \left\{ \frac{f_{\mathbf{k}+\mathbf{q}}(1 + N_{\mathbf{q}})}{\omega + \omega_{\mathbf{q}} - \epsilon_{\mathbf{k}+\mathbf{q}} - i\delta} + \frac{N_{\mathbf{q}}(1 - f_{\mathbf{k}+\mathbf{q}})}{\omega + \omega_{\mathbf{q}} - \epsilon_{\mathbf{k}+\mathbf{q}} + i\delta} \right. \\ \left. + \frac{f_{\mathbf{k}+\mathbf{q}}N_{\mathbf{q}}}{\omega - \omega_{\mathbf{q}} - \epsilon_{\mathbf{k}+\mathbf{q}} - i\delta} + \frac{(1 + N_{\mathbf{q}})(1 - f_{\mathbf{k}+\mathbf{q}})}{\omega - \omega_{\mathbf{q}} - \epsilon_{\mathbf{k}+\mathbf{q}} + i\delta} \right\} d\mathbf{q}. \quad (17.12)$$

⁴⁵ See e.g. Abrikosov *et al.*⁴⁵

⁴⁶ See e.g. Kadanoff and Baym.⁴⁶

This result has the correct zero temperature limit, and it gives the correct real part of Σ at finite temperatures. The spectral function A for the electron Green function [see Eq. (17.7)] is, however, not given by $\pi^{-1} \text{Im}(\omega - \epsilon_{\mathbf{k}} - \Sigma)^{-1}$ but instead by an expression $\pi^{-1} \text{Im}[\omega - \epsilon_{\mathbf{k}} - \Sigma^R(\mathbf{k}, \omega)]^{-1}$, where Σ^R is obtained from Σ by the somewhat arbitrary procedure

$$\begin{aligned}\Sigma^R(\mathbf{k}, \omega) &= \lim_{\Delta \rightarrow 0, \Delta > \delta} \Sigma(\mathbf{k}, \omega - i\Delta) \\ &= \frac{1}{(2\pi)^3} \int |g_{\mathbf{q}}|^2 \left\{ \frac{N_{\mathbf{q}} + f_{\mathbf{k}+\mathbf{q}}}{\omega + \omega_{\mathbf{q}} - \epsilon_{\mathbf{k}+\mathbf{q}} - i\Delta} + \frac{N_{\mathbf{q}} + 1 - f_{\mathbf{k}+\mathbf{q}}}{\omega - \omega_{\mathbf{q}} - \epsilon_{\mathbf{k}+\mathbf{q}} - i\Delta} \right\} d\mathbf{q}.\end{aligned}\quad (17.13)$$

This section summarizes some formulas to serve as a background to the discussion of results to be given in Part VIII.

V. The Landau Fermi Liquid Theory

18. INTRODUCTORY REMARKS

Our discussion so far has been based on the Green function formulation of the many-body problem. There is, however, an alternative formulation of many properties that uses a single-particle distribution function $f(\mathbf{k}, \mathbf{r}, t)$ of the Boltzmann type. A particular distribution function of this type was introduced by Wigner⁴⁷

$$f_w(\mathbf{k}; \mathbf{r}, t) = \int d\mathbf{r} \exp(-i\mathbf{k} \cdot \mathbf{r}) \langle \psi^+(\mathbf{R} - \frac{1}{2}\mathbf{r}, t) \psi(\mathbf{R} + \frac{1}{2}\mathbf{r}, t) \rangle. \quad (18.1)$$

We note that the Wigner distribution function is simply related to the one-particle Green function since

$$\langle \psi^+(\mathbf{r}, t) \psi(\mathbf{r}', t) \rangle = -iG(\mathbf{r}'t, \mathbf{r}t').$$

The bracket in Eq. (18.1) stands for a statistical average, which means that G is a temperature Green function, and we allow for the presence of external time-dependent fields. For a uniform system with no fields present, f_w reduces to the momentum distribution function

$$f_w(\mathbf{k}; \mathbf{r}, t) = \langle a_k^+ a_k \rangle, \quad (18.2)$$

and we may think of $f_w(\mathbf{k}; \mathbf{r}, t)$ as a momentum distribution that changes slowly with position and time. The particle and current densities are related

⁴⁷ E. Wigner, *Phys. Rev.* **40**, 749 (1932).

to f_W by

$$\begin{aligned}\rho(\mathbf{r}, t) &\equiv \langle \psi^+(\mathbf{r}, t) \psi(\mathbf{r}, t) \rangle = \int f_W(\mathbf{k}; \mathbf{r}, t) \frac{d\mathbf{k}}{(2\pi)^3} \\ \mathbf{j}(\mathbf{r}, t) &\equiv \frac{1}{2} \left\langle \psi^+(\mathbf{r}, t) \left(-\frac{i}{m} \frac{\partial}{\partial \mathbf{r}} \right) \psi(\mathbf{r}, t) + \text{h.c.} \right\rangle = \int \frac{\mathbf{k}}{m} f_W(\mathbf{k}; \mathbf{r}, t) \frac{d\mathbf{k}}{(2\pi)^3}. \end{aligned} \quad (18.3)$$

The Landau Fermi liquid theory uses a single-particle distribution function, however, i.e. not the Wigner function f_W but the distribution function of a noninteracting model system. The Landau theory is limited to situations where there is a simple correspondence between states of the model system and states of the actual system. A detailed discussion of the relations between the Green function theory, the Wigner distribution function, and the Landau theory is clearly outside the scope of this article, and we refer to the original papers by Pitaevskii,⁴⁸ Luttinger and Nozières,⁴⁹ Kadanoff and Baym,⁵⁰ and Holstein.⁵¹ We confine ourselves to a brief summary of the static properties of the phenomenological Landau theory in this section and will give a somewhat more detailed discussion of the transport equation and wavelike excitations in the following section. The aim of these sections is to discuss the effects of interactions on various properties of a Fermi liquid, using a uniform Fermi liquid as a model for the conduction electrons in simple metals.

The key assumption in the Landau theory is a one-to-one correspondence between the states of a noninteracting model system and the actual physical system. To characterize the states we use a distribution $n(\mathbf{k})$, omitting spin variables temporarily. The Landau theory is applicable when we have small deviations $\Delta n(\mathbf{k}) = n(\mathbf{k}) - n^{(0)}(\mathbf{k})$ from the equilibrium distribution $n^{(0)}(\mathbf{k}) = \Theta(k_F - |\mathbf{k}|)$. In an independent-particle model the total energy is simply $E = \sum_{\mathbf{k}} E(\mathbf{k}) n(\mathbf{k})$ and the excitation energies are given by $\Delta E = \sum_{\mathbf{k}} E(\mathbf{k}) \Delta n(\mathbf{k})$. In the Landau theory the interaction between quasi particles is taken into account and has to be included in the excitation energy by going to next order, thus

$$\Delta E = \sum_{\mathbf{k}} E^{(0)}(\mathbf{k}) \Delta n(\mathbf{k}) + \frac{1}{2} \sum_{\mathbf{k}\mathbf{k}'} f_{\mathbf{k}\mathbf{k}'} \Delta n(\mathbf{k}) \Delta n(\mathbf{k}'). \quad (18.4)$$

⁴⁸ L. P. Pitaevskii, *Soviet Phys. JETP (English Transl.)* **10**, 1267 (1960).

⁴⁹ P. Nozières and J. M. Luttinger, *Phys. Rev.* **127**, 1423 (1962); J. M. Luttinger and P. Nozières, *ibid.* **127**, 1431 (1962).

⁵⁰ L. P. Kadanoff and G. Baym.⁵⁵

⁵¹ T. Holstein, *Ann. Phys.* **29**, 410 (1964).

$E^{(0)}(\mathbf{k})$ is the change in energy when we add one quasi particle to the system, and $f_{\mathbf{kk}'}$ is the interaction energy between two quasi particles in states \mathbf{k} and \mathbf{k}' , respectively. In the presence of a distribution $\Delta n(\mathbf{k})$ of quasi particles, the energy of a given quasi particle \mathbf{k} changes because of the interaction and is given by

$$E(\mathbf{k}) = \delta \Delta E / \delta \mathbf{k} = E^{(0)}(\mathbf{k}) + \sum_{\mathbf{k}'} f_{\mathbf{kk}'} \Delta n(\mathbf{k}'). \quad (18.5)$$

The last term in Eq. (18.5) is numerically small compared to $E^{(0)}(\mathbf{k})$. It is nevertheless very important, because what matters is not the magnitude of $E(\mathbf{k})$ itself but rather the energy relative to the Fermi level, i.e. $E(\mathbf{k}) - \mu$. Inclusion of the interaction term in Eq. (18.5) makes the Landau theory differ in a fundamental way from an independent-particle theory and brings out in a simple way essential effects of the interaction on various physical properties.

$E^{(0)}(\mathbf{k})$ and $f_{\mathbf{kk}'}$ are defined formally from the expression of the total energy E as a functional of the distribution $n(\mathbf{k})$,

$$E^{(0)}(\mathbf{k}) = [\delta E / \delta n(\mathbf{k})]_{n=n^{(0)}}; \quad f_{\mathbf{kk}'} = \delta^2 E / \delta n(\mathbf{k}) \delta n(\mathbf{k}'), \quad (18.6)$$

or alternatively from the Dyson equation,

$$E(\mathbf{k}) = \epsilon(\mathbf{k}) + \Sigma[\mathbf{k}, E(\mathbf{k})]; \quad f_{\mathbf{kk}'} = \delta E(\mathbf{k}) / \delta n(\mathbf{k}'). \quad (18.7)$$

The index \mathbf{k} in these relations may be taken to specify a Bloch state and also to include a spin index. For an electron gas we have to lowest order in the screened interaction

$$\begin{aligned} f_{\mathbf{kk}'} &= -\Omega^{-1} W(\mathbf{k} - \mathbf{k}'; 0), && \text{parallel spins} \\ &= 0, && \text{otherwise,} \end{aligned} \quad (18.8)$$

where Ω is the total volume of the system and $W(\mathbf{k}; 0)$ is a static screened potential of roughly the form

$$W(\mathbf{k}; 0) = 4\pi e^2 / (k^2 + k_{TF}^2). \quad (18.9)$$

The energy of a quasi particle is thus decreased by the presence of other quasi particles with the same spin. We should further note that the energy of a quasi particle depends on the presence of other quasi particles only through the distribution function $n(\mathbf{k})$ just as in a self-consistent field problem.

The distribution function in equilibrium is given by the same formula as for independent fermions, i.e.

$$n(\mathbf{k}) = [\exp([E(\mathbf{k}) - \mu]/k_B T) + 1]^{-1}. \quad (18.10)$$

Because $E(\mathbf{k})$ depends on $n(\mathbf{k})$, Eq. (18.10) is an implicit equation to be

solved for $n(\mathbf{k})$. At low temperature, however, we find, barring exceptional circumstances, that $n(\mathbf{k})$ approaches the unit step function $n^{(0)}(\mathbf{k}) = \Theta[\mu - E(\mathbf{k})]$ in the limit $T \rightarrow 0$. We should observe that the Landau distribution function describes the distribution of quasi-particle states of given momentum and should not be confused with the true momentum distribution of the physical system Eq. (18.2), which is not a unit step function for an interacting system. The self-consistency requirement on $n(\mathbf{k})$ and $E(\mathbf{k})$ in Eq. (18.10) is trivial in many applications, namely, when there is an equal number of electrons and holes of each spin within a given solid angle of the Fermi surface. The interaction term in Eq. (18.5) then does not contribute and $E(\mathbf{k}) = E^{(0)}(\mathbf{k})$. As a result the density of states, which is given by $\nabla E(\mathbf{k})$, does not change from its zero temperature value.

Before discussing some important effects of the quasi-particle interaction, we need to comment on the nature of the interaction $f_{\mathbf{kk}'}$. The interaction depends on the spin as well as on the momentum variables. For a spatially uniform system with a paramagnetic ground state we need only to distinguish between a spin-independent "ordinary" interaction $f_{\mathbf{kk}'}^0$ and an "exchange" interaction $f_{\mathbf{kk}'}^e$, thus

$$f_{\mathbf{kk}'} = f_{\mathbf{kk}'}^0 + f_{\mathbf{kk}'}^e \delta_{\sigma\sigma'}. \quad (18.11)$$

In the Landau theory, one considers only small changes in the distribution close to the Fermi surface. One can therefore take $|\mathbf{k}| = |\mathbf{k}'| = k_F$, the Fermi momentum, and for a spherical Fermi surface f^0 and f^e will depend only on the angle $\theta_{\mathbf{kk}'}$ between the momentum \mathbf{k} and \mathbf{k}' . Furthermore, the calculation of physical properties will invoke only certain integrals of f^0 and f^e . These integrals are essentially the coefficients in an expansion of f^0 and f^e in terms of Legendre polynomials in $\cos \theta_{\mathbf{kk}'}$. It is expedient to note that the proper combinations entering the end results will be

$$a = f^0 + \frac{1}{2}f^e, \quad b = \frac{1}{2}f^e. \quad (18.12)$$

Absorbing the algebraic factors entering the integrals, we define two new quantities

$$A = (\Omega k_F m^*/\pi^2)a; \quad B = (\Omega k_F m^*/\pi^2)b, \quad (18.13)$$

where Ω is the total volume of the system and m^* is the density of states effective mass, $dE(\mathbf{k})/d\mathbf{k} = \mathbf{k}_F/m^*$. We expand A and B in Legendre polynomials

$$\begin{aligned} A_{\mathbf{kk}'} &= \sum_{l=0}^{\infty} (2l+1) A_l P_l(\cos \theta_{\mathbf{kk}'}) \\ B_{\mathbf{kk}'} &= \sum_{l=0}^{\infty} (2l+1) B_l P_l(\cos \theta_{\mathbf{kk}'}) \end{aligned} \quad (18.14)$$

The final formulas giving the effects of the interaction on various physical properties will contain the coefficients A_l and B_l . In the cases of interest known, only the first few values of l will occur. A small set of numbers will thus characterize the effects of interaction in the Landau theory and these numbers can be calculated from any particular theoretical model.

We wish to conclude this section by stating a few results relating to static properties of a Fermi liquid, and refer to textbooks⁵² for a detailed discussion.

The spin susceptibility is appreciably enhanced because of the interactions. The distributions of spins parallel and antiparallel to an external magnetic field H_0 are shifted relative to each other, which results in a shift of the quasi-particle energies because of the exchange interaction. This change in the interaction energy contributes to the spin susceptibility, and we obtain

$$\chi/\chi_F = (m^*/m)(1 + B_0)^{-1}, \quad (18.15)$$

where χ_F is the value for independent fermions of mass m . Because the exchange contribution is negative and m^*/m is close to one, χ is generally enhanced. B_0 is of the order -0.25 to -0.40 at metallic densities.

The compressibility κ is conventionally defined as a pressure derivative but is also related to the change in the chemical potential with particle density. This change has two components, one because the energy of an isolated quasi particle changes with the change of Fermi momentum plus a second coming from the change in interaction associated with the change of Fermi momentum. These effects result in the modification

$$\kappa/\kappa_F = (m^*/m)(1 + A_0)^{-1}, \quad (18.16)$$

where κ_F is the compressibility for the noninteracting gas. A_0 is of the order $-r_s/6$ (for r_s values of typical metals, see Table I in Sect. 23).

Finally we wish to mention the relation between the effective mass m^* and the Landau interaction, which follows from the Galilean invariance of a uniform system: The momentum of a unit volume of the liquid must equal the flow of mass. This condition gives the relation

$$m^*/m = 1 + A_1. \quad (18.17)$$

For a real solid we cannot require Galilean invariance. If, in particular, we wish to calculate the effective mass due to electron-phonon interaction, we must do so from the definition $\mathbf{k}/m^* = \nabla E^{(0)}(\mathbf{k})$. It so happens that the phonon contribution to m^* can be expressed in terms of the phonon contribution to the Landau interaction, but in this case it is the $l = 0$

⁵² D. Pines and P. Nozières, "The Theory of Quantum Liquids," Vol. I. Benjamin, New York, 1966; or P. Nozières.²⁴

component rather than the $l = 1$ component that enters.⁵³ This has the consequence that in the expression for the paramagnetic susceptibility, $\chi_F/\chi = (m/m^*) + (m/m^*)B_0$, the phonon contribution vanishes to lowest order.⁵⁴

19. THE KINETIC EQUATION AND WAVELIKE EXCITATIONS

There is in principle a straight path starting from the equation of motion (13.4) for the one-electron Green function to the Landau kinetic equation, using the relation between the Wigner distribution function and Green function. In practice, this path involves a number of delicate considerations in particular with respect to the collision terms. We will here only indicate this path by starting from a Green function equation where we neglect the frequency dependence of the self-energy. This corresponds to some kind of self-consistent theory which leaves out explicit dynamical effects. This approximation is, however, good enough to demonstrate features of key interest in the derivation of the Landau kinetic equation. The collision terms are, however, deliberately neglected on this level of approximation.

A static self-energy is local in time, i.e., $\Sigma(\mathbf{x}t, \mathbf{x}'t') = \Sigma(\mathbf{x}, \mathbf{x}') \delta(t - t')$. Adding Eq. (13.4) and its complex conjugate, we obtain, in the same matrix notation as in Section 5, the following equation for the density matrix $\rho(\mathbf{x}, \mathbf{x}'; t) = \langle \psi^+(\mathbf{x}'t)\psi(\mathbf{x}t) \rangle$:

$$i(\partial/\partial t)\rho + [\rho, h + \Sigma] = 0. \quad (19.1)$$

We include in the single-particle Hamiltonian h the effect of an external magnetic field \mathbf{H} on the electron spin. It is therefore convenient to consider the spin explicitly and to this effect we represent Σ , h , and ρ as 2×2 matrices in spin space, e.g.,

$$\begin{aligned} \Sigma_{\alpha\beta}(\mathbf{r}, \mathbf{r}') &= \int \chi_\alpha^*(\xi) \Sigma(\mathbf{r}\xi, \mathbf{r}'\xi') \chi_\beta(\xi') d\xi d\xi' \\ h_{\alpha\beta}(\mathbf{r}, \mathbf{r}') &= \{[(\mathbf{p}^2/2m) + V(\mathbf{r})] \delta_{\alpha\beta} - \beta_0 \mathbf{H} \cdot \sigma_{\alpha\beta}\} \delta(\mathbf{r} - \mathbf{r}'), \end{aligned} \quad (19.2)$$

where σ is the Pauli spin operator and $\beta_0 = e\hbar/2mc$ is the Bohr magneton. Similarly, the Wigner distribution becomes a matrix

$$f_{\alpha\beta}(\mathbf{k}, \mathbf{R}; t) = \int \exp[-ik \cdot (r - r')] \rho_{\alpha\beta}(r, r'; t) d(r - r'); \quad \mathbf{R} = \frac{1}{2}(r + r'). \quad (19.3)$$

⁵³ V. Heine, P. Nozières, and J. W. Wilkins, *Phil. Mag.* **13**, 741 (1966).

⁵⁴ J. J. Quinn, in "The Fermi Surface" (W. A. Harrison and M. B. Webb, eds.). Wiley, New York, 1960.

The particle and spin densities are obtained by forming the following traces:

$$\rho(\mathbf{r}, t) = \text{tr} \int f(\mathbf{k}, \mathbf{r}; t) [d\mathbf{k}/(2\pi)^3], \quad \delta(\mathbf{r}, t) = \text{tr} \int \delta f(\mathbf{k}, \mathbf{r}; t) [d\mathbf{k}/(2\pi)^3]. \quad (19.4)$$

In order to obtain the Landau kinetic equation we transform the effective Hamiltonian $H = h + \Sigma$ in the same way as ρ is transformed into f in Eq. (19.3). We assume that both $f(\mathbf{k}, \mathbf{R}; t)$ and $H(\mathbf{k}, \mathbf{r}; t)$ vary slowly with \mathbf{r} and can then transform Eq. (19.1) for the density matrix into the classical form

$$(\partial f/\partial t) + \{f, H\} = 0, \quad (19.5)$$

where the commutator has turned into something that would have been a Poisson bracket if we had neglected spin properties. Because the spin matrices do not generally commute, we obtain the obvious generalization of the ordinary Poisson bracket:

$$\{f, H\} = -i[f, H] + \frac{1}{2} \left[\frac{\partial f}{\partial \mathbf{r}} \cdot \frac{\partial H}{\partial \mathbf{k}} + \frac{\partial H}{\partial \mathbf{k}} \cdot \frac{\partial f}{\partial \mathbf{r}} \right] - \frac{1}{2} \left[\frac{\partial f}{\partial \mathbf{k}} \cdot \frac{\partial H}{\partial \mathbf{r}} + \frac{\partial H}{\partial \mathbf{r}} \cdot \frac{\partial f}{\partial \mathbf{k}} \right]. \quad (19.6)$$

With our choice of the self-energy there are no renormalization effects in the momentum distribution, and the Wigner and Landau distributions are the same. Thus Eq. (19.5) is the Landau kinetic equation. We refer to e.g. Kadanoff and Baym³⁶ for the derivation in the general case.

We now consider small disturbances around the equilibrium in a uniform Fermi liquid and separate zero and first order terms according to

$$\begin{aligned} H(\mathbf{k}, \mathbf{r}; t) &= E^{(0)}(\mathbf{k}) + \epsilon_1(\mathbf{k}, \mathbf{r}; t) \\ E^{(0)}(\mathbf{k}) &= (k^2/2m) + \Sigma^{(0)}(\mathbf{k}) \\ \epsilon_1(\mathbf{k}, \mathbf{r}; t) &= \delta\Sigma(\mathbf{k}, \mathbf{r}; t) - \beta_0 \mathbf{H} \cdot \boldsymbol{\sigma} \\ f(\mathbf{k}, \mathbf{r}; t) &= n^{(0)}(\mathbf{k}) + \Delta n(\mathbf{k}) = n^{(0)}(\mathbf{k}) + \delta[E^{(0)}(\mathbf{k}) - \mu]n_1(\mathbf{k}, \mathbf{r}; t) \\ n^{(0)}(\mathbf{k}) &= \Theta[\mu - E^{(0)}(\mathbf{k})]. \end{aligned} \quad (19.7)$$

The deviation $\Delta n(\mathbf{k}, \mathbf{r}; t)$ is localized to the immediate neighborhood of the Fermi surface, as is explicitly written in Eq. (19.7). In order to allow for diamagnetic effects, we replace \mathbf{k} by $\mathbf{k} - (e/c)\mathbf{A}$. Performing the differentiations in Eq. (19.6) and replacing $\mathbf{k} - (e/c)\mathbf{A}$ by \mathbf{k} afterwards, and finally linearizing the equation, one obtains ($v_F = k_F/m^*$)

$$\frac{\partial n_1}{\partial t} + \left[\frac{e}{c} (\mathbf{v}_F \times \mathbf{H}) \cdot \frac{\partial}{\partial \mathbf{k}} + \mathbf{v}_F \cdot \frac{\partial}{\partial \mathbf{r}} \right] [n_1 + \epsilon_1] + i(\epsilon_1 n_1 - n_1 \epsilon_1) = e \mathbf{E} \cdot \mathbf{v}_F, \quad (19.8)$$

where \mathbf{E} denotes the total field arising from external as well as from induced charges.

The linear term in the change of the self-energy will be of the form (suppressing the variables \mathbf{r}, t for the moment)

$$\delta\Sigma_{\alpha\beta}(\mathbf{k}) = \sum_{\gamma,\delta} \int [d\mathbf{k}'/(2\pi)^3] f_{\alpha\beta\gamma\delta}(\mathbf{k}, \mathbf{k}') \Delta n_{\gamma\delta}(\mathbf{k}'). \quad (19.9)$$

The symmetry of the system restricts the form of the interaction function f , and for a uniform system with a paramagnetic ground state one is limited to the form

$$\delta\Sigma_{\alpha\beta}(\mathbf{k}) = \int [d\mathbf{k}'/(2\pi)^3] \{ a_{kk'} \delta_{\alpha\beta} \operatorname{tr} \Delta n(\mathbf{k}') + b_{kk'} \delta_{\alpha\beta} \cdot \operatorname{tr} [\sigma \Delta n(\mathbf{k}')] \}. \quad (19.10)$$

A comparison with the representation in terms of ordinary and exchange contributions f^0 and f^e from the preceding section [cf. Eqs. (18.5) and (18.11)] gives the relations

$$a = f^0 + \frac{1}{2}f^e, \quad b = \frac{1}{2}f^e. \quad (19.11)$$

Using the relation $\Delta n(\mathbf{k}) = \delta[E^{(0)}(\mathbf{k}) - \mu]n_1(\mathbf{k})$, we can transform Eq. (19.10) into an integral over the Fermi surface, using the formula $\delta[E^{(0)}(\mathbf{k}) - \mu] = \delta(k - k_F)/v_F$, thus

$$\begin{aligned} \delta\Sigma(\mathbf{k}) &= \operatorname{tr}_\sigma \int [d\mathbf{k}'/(2\pi)^3] (a_{kk'} + b_{kk'} \sigma \cdot \sigma') [\delta(k' - k_F)/v_F] n_1(\mathbf{k}') \\ &= \frac{1}{2} \operatorname{tr}_\sigma \int (dk'/4\pi) [A_{kk'} + B_{kk'} \sigma \cdot \sigma'] n_1(\mathbf{k}'), \end{aligned} \quad (19.12)$$

with $A = \Omega k_F m^* a / \pi^2$ and $B = \Omega k_F m^* b / \pi^2$. The momentum \mathbf{k}' is on the Fermi surface and the integration extends over the full solid angle, $\int d\hat{\mathbf{k}}' = 4\pi$. In applications to specific problems it is convenient to use the expansion of the A and B functions in Legendre polynomials given in Eq. (18.14).

Instead of working with the four components of the matrix n_1 , we define density and spin density distributions by⁵⁵

$$f(\mathbf{k}, \mathbf{r}; t) = \operatorname{tr} n_1(\mathbf{k}, \mathbf{r}; t), \quad \sigma(\mathbf{k}, \mathbf{r}; t) = \operatorname{tr} [\sigma n_1(\mathbf{k}, \mathbf{r}; t)]. \quad (19.13)$$

⁵⁵ The function $f(\mathbf{k}, \mathbf{r}; t)$ should not be confused with the Wigner distribution f_W used earlier; f corresponds to the ordinary distribution function for spinless particles, while f_W is a matrix.

The transport equation in Eq. (19.8) now splits into the two sets

$$\begin{aligned}
 & \frac{\partial f(\mathbf{k}, \mathbf{r}; t)}{\partial t} + \left[\frac{e}{c} (\mathbf{v}_F \times \mathbf{H}) \cdot \frac{\partial}{\partial \mathbf{k}} + \mathbf{v}_F \cdot \frac{\partial}{\partial \mathbf{r}} \right] \left(f(\mathbf{k}, \mathbf{r}; t) + \int A_{\mathbf{kk}'} f(\mathbf{k}', \mathbf{r}; t) \frac{d\hat{k}'}{4\pi} \right) \\
 & \quad = 2e\mathbf{E} \cdot \mathbf{v}_F \\
 & \frac{\partial \sigma(\mathbf{k}, \mathbf{r}; t)}{\partial t} \\
 & \quad + \left[\frac{e}{c} (\mathbf{v}_F \times \mathbf{H}) \cdot \frac{\partial}{\partial \mathbf{k}} + \mathbf{v}_F \cdot \frac{\partial}{\partial \mathbf{r}} \right] \left(\sigma(\mathbf{k}, \mathbf{r}; t) + \int B_{\mathbf{kk}'} \sigma(\mathbf{k}', \mathbf{r}; t) \frac{d\hat{k}'}{4\pi} - 2\beta_0 \mathbf{H} \right) \\
 & \quad + \sigma(\mathbf{k}, \mathbf{r}; t) \left(\int B_{\mathbf{kk}'} \sigma(\mathbf{k}', \mathbf{r}; t) \frac{d\hat{k}'}{4\pi} - 2\beta_0 \mathbf{H} \right) = 0. \tag{19.14}
 \end{aligned}$$

A case of particular interest is when we have a constant magnetic field \mathbf{H}_0 , possibly a small oscillating field \mathbf{H} , and in addition an external electric field \mathbf{E}_{ext} . We write accordingly $\sigma = \sigma_0 + \sigma_1$ and use the result from the paramagnetic spin susceptibility that $\sigma_0 = 2\beta_0 \mathbf{H}_0 (1 + B_0)$. Choosing the z axis along the field \mathbf{H}_0 we obtain for the components σ_1^z and $\sigma_1^\pm = \sigma_1^x \pm i\sigma_1^y$,

$$\begin{aligned}
 & \frac{\partial \sigma_1^z}{\partial t} + \left[\frac{e}{c} (\mathbf{v}_F \times \mathbf{H}_0) \cdot \frac{\partial}{\partial \mathbf{k}} + \mathbf{v}_F \cdot \frac{\partial}{\partial \mathbf{r}} \right] \\
 & \quad \times \left[\sigma_1^z + \int B_{\mathbf{kk}'} \sigma_1^z(\mathbf{k}') \frac{d\hat{k}'}{4\pi} - 2\beta_0 H_1^z \right] = 0 \\
 & \frac{\partial \sigma_1^\pm}{\partial t} + \left[\frac{e}{c} (\mathbf{v}_F \times \mathbf{H}_0) \cdot \frac{\partial}{\partial \mathbf{k}} + \mathbf{v}_F \cdot \frac{\partial}{\partial \mathbf{r}} \pm i \frac{2\beta_0 H_0}{1 + B_0} \right] \\
 & \quad \times \left[\sigma_1^\pm + \int B_{\mathbf{kk}'} \sigma_1^\pm(\mathbf{k}') \frac{d\hat{k}'}{4\pi} - 2\beta_0 H_1^\pm \right] = 0. \tag{19.15}
 \end{aligned}$$

We wish to study solutions corresponding to wave motions in space and time. The associated distortions of the Fermi surface are expanded in spherical harmonics. Thus we make the following ansatz:

$$f(\mathbf{k}, \mathbf{r}; t) = \exp[i(\mathbf{q} \cdot \mathbf{r} - \omega t)] \sum_{lm} \alpha_{lm}^{(1)} Y_{lm}(\hat{k}), \tag{19.16}$$

and similar ones for σ_1^z and σ_1^\pm with expansion coefficients $\alpha_{lm}^{(2)}$ and $\alpha_{lm}^{(3)}$.

We illustrate the nature of the resulting equations for the simple case that we have no oscillating field \mathbf{H}_1 and no external field \mathbf{E}_{ext} . In this case

we obtain

$$\sum_{lm} [\omega + (m\omega_c - \mathbf{v}_F \cdot \mathbf{q})(1 + A_l)] \alpha_{lm}^{(1)} Y_{lm}(\hat{k}) = i \exp[-i(\mathbf{q} \cdot \mathbf{r} - \omega t)] 2e \mathbf{E} \cdot \mathbf{v}_F \quad (19.17a)$$

$$\sum_{lm} [\omega + (m\omega_c - \mathbf{v}_F \cdot \mathbf{q})(1 + B_l)] \alpha_{lm}^{(2)} Y_{lm}(\hat{k}) = 0 \quad (19.17b)$$

$$\sum_{lm} [\omega + (m\omega_c - \mathbf{v}_F \cdot \mathbf{q} \mp \Omega_0)(1 + B_l)] \alpha_{lm}^{(3)} Y_{lm}(\hat{k}) = 0, \quad (19.17c)$$

where we have introduced the cyclotron frequency $\omega_c = eH_0/(m^*c)$ and the enhanced spin resonance frequency $\Omega_0 = \omega_s/(1 + B_0)$, and where ω_s is the ordinary spin resonance frequency $2\beta_0 H_0$. The derivation of these equations has closely followed that given by Silin.⁵⁶

We now summarize briefly some important results obtained for the normal modes of the system.⁵⁷⁻⁵⁹

a. The Long-Wavelength Limit in the Case $\mathbf{E} = 0$

The results are immediately obtained from Eq. (19.17) and we obtain the following sequence of modes, corresponding to different distortions of the Fermi surface ($l = 0, 1, 2, \dots; m = 0, \pm 1, \dots, \pm l$):

$$\begin{aligned} f: \quad \omega_{lm} &= m\omega_c(1 + A_l) \\ \sigma_1^s: \quad \omega_{lm} &= m\omega_c(1 + B_l) \\ \sigma_1^\pm: \quad \omega_{lm} &= (m\omega_c \mp \Omega_0)(1 + B_l). \end{aligned} \quad (19.18)$$

These results were first obtained by Silin.⁵⁶ We note that the most well-known case, the cyclotron frequency ω_c measured in an Azbel-Kaner experiment (AKCR), does not appear in this spectrum, whereas for $l = 1$ we would obtain, if phonon effects are neglected, the free electron cyclotron frequency $\omega_c(1 + A_1) = eH_0/mc$.⁶⁰

⁵⁶ V. P. Silin, *Soviet Phys. JETP (English Transl.)* **8**, 870 (1959).

⁵⁷ P. M. Platzman and P. A. Wolff, *Phys. Rev. Letters* **18**, 280 (1967).

⁵⁸ P. M. Platzman, W. M. Walsh, Jr., and E-Ni Foo, *Phys. Rev.* **172**, 689 (1968).

⁵⁹ N. D. Mermin and Y. C. Cheng, *Phys. Rev. Letters* **20**, 839 (1968).

⁶⁰ The reason for this is that in the Azbel-Kaner experiment there is no coupling to the bulk modes of the sample. The microwave electric field penetrates only a thin surface layer in which it couples individually to the quasiparticles in a small portion of the orbit as they spiral in the constant magnetic field parallel to the surface. If we could have the electric field penetrate the metal uniformly, we should indeed observe a resonance at the free electron cyclotron frequency, as was first discussed by Kohn,⁶¹ who gave a very simple argument to show this.

⁶¹ W. Kohn, *Phys. Rev.* **123**, 1242 (1961).

So far only two modes of the spectrum have been measured, namely, *transverse spin waves* (ω_{00} of σ_1^\pm) and *magnetoplasma waves* (ω_{21} of f). In both cases standing waves were set up in thin slabs of alkali metals. In the first case extra structure was observed in a spin resonance experiment⁶² and in the second case additional structure occurred in an AKCR experiment.⁶³

b. Dispersion of Transverse Spin Waves

The dispersion relation to order k^2 is obtained by applying second order perturbation theory to Eq. (19.17c) which gives

$$\begin{aligned} \omega_{00}(q) = \omega_s + & \frac{(v_F q)^2 (B_0 - B_1)(1 + B_1)}{3\omega_s} \\ & \times \left\{ \cos^2 \vartheta \left(\frac{B_0 - B_1}{1 + B_0} \right)^{-2} + \sin^2 \vartheta \left[\left(\frac{B_0 - B_1}{1 + B_0} \right)^2 - \left(\frac{\omega_c(1 + B_1)}{\omega_s} \right)^2 \right]^{-1} \right\}. \end{aligned} \quad (19.19)$$

Here ϑ is the angle between the magnetic field H_0 and the direction of q . This result was derived by Silin⁵⁶ for $\vartheta = 0$ and for general ϑ by Platzman and Wolff.⁵⁷ The observations on spin waves by Schultz and Dunifer⁶² agree well with this formula and from their data B_0 and B_1 can be determined.

c. Dispersion of Magnetoplasma Waves

In this case the induced electric field must be taken into account. The geometry is such that the magnetic field is parallel to the slab and thus the angle ϑ is effectively 90° . Again, second order perturbation theory gives to leading order

$$\omega_{21}(q) = \omega_c \left[1 + A_2 - \left(\frac{qv_F}{\omega_c} \right)^2 \frac{(1 + A_3)(7 + 13A_2 - 6A_3)}{70(1 - A_2 + 2A_3)} \right]. \quad (19.20)$$

This formula agrees well with experimental results by Walsh and Platzman,⁶³ and from their data A_2 and A_3 can be estimated.

d. The Plasmon Dispersion Relation

One may argue that plasma oscillations fall outside the regime of the Landau theory because of the high frequency involved, and that instead a dielectric response formulation should be used. Presently available approx-

⁶² S. Schultz and G. Dunifer, *Phys. Rev. Letters* **18**, 283 (1967).

⁶³ W. M. Walsh, Jr., and P. M. Platzman, *Phys. Rev. Letters* **15**, 784 (1965).

imations of the dielectric function are, however, no better than assuming a static self-energy, and on that level of approximation the Landau theory would apply to the plasma oscillations. Solving the equation with no magnetic field present, we obtain, using again second order perturbation theory,⁶⁴

$$\omega_{10}^2 = \omega_p^2 + \frac{3}{8}(v_F q)^2(1 + A_1)(1 + \frac{5}{8}A_0 + \frac{3}{8}A_2). \quad (19.21)$$

It seems intuitively clear that no phonon effects should be included in this case, due to the high frequency involved in the plasma waves. Since A_2 is small compared to A_0 , the dispersion law is determined essentially by the effective mass (A_1) and the compressibility (A_0). The result in Eq. (19.21) is pertinent to real metals. For plasma oscillations it is the electron gas compressibility not the compressibility of the solid that should enter.

These remarks conclude our discussion of the Fermi Liquid. The main emphasis has been on giving representative examples showing explicitly how the Landau interaction parameters A_1 and B_1 effect various physical properties. We shall come back to these problems in Section 27 where we discuss the electron gas and in Section 43 where we discuss the experimental results.

VI. Wave-Packet States in Many-Particle Systems

20. INTRODUCTORY REMARKS ON WAVE PACKETS

The purpose of this part is to demonstrate and discuss how quasi-particle states can be constructed, and show how their velocity and lifetime is related to the structure of the spectral function. This is far from trivial in an interacting system. The spectral function $A(\omega)$ contains contributions from a practically infinite number of exact eigenstates of the system, from which we have to construct a localized wave packet with a finite spread in energy as well as in momentum.

The usual discussion of quasi particles in textbooks makes use of rather complicated arguments, using the properties of the analytical continuation of the Green function into the complex ω plane. In this section we prefer to follow a more direct path and construct the wave packets along similar lines as for free particles. In doing so one needs an obvious extension of the argument. For a free particle or in an independent-particle model, the energy and momentum are coupled by the dispersion relation $E = E(\mathbf{k})$. This is not so in an interacting system. The situation is described by a spectral function $A(\mathbf{k}, \omega)$ (for a uniform system), and this implies that we have to

⁶⁴ V. P. Silin, *Soviet Phys. JETP (English Transl.)* **7**, 538 (1958); S. Misawa, *Progr. Theoret. Phys.* **30**, 786 (1963).

consider first, say, a wave packet in momentum space and in addition to filter out a particular energy region. We shall show that one can define a good quasi-particle state for every well-defined peak structure in the spectral function. The decay of these quasi particles is determined by the form of the peak—for a pure Lorentz peak the decay is exponential.

It will also be shown that the wave packets under certain conditions can be described by the homogeneous Green function equation, with the self-energy playing the role of an optical potential. The conditions for this are easily fulfilled in scattering on atoms or surfaces, in which cases the asymptotic in- and outgoing solutions satisfy simple equations. For motion in an extended medium, the conditions are more limiting.

We start reviewing the form of the wave packet state for free particles, and write the defining equations

$$\begin{aligned}\varphi(\mathbf{r}) &= (2\pi)^{-3/2} \int \alpha(\mathbf{k}) \exp(i\mathbf{k}\cdot\mathbf{r}) d\mathbf{k} \\ \alpha(\mathbf{k}) &= (2\pi)^{-3/2} \int \varphi(\mathbf{r}) \exp(-i\mathbf{k}\cdot\mathbf{r}) d\mathbf{r} \quad (20.1)\end{aligned}$$

$$\int |\varphi(\mathbf{r})|^2 d\mathbf{r} = \int |\alpha(\mathbf{k})|^2 d\mathbf{k} = 1.$$

We prepare a wave packet state in a many-particle system as follows:

$$|N+1, \varphi\rangle = \int \varphi(\mathbf{r}) \psi^+(\mathbf{r}) d\mathbf{r} |N\rangle. \quad (20.2)$$

The meaning of this formula in a configuration space picture is given by the expression

$$(N+1)^{-1/2} \sum_{k=1}^{N+1} (-1)^{k+1} \varphi(\mathbf{r}_k) \Phi_N(\mathbf{r}_1 \cdots \mathbf{r}_{k-1} \mathbf{r}_{k+1} \cdots \mathbf{r}_{N+1}), \quad (20.3)$$

where Φ_N is the wave function corresponding to $|N\rangle$. We next calculate the particle density of the state $|N+1, \varphi\rangle$ and obtain

$$\begin{aligned}\rho(\mathbf{r}) &= \frac{\langle N+1, \varphi | \psi^+(\mathbf{r}) \psi(\mathbf{r}) | N+1, \varphi \rangle}{\langle N+1, \varphi | N+1, \varphi \rangle} \\ &= \rho^0(\mathbf{r}) + \left(\varphi^*(\mathbf{r}) \Theta \varphi(\mathbf{r}) / \int d\mathbf{r} \varphi^*(\mathbf{r}) \Theta \varphi(\mathbf{r}) \right) + \Delta \rho(\mathbf{r}) \quad (20.4)\end{aligned}$$

where

$$\begin{aligned}\rho^0(\mathbf{r}) &= \langle N | \psi^+(\mathbf{r})\psi(\mathbf{r}) | N \rangle \\ \Theta\varphi(\mathbf{r}) &= \int d\mathbf{r}' [\delta(\mathbf{r} - \mathbf{r}') - \rho^0(\mathbf{r}, \mathbf{r}')] \varphi(\mathbf{r}') \\ \rho^0(\mathbf{r}, \mathbf{r}') &= \langle N | \psi^+(\mathbf{r}')\psi(\mathbf{r}) | N \rangle \\ \Delta\rho(\mathbf{r}) &= \frac{-\int d\mathbf{r}' d\mathbf{r}'' \varphi^*(\mathbf{r}'') \langle N | \{\psi^+(\mathbf{r})\psi(\mathbf{r}) - \rho^0(\mathbf{r})\} \psi^+(\mathbf{r}')\psi(\mathbf{r}'') | N \rangle \varphi(\mathbf{r}')}{\int d\mathbf{r} \varphi^*(\mathbf{r}) \Theta\varphi(\mathbf{r})}.\end{aligned}\quad (20.5)$$

The operator Θ acts as a projection that suppresses components of the wave packet φ already represented in the ground state (e.g. in the HF theory the operator Θ makes the function orthogonal to all occupied states). It therefore gives a distortion of the wave packet. A further distortion occurs because of the last term $\Delta\rho$, which, however, gives no net contribution, since $\int \Delta\rho d\mathbf{r} = 0$.

The wave packet thus prepared is properly localized in \mathbf{r} space if $\varphi(\mathbf{r})$ is, and in \mathbf{k} space if we build it from Bloch states within a narrow range of \mathbf{k} space around some \mathbf{k}_0 . The wave packet does not, however, have a well-defined energy. In one-electron theory the choice of a range in \mathbf{k} space around \mathbf{k}_0 implies a limited spread in energy around the representative value $\epsilon = \epsilon(\mathbf{k}_0)$. In a many-particle state we have to specify a region in energy space separately. This can be done by means of a form factor g for energy selection,⁶⁶ and we write the wave packet as

$$|N + 1, \varphi\rangle = \int d\mathbf{r} dt g(t) \varphi(\mathbf{r}) \psi^+(\mathbf{r}, t) |N\rangle, \quad (20.6)$$

where $\psi^+(\mathbf{r}, t)$ is the Heisenberg operator, and $g(t)$ may be chosen, e.g., as

$$g(t) = (W/2)e^{-iEt}e^{-W|t|}. \quad (20.7)$$

This choice shows explicitly that the wave packet is localized in \mathbf{r} -space if $\varphi(\mathbf{r})$ is. Alternatively we could define a form of the wave packet which explicitly shows that the energy is well defined by choosing

$$\begin{aligned}|N + 1, \varphi\rangle &= \sum_s |N + 1, s\rangle \frac{W^2}{(\epsilon_s - E)^2 + W^2} \\ &\times \langle N + 1, s | \int d\mathbf{r} \varphi(\mathbf{r}) \psi^+(\mathbf{r}) | N \rangle.\end{aligned}\quad (20.8)$$

The two choices in Eqs. (20.6) and (20.8) are actually identical. Note that

⁶⁶ P. Nozières,⁶⁵ p. 94.

the form factor is introduced only to define the energy within a chosen spread, and has nothing to do with the actual dynamics of the quasi particle.

21. THE OPTICAL POTENTIAL. SCATTERING ON ATOMS AND SURFACES

In this section we discuss elastic scattering with the electron well outside the scattering system in the initial and final states. We then need no energy filtering. With a suitable choice of wave packet $\varphi(\mathbf{r})$, the state vector

$$|N + 1, \varphi\rangle = \int d\mathbf{r} \varphi(\mathbf{r}) \psi^+(\mathbf{r}) |N\rangle \quad (21.1)$$

describes an electron well outside the system and moving toward it. The subsequent motion and scattering is described by the time-evolution operator e^{-iHt} . After a long time T we have, measuring energy relative to the energy of the system,

$$\begin{aligned} & \exp[-i(H - E_0)T] |N + 1, \varphi\rangle \\ &= \int \psi^+(\mathbf{r}) |N\rangle \varphi_{sc}(\mathbf{r}) d\mathbf{r} + \int \sum_i \psi^+(\mathbf{r}) |N, i\rangle \varphi_{sc}^{(i)}(\mathbf{r}) d\mathbf{r} \\ &+ \sum_j \beta_j |N + 1, j\rangle, \end{aligned} \quad (21.2)$$

i.e. a state with elastically (φ_{sc}) and inelastically ($\varphi_{sc}^{(i)}$) scattered wavelets and possibly also bound states of $(N + 1)$ electrons. Let us now describe the dynamics by introducing a model wave function of the form⁶⁶

$$\phi(\mathbf{r}, t) = \int \langle N | \psi(\mathbf{r}, t) \psi^+(\mathbf{r}') | N \rangle \varphi(\mathbf{r}') d\mathbf{r}'. \quad (21.3)$$

Before the scattering, at $t = 0$, we have

$$\phi(\mathbf{r}, 0) = \varphi(\mathbf{r}) - \int \rho^0(\mathbf{r}, \mathbf{r}') \varphi(\mathbf{r}') d\mathbf{r}' = \varphi(\mathbf{r}), \quad (21.4)$$

because $\rho^0(\mathbf{r}, \mathbf{r}') = 0$ for \mathbf{r}' outside the system. After a long time T we have from Eqs. (21.1)–(21.3)

$$\begin{aligned} \phi(\mathbf{r}, T) &= \int \langle N | \psi(\mathbf{r}, T) \psi^+(\mathbf{r}') | N \rangle \varphi(\mathbf{r}') d\mathbf{r}' \\ &= \int \langle N | \psi(\mathbf{r}) \exp[-i(H - E_0)T] | N + 1, \varphi \rangle \\ &= \varphi_{sc}(\mathbf{r}) + \sum_j \beta_j \langle N | \psi(\mathbf{r}) | N + 1, j \rangle. \end{aligned} \quad (21.5)$$

⁶⁶ J. S. Bell and E. J. Squires, *Phys. Rev. Letters* **3**, 96 (1959).

For \mathbf{r} well outside the system, the last part vanishes leaving

$$\phi(\mathbf{r}, T) = \varphi_{\text{sc}}(\mathbf{r}).$$

Thus the model wave function $\phi(\mathbf{r}, t)$ correctly describes the incoming and elastically scattered waves.

We shall now show that $\phi(\mathbf{r}, t)$ satisfies the homogeneous equation for the one-particle Green function. From Eq. (13.4) we have for $t > 0$

$$\begin{aligned} & [i(\partial/\partial t) - h(\mathbf{r})] \langle N | \psi(\mathbf{r}, t) \psi^+(\mathbf{r}') | N \rangle \\ & - \int_0^\infty \Sigma(\mathbf{r}, \mathbf{r}''; t - t'') \langle N | \psi(\mathbf{r}'', t'') \psi^+(\mathbf{r}') | N \rangle d\mathbf{r}'' dt'' \\ & + \int_{-\infty}^0 \Sigma(\mathbf{r}, \mathbf{r}''; t - t'') \langle N | \psi^+(\mathbf{r}') \psi(\mathbf{r}'', t'') | N \rangle d\mathbf{r}'' dt'' = 0. \end{aligned} \quad (21.6)$$

The self-energy operator $\Sigma(\mathbf{r}, \mathbf{r}', \tau)$ tends to zero when $|\tau|$ becomes larger than some time typical for the electrons in the system. For t larger than that characteristic time, the last term in Eq. (21.6) vanishes, and we obtain

$$[i(\partial/\partial t) - h(\mathbf{r})] \phi(\mathbf{r}, t) - \int_{-\infty}^{+\infty} \Sigma(\mathbf{r}, \mathbf{r}''; t - t'') \phi(\mathbf{r}'', t'') d\mathbf{r}'' dt'' = 0. \quad (21.7)$$

The wave-packet state has a well-defined energy $E_0 + \epsilon_0$, $\epsilon_0 = \hbar^2 k_0^2 / 2m$, with an energy spread due only to the small spread in \mathbf{k} vectors defining $\varphi(\mathbf{r})$. If $\Sigma(\mathbf{r}, \mathbf{r}''; \omega)$ varies slowly with ω over the corresponding small range around $\omega = \epsilon_0$, we have

$$[i(\partial/\partial t) - h(\mathbf{r})] \phi(\mathbf{r}, t) - \int \Sigma(\mathbf{r}, \mathbf{r}''; \epsilon_0) \phi(\mathbf{r}'', t) d\mathbf{r}'' = 0. \quad (21.8)$$

We can therefore calculate the elastic scattering as if we had a one-electron problem with a complex nonlocal potential $\Sigma(\mathbf{r}, \mathbf{r}''; \epsilon_0)$. This is called an *optical potential* since it describes the losses due to absorption and inelastic scattering as well as it describes elastic scattering.

22. MOTION OF WAVE PACKETS IN AN EXTENDED MEDIUM

A direct application on intuitive grounds can be made of the results from the preceding section. Let us introduce for a uniform system a complex local potential $U = U_1 - iU_2$, where U_1 and U_2 are constants. The real part U_1 will shift the energy levels whereas the imaginary part will give an exponential damping of the wave function amplitude. Thus the quasi

particle has a *lifetime* $\tau = \hbar/(2U_2)$ and a *mean free path* $\Lambda = v\tau = \hbar v/(2U_2)$. These results are essentially correct as the somewhat closer analysis below will demonstrate. In the preceding section the initial and final states were defined as wave packets for a free particle. In an extended medium we must localize the wave packet in space and time as well as in momentum and energy space as we did in Section 20. We must also look closer into the question of how the quasi-particle wave packets are related to the spectral density function. Most of the discussion in this section refers to an electron gas but can easily be extended to periodic media.

It is convenient to write the wave-packet state in the form

$$|N + 1, \varphi, t\rangle = \int \varphi(\mathbf{r}, t) g(t') \psi^+(\mathbf{r}, t') |N\rangle d\mathbf{r} dt' \quad (22.1)$$

with

$$\varphi(\mathbf{r}, t) = (2\pi)^{-3/2} \int d\mathbf{k} \alpha(\mathbf{k}) \exp[i(\mathbf{k} \cdot \mathbf{r} - E_{\mathbf{k}}t)], \quad (22.2)$$

where $E_{\mathbf{k}}$ will later on be identified with the quasi-particle energy.

The state $|N + 1, \varphi, t\rangle$ is localized in the same region of space as the function $\varphi(\mathbf{r}, t)$ but this does not necessarily mean that it has the same dynamic propagation as $\varphi(\mathbf{r}, t)$. The propagation of the state $|N + 1, \varphi, 0\rangle$ is determined by the full many-body Hamiltonian H , and a suitable measure of the decay of the quasi particle is the amplitude

$$\begin{aligned} S(\tau) &= \langle N + 1, \varphi, \tau | \exp[-i(H - E_0)\tau] | N + 1, \varphi, 0 \rangle \\ &= \int d\mathbf{r}' d\mathbf{r}'' dt' dt'' \langle N | \psi(\mathbf{r}'', \tau + t'') \psi^+(\mathbf{r}', t') | N \rangle \\ &\quad \times \varphi^*(\mathbf{r}'', \tau) \varphi(\mathbf{r}', 0) g^*(t'') g(t'). \end{aligned} \quad (22.3)$$

We now use the formula (cf. Eqs. (9.2) and (10.1)),

$$\langle N | \psi(\mathbf{r}, t) \psi^+(\mathbf{r}', t') | N \rangle = \int_{-\infty}^{\infty} e^{-i\omega(t-t')} A(\mathbf{r}, \mathbf{r}'; \omega) d\omega, \quad (22.4)$$

where A is the spectral function of G , and μ is the chemical potential. Using the form factor defined in Eq. (20.7), we obtain after performing the space and time integrations the result

$$S(\tau) = \int_{-\infty}^{\infty} \exp[i(E_{\mathbf{k}} - \omega)\tau] \left(\frac{W^2}{(\omega - E)^2 + W^2} \right)^2 [\alpha(\mathbf{k})]^2 A(\mathbf{k}, \omega) d\mathbf{k} d\omega. \quad (22.5)$$

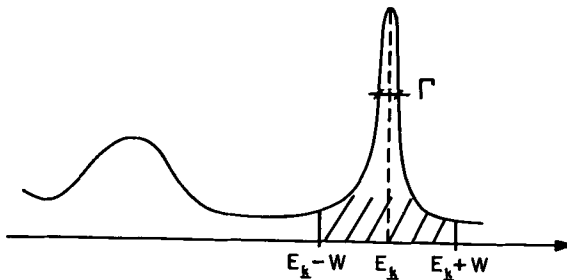


FIG. 11. A quasi-particle peak in the spectral function and a filtering region.

The choice of form factor means that we are looking into an energy interval $\omega \approx E \pm W$, and by varying E and W we can scan different portions of the energy axis. A quasi particle is associated with a peak in the spectral function. Suppose that we find, inside the scanning interval $E \pm W$, a quasi-particle peak of the approximate form (see Fig. 11)

$$A(\mathbf{k}, \omega) \cong (Z/\pi) \{ \Gamma / [(\omega - E_{\mathbf{k}})^2 + \Gamma^2] \}. \quad (22.6)$$

We now choose $E = E_{\mathbf{k}}$ and $W \gg \Gamma$ but small enough to filter away any additional structure in A beside the quasi-particle peak.

We should also have W small compared to $E_{\mathbf{k}} - \mu$ so that the integrations over ω in Eq. (22.5) can be extended down to $-\infty$. We then obtain the desired result

$$S(\tau) = \iint_{-\infty}^{+\infty} d\mathbf{k} d\omega \exp[i(E_{\mathbf{k}} - \omega)\tau] [\alpha(\mathbf{k})]^2 \frac{Z}{\pi} \frac{\Gamma}{(\omega - E_{\mathbf{k}})^2 + \Gamma^2} = Ze^{-\Gamma\tau}, \quad (22.7)$$

as intuitively expected.

The appropriate filtering requirements are well satisfied for \mathbf{k} close to the Fermi surface, where $\Gamma \sim (E_{\mathbf{k}} - \mu)^2$, which is much smaller than the excitation energy $E_{\mathbf{k}} - \mu$. In a normal metal it actually seems possible to construct approximate quasi-particle states for all energies except for the small (but important) region close to the Fermi surface where the phonons may give rise to complicated structure.

The analysis just completed enables us to proceed in analogy with the preceding section. We introduce a model wave function $\phi(\mathbf{r}, t)$ related to $S(t)$ by

$$S(t) = \int \varphi^*(\mathbf{r}, t) \phi(\mathbf{r}, t) d\mathbf{r}. \quad (22.8)$$

A comparison with Eq. (22.3) shows that

$$\phi(\mathbf{r}, t) = \int \langle N | \psi(\mathbf{r}, t + t'')\psi^+(\mathbf{r}', t') | N \rangle g^*(t'')\varphi(\mathbf{r}', 0)g(t') d\mathbf{r}' dt' dt''. \quad (22.9)$$

Using again the same form factor we obtain after integrations

$$\begin{aligned} \phi(\mathbf{r}, t) &= (2\pi)^{-3/2} \int \exp[i(\mathbf{k}\cdot\mathbf{r} - \omega t)] \left(\frac{W^2}{(\omega - E)^2 + W^2} \right)^2 \\ &\quad \times \alpha(\mathbf{k}) A(\mathbf{k}, \omega) d\mathbf{k} d\omega, \end{aligned} \quad (22.10)$$

which for a Lorentzian peak in $A(\mathbf{k}, \omega)$ within the interval $E \pm W$ gives

$$\phi(\mathbf{r}, t) = Z(2\pi)^{-3/2} \int d\mathbf{k} \alpha(\mathbf{k}) \exp\{i[\mathbf{k}\cdot\mathbf{r} - (E_{\mathbf{k}} - i\Gamma)t]\}. \quad (22.11)$$

The relation to the Green function equation now requires much more limiting conditions than in the preceding section.⁶⁷ If these requirements are fulfilled, we obtain for an electron gas

$$i(\partial/\partial t)\phi(\mathbf{r}, t) = -(\hbar^2/2m) \nabla^2 \phi(\mathbf{r}, t) + \Sigma(\mathbf{k}_0, E_{\mathbf{k}_0})\phi(\mathbf{r}, t), \quad (22.12)$$

using the fact that the wave packet is well centered around \mathbf{k}_0 . Equation (22.12) expresses the result stated at the beginning of this section on intuitive grounds.

We finally remark that the results of this section are easily extended to the case of Bloch functions, if we diagonalize the spectral function $A(\mathbf{r}, \mathbf{r}'; \omega)$, which is possible if we work within a *narrow* energy range for ω .

With our discussion of wave-packet states or quasi particles we have tried to demonstrate in an explicit and convincing manner results for elastic scattering (Section 21) and the decay of quasi particles. In particular we have given a procedure to handle the propagation of quasi-particles that do not have an extremely long lifetime.

The quasi-particle wave function in Eq. (22.9) is always directly related to the spectral function [see Eq. (22.4)], but only under more specialized conditions to the imaginary part of the self-energy. Except for the very ideal quasi particles, where we can confine ourselves to look at $\text{Im } \Sigma(\mathbf{k}, E_{\mathbf{k}})$, we shall thus have to study the actual structure of the spectral function.

We finally remark that our considerations apply only to the motion of quasi particles and tell us nothing about the oscillator strength and how to excite them. But that, to cite Kipling, is another story.

⁶⁷ Besides the condition stated at Eq. (21.8) we must require that $\Sigma(\mathbf{r}, \tau)$ tends to zero with $|\tau|$ while $|\tau|$ is still small compared to the lifetime of the quasiparticle [cf. Eqs. (21.6) and (21.7)].

VII. Properties of an Electron Gas

23. INTRODUCTION

The electron gas and the jellium model have been extensively discussed and used to demonstrate the key effects of the electron-electron and the electron-phonon interaction, and they have also been used as a testing ground for numerous approximation schemes. The *jellium model* is a simplified model in which the valence electrons move in a vibrating continuous charge and mass distribution obtained by smearing out the ions over the lattice; in spite of this obvious oversimplification the model is capable to demonstrate some key characteristic features of electron-phonon interaction in metals. The jellium is in equilibrium at a density approximately corresponding to that of sodium ($r_s = 4$); so that in order to simulate other metals one would have to consider external forces acting on the system. If we freeze the positive charge in the jellium at a given uniform density, we have the model referred to as the *electron gas*. We shall in this section discuss in considerable detail the properties of an electron gas. In later sections we shall show how some key results can be used and how indeed complete blocks of information concerning the electron gas can be carried over with only minor modifications for the description of real metals, and of course in particular the so called simple metals. We shall refrain from any attempt to review the vast literature on the electron gas problem,⁶⁸ and shall only discuss some selected aspects that are pertinent for our subsequent discussions.

The properties of an electron gas are usually expressed in terms of a dimensionless parameter r_s , related to the electron density by $4\pi r_s^3 a_0^3 / 3 = \Omega/N = \rho^{-1}$, where a_0 is the Bohr radius. Since the density is given in terms of the Fermi momentum, k_F , as $\rho = k_F^3 / 3\pi^2$, we have the relation

$$k_F = (\alpha r_s a_0)^{-1}; \quad \alpha = (4/9\pi)^{1/3} = 0.521. \quad (23.1)$$

In Table I we give the values of r_s for some metals.

The sum of the charge densities of the electrons and of the uniform background is zero except in a surface layer.⁶⁹ The electrostatic potential is constant in the interior and has some sort of surface barrier. If we consider only the average electrostatic interaction, we have the Hartree approximation, which for the electron gas is identical to the Sommerfeld model. The one-electron energy measured from the average potential is simply $\epsilon_k =$

⁶⁸ Extensive discussions of the electron gas and jellium models can be found in R. Brout and P. Carruthers, "Lectures on the Many-Electron Problem," Wiley (Interscience), New York, 1963; and in Pines and Nozières.⁶²

⁶⁹ As long as the electrons are itinerant and have not formed a Wigner lattice.²

TABLE I. VALUES OF r_s FOR SOME METALS

Be	Al	Pb	Mg	Cu	Li	Na	K	Rb	Cs
1.88	2.07	2.30	2.66	2.67	3.26	4.00	4.94	5.25	5.64

$\hbar^2 k^2 / 2m$ and the average energy per particle is $\frac{3}{5} \epsilon_F$, where $\epsilon_F = \hbar^2 k_F^2 / 2m = (\alpha r_s)^{-2}$ Ry. In passing from the Hartree to the HF approximation we include the exchange interaction. Assuming a paramagnetic ground state the one-electron wave functions are still plane waves and the electron density is uniform; however, taking the HF exchange into account, the dispersion law is given by

$$\epsilon_k^{\text{HF}} = \frac{\hbar^2 k^2}{2m} - \frac{e^2 k_F}{2\pi} \left[2 + \frac{k_F^2 - k^2}{k_F k} \ln \left| \frac{k_F + k}{k_F - k} \right| \right]. \quad (23.2)$$

The contribution from the exchange term varies rapidly in the neighborhood of k_F . This results in an infinite derivative of ϵ_k^{HF} for $k = k_F$, which implies that the density of states vanishes at the Fermi surface. Furthermore, the bandwidth becomes too large, whereas average properties, such as the total energy per electron

$$\bar{\epsilon}_{\text{HF}} = \frac{3}{5} \epsilon_F + \epsilon_{\text{ex}} = \left(\frac{3}{5\alpha^2 r_s^2} - \frac{3}{2\pi\alpha r_s} \right) \text{ Ry} = \left(\frac{2.21}{r_s^2} - \frac{0.916}{r_s} \right) \text{ Ry}, \quad (23.3)$$

have quite reasonable values.

In the high density limit the kinetic energy dominates over the potential energy, and the Hartree theory becomes exact taking the limit $r_s \rightarrow 0$. At the opposite extreme, very low densities $r_s \geq 20$, the electrostatic interaction dominates and the electrons tend to condensate on a Wigner lattice.² Taking into account the energy due to the vibrations of the electrons around their equilibrium positions, one obtains the energy per electron⁷⁰:

$$\epsilon_W = \left(\frac{-1.792}{r_s} + \frac{2.65}{r_s^{3/2}} - \frac{0.73}{r_s^2} \right) \text{ Ry}. \quad (23.4)$$

The Hartree and HF approximations provide some very useful results about the properties of the electron gas but fail in important aspects. If one attempts to improve on the HF approximation by using perturbation theory, one finds divergencies in every order. These divergencies derive from the long range of the Coulomb potential and the resulting singular behavior of its Fourier transform $4\pi e^2/q^2$. In the early fifties a systematic approach was developed by Bohm and Pines.²² They bypassed the diffi-

⁷⁰ W. J. Carr, Jr., R. A. Coldwell-Horsfall, and A. E. Fein, *Phys. Rev.* **124**, 747 (1961).

culties with perturbation theory by introducing collective coordinates and canonical transformations. In 1957 Gell-Mann and Brueckner²⁶ reexamined the perturbation series and showed how to sum the most divergent terms in each order to obtain a meaningful result, which they expressed as an expansion in r_s . Shortly after, Hubbard^{25,27} applied the field-theoretical approach and showed that the perturbation series could be written in powers of a screened interaction in such a way that no divergencies occurred.

We wish to emphasize strongly that, in spite of numerous statements in the literature to the opposite effect, the RPA method, the Gell-Mann and Brueckner r_s expansions, and the Green function methods using expansions in a screened interaction, are not at all equivalent. Indeed, when expanding in terms of a screened interaction, the expansion parameter in the Green function formulation is not r_s but rather something like $r_s/(1 + r_s)$, which at least indicates no breakdown when $r_s > 1$.^{25,27,71,72}

We shall start our discussion of the electron gas with the quantities we know best, namely, the total energy and the compressibility. We then turn to the more complicated properties than can be derived from first and second functional derivatives of the total energy, namely, the self-energy Σ and the Landau quasi-particle interaction function f . In the last section of this part we shall discuss different approximations for the dielectric function.

24. THE TOTAL ENERGY AND THE COMPRESSIBILITY

We shall in this section briefly review a few calculations of the energy of an electron gas, and the results for the compressibility which they imply. We do not discuss the total energy ϵ but rather the correlation energy ϵ_c , defined as the difference between the total energy and the HF energy (per electron in rydbergs) :

$$\epsilon = \frac{2}{3}\epsilon_F + \epsilon_{ex} + \epsilon_c. \quad (24.1)$$

We regard ϵ_c as a function of r_s rather than the density $\rho \sim r_s^{-3}$. We consider the positive background to be uniform and will not discuss questions such as mechanical instabilities and phase transitions of a jellium.⁷³ We will, however, comment on the possibilities of transitions from the paramagnetic state to the ferromagnetic state and to the Wigner lattice.

There is a simple relation derived by Hubbard²⁵ between the total energy and the imaginary part of the inverse dielectric function. The derivation of this relation is well known and we only briefly indicate the key arguments. By definition ϵ^{-1} involves the density-density correlation function, Eq. (12.10), and hence the expectation value of the potential energy can be

⁷¹ J. C. Phillips, *Phys. Rev.* **123**, 420 (1961).

⁷² D. J. W. Geldart, A. Houghton, and S. H. Vosko, *Can. J. Phys.* **42**, 1938 (1964).

⁷³ N. Wiser and M. H. Cohen, *J. Phys.* **C2**, 193 (1969).

expressed in terms of ϵ^{-1} . The total energy is obtained by integration over the interaction strength, a well-known procedure that is said to have first been used by Pauli. The integration over interaction strength can be transformed into an integration over r_s and ϵ_c written as

$$\epsilon_c = r_s^{-2} \int_0^{r_s} V_c(x) dx, \quad (24.2)$$

where V_c according to a theorem by Ferrell⁷⁴ always has a negative derivative.³⁷

We will introduce a few rather awkward formulas, which however are convenient for the following discussion. We write the relation between V_c and the dielectric function $\epsilon(q, \omega; r_s)$ in the form

$$V_c(r_s) = \frac{6}{\alpha\pi^2} \int_0^\infty q dq \int_0^\infty \left[\frac{\beta(q, w; r_s)}{1 + (4\alpha r_s/\pi)q^{-2}\beta(q, w; r_s)} - \beta_0(q, w) \right] dw,$$

$$\epsilon(q, iw; r_s) = 1 + (4\alpha r_s/\pi)q^{-2}\beta(q, w/2q; r_s). \quad (24.3)$$

Here $\beta(q, w; r_s)$ is a real function of order unity which for the case of the Lindhard dielectric function equals

$$\beta_0(q, w) = \frac{1}{2} + \frac{w^2 + 1 - q^2/4}{4q} \ln \frac{w^2 + (1 + \frac{1}{2}q)^2}{w + (1 - \frac{1}{2}q)^2}$$

$$- \frac{1}{2}w \left[\arctan \frac{1 + \frac{1}{2}q}{w} + \arctan \frac{1 - \frac{1}{2}q}{w} \right]. \quad (24.4)$$

In the limit of small q we have

$$\lim_{q \rightarrow 0} \beta_0(q, w) = \beta_0(w) = 1 - w \arctan w^{-1}. \quad (24.5)$$

We now make a comparison between the Hubbard²⁷ and the Gell-Mann and Brueckner²⁸ calculations of the energy.

Hubbard calculated the correlation energy using the Lindhard dielectric function,⁷⁵ and then improved the result slightly by approximately including higher order exchange effects. Gell-Mann and Brueckner's infinite summation of the "ring diagrams" mentioned in the previous section gave a result for the energy equivalent to using the Lindhard dielectric function. Unlike Hubbard, however, they did not evaluate this result at metallic densities but only gave a representation of it in terms of $\log r_s$ and r_s that is valid in the limit of small r_s . We give a brief demonstration of the Gell-Mann and

⁷⁴ R. A. Ferrell, *Phys. Rev. Letters* **1**, 443 (1958).

⁷⁵ The Lindhard dielectric function satisfies the Ferrell criterion as shown by Hedin³⁷ and by S. Misawa, *Progr. Theoret. Phys.* **39**, 1426 (1968).

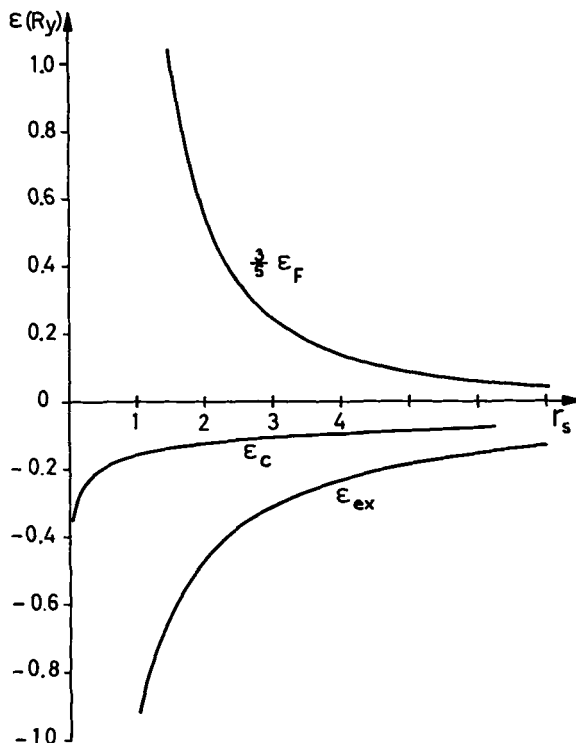


FIG. 12. The correlation energy calculated from the Lindhard dielectric function compared to the HF energy, $\frac{3}{2}\epsilon_F + \epsilon_{ex}$.

Brueckner derivation. With β replaced by β_0 we obtain for V_c the formula

$$V_c(r_s) = -\frac{12r_s}{\pi^3} \int_0^\infty d(q^2) \int_0^\infty \frac{\beta_0^2(q, w)}{q^2 + (4\alpha r_s/\pi)\beta_0(q, w)} dw. \quad (24.6)$$

While Hubbard made a numerical calculation of V_c and ϵ_c , Gell-Mann and Breuckner only considered the leading terms in a high density expansion. This was done by splitting the integration over q in two intervals, $0 \rightarrow 1$ and $1 \rightarrow \infty$. The last integral gives rise to a well-behaved power series in r_s and contributes a constant in leading order. In the first interval, $0 \rightarrow 1$, one can replace $\beta_0(q, w)$ by the small q limit $\beta_0(w)$. The integration over q can then be done analytically and gives

$$V_c(r_s) = -\frac{12r_s}{\pi^3} \int_0^\infty \beta_0^2(w) \ln \frac{1 + (4\alpha r_s/\pi)\beta_0(w)}{(4\alpha r_s/\pi)\beta_0(w)} dw. \quad (24.7)$$

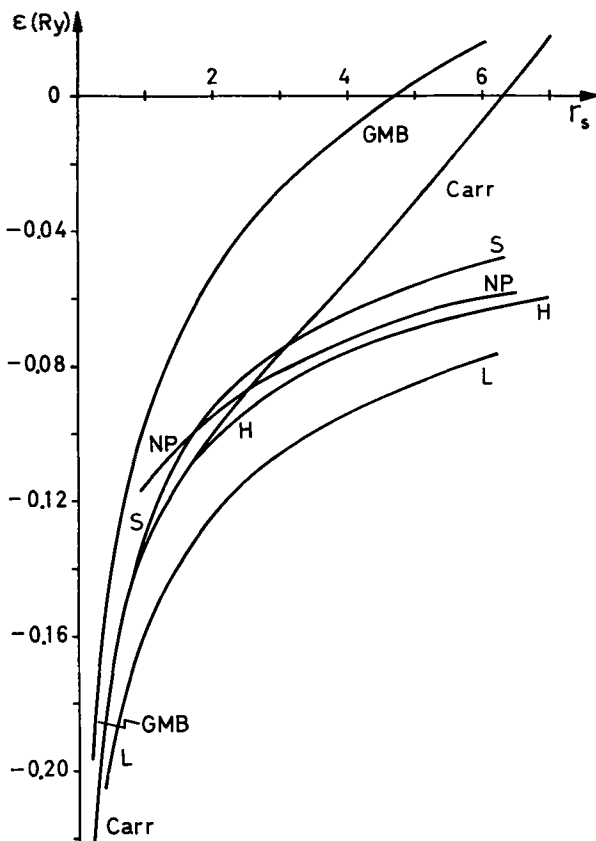


FIG. 13. Results from different calculations of the correlation energy. GMB: M. Gell-Mann and K. Brueckner, *Phys. Rev.* **106**, 364 (1957). Carr: W. J. Carr, Jr., and A. A. Maradudin, *Phys. Rev.* **133**, A371 (1964). S: K. S. Singwi, M. P. Tosi, R. H. Land, and A. Sjölander, *Phys. Rev.* **176**, 589 (1968). NP: P. Nozières and D. Pines, *Phys. Rev.* **111**, 442 (1958). H: J. Hubbard, *Proc. Roy. Soc. A* **243**, 336 (1957). L: Lindhard dielectric constant.

The leading contribution to V_c in the limit of small r_s is clearly proportional to $r_s \ln r_s$, which according to Eq. (24.2) contributes a $\ln r_s$ term to ϵ_c .

In Fig. 12 we have plotted the result of a numerical integration using the Lindhard function and as a comparison $\frac{2}{3}\epsilon_F$ and ϵ_{ex} are also shown. The narrow dip in the ϵ_c curve for small r_s is due to the $\ln r_s$ singularity. In Fig. 13 the same curve, marked L, is redrawn on a larger scale and is compared with other calculations. The curve marked GMB gives the result of Gell-Mann and Brueckner⁷⁶ in the high density limit. Carr and Maradudin⁷⁶

⁷⁶ W. J. Carr, Jr., and A. A. Maradudin, *Phys. Rev.* **133**, A371 (1964).

TABLE II. VALUES OF THE COMPRESSIBILITY RATIO κ_F/κ FROM EQ. (24.9)

$r_s:$	1	2	3	4	5	6
HF ^a	0.83	0.67	0.50	0.34	0.17	0.00
L ^b	0.83	0.64	0.45	0.24	0.03	-0.19
NP ^c	0.83	0.65	0.46	0.27	0.07	-0.15
H ^d	0.83	0.65	0.46	0.26	0.06	-0.15
W ^e	0.83	0.66	0.48	0.29	0.09	-0.13
S ^f	0.83	0.64	0.45	0.25	0.05	-0.17

^a Hartree-Fock approximation.^b Lindhard dielectric function.^c P. Nozières and D. Pines, *Phys. Rev.* **111**, 442 (1958).^d J. Hubbard, *Proc. Roy. Soc. A* **243**, 336 (1957).^e E. P. Wigner, *Trans. Faraday Soc.* **34**, 678 (1938).^f K. S. Singwi, M. P. Tosi, R. H. Land, and A. Sjölander, *Phys. Rev.* **176**, 589 (1968).

improved on the GMB result by including some higher order diagrams. The r_s expansions fail badly at metallic densities. The curves marked NP and H refer to interpolation results by Nozières and Pines⁷⁷ and Hubbard⁷⁷ and are generally believed to be quite accurate. The recently given modification of the dielectric function by Singwi *et al.*⁷⁸ is denoted by S and gives values that seem slightly high. A detailed discussion of the accuracy of the different energy curves is given by Pines.⁷⁸ The conclusion from the numerical comparison in Fig. 13 seems to be that the various approximation schemes give results that are consistent within 0.01–0.02 Ry over a large density interval covering the full range of metallic densities.

The curve for ϵ_c in Fig. 12 is remarkably flat compared with the variations in $\frac{2}{3}\epsilon_F$ and ϵ_{ex} , except for the singular dip at small r_s . This dip is, however, only of little importance, since it is very small compared to the much stronger singularities in the other energy terms. The insensitivity of the correlation energy to the density is a well-known empirical fact for atoms.⁷⁹

Due to the small density variation of ϵ_c , the correlation gives only a small contribution to the compressibility, which is given by the formula

$$\kappa^{-1} = -\Omega \frac{\partial P}{\partial \Omega} = \frac{P_0}{r_s^2} \left(r_s \frac{d^2 \epsilon}{dr_s^2} - 2 \frac{d \epsilon}{dr_s} \right), \quad (24.8)$$

where $P_0 = 75 \cdot 10^{11}$ dyn/cm². In terms of the compressibility in the Hartree

⁷⁷ P. Nozières and D. Pines, *Phys. Rev.* **111**, 442 (1958).⁷⁸ D. Pines, "Elementary Excitations in Solids," Benjamin, New York, 1963.⁷⁹ E. Clementi, *J. Chem. Phys.* **38**, 2248 (1963); **39**, 175 (1963). If we consider the correlation energy per electron for neutral atoms from He to Ar, we find a rather constant value of 0.075 Ry. Also the correlation energy within one isoelectronic series stays fairly constant over a wide range of electron densities.

approximation ($\kappa_F \sim r_s^5$), we obtain

$$\frac{\kappa_F}{\kappa} = 1 - \frac{\alpha r_s}{\pi} + \frac{\alpha^2 r_s^3}{6} \left(r_s \frac{d^2 \epsilon_c}{dr_s^2} - 2 \frac{d \epsilon_c}{dr_s} \right). \quad (24.9)$$

In Table II we give values of κ_F/κ calculated using different expressions for the correlation energy. Since the contribution from ϵ_c is quite small and not very sensitive to the approximation used, the compressibility of an electron gas is known fairly accurately.

We note that the compressibility becomes negative at $r_s \approx 5$, that is, at about twice the equilibrium volume ($r_s \approx 4$). The instability has the consequence that the dielectric response function $\epsilon(q, 0)$ tends to $-\infty$ instead of $+\infty$ for $q \rightarrow 0$. This anomaly seems to have little influence on properties such as the screening of a point charge (see Section 27). It could, however, in principle effect plasma vibrations which are long-wavelength phenomena. It should also be noted that the compressibility of real solids, due to the presence of the ions, has little relation to that of the electron gas. The trends of the two compressibilities as functions of r_s are actually opposite.⁸⁰

Many attempts have been made to estimate for what r_s a transition from the paramagnetic to the ferromagnetic state might occur. It seems that the transition is very unlikely to occur for $r_s < 7$,⁸¹ and probably does not come⁸¹ until at $r_s = 10$, or perhaps not until $r_s = 19$.⁸² The transition to the Wigner lattice has been proposed to occur at $r_s \cong 20$,^{28,77} $r_s \cong 50$,⁸³ and $r_s \cong 30$.⁸⁴ Both types of transitions thus seem to occur (if they occur, which is not quite certain) at such low densities that they are of minor direct interest.

25. THE ELECTRON SELF-ENERGY

a. Introductory Remarks

In this section we shall discuss in considerable detail the overall properties of the self-energy as a function of both momentum and frequency. We shall also discuss the structure of the spectral weight function for electrons and holes, review results obtained for the momentum distribution and the density of states, and comment on the damping and dispersion

⁸⁰ N. W. Ashcroft and D. C. Langreth, *Phys. Rev.* **155**, 682 (1967).

⁸¹ S. Misawa, *Phys. Rev.* **140**, A1645 (1965); S. F. Edwards and A. J. Hillel, *J. Phys. C1*, 61 (1968).

⁸² Y. Osaka, *J. Phys. Soc. (Japan)* **22**, 1513 (1967).

⁸³ F. W. de Wette, *Phys. Rev.* **135**, A287 (1964).

⁸⁴ H. M. Van Horn, *Phys. Rev.* **157**, 342 (1967).

of quasi-particle states, and also discuss "plasmaron" excitations. The discussion of Fermi surface properties will be deferred to the next section.

Most of our present knowledge about the self-energy $\Sigma(\mathbf{k}, \omega)$ has been based on calculations, where vertex corrections have been neglected, i.e. using the formula⁸⁵

$$\Sigma(\mathbf{k}, \omega) = (i/(2\pi)^4) \int e^{i\omega' t} W(\mathbf{k}', \omega') G(\mathbf{k} + \mathbf{k}', \omega + \omega') d\mathbf{k}' d\omega'. \quad (25.1)$$

In applications of this formula one has often introduced further approximations such as replacing G by the zero order approximation G_0 and using the time-dependent Hartree approximation or even further approximations thereof when calculating the screened interaction W .

It has often been remarked that Eq. (25.1) is valid only at high densities and that the effect of vertex corrections may be so large at metallic densities that the results are no longer meaningful. One has, however, to remember that our present understanding of one-electron properties is based mainly on Hartree or HF type approximations, the validity of which, using the same kind of argument, is even much more restricted. We take a more optimistic point of view and would like to emphasize that Eq. (25.1) represents a major step beyond the HF approximation by including dynamical effects of the interaction. The dynamical effects give rise to important features that are not accounted for by a HF type theory, such as damping of quasi particles and characteristic structure in the spectral function. We believe that the effects in their gross features are described in a physically and qualitatively acceptable way by Eq. (25.1) over a considerable density range, and that while vertex corrections might give rise to new unknown features, their main effect would be numerical changes, not qualitative changes. We cannot of course substantiate our belief with any kind of rigorous mathematical proof, but we would like to mention some rather direct evidence from calculations over a density range up to $r_s \sim 5-6$, which support our point of view: (i) The next term in the expansion of Σ in powers of W , schematically $GWGWG$, gives a small contribution compared to GW . (ii) The value of the chemical potential is given quite well by Eq. (25.1). (iii) The gross properties of Σ are very insensitive to the form of the dielectric function used when calculating $W = v\epsilon^{-1}$, as long as ϵ^{-1} has a plasmon pole and the sum rule for the oscillator strength is satisfied. (iv) If the Dyson equation is solved by iteration starting with $\Sigma_1 = WG_0$, one finds that the second iteration, $\Sigma_2 = WG_1$, with $G_1 = (\omega - \epsilon_k - \Sigma_1)^{-1}$ differs fairly little from Σ_1 .

⁸⁵ The first comprehensive discussion of this approximation for Σ was given by J. J. Quinn and R. A. Ferrell, *Phys. Rev.* **112**, 812 (1958), however only in the small r_s limit.

b. Formal Discussion of the Self-Energy

We first illustrate the convergence properties of the present approach. Each new term in an expansion of Σ in powers of W adds a dimensionless factor $(2\pi)^{-4}GGW dk d\omega$. Using the facts that the scales for energy and momentum are given by ϵ_F and k_F , respectively, we find that the dimensionless factor will be of the order

$$\frac{1}{(2\pi)^4} \frac{1}{\epsilon_F} \frac{1}{\epsilon_F} \frac{4\pi e^2}{k_F^2 + k_{TF}^2} \frac{4\pi k_F^3}{3} \epsilon_F = \frac{1}{6\pi} \frac{\lambda}{1 + \lambda}, \quad (25.2)$$

where k_{TF} is the inverse Thomas-Fermi screening length

$$k_{TF}^2 = \lambda k_F^2; \quad \lambda = 4\alpha r_s/\pi \approx 0.66r_s. \quad (25.3)$$

The expansion parameter is therefore of the order $\lambda(1 + \lambda)^{-1}$. If we were considering an r_s expansion, we would expand $\lambda(1 + \lambda)^{-1}$ into $\lambda - \lambda^2 + \lambda^3 \dots$, and would have no reason to expect convergence in the metallic density region. The argument we have given is of course only indicative of how things may go. Both G and W have poles and the integrand is highly singular. Still, when the frequency integrations are done, the result turns out to be built from factors of the type in Eq. (25.2), both for the first order and the second order terms. The second order terms are further fairly small on the average, meaning that where peaks occur in $\text{Im } \Sigma(\omega)$, the integrated strength is small.⁸⁶

In connection with point (ii), we notice that the chemical potential is related to the energy per electron by the relation⁸⁷

$$\mu = \epsilon - \frac{r_s}{3} \frac{d\epsilon}{dr_s} = \frac{1}{\alpha^2 r_s^2} - \frac{2}{\pi \alpha r_s} + \epsilon_c - \frac{r_s}{3} \frac{d\epsilon_c}{dr_s}. \quad (25.4)$$

In Table III are given values for $\mu - \epsilon_F$ obtained using Eq. (25.4) with the different expressions for ϵ_c defined in Table II. Also listed are the values obtained by solving the Dyson equation with Σ from Eq. (25.1):

$$\mu = \epsilon_F + \Sigma(k_F, \mu). \quad (25.5)$$

Two approximations for W were used, one with the LTH dielectric function⁸⁷ and one with a simplified formula only containing the plasmon pole.⁸⁸ In both calculations the approximation $G_0 = (\omega - \epsilon_k)^{-1}$ was used. The values obtained agree with each other within 5%.

Certain characteristic features of the real and imaginary parts of Σ

⁸⁶ L. Hedin, (to be published).

⁸⁷ F. Seitz,⁴ p. 343.

⁸⁸ B. I. Lundqvist, *Physik Kondensierten Materie* **6**, 206 (1967).

TABLE III. CORRELATION AND EXCHANGE CONTRIBUTIONS $\mu - \epsilon_F$
TO THE CHEMICAL POTENTIAL IN RY

	$r_s:$	1	2	3	4	5	6
Eq. (25.4)	L ^a	-1.398	-0.750	-0.527	-0.411	-0.340	-0.294
	H ^a	-1.370	-0.727	-0.506	-0.392	-0.324	-0.278
	S ^a	-1.364	-0.718	-0.496	-0.381	-0.311	-0.266
	W ^a	-1.326	-0.707	-0.498	-0.388	-0.323	-0.282
Eq. (25.5)	L ^a	-1.397	-0.749	-0.526	-0.411	-0.341	-0.293
	PP ^b	-1.382	-0.738	-0.516	-0.403	-0.333	-0.286

^a See Table II.

^b Plasmon pole dielectric constant, see Eq. (25.11).

follow from quite general considerations and we shall discuss this before surveying detailed calculations. The self-energy has a spectral resolution

$$\Sigma(\mathbf{k}, \omega) = \epsilon_{\mathbf{k}}^{\text{ex}} + \frac{1}{\pi} \int_C \frac{|\text{Im } \Sigma(\mathbf{k}, \omega')|}{\omega - \omega'} d\omega', \quad (25.6)$$

where C is the contour shown in Fig. 2. The quantity $\epsilon_{\mathbf{k}}^{\text{ex}}$ is a HF exchange potential in which the true momentum distribution $n(\mathbf{k})$ appears:

$$\epsilon_{\mathbf{k}}^{\text{ex}} = - \sum_{\mathbf{k}'} v(\mathbf{k}') n(\mathbf{k} - \mathbf{k}'). \quad (25.7)$$

It follows from a general consideration that in the neighborhood of the Fermi surface⁸⁹

$$|\text{Im } \Sigma(\mathbf{k}, \omega)| \sim (\omega - \mu)^2. \quad (25.8)$$

If no additional structure occurs in $|\text{Im } \Sigma|$, it will look like in Fig. 14. Using the dispersion relation in Eq. (25.6) one concludes that $\text{Re } \Sigma(\mathbf{k}, \omega)$ must have the qualitative form given in the same figure. In particular, $\text{Re } \Sigma$ must have at least two maxima and two minima. We also see that $(\partial \Sigma(\mathbf{k}, \omega) / \partial \omega) < 1$ at $\omega = \mu$, which is necessary for the interpretation of the theory, since the renormalization constant Z in Eq. (11.2), $Z = (1 - \partial \Sigma / \partial \omega)^{-1}$, which is equal to the step in the $n(\mathbf{k})$ distribution, obviously must be smaller than unity, cf. Fig. 6.

We next turn to a more detailed discussion of the self-energy. The difference between the approximation in Eq. (25.1), symbolically $GW = Gv\epsilon^{-1}$, and the HF approximation Gv shows up most clearly in the small q behavior of $v(\mathbf{q})\epsilon^{-1}(\mathbf{q}, \omega)$. It is convenient to study $\text{Im } \epsilon^{-1}(\mathbf{q}, \omega)$ and then obtain $\text{Re } \epsilon^{-1}(\mathbf{q}, \omega)$ using the dispersion relation. In Fig. 1 we have drawn

⁸⁹ J. M. Luttinger, *Phys. Rev.* **121**, 942 (1961).

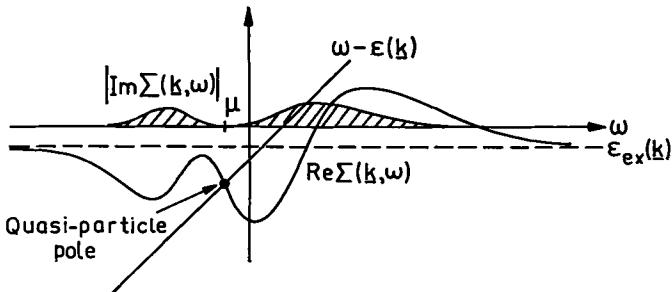


FIG. 14. Qualitative behavior of the self-energy Σ deduced from general principles.

the regions in (\mathbf{q}, ω) space where the LTH result for $\text{Im } \epsilon(\mathbf{q}, \omega)$ is nonzero. $\text{Im } \epsilon^{-1}(\mathbf{q}, \omega)$ is nonzero in the same regions and also along the plasmon line $\epsilon(\mathbf{q}, \omega) = 0$, where it has a δ -function contribution. The exact $\text{Im } \epsilon^{-1}(\mathbf{q}, \omega)$ will for small q behave as indicated in Fig. 15. The small bump at low energies is associated with particle-hole scattering. These processes have little weight because of phase-space limitations, and the plasmon state will at small q essentially exhaust the sum rule [ω_p is defined in Eq. (5.35)]

$$\int_0^\infty \omega \text{Im } \epsilon^{-1}(\mathbf{q}, \omega) d\omega = -(\pi/2)\omega_p^2. \quad (25.9)$$

In some applications one does not need the full dielectric function or the LTH dielectric function. An approximation, which we have found most useful, is to take a plasmonlike sharp absorption for all \mathbf{q} according to the choice

$$\text{Im } \epsilon^{-1}(\mathbf{q}, \omega) = -(\pi/2)[\omega_p^2/\omega_1(\mathbf{q})]\delta[\omega - \omega_1(\mathbf{q})], \quad (25.10)$$

which gives

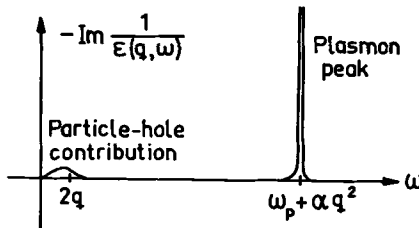
$$[\epsilon(\mathbf{q}, \omega)]^{-1} = 1 + \{\omega_p^2/[\omega^2 - \omega_1^2(\mathbf{q})]\}. \quad (25.11)$$

The quantity $\omega_1(\mathbf{q})$ must reduce to ω_p in the limit when $q \rightarrow 0$ and be proportional to q^2 for large q (cf. Fig. 1). In energy momentum units of ϵ_F and k_F , we choose the dispersion law:

$$\omega_1^2(q) = \omega_p^2 + (16/3)q^2 + q^4; \quad \omega_p = 4(\alpha r_s/3\pi)^{1/2}, \quad (25.12)$$

which gives for the dielectric function itself

$$\epsilon(q, \omega) = 1 + k_{TF}^2/[q^2 + (3/16)(q^4 - \omega^2)]; \quad k_{TF} = (4\alpha r_s/\pi)^{1/2}. \quad (25.13)$$

FIG. 15. Qualitative behavior of $\text{Im } \epsilon^{-1}(q\omega)$ for small q .

The coefficient $16/3$ in the quadratic term is a bit larger than the Lindhard value $12/5$, but we have chosen to sacrifice this in order to obtain the correct static limit for $\epsilon(q, 0)$ when $q \rightarrow 0$. The results are quite insensitive to the particular dispersion coefficient that is used. Using this simple type of dielectric function one can perform the frequency integration in Eq. (25.1) and obtain

$$\begin{aligned} \Sigma(\mathbf{k}, \omega) = & -\frac{1}{(2\pi)^3} \int d\mathbf{q} \frac{v(\mathbf{q}) n(\mathbf{k} + \mathbf{q})}{\epsilon[\mathbf{q}, \epsilon(\mathbf{k} + \mathbf{q}) - \omega]} \\ & - \frac{\omega_p^2}{(2\pi)^3} \int \frac{v(\mathbf{q})}{2\omega_1(\mathbf{q})} \frac{d\mathbf{q}}{\omega_1(\mathbf{q}) + \omega - \epsilon(\mathbf{k} + \mathbf{q})}. \end{aligned} \quad (25.14)$$

The first term in Eq. (25.14) is a screened exchange potential and the second term describes the Coulomb hole (cf. Section 14).

Let us first consider the behavior approximately at the quasi-particle peak, i.e. put $\omega = \epsilon_{\mathbf{k}}$. It is evident that the screened potential $W(\mathbf{q}, \epsilon_{\mathbf{k}+\mathbf{q}} - \epsilon_{\mathbf{k}})$ has a finite limit when $q \rightarrow 0$. Therefore the screened exchange term gives no anomaly like the unscreened HF exchange. The Coulomb hole term has a smooth \mathbf{k} dependence, and therefore $\Sigma(\mathbf{k}, \epsilon_{\mathbf{k}})$ varies smoothly as a function of \mathbf{k} .

Let us next consider the self-energy as function of ω for fixed \mathbf{k} . It is sufficient to use the simplified dielectric function in Eq. (25.13) to demonstrate the key features which are indeed similar to those of the polaron problem. Performing the frequency integration in Eq. (25.1), we obtain

$$\begin{aligned} \text{Im } \Sigma(\mathbf{k}, \omega) = & \frac{\pi \omega_p^2}{2} \frac{1}{(2\pi)^3} \int \frac{v(\mathbf{q}) d\mathbf{q}}{\omega_1(\mathbf{q})} \{ n_{\mathbf{k}+\mathbf{q}} \delta(\epsilon_{\mathbf{k}+\mathbf{q}} - \omega_1(\mathbf{q}) - \omega) \\ & - (1 - n_{\mathbf{k}+\mathbf{q}}) \delta(\epsilon_{\mathbf{k}+\mathbf{q}} + \omega_1(\mathbf{q}) - \omega) \}. \end{aligned} \quad (25.15)$$

From the restrictions in the integration region we see that $\text{Im } \Sigma(\mathbf{k}, \omega) = 0$ for $\mu - \omega_p < \omega < \mu + \omega_p$. Performing the integrations we find that $\text{Im } \Sigma(\mathbf{k}, \omega)$ has a logarithmic singularity at $\omega = \epsilon_{\mathbf{k}} - \omega_p$ ($k < k_F$) and

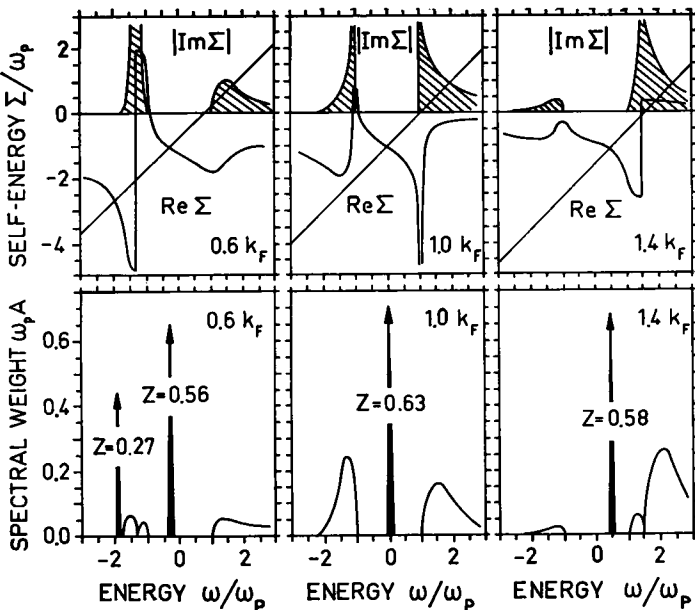


FIG. 16. The self-energy Σ and the corresponding spectral function A for $r_s = 5$ calculated with the plasmon-pole dielectric function by B. I. Lundqvist, *Physik Kondensierter Materie* 6, 193 (1967). The crossings between the straight line and $\text{Re } \Sigma$ give the solutions of the Dyson equation.

at $\omega = \epsilon_k + \omega_p$ ($k > k_F$). Logarithmic singularities in $\text{Im } \Sigma(\mathbf{k}, \omega)$ give rise to finite discontinuities in the real part, as can be verified using the dispersion relation. We summarize this behavior in the following relations:

$$\begin{cases}
 \begin{aligned}
 &\text{Im } \Sigma(\mathbf{k}, \omega) \cong -\frac{\omega_p}{2ka_0} \ln |\epsilon_k - \omega_p - \omega| \\
 &\text{Re } \Sigma(\mathbf{k}, \omega) \text{ has a step} = \frac{\pi\omega_p}{2ka_0}
 \end{aligned} \\
 k < k_F, \quad \omega \cong \epsilon_k - \omega_p:
 \end{cases} \quad (25.16)$$

$$\begin{cases}
 \begin{aligned}
 &\text{Im } \Sigma(\mathbf{k}, \omega) \cong \frac{\omega_p}{2ka_0} \ln |\epsilon_k + \omega_p - \omega| \\
 &\text{Re } \Sigma(\mathbf{k}, \omega) \text{ has a step} = \frac{\pi\omega_p}{2ka_0}.
 \end{aligned} \\
 k > k_F, \quad \omega \cong \epsilon_k + \omega_p:
 \end{cases}$$

For $k = k_F$ the finite discontinuity in $\text{Re } \Sigma$ becomes a logarithmic singularity. This behavior of the electron gas and its implications seems to have been first noticed and discussed by Hedin *et al.*⁹⁰ and has been studied in

⁹⁰ L. Hedin, B. I. Lundqvist, and S. Lundqvist, *Solid State Comm.* 5, 237 (1967).

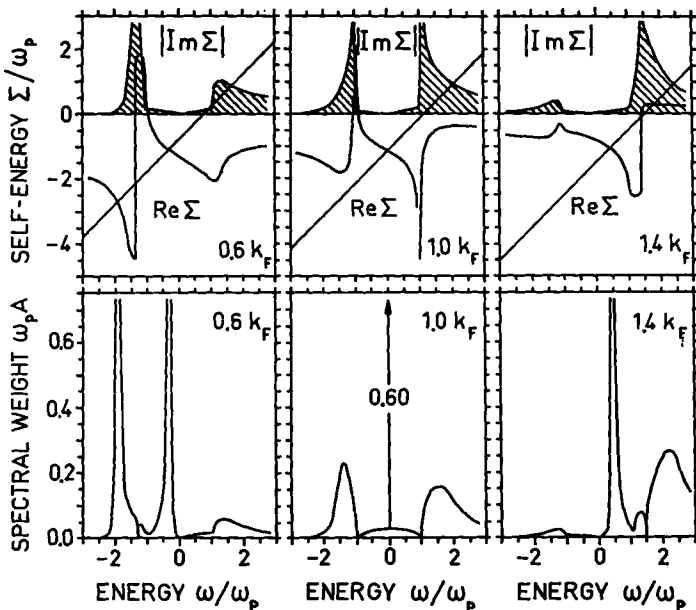


FIG. 17. The self-energy Σ and the corresponding spectral function A for $r_s = 5$ calculated with the Lindhard dielectric function by B. I. Lundqvist, *Physik Kondensierten Materie* 7, 117 (1968).

detail by Lundqvist. Typical curves for Σ obtained with this dielectric function are shown in the upper half of Fig. 16.⁹¹ Typical results when the full Lindhard dielectric function is used are shown in the upper part of Fig. 17.⁹² The difference is due mainly to the effects of particle hole excitations in the frequency region $\mu - \omega_p < \omega < \mu + \omega_p$, which are not described by the simplified form of the dielectric function.

c. Structure of the Spectral Function

The propagation and damping of quasi particles are determined by the peaks in the spectral function $A(\mathbf{k}, \omega)$, as discussed in Part VI. In the lower parts of Figs. 16 and 17 we have given the results for $A(\mathbf{k}, \omega)$ corresponding to the upper parts as calculated from the general formula Eq. (10.9):

$$\begin{aligned} A(\mathbf{k}, \omega) &= \pi^{-1} |\operatorname{Im} G(\mathbf{k}, \omega)| \\ &= \pi^{-1} \frac{|\operatorname{Im} \Sigma(\mathbf{k}, \omega)|}{|\omega - \epsilon_{\mathbf{k}} - \operatorname{Re} \Sigma(\mathbf{k}, \omega)|^2 + |\operatorname{Im} \Sigma(\mathbf{k}, \omega)|^2}. \end{aligned} \quad (25.17)$$

⁹¹ B. I. Lundqvist, *Physik Kondensierten Materie* 6, 193 (1967).

⁹² B. I. Lundqvist, *Physik Kondensierten Materie* 7, 117 (1968).

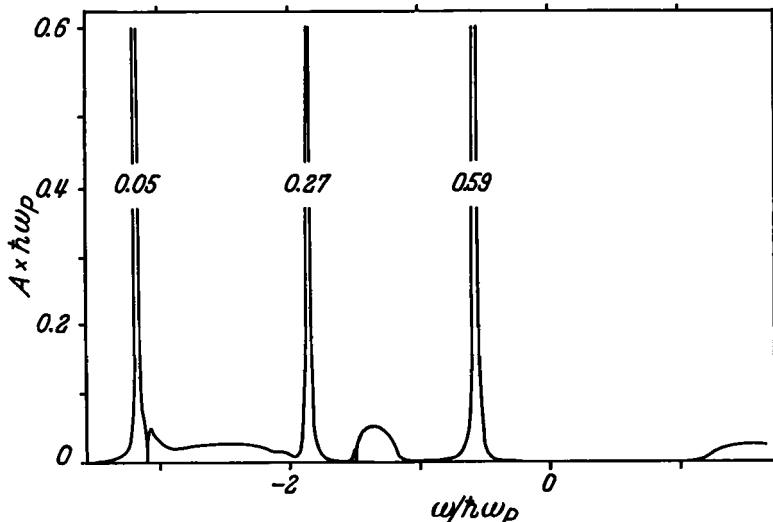


FIG. 18. Typical behavior of the spectral function A at low momenta according to a second iteration of the Dyson equation ($r_s = 4$, $k = 0.2k_F$) from B. I. Lundqvist, *Physik Kondensierten Materie* **6**, 206 (1967).

For $\text{Im } \Sigma$ infinitesimal, the peak becomes a δ -function,

$$A(\mathbf{k}\omega) = \delta(\omega - \epsilon_{\mathbf{k}} - \Sigma(\mathbf{k}\omega)) = Z \delta(\omega - E_{\mathbf{k}}).$$

The strength Z of the peak is given by the quasi-particle renormalization factor $Z = (1 - \partial\Sigma/\partial\omega)^{-1}$, and the energy $E_{\mathbf{k}}$ by the Dyson equation $E_{\mathbf{k}} = \epsilon_{\mathbf{k}} + \Sigma(\mathbf{k}, E_{\mathbf{k}})$.

For $k = k_F$ there is only one strong peak in the spectral function, corresponding to the usual quasi particle. For the other k values in the figures, we find three solutions of the Dyson equation $\omega - \epsilon_{\mathbf{k}} - \text{Re } \Sigma(\mathbf{k}, \omega) = 0$. One of them, however, falls at $\omega = \epsilon_{\mathbf{k}} \pm \omega_p$ where the damping is infinite (or very strong in a more refined treatment), and therefore this solution will be totally (or partly) suppressed. Of the two remaining solutions, one corresponds to the usual quasi particle, i.e. a bare particle surrounded by a cloud of virtual plasmons and particle-hole excitations. The new state has an energy lower than that corresponding to a hole plus a plasmon, i.e., $\epsilon_{\mathbf{k}} - \omega_p$. The new peak describes a resonant coupling between a hole and plasmons of different wavelengths and may be thought of as a hole coupled to a cloud of real plasmons. This coupled plasma-electron state which we call a *plasmaron*, has a large "oscillator strength" with respect to one-particle excitations. It will be discussed further in connection with soft X-ray emission in Section 39.

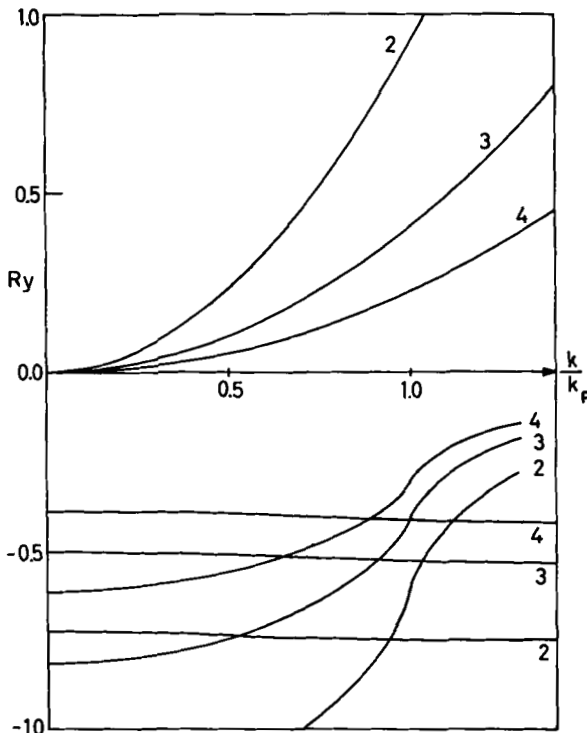


FIG. 19. Quasi-particle energy $E(k)$ from L. Hedin, *Phys. Rev.* **139**, A796 (1965). The upper curves show the kinetic part $\epsilon(k)$ and the lower curves the exchange-correlation part $V(k)$, of Eq. (25.18). The r_s value is marked on each curve. The almost flat $V(k)$ curves include both correlation and exchange, while the curves with a logarithmic singularity in their derivative at $k = k_F$ only include exchange (HF approximation).

Before discussing the physical implications, we will remark on the question of how much the results depend on the approximations used to calculate the self-energy. The characteristic structure of the spectral function has to do with the possibility to have more than one solution of the Dyson equation. This in turn has to do with the existence of a strong resonance in the system, or equivalently a strong peak in $\text{Im } \Sigma$, and these features are qualitatively not very sensitive to the approximations used. For example, using the exact dielectric function and the exact Green function would scale down the peak in $\text{Im } \Sigma$ by the renormalization constant Z and broaden it due to the broadening of the quasi-particle peak in G and the plasmon width in ϵ^{-1} . No drastic changes in the results would result from this. The type of change to be expected from the use of G rather than G_0

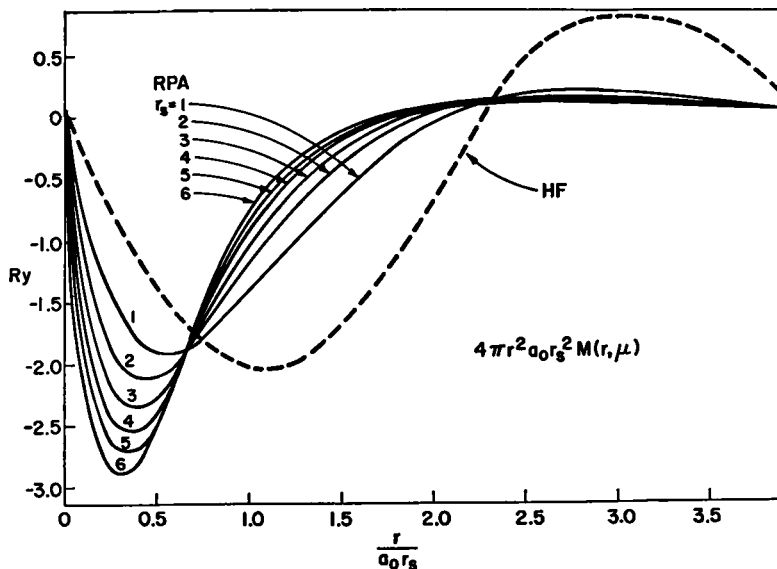


FIG. 20. Self-energy operator M ($= \Sigma$) as a nonlocal potential for particles at the Fermi surface, $(\Sigma\varphi)_r = \int \Sigma(\mathbf{r} - \mathbf{r}'; \mu)\varphi(\mathbf{r}') d\mathbf{r}'$, from L. Hedin, *Phys. Rev.* **139**, A796 (1965).

is illustrated in Fig. 18, which gives the spectral function A calculated with

$$\Sigma = [\omega - \epsilon_{\mathbf{k}} - \Sigma_1(\mathbf{k}, \omega)]^{-1} v \epsilon^{-1}, \text{ where } \Sigma_1 = G_0 v \epsilon^{-1}.$$

For the dielectric function, the plasmon pole approximation defined in Eq. (25.13) was used.⁸⁸

The possible influence of vertex corrections is difficult to assess rigorously, but work by Layzer⁸⁸ indicates that the vertex function varies slowly in the region of importance. Direct estimates of the lowest order correction to the GW approximation, Eq. (25.1), gives only a relatively small result, which acts to slightly sharpen the plasmaron peak.⁸⁶ We conclude this section by summarizing some of the results of physical interest that has followed from calculations of the self-energy.

d. Quasi-Particle Dispersion Law

After solving the Dyson equation one can write the resulting quasi-particle energy in the form

$$E(\mathbf{k}) = \epsilon(\mathbf{k}) + V(\mathbf{k}) \quad (25.18)$$

⁸⁸ A. J. Layzer, *Phys. Letters* **13**, 121 (1964); *Ann. Phys. (N. Y.)* **35**, 67 (1965).

TABLE IV. BANDWIDTH OF AN ELECTRON GAS IN Ry

r_s :	1	2	3	4	5	6
H ^a	3.683	0.921	0.409	0.230	0.147	0.102
L ^b -H ^a	0.073	-0.021	-0.024	-0.020	-0.017	-0.014
PP ^c -H ^a	0.087	-0.006	-0.013	-0.012	-0.010	-0.008
HF ^d -H ^a	1.222	0.611	0.407	0.305	0.244	0.204

^a Sommerfeld or Hartree model.^b Lindhard dielectric function in $\Sigma = G_0 W$. L. Hedin, *Phys. Rev.* **139**, A796 (1965).^c Plasmon pole dielectric function in $\Sigma = G_0 W$. B. I. Lundqvist, *Physik Kondensierten Materie* **6**, 206 (1967).^d Hartree-Fock approximation, $\Sigma = G_0 v$.

where $V(\mathbf{k})$ can be interpreted as an effective exchange and correlation potential for quasi-particle states. Figure 19 shows the results by Hedin³⁷ for several metallic densities. The HF results for $V(\mathbf{k})$ are shown as a comparison. It is remarkable how the interactions wipe out essentially all \mathbf{k} dependence and leave a potential that is almost constant. That means that the effective interaction in ordinary space is almost local. This is shown in Fig. 20 giving Σ as a nonlocal potential for particles at the Fermi surface.³⁷ These results provide some a posteriori justification for simplified procedures in energy band calculations where the effects of exchange and correlation have been simulated using a local potential, such as e.g. the Slater exchange potential. The constancy of $V(\mathbf{k})$ further indicates that there will be no serious distortions of the shape of energy band curves in simple metals due to many-electron interactions. Some further electron gas results on this point are given in Sect. 38, which deals with local density approximations.

e. Bandwidths

One may ask how much the bandwidth for the quasi-particle band differs compared to the Sommerfeld model. In Table IV we compare the results obtained with $\Sigma = 0$, and two approximations using Eq. (25.1), one with the full Lindhard dielectric function and the other using the simplified formula Eq. (25.13). The numbers indicate that the effects of exchange and correlation decreases the bandwidth by about 5% at metallic densities. Such a small effect cannot be considered as significant and we conclude that bandwidths are not influenced by exchange and correlation within the accuracy of the theory. For comparison, the HF values are also given, and we see that if only exchange but not correlation were included, the bandwidth would become too large at metallic densities by roughly a factor of 2.

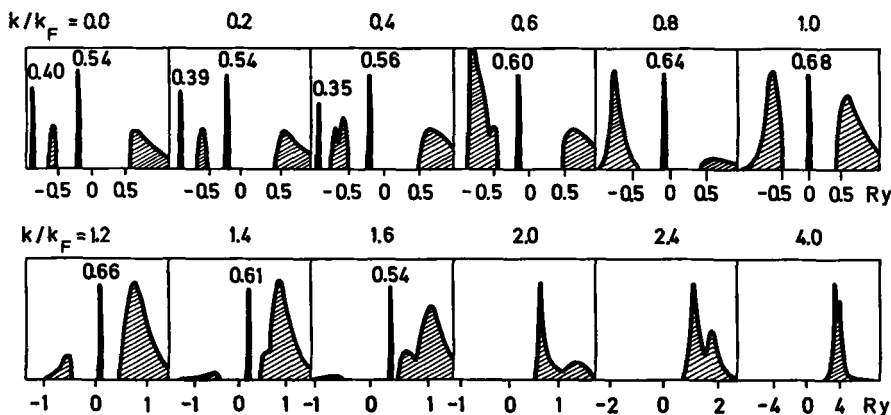


FIG. 21. Survey of the spectral function from $k = 0$ to $k = 4k_F$ for $r_s = 4$ calculated with the plasmon pole dielectric function from B. I. Lundqvist, *Physik Kondensierten Materie* **6**, 206 (1967). The Z values marked in the figure show the parts of the total "oscillator strength" $\int A(k\omega) d\omega = 1$, which falls on δ -function peaks. The scale on the ordinate is different for different k values.

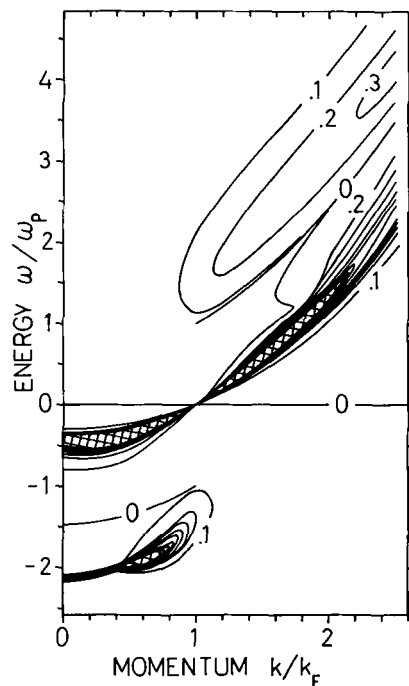


FIG. 22. Map in the $k\omega$ plane of the spectral function $A(k\omega)$ by level curves for constant A , according to a calculation with the Lindhard dielectric function for $r_s = 4$ by B. I. Lundqvist, *Physik Kondensierten Materie* **7**, 117 (1968).

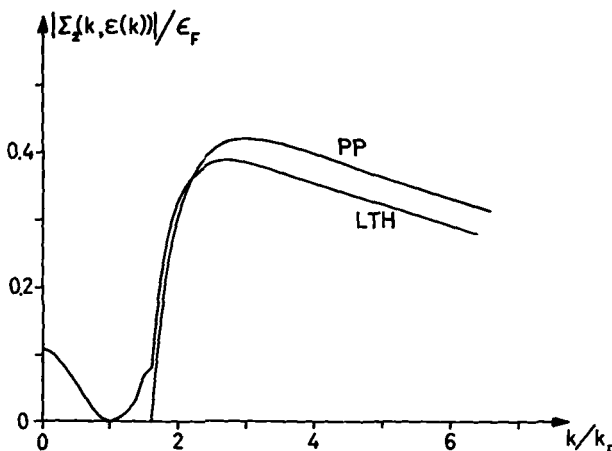


FIG. 23. The imaginary part of the quasi-particle energy for $r_s = 2$ calculated with the Lindhard (LTH) and the plasmon-pole (PP) dielectric constants (see text).

f. Damping of Quasi-Particle States

Figure 21 gives a survey of the spectral function from the bottom of the Fermi sea up to $k = 4k_F$.⁹⁴

In Fig. 22 we have mapped the spectral function A by niveau curves in the $k\omega$ plane.⁹² We notice the approximate parabola for the quasi particle, which has zero width at $k = k_F$. In the upper right part we have the broad effects due to plasmons. In the lower part we have a cutoff "parabola" that describes the dispersion and width of the coupled hole-plasmon states, the plasmarons. We see that the quasi particles have small damping and are well defined only in a narrow region around the Fermi surface. The important aspect in our opinion is not, however, whether the damping is mathematically small and corresponds to a pole infinitesimally close to the real ω axis, but whether it can be identified as a bona fide resonance state in an experiment.

We note that the plasmaron state for sufficiently small k is even more narrow than the regular quasi-particle peak. This seems to be an effect of the small phase-space available for decay.

In Fig. 23 we give a curve of the damping of quasi-particle states as a function of momentum for the electron density of aluminium ($r_s = 2$). The curve shows $\text{Im } \Sigma(k, \epsilon_k)$ as obtained with the LTH dielectric function by Quinn⁹⁵ for $k > k_F$ and by Hedin⁹⁷ for $k < k_F$. As a comparison the results⁹⁸ with the simple dielectric function are also drawn (PP) to show

⁹⁴ Curves drawn from data of Lundqvist.⁹⁸

⁹⁵ J. J. Quinn, *Phys. Rev.* **126**, 1453 (1962). The curve is drawn after an accurate re-calculation by Lundqvist.

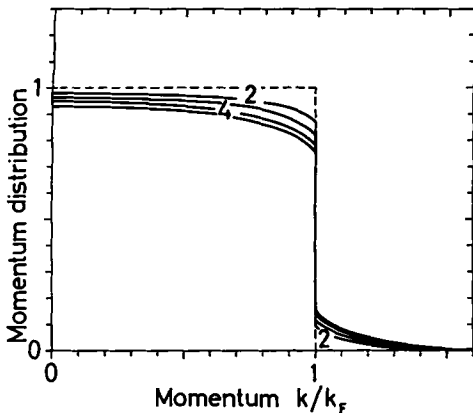


FIG. 24. The momentum distribution function for $r_s = 2, 3, 4$, and 5 .

the relative importance of plasmon damping as compared to particle-hole damping. We should note, however, that the damping given in Fig. 23 only tells the total decay rate of a quasi-particle state (cf. Part VI). If we want to calculate, say, a photoemission yield, we need the angular and energy-dependence of the scattering cross section, not just the total cross section.

g. Momentum Distribution and Density of States

Results for the momentum distribution $n(\mathbf{k})$ and the density of states $g(\omega)$,

$$n(\mathbf{k}) = \int_{-\infty}^{\mu} A(\mathbf{k}, \omega) d\omega, \quad g(\omega) = \int A(\mathbf{k}, \omega) d\mathbf{k}, \quad (25.19)$$

are given in Figs. 24 and 25 from calculations using Eq. (25.1) and (25.17) with the Lindhard dielectric function.⁹² The first calculations of the $n(\mathbf{k})$ curves were made by Dániel and Vosko,⁹⁶ and higher order corrections have been examined by Geldart, Houghton, and Vosko.^{72,97} The curve for $g(\omega)$ shows not only the part coming from the quasi-particle peaks, which is approximately parabolic in shape, but also a low energy satellite, which comes from the coupled hole-plasmon states. This structure is of relevance

⁹⁶ E. Daniel and S. H. Vosko, *Phys. Rev.* **120**, 2041 (1960).

⁹⁷ In the calculations of Geldart *et al.*⁷² and Daniel and Vosko,⁹⁶ the spectral function A was approximated by an expansion to first order in the self-energy

$$A = \pi^{-1} \operatorname{Im}(G + G\Sigma G)$$

which at metallic densities gives quite a different result than Eq. (25.17), which was used by Lundqvist.⁹²

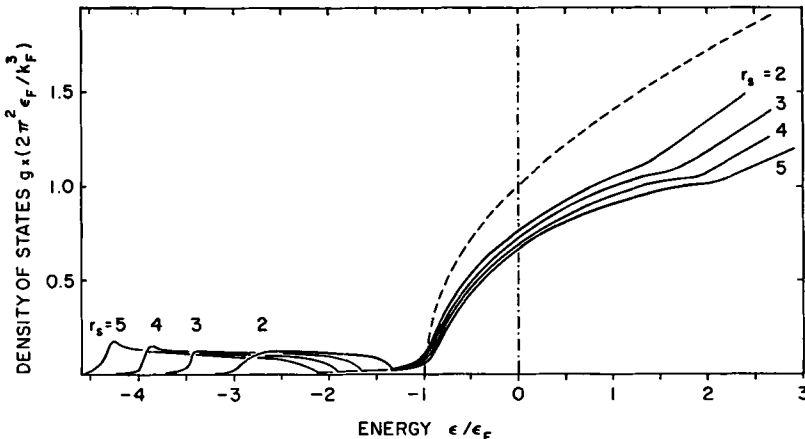


FIG. 25. The density of states for $r_s = 2, 3, 4$, and 5 . The dashed curve is the result in the Hartree approximation and the vertical broken line indicates the Fermi level.

in discussing soft X-ray emission and we shall return to this question in Section 39.

The step in the momentum distribution function $n(\mathbf{k})$ is given by the quasi-particle renormalization factor $Z = (1 - \partial\Sigma/\partial\omega)^{-1}$. Using the dispersion relation of Eq. (25.6) we have

$$\frac{\partial\Sigma}{\partial\omega} = -\frac{1}{\pi} \int \frac{|\text{Im } \Sigma(k_F, \omega')|}{(\omega' - \mu)^2} d\omega', \quad (25.20)$$

which shows that Z is smaller than 1, as it should. In Fig. 26 are given results for Z as obtained from Eq. (25.1) using the LTH dielectric function^{37,96} and the simple dielectric function.⁸⁸ In the latter case $\text{Im } \Sigma(k_F, \omega)$ is zero for $|\omega - \mu| < \omega_p$, and the close agreement between the two curves shows the dominance of the plasmon-induced structure in $\text{Im } \Sigma$. In Fig. 26 are also drawn results obtained by Geldart *et al.*⁷² which include second order terms in Σ in powers of the screened interaction W . These results, however, seem to give somewhat small values for Z as discussed by Hedin.⁸⁶

It should be noted that our arguments have been based on the tacit assumption that we have a paramagnetic state. If we are interested in more complicated situations, we must allow G to have a less restricted form than being diagonal in spin and plane wave labels. Already the first order term for Σ seems to have a sufficiently complicated dynamical structure to make it capable of giving rise to a large variety of unconventional solutions—indeed, we may not yet have exhausted all unconventional HF solutions. The topic of unrestricted dynamical solutions remains an essentially unexplored and highly interesting area, particularly for applications outside the simple electron gas model.

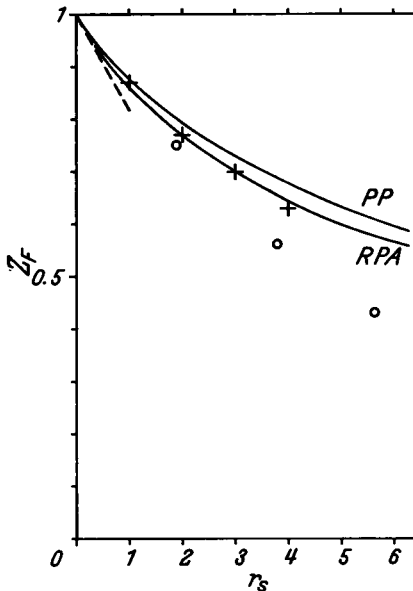


FIG. 26. The renormalization constant Z for a quasi-particle on the Fermi surface. PP: Plasmon-pole dielectric function, B. I. Lundqvist, *Physik Kondensierter Materie* **6**, 206 (1967). RPA: Lindhard dielectric function, E. Daniel and S. H. Vosko, *Phys. Rev.* **120**, 2041 (1960). +: Hubbard dielectric function, T. M. Rice, *Ann. Phys. (N. Y.)* **31**, 100 (1965). ○: Including higher order contributions, D. J. W. Geldart, A. Houghton, and S. H. Vosko, *Can. J. Phys.* **42**, 1938 (1964).

26. THE FERMI LIQUID PARAMETERS

a. Equation for the Landau Interaction Function $f_{kk'}$

Small disturbances around the Fermi surface are conveniently described in terms of the parameters of the Fermi liquid theory as was discussed in Sections 18 and 19. The key quantity is the Landau interaction function $f_{kk'}$. It depends not only on the gross properties of the self-energy Σ but in particular on how Σ changes when we change the distribution of quasi particles, or explicitly⁹⁸

$$f_{kk'} = \frac{\delta E_k}{\delta n_{k'}} = \frac{\delta \Sigma(\mathbf{k}, E_k)}{\delta n_{k'}}. \quad (26.1)$$

From Eq. (26.1) we obtain

$$f_{kk'} = \frac{\partial \Sigma(\mathbf{k}, E_k)}{\partial \omega} \frac{\delta E_k}{\delta n_{k'}} + \left(\frac{\delta \Sigma(\mathbf{k}, \omega)}{\delta n_{k'}} \right)_{\omega=E_k} = Z \left(\frac{\delta \Sigma(\mathbf{k}, \omega)}{\delta n_{k'}} \right)_{\omega=E_k}, \quad (26.2)$$

⁹⁸ For a detailed discussion we refer to standard texts.^{35,52}

where Z is the renormalization constant, $Z = (1 - \partial\Sigma/\partial\omega)^{-1}$. The self-energy varies with $n_{\mathbf{k}}$ only through the variation of G , thus

$$\frac{\partial\Sigma(k)}{\partial n_{\mathbf{k}'}} = \int \frac{\delta\Sigma(k)}{\delta G(q)} \frac{\delta G(q)}{\delta n_{\mathbf{k}'}} d^4q. \quad (26.3)$$

If we replace G by $G_0(\mathbf{k}, \omega) = (\omega - \epsilon_{\mathbf{k}})^{-1}$, we have the simple result

$$\begin{aligned} \frac{\delta G_0(\mathbf{k}, \omega)}{\delta n_{\mathbf{k}'}} &= \frac{\delta}{\delta n_{\mathbf{k}'}} \left[\frac{n_{\mathbf{k}}}{\omega - \epsilon_{\mathbf{k}} - i\delta} + \frac{1 - n_{\mathbf{k}}}{\omega - \epsilon_{\mathbf{k}} + i\delta} \right] \\ &= 2\pi i \delta_{\mathbf{k}\mathbf{k}'} \delta(\omega - \epsilon_{\mathbf{k}}), \end{aligned} \quad (26.4)$$

while in the general case, $G = [\omega - \epsilon_{\mathbf{k}} - \Sigma(\mathbf{k}, \omega)]^{-1}$, we have

$$\frac{\delta G(\mathbf{k}, \omega)}{\delta n_{\mathbf{k}'}} = 2\pi i \delta_{\mathbf{k}\mathbf{k}'} \delta[\omega - \epsilon_{\mathbf{k}} - \Sigma(\mathbf{k}, \omega)] + G^2(\mathbf{k}, \omega) \frac{\delta\Sigma(\mathbf{k}, \omega)}{\delta n_{\mathbf{k}'}}. \quad (26.5)$$

Using the correspondence $\delta_{\mathbf{k}\mathbf{k}'} = \delta(\mathbf{k} - \mathbf{k}')[(2\pi)^3/\Omega]$ we obtain⁹⁹

$$\frac{\delta\Sigma(k)}{\delta n_{\mathbf{k}'}} = 2\pi i Z \frac{(2\pi)^3}{\Omega} \frac{\delta\Sigma(k)}{\delta G(\mathbf{k}', E_{\mathbf{k}'})} + \int \frac{\delta\Sigma(k)}{\delta G(q)} G^2(q) \frac{\delta\Sigma(q)}{\delta n_{\mathbf{k}'}} d^4q. \quad (26.6)$$

Equation (26.6) can in principle be solved provided we know Σ as a functional of G . In practice this scheme involves some difficulties which will be further discussed in the following subsection.

b. Approximate Equations and Results for $f_{\mathbf{k}\mathbf{k}'}$

The simplest choice which has a considerable intuitive appeal is obtained by taking $\delta\Sigma/\delta G = W$, the screened interaction, neglect the integral in Eq. (26.6), and finally put the renormalization constant $Z = 1$, thus

$$f_{\mathbf{k}\mathbf{k}'} = -\Omega^{-1} W(\mathbf{k} - \mathbf{k}'; 0) \delta_{\sigma\sigma'}. \quad (26.7)$$

This expression has been extensively used by Quinn and Ferrell,¹⁰⁰ Watabe,¹⁰¹ Misawa,¹⁰² and by Brouers and Deltour.¹⁰³ This choice neglects the spin independent part of f . The predictions are reasonable for some

⁹⁹ In the notation used by Nozières,²⁵ this integral equation has the form

$${}^0\Gamma^0(k, k') = {}^0I(k, k') + \int {}^0I(k, q) G^2(q) {}^0\Gamma^0(qk') d^4q',$$

where ${}^0I(kk') = \delta\Sigma(k)/\delta G(k')$ is the “irreducible two-body interaction” and ${}^0\Gamma^0 \sim Z^{-1} \delta\Sigma/\delta n \sim Z^{-1} f$ is a limiting value of the two-particle scattering amplitude ${}^0\Gamma$.

¹⁰⁰ J. J. Quinn and R. A. Ferrell, *Plasma Phys.—Accelerators-Thermonucl. Res. (GB)* **2**, 18 (1961).

¹⁰¹ M. Watabe, *Progr. Theoret. Phys.* **29**, 519 (1963).

¹⁰² S. Misawa, *Phys. Letters* **7**, 249 (1963).

¹⁰³ F. Brouers and J. Deltour, *Phys. Status Solidi* **11**, K29 (1965).

properties while for others, such as the compressibility, the results are not good.

The integral equation (26.6) is quite difficult to handle numerically. A simple alternative procedure is to calculate first the total energy E as a functional of $G_0 = (\omega - \epsilon_{\mathbf{k}})^{-1}$ and then use the formulas

$$\begin{aligned} E_{\mathbf{k}} &= \delta E / \delta n_{\mathbf{k}} \\ f_{\mathbf{kk}'} &= \delta E_{\mathbf{k}} / \delta n_{\mathbf{k}'} = \delta^2 E / \delta n_{\mathbf{k}} \delta n_{\mathbf{k}'}. \end{aligned} \quad (26.8)$$

A discussion of $E_{\mathbf{k}}$ from this point of view was first given by Phillips.⁷¹ If the Hubbard formula for the energy is used, we obtain

$$E_{\mathbf{k}} = \epsilon_{\mathbf{k}} + \frac{i}{(2\pi)^4} \lim_{\delta \rightarrow 0} \int \frac{v(\mathbf{q}) e^{i\omega\delta}}{\epsilon_s(\mathbf{q}, \omega)} \frac{d\omega d\mathbf{q}}{\epsilon_{\mathbf{k}} + \omega - \epsilon_{\mathbf{k}+\mathbf{q}}} \quad (26.9)$$

with (cf. Section 27)

$$\epsilon_s(\mathbf{q}, \omega) = 1 - [1 - g(\mathbf{q})] v(\mathbf{q}) P_0(\mathbf{q}, \omega). \quad (26.10)$$

When the Hubbard exchange correction $g(\mathbf{q}) \rightarrow 0$, then $\epsilon_s(\mathbf{q}, \omega)$ reduces to the Lindhard dielectric function. The corresponding formula for $f_{\mathbf{kk}'}$ was derived by Rice¹⁰⁴ and discussed in detail by him. From Eq. (26.9) one obtains¹⁰⁵

$$\begin{aligned} f_{\mathbf{kk}'} &= -\frac{1}{\Omega} \frac{v(\mathbf{k} - \mathbf{k}')}{\epsilon_s(\mathbf{k} - \mathbf{k}', 0)} \\ &\quad - \frac{2}{\Omega} \frac{i}{(2\pi)^4} \int \frac{v^2(\mathbf{k}'') g(\mathbf{k}'')}{\epsilon_s^2(\mathbf{k}'')} G_0(\mathbf{k} + \mathbf{k}'') \\ &\quad \times [G_0(\mathbf{k}' + \mathbf{k}'') + G_0(\mathbf{k}' - \mathbf{k}'')] d^4\mathbf{k}''. \end{aligned} \quad (26.11)$$

$$f_{\mathbf{kk}'} = \frac{1}{\Omega} \frac{i}{(2\pi)^4} \int \frac{v^2(\mathbf{k}'')}{\epsilon_s^2(\mathbf{k}'')} G_0(\mathbf{k} + \mathbf{k}'') [G_0(\mathbf{k}' + \mathbf{k}'') + G_0(\mathbf{k}' - \mathbf{k}'')] d^4\mathbf{k}''.$$

An attempt to solve Eq. (26.6) by expansion in the screened interaction W was developed by Hedin.³⁷ The result to second order in W is schematically (suppressing variables)

$$\begin{aligned} f^e &= -(Z^2/\Omega) \left\{ W + \int [2WWGG + WWG(G + G)] \right\} \\ f^0 &= (Z^2/\Omega) \int W^2 G(G + G). \end{aligned} \quad (26.12)$$

¹⁰⁴ T. M. Rice, *Ann. Phys. (N. Y.)* **31**, 100 (1965).

¹⁰⁵ From Eq. (26.9) actually follows that the term involving the Hubbard g factor appears in f^0 , not in f^e . Rice, however, argued from a diagrammatic analysis that Eq. (26.11) was a more correct expression to use.

The key difference between the formulas by Rice and Hedin is the appearance of the factors Z^2 . Since this factor is about 0.5 at metallic densities, the difference between the two approaches is a crucial one. The comparison shows that two a priori sensible schemes lead to quite different results. A comparison of the results for the compressibility with those obtained from the total energy in Eq. (24.9) indicates that the Z^2 factors should be left out.

We shall briefly outline a modified procedure that replaces the original integral by one that can be easily solved. To this end we introduce a model Green function $G_0 = [\omega - \epsilon_k - \epsilon_0(\hat{k})]^{-1}$, where we let the energy shift depend on the direction and spin of \mathbf{k} but not on the magnitude.¹⁰⁶ A convenient choice of ϵ_0 is

$$\epsilon_0(\hat{k}) = \Sigma(\mathbf{k}, E_{\mathbf{k}}) \Big|_{|\mathbf{k}|=k_F}, \quad (26.13)$$

since this gives

$$f_{kk'} = \delta E_k / \delta n_{k'} = \delta \epsilon_0(\hat{k}) / \delta n_{k'}. \quad (26.14)$$

Retracing the steps leading to Eq. (26.6), we obtain

$$\begin{aligned} f_{kk'} &= \frac{\partial \Sigma}{\partial \omega} \frac{\delta E_k}{\delta n_{k'}} + 2\pi i \frac{(2\pi)^3}{\Omega} \frac{\delta \Sigma(\mathbf{k}, E_{\mathbf{k}})}{\delta G_0(\mathbf{k}', E_{\mathbf{k}'})} \\ &\quad + \int \frac{\delta \Sigma(\mathbf{k}, E_{\mathbf{k}})}{\delta G_0(\mathbf{q}, \omega)} G_0^2(\mathbf{q}, \omega) \frac{\delta \epsilon_0(\hat{\mathbf{q}})}{\delta n_{k'}} d\mathbf{q} d\omega, \end{aligned} \quad (26.15)$$

which can be written as an integral equation for $f_{kk'}$, thus

$$f_{kk'} = Z \left\{ h_{kk'} + \int Q_{kk''} f_{k''k'}(d\hat{k''}/8\pi) \right\}, \quad (26.16)$$

with

$$h_{kk'} = 2\pi i \frac{(2\pi)^3}{\Omega} \frac{\delta \Sigma(\mathbf{k}, E_{\mathbf{k}})}{\delta G_0(\mathbf{k}', E_{\mathbf{k}'}),} \quad (26.17)$$

and^{108a}

$$Q_{kk'} = 8\pi \int \frac{\delta \Sigma(\mathbf{k}, E_{\mathbf{k}})}{\delta G_0(\mathbf{k}', \omega)} G_0^2(\mathbf{k}', \omega) \mathbf{k}'^2 dk' d\omega. \quad (26.18)$$

The integral equation is trivially solved in terms of the Legendre coefficients

¹⁰⁶ Such an energy shift was used by Luttinger and Ward¹⁰⁷ to avoid the anomalous graphs in a finite temperature expansion. With the use of ϵ_0 the large cancellations noted by DuBois¹⁰⁸ can be avoided.

¹⁰⁷ J. M. Luttinger and J. C. Ward, *Phys. Rev.* **118**, 1417 (1960).

¹⁰⁸ D. F. DuBois, *Ann. Phys. (N. Y.)* **8**, 24 (1959); see p. 54.

^{108a} The integration over k' is only over magnitude not over angles.

TABLE V. EFFECTIVE Z FACTOR IN EQ. (26.19)

	$r_s:$	1	2	3	4	5	6
Z_{eff}^a	$l = 0$	1.00	1.00	1.00	1.00	1.00	1.00
	1	0.99	0.98	0.96	0.95	0.93	0.92
	2	0.98	0.95	0.92	0.90	0.87	0.85
	3	0.96	0.93	0.89	0.86	0.83	0.80
Z^b		0.86	0.77	0.70	0.65	0.60	0.57

^a We have used $Q^0 = 0$, $Q^e = WG_0^2$ and the plasmon-pole dielectric function in Eq. (25.11).

^b The actual Z value calculated from $\Sigma = G_0 W$ with the Lindhard dielectric function.

of f , h , Q . Writing

$$f_{kk'} = \sum_l (2l + 1) f_l P_l(\cos \theta_{kk'}), \quad f_l = f_l^0 + f_l^e \delta_{ee'},$$

and similarly for h and Q , one obtains the explicit solution

$$\begin{aligned} f_l^0 + \frac{1}{2} f_l^e &= Z_{\text{eff}}(h_l^0 + \frac{1}{2} h_l^e), & Z_{\text{eff}} &= Z[1 - Z(Q_l^0 + \frac{1}{2} Q_l^e)]^{-1} \\ \frac{1}{2} f_l^e &= Z_{\text{eff}}' \frac{1}{2} h_l^e, & Z_{\text{eff}}' &= Z[1 - Z \frac{1}{2} Q_l^e]^{-1}. \end{aligned} \quad (26.19)$$

For $l = 0$ the equations reduce to $f_0^0 = h_0^0$ and $f_0^e = h_0^e$. The numerical results in Table V show that the effective Z factors are indeed very close to 1.

The integrals $h_{kk'}^0$ and $h_{kk'}^e$ are of the same structure as the integrals considered by Rice. To second order in $W_0 = v(1 - P_0 v)^{-1}$, one obtains

$$\begin{aligned} h_{kk'}^0 &= \Omega^{-1}(i/(2\pi)^4) \int W_0^2(\mathbf{k}'') G_0(\mathbf{k} + \mathbf{k}'') \\ &\quad \times [G_0(\mathbf{k}' + \mathbf{k}'') + G_0(\mathbf{k}' - \mathbf{k}'')] d\mathbf{k}'' \\ h_{kk'}^e &= -\Omega^{-1} W_0(\mathbf{k} - \mathbf{k}', 0) \\ &\quad - \Omega^{-1}(i/(2\pi)^4) \int W_0(\mathbf{k}'') \{2W_0(\mathbf{k} - \mathbf{k}') G_0(\mathbf{k} + \mathbf{k}'') G_0(\mathbf{k}' + \mathbf{k}'') \\ &\quad + W_0(\mathbf{k} + \mathbf{k}'' - \mathbf{k}') G_0(\mathbf{k} + \mathbf{k}'') G_0(\mathbf{k} - \mathbf{k}'') \\ &\quad - W_0(\mathbf{k} - \mathbf{k}') G_0^2(\mathbf{k}' + \mathbf{k}'') + W_0(\mathbf{k} + \mathbf{k}'' - \mathbf{k}') G_0^2(\mathbf{k}' - \mathbf{k}'') \\ &\quad - W_0(\mathbf{k}' - \mathbf{k}_F) G_0^2(\mathbf{k} + \mathbf{k}'')\} d\mathbf{k}'', \end{aligned} \quad (26.20)$$

where \mathbf{k} , \mathbf{k}' , and \mathbf{k}_F stand for (\mathbf{k}, μ) , etc., and \mathbf{k}_F has the same direction and spin as $\mathbf{k} + \mathbf{k}'$.

Thus this procedure combines the intuitive appeal of the approach by Rice with the requirements of having a systematic approach.

c. Numerical Results

In Sections 18 and 19 we discussed the relation between the Landau parameters A_i and B_i and the properties of the system

$$\begin{aligned}\kappa_F/\kappa &= (m/m^*)(1 + A_0), \\ m^*/m &= 1 + A_1, \\ \chi_F/\chi &= (m/m^*)(1 + B_0)\end{aligned}\quad (26.21)$$

magnetoplasma waves $\Rightarrow A_2, A_3$, spin waves $\Rightarrow B_0, B_1$.

We would like to compare the calculation by Rice with that based on Eqs. (26.19) and (26.20). The two formulas differ in three respects: (i) the factor Z_{eff} , (ii) the choice of dielectric function, (iii) in the second order terms. The factor Z_{eff} is close to 1, and the Hubbard exchange modification has only a minor effect. The main difference is therefore in the second order terms in Eqs. (26.11) and (26.20).

An important check on calculations is given by the sum rule derived by Brinkman *et al.*,¹⁰⁹

$$1 + \frac{B_0}{1 + B_0} + \sum_{l=1}^{\infty} (2l + 1) \left(\frac{A_l}{1 + A_l} + \frac{B_l}{1 + B_l} \right) = 0, \quad (26.22)$$

which can be rewritten as¹¹⁰

$$\begin{aligned}S &\equiv 1 + A(0) + B(0) - A_0 - \frac{B_0^2}{1 + B_0} \\ &- \sum_{l=1}^{\infty} (2l + 1) \left[\frac{A_l^2}{1 + A_l} + \frac{B_l^2}{1 + B_l} \right] = 0,\end{aligned}\quad (26.23)$$

where $A(0)$ and $B(0)$ are the values of $A_{kk'}$ and $B_{kk'}$ when $\mathbf{k} = \mathbf{k}'$. The sum rule is essentially a condition on $A(0)$, $B(0)$, A_0 , and B_0 . The coefficients A_i and B_i are listed in Table VI, using three approximations: (i) the screened exchange approximation, Eq. (26.7), (ii) Rice's results, Eq. (26.11), (iii) according to Eqs. (26.19) and (26.20).¹¹¹

¹⁰⁹ W. F. Brinkman, P. M. Platzmann, and T. M. Rice, *Phys. Rev.* **174**, 495 (1968).

¹¹⁰ From the Legendre expansion $A(\theta) = \Sigma(2l + 1)A_l P_l(\cos \theta)$ we obtain $A(0) = \Sigma(2l + 1)A_l$ and similarly for B .

¹¹¹ The second order term in h^* [Eq. (26.20)] was calculated with a static dielectric function.³⁷ The G^2 term then drops out, and as stressed by Rice¹⁰⁴ the contribution from $W(k'')2W(k - k')G(k + k')G(k' + k'')$ comes out too small. If on the other hand we used a dynamic W , there would be large cancellations between this term and the G^2 terms, and the static approximation may thus by cancellation of errors yield a reasonable result.

TABLE VI. LANDAU A_l AND B_l COEFFICIENTS

	r_s :	Screened exchange ^a		Rice ^b		Expansion method ^c	
		2	4	2	4	2	4
A_l	$l = 0$	-0.234	-0.324	-0.35	-0.69	-0.367	-0.706
	1	-0.048	-0.038	-0.001	+0.06	-0.042	+0.005
	2	-0.013	-0.007	-0.03	-0.05		
	3	-0.003	-0.001	+0.004	+0.004		
B_l	$l = 0$	-0.234	-0.324	-0.235	-0.28	-0.253	-0.325
	1	-0.048	-0.038	-0.06	-0.06	-0.083	-0.098
	2	-0.013	-0.007	-0.03	-0.02	-0.014	-0.002
	3	-0.003	-0.001	+0.004	-0.001	-0.008	-0.007
S^d		0.195	0.198	0.20	0.23	-0.053	+0.018

^a Screened exchange according to Eq. (26.7).

^b Rice's expression, Eq. (26.11).

^c Expansion method according to Eqs. (26.19) and (26.20). The terms of second order in W were evaluated with a static approximation.

^d The sum rule constant in Eq. (26.23).

The values for $l = 0$ agree quite well in cases (ii) and (iii), while A_0 is distinctly different in case (i). The sum rule is satisfied best in case (iii). For $l > 0$ the coefficients in cases (ii) and (iii) show only a rough correlation. As suggested by Rice,¹¹² the size of the difference between calculations (ii) and (iii) may be taken as indicative of the errors involved.

It should be remarked that the equilibrium properties κ , m^* , and χ can of course be calculated without using the Landau theory. The compressibility is obtained from the total energy, the effective mass can be obtained from the Dyson equation, and the susceptibility can be calculated from the total energy in the presence of a magnetic field. Calculations of the specific heat ratio $c/c_F = m^*/m$ and spin susceptibility along these lines were carried out by Silverstein¹¹³ using an interpolation procedure by Nozières and Pines,⁷⁷ which divided the contribution into parts corresponding to small and large momentum transfers, respectively. For small momentum transfers the Lindhard formula was used, whereas the contribution for large momentum transfers was calculated in second order perturbation theory. An interpolation was used in the intermediate region.

¹¹² T. M. Rice, *Phys. Rev.* **175**, 858 (1968).

¹¹³ S. D. Silverstein, *Phys. Rev.* **128**, 631 (1962); **130**, 1703 (1963).

TABLE VII. RESULTS FOR THE COMPRESSIBILITY, SUSCEPTIBILITY,
AND EFFECTIVE MASS

	r_s :	1	2	3	4	5
κ_F/κ	E ^a	0.835	0.661	0.497	0.292	0.100
	R ^b		0.66	0.47	0.29	
	NP ^c	0.83	0.65	0.46	0.27	
	SX ^d	0.88	0.81	0.75	0.70	0.67
χ/χ_F	E	1.151	1.282	1.396	1.489	1.561
	R	1.15	1.27	1.39	1.48	
	S ^e		1.27	1.28	1.30	
	SX	1.14	1.24	1.34	1.42	1.50
m^*/m	E	0.950	0.958	0.979	1.005	1.035
	R	0.96	0.99	1.02	1.06	
	S		1.02	1.05	1.10	
	SX	0.95	0.95	0.95	0.96	0.97

^a Expansion method, Eq. (26.20)^b Rice, Eq. (26.11).^c P. Nozières and D. Pines, *Phys. Rev.* **111**, 442 (1958).^d Screened exchange, Eq. (26.7).^e S. D. Silverstein, *Phys. Rev.* **128**, 631 (1962); *ibid.* **130**, 912 (1963).

Table VII shows values for κ , χ and m^* obtained from the A and B coefficients in Table VI. The row S refers to Silverstein¹¹³ who used the interpolation idea of Nozières and Pines⁷⁷ as just described. The agreement between the first two calculations for κ and χ is excellent, actually better than the agreement for A_0 and B_0 , while the results by Silverstein for the susceptibility (when $r_s \geq 3$) seem to be somewhat small. For m^*/m the values labeled S are taken from Rice¹⁰⁴ who found a numerical error in Silverstein's calculation and reevaluated the numbers.

In screened exchange approximation the choice of dielectric screening, e.g. the Lindhard formula, the Hubbard modification, or the simple Thomas-Fermi screening, makes little difference. The values of κ_F/κ are much too large, and the values of χ_F/χ are somewhat small. Watabe¹⁰¹ and Misawa¹⁰² have used the screened exchange approximation in conjunction with a self-consistency procedure, which however only increased the discrepancies.

27. THE DIELECTRIC FUNCTION

Most one-electron properties are indeed quite insensitive to the details of the dielectric function and the two previous sections have illustrated

this point. Therefore, the dielectric function is not a primary object to study in this context and we shall confine ourselves to some pertinent points for discussion. Extensive reviews on the subject have recently been published by Pines,⁷⁸ Nozières and Pines,⁵² and Tosi.¹¹⁴

The Lindhard dielectric function was derived in Section 5 from the time-dependent Hartree theory. An induced charge density is calculated from the response of electrons moving independently under the total potential, thus

$$\rho^{\text{ind}}(\mathbf{q}, \omega) = P_0(\mathbf{q}, \omega)[V^{\text{ext}}(\mathbf{q}, \omega) + V^{\text{ind}}(\mathbf{q}, \omega)], \quad (27.1)$$

where P_0 is the polarization propagator for independent particles [see Eqs. (5.21) and (14.5)]. The dielectric function is defined by

$$\rho^{\text{ind}} = [\epsilon^{-1} - 1]\rho^{\text{ext}}, \quad (27.2)$$

and using the relations

$$V^{\text{ext}}(\mathbf{q}, \omega) = v(\mathbf{q})\rho^{\text{ext}}(\mathbf{q}, \omega),$$

$$V^{\text{ind}}(\mathbf{q}, \omega) = v(\mathbf{q})\rho^{\text{ind}}(\mathbf{q}, \omega),$$

we obtain the Lindhard formula

$$\epsilon(\mathbf{q}, \omega) = 1 - P_0(\mathbf{q}, \omega)v(\mathbf{q}). \quad (27.3)$$

The Lindhard dielectric function properly describes the screening properties, but is inaccurate in detailed predictions outside the long-wavelength regime. A simple way to obtain an improved result is to write

$$V^{\text{ind}} = v(1 - G)\rho^{\text{ind}}. \quad (27.4)$$

This is the type of local field correction discussed by Nozières and Pines,¹¹⁵ which is associated with the local hole in the charge distribution around an individual electron. Inserting Eq. (27.4) in the previous equation we obtain

$$\frac{1}{\epsilon(\mathbf{q}, \omega)} = 1 + \frac{P_0(\mathbf{q}, \omega)v(\mathbf{q})}{1 - [1 - G(\mathbf{q})]P_0(\mathbf{q}, \omega)v(\mathbf{q})}. \quad (27.5)$$

This result reminds us about the approximate treatment of exchange in Eq. (5.41) and shows that Gv is of the order $\frac{1}{2}v_{\text{av}}$. An improvement of this type was first suggested by Hubbard,²⁷ who derived from a diagrammatic analysis the approximate formula

$$G(q) = \frac{1}{2}[q^2/(q^2 + k_F^2 + \xi k_{\text{TF}}^2)] \quad (27.6)$$

with $\xi = 0$ in the original work and with $\xi = 1$ in later work as e.g. used by Rice.¹⁰⁴

¹¹⁴ M. P. Tosi, *Riv. Nuovo Cimento*, **1**, 160 (1969).

¹¹⁵ P. Nozières and D. Pines, *Nuovo Cimento* **9**, 470 (1958).

The Hubbard correction was introduced for an improved calculation of the total energy. For large q values it is easy to see that the second order exchange contribution to the energy cancels half the direct second order term, and the correction factor has precisely this effect at large q .¹¹⁶

In a recent paper by Singwi *et al.*,²⁸ a different choice of the factor G has been proposed. They consider a relation

$$V^{\text{ind}}(\mathbf{r}, \omega) = \int u(\mathbf{r} - \mathbf{r}') \rho^{\text{ind}}(\mathbf{r}', \omega) d\mathbf{r}', \quad (27.7)$$

where the effective interaction $u(\mathbf{r})$ is defined by

$$\nabla_{\mathbf{r}} \int u(\mathbf{r} - \mathbf{r}') \rho^{\text{ind}}(\mathbf{r}') d\mathbf{r}' = \int g(\mathbf{r} - \mathbf{r}') \nabla_{\mathbf{r}} v(\mathbf{r} - \mathbf{r}') \rho^{\text{ind}}(\mathbf{r}') d\mathbf{r}'.$$

Thus, the field from the induced charge is reduced through the pair-correlation function $g(\mathbf{r})$. This leads to the correction

$$G(\mathbf{k}) = 1 - \int (\mathbf{k}\mathbf{k}'/\mathbf{k}'^2) g(\mathbf{k} - \mathbf{k}') (d\mathbf{k}'/(2\pi)^3), \quad (27.8)$$

$g(\mathbf{k})$ being the Fourier transform of $g(\mathbf{r})$. With this choice the dielectric function will depend on $g(\mathbf{r})$ and because $g(\mathbf{r})$ in turn can be expressed as an integral $g(\mathbf{r}) \sim \int (\epsilon^{-1} - 1) d\omega$, a self-consistency procedure can be set up. This approach has also been discussed by Hubbard.²⁹ If the HF formula for $g(\mathbf{k} - \mathbf{k}')$ is used in Eq. (27.8), the original Hubbard correction is retrieved.

We will now shortly review some results obtained with the three dielectric functions, the Lindhard, the Hubbard, and the Singwi *et al.* Results for the correlation energy have already been presented in Section 27 (see Fig. 13). It should be noted that the $q \rightarrow \infty$ limit of $G(q)$ is $1 - g(0)$ in the self-consistent treatment. In the Lindhard and Hubbard cases this limit is 0 and $\frac{1}{2}$, respectively, while at metallic densities $1 - g(0) \approx 1$ according to Singwi *et al.* From Fig. 13 we see that the Singwi *et al.* curve (S) comes roughly as much above the Hubbard (H) and the Nozières and Pines (NP) curves as the Lindhard (L) curve comes below. This indicates that either the H and NP methods of correcting the L result are quite crude, or that the S method is not particularly good for correlation energies.^{116a} For the pair correlation function $g(\mathbf{r})$, on the other hand, the

¹¹⁶a It should be noted that the Hubbard dielectric function ϵ_H given by Eqs. (27.5) and (27.6) is not the same as the effective dielectric function ϵ_s in Eq. (26.10). A recent discussion of different effective dielectric functions has been given by L. Kleinman, *Phys. Rev.* **160**, 585 (1967); **172**, 383 (1968).

^{116a} A recent investigation by D. C. Langreth, *Phys. Rev.* **181**, 753 (1969), of the large q behavior of the dielectric function supports the H and NP results.

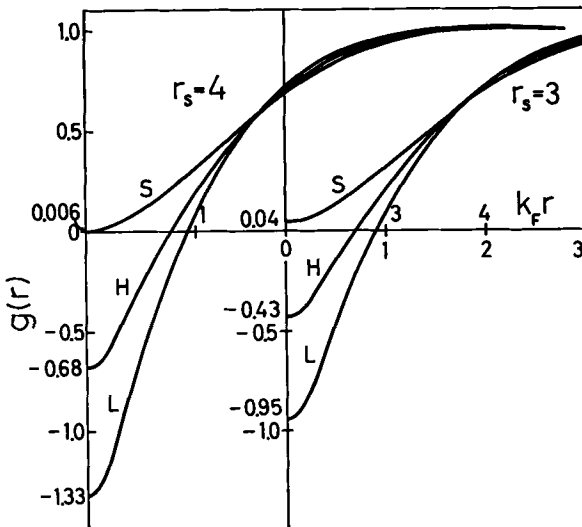


FIG. 27. The pair correlation function for $r_s = 3$ and 4 from different approximations for the dielectric function taken from K. S. Singwi, M. P. Tosi, R. H. Land, and A. Sjölander, *Phys. Rev.* **176**, 589 (1968). S: Singwi *et al.* H: Hubbard. L: Lindhard.

Singwi *et al.* results no doubt represent a dramatic improvement compared to H and L since their $g(r)$ curve is positive for all r (see Fig. 27).

The results for the screening of a fixed point charge are shown in Fig. 28. The overall results are quite similar in the three cases, while as a contrast the Thomas-Fermi result tends to infinity for $r \rightarrow 0$. The amplitudes of the first Friedel wiggle are, however, quite different. Although the amplitudes are very small they may still be of importance in problems about lattice stability and phonon dispersion curves.

We next turn to the regime of small q and large frequencies and comment on the plasmon dispersion law obtained from the condition $\epsilon(q, \omega) = 0$. In units of ϵ_F and k_F one obtains from Eq. (27.5) that

$$\omega^2 = \omega_p^2 + (12/5)[1 - (20\alpha r_s/9\pi)\gamma]q^2, \quad (27.9)$$

where γ is a constant defined by the relation

$$\lim_{q \rightarrow 0} G(q) = \gamma q^2. \quad (27.10)$$

The results for γ in the approximations by Hubbard and by Singwi *et al.* are quite close, giving $\gamma \approx 0.5$ at metallic densities. The effects of exchange on plasmon dispersion, calculated by Pines and Nozières⁷⁷ and by Kanazawa *et al.*,¹¹⁷ gave a result corresponding to $\gamma = 0.15$. Pines and Nozières used

¹¹⁷ H. Kanazawa, S. Misawa, and E. Fujita, *Progr. Theoret. Phys.* **23**, 426 (1960).

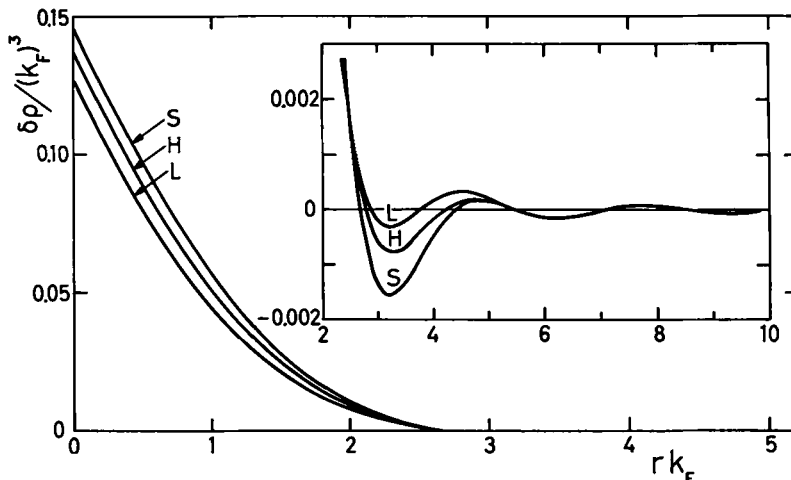


FIG. 28. Induced charge density around an impurity charge for $r_s = 3$ according to the same approximations for the dielectric function as in Fig. 27, taken from K. S. Singwi and M. P. Tosi, *Phys. Rev.* **181**, 784 (1969).

the method by Bohm and Pines, and Kanazawa *et al.* calculated a modified polarization propagator containing a screened interaction.

The plasmon dispersion coefficient can also be obtained from the Landau theory, and one obtains the dispersive term [see Eq. (19.21)]

$$(12/5)(1 + A_1)[1 + (5/9)A_0 + (4/9)A_2]q^2. \quad (27.11)$$

At metallic densities A_1 and A_2 are small compared to A_0 and since $A_0 \approx -\alpha r_s/\pi$, this result corresponds to $\gamma \cong \frac{1}{4}$.

Thus there are three different recommendations for the correction factor γ in Eq. (27.9) ranging from 0.15 to 0.25 and 0.50. We find no a priori reason to prefer one of the three before the others.

We finally comment on the limiting value of $\epsilon(q, 0)$ for $q \rightarrow 0$. This limit is related to the compressibility ratio κ/κ_F by the formula¹¹⁸

$$\lim_{q \rightarrow 0} \epsilon(q, 0) = 1 + (k_{TF}^2/q^2)(\kappa/\kappa_F). \quad (27.12)$$

In the Lindhard approximations we shall have $\kappa/\kappa_F = 1$, while the approximation by Singwi *et al.* gives $\kappa_F/\kappa = 1 - (4\alpha r_s/\pi)\gamma$, and the exact result is $\kappa_F/\kappa = (m/m^*)(1 + A_0) \cong 1 - (\alpha r_s/\pi)$. Again the spread in values is fairly wide.

The examples just mentioned show that the questions about the detailed structure of the dielectric function are still unsettled in important

¹¹⁸ See e.g. P. Nozières.³⁵

respects. Fortunately these uncertainties and ambiguities have only little effect on most one-electron properties because they usually depend on various averages over the dielectric function.

VIII. Phonon Contributions to the Electron Self-Energy

28. SOME GENERAL RESULTS AND FORMULAS

We shall in this part deal with properties related to the phonon contributions to the electron self-energy and the electron spectral function. After giving the general formulas and a brief discussion of the effects, we shall review some recent calculations and illustrate the nature of the results obtained, in particular for the spectral function and the density of states. The strong temperature dependence reflects itself on the properties of the electrons and gives rise to temperature variations in cyclotron resonance and in the specific heat. We shall briefly comment on these effects, although they are marginal with present experimental accuracy.

We will discuss only the phonon contributions to the self-energy and the spectral function with the system in equilibrium, and will not enter the topic of phonon contributions to the Landau interaction function. This topic and the still more specialized one about the coupling of the system to various external probes we find to be outside the scope of this article. We will thus not at all take up questions such as wave function renormalization and the cancellation or noncancellation of phonon effect for various properties, which is a long and specialized affair deserving a separate review.¹¹⁹

We shall now list a number of formulas and general results which will be of relevance for the later discussion. We shall use the Migdal argument⁴² that vertex corrections are small of order $(m/M)^{1/2}$ and therefore neglect them. The phonon contribution to the self-energy of the electron is then given by [cf. Eq. (16.14)]

$$\Sigma^{\text{ph}}(\mathbf{k}, \omega) = i \sum_{\lambda} \int \frac{d\mathbf{q} d\omega'}{(2\pi)^4} |g_{\mathbf{q}\lambda}|^2 D_{\mathbf{q}\lambda}(\omega') G(\mathbf{k} - \mathbf{q}, \omega - \omega'). \quad (28.1)$$

Because $G(\mathbf{k}, \omega) = [\omega - \epsilon(\mathbf{k}) - \Sigma(\mathbf{k}, \omega)]^{-1}$, this is an integral equation to be solved for $\Sigma(\mathbf{k}, \omega)$. However, Migdal made the important observation that $\Sigma^{\text{ph}}(\mathbf{k}, \omega)$ is essentially independent of \mathbf{k} in the region where it affects the integral. This implies that we can neglect $\Sigma^{\text{ph}}(\mathbf{k}, \omega)$ in $G(\mathbf{k}, \omega)$ and the problem is then reduced to quadratures. A detailed discussion of this point

¹¹⁹ See Abrikosov *et al.*³⁸; Holstein⁵¹; Heine *et al.*⁵³; R. E. Prange and L. P. Kadanoff, *Phys. Rev.* **134**, A566 (1964); R. E. Prange and A. Sachs, *ibid.* **158**, 672 (1967).

is given by Schrieffer.¹²⁰ Here we give the slightly more general formula derived by Grimvall¹²¹:

$$\begin{aligned} \text{Re } \Sigma^{\text{ph}}(\mathbf{p}, \omega) &= -\frac{m}{2 | \mathbf{p} | (2\pi)^3} \sum_{\lambda} \int_0^{2\pi} d\varphi \int_0^{2k_F} \frac{q (\hat{e}_{\lambda q} \cdot \mathbf{q})^2 h^2(q)}{\omega_{\lambda}(\mathbf{q})} \\ &\quad \times \ln \left| \frac{\omega + \omega_{\lambda}(\mathbf{q})}{\omega - \omega_{\lambda}(\mathbf{q})} \right| dq \\ \text{Im } \Sigma^{\text{ph}}(\mathbf{p}, \omega) &= -\frac{m}{4 | \mathbf{p} | (2\pi)^2} \sum_{\lambda} \int_0^{2\pi} d\varphi \int_0^{| \omega_{\lambda}(\mathbf{q}) | < \omega} \frac{q (\hat{e}_{\lambda q} \cdot \mathbf{q})^2 h^2(q)}{\omega_{\lambda}(\mathbf{q})} dq. \end{aligned} \quad (28.2)$$

In Eq. (28.2) $\omega_{\lambda}(\mathbf{q})$ is the phonon frequency of branch λ , $(\hat{e}_{\lambda q} \cdot \mathbf{q})h(q)$ denotes the screened matrix element between an electron and an ion, φ is the angle of rotation round the axis \mathbf{p} , and \mathbf{q} is the total momentum transfer in the interaction with phonons and is always taken between \mathbf{p} and another point on the Fermi surface. The formula assumes a spherical Fermi surface, but accounts fully for the anisotropic properties of the phonons. The energy is measured relative to the electron energy at the Fermi surface.

The following general characteristics follow from Eq. (28.2) but can to some extent be understood on intuitive grounds. The real part is zero at $\omega = 0$, rises to maximum when ω is of the order of the typical lattice frequency i.e. $\omega = \omega_{\text{Debye}}$, and then goes to zero when $\omega \gg \omega_{\text{Debye}}$. The absolute value of $\text{Im } \Sigma^{\text{ph}}$ starts from the value zero at $\omega = 0$, rises to a maximum at $\omega \approx \omega_{\text{Debye}}$, and is essentially constant for frequencies large compared with the typical lattice frequency. Structure due to phonon effects is thus confined to a narrow region of order $\omega \approx \omega_{\text{Debye}}$ around the Fermi surface. Outside this region the only effect due to phonons is an essentially constant damping rate. Far away from the Fermi surface, however, the damping due to phonon exchange can be neglected in comparison with the effect of electron-electron interaction.

These remarks hold at zero absolute temperature. At finite temperature the expression for Σ^{ph} is [cf. Eq. (17.12)]

$$\begin{aligned} \Sigma^{\text{ph}}(\mathbf{k}, \omega; T) &= \sum_{\lambda} \int \frac{d\mathbf{q}}{(2\pi)^3} | g_{\mathbf{q}\lambda} |^2 \\ &\quad \times \left\{ \frac{1 - f_{\mathbf{k}-\mathbf{q}} + N_{\mathbf{q}\lambda}}{\omega - \epsilon_{\mathbf{k}-\mathbf{q}} + \mu - \omega_{\mathbf{q}\lambda}} + \frac{f_{\mathbf{k}-\mathbf{q}} + N_{\mathbf{q}\lambda}}{\omega - \epsilon_{\mathbf{k}-\mathbf{q}} + \mu + \omega_{\mathbf{q}\lambda}} \right\}. \end{aligned} \quad (28.3)$$

¹²⁰ Schrieffer,²⁶ p. 162.

¹²¹ G. Grimvall, *Phys. Kondensierten Materie* **6**, 15 (1967).

TABLE VIII. ELECTRON-PHONON CONTRIBUTION TO EFFECTIVE MASS

		Li	Na	K	Rb	Cs	Pb	Al
	r.:	3.22	3.96	4.87	5.18	5.57		
$(\delta m/m)_{ph}$	Q ^a	0.35	0.45	0.59	0.61	0.69		
	AW ^b		0.18				1.05	0.49
	A ^c	0.14	0.15	0.16	0.18	0.22		
	T ^d						1.3	0.38

^a J. J. Quinn, "The Fermi Surface" (*Proc. Intern. Conf., Cooperstown*) (W. A. Harrison and M. B. Webb, eds.). New York, Wiley, 1960.

^b N. W. Ashcroft and J. W. Wilkins, *Phys. Letters* **14**, 285 (1965).

^c A. O. E. Animalu, F. Bonsignori, and V. Bortolani, *Nuovo Cimento* **42B**, 83 (1966).

^d W. L. McMillan, *Phys. Rev.* **167**, 331 (1968).

The temperature factors cause a blurring of the phonon effects. Indeed, the electron-phonon interaction is a typical quantum effect to be discussed in terms of phonon emission and absorption. In the limit of high temperature $T \gtrsim \Theta_{Debye}$, the lattice behaves just as a classical system with density fluctuations and in that limit no *structured effects of the electron-phonon interaction will remain*. A direct calculation of Eq. (28.2) or (28.3) is quite difficult, due to the complication with phonon polarization vectors and umklapp processes. A complete numerical calculation has, however, been performed by Grimvall^{121,122} for the case of Na, and will be reviewed later.

If one is mainly interested in the results for Σ^{ph} , one can take the information about the phonon spectrum from the inversion of the gap ϵ equations in an analysis of tunneling data for superconductors. Let $\alpha^2(\omega)F(\omega)$ be the product of the electron-phonon interaction $\alpha^2(\omega)$, and the density of phonon states $F(\omega)$, or explicitly¹²³

$$\alpha^2(\omega)F(\omega) = \sum_{\lambda} \frac{\iint (dS'/V_F') (dS/V_F) |g_{q\lambda}|^2 \delta(\omega - \omega_{q\lambda})}{(2\pi)^3 \int (dS/V_F)} . \quad (28.4)$$

The integrations in Eq. (28.4) extend over the Fermi surface. The average $\Sigma^{ph}(p, \omega; T)$ over all directions p at the Fermi surface can now [cf. Eq. (28.3)], be written¹²⁴

$$\begin{aligned} \Sigma^{ph}(p, \omega; T) &= \int d\epsilon \int d\omega' \alpha^2(\omega') F(\omega') \\ &\times \left\{ \frac{1 - f(\epsilon) + N(\omega')}{\omega - \epsilon + \mu - \omega'} + \frac{f(\epsilon) + N(\omega')}{\omega - \epsilon + \mu + \omega'} \right\}, \end{aligned} \quad (28.5)$$

¹²² G. Grimvall, *J. Phys. Chem. Solids* **29**, 1221 (1968).

¹²³ W. L. McMillan and J. M. Rowell, in "Superconductivity" (R. D. Parks, ed.), Marcel Dekker, New York, 1968.

¹²⁴ W. L. McMillan, *Phys. Rev.* **167**, 331 (1968).

where $f(\epsilon)$ and $N(\omega)$ are the fermion and boson factors. It is far from obvious that the average in Eq. (28.5) should give an accurate representation of Σ . We refer to the numerical calculations and discussions by Grimvall,¹²⁵ who concludes that the average Σ should be sufficiently accurate for calculation of e.g. cyclotron resonance and specific heat effective masses, while the average gives a very poor representation of the imaginary part of Σ .

29. EARLY CALCULATIONS OF THE EFFECTIVE MASS. THE WORK OF ENGELSBERG AND SCHRIEFFER

The early investigations of electron-phonon effects in normal metals were mainly concerned with the enhancement of the density of states at the Fermi surface, or what amounts to the same thing, the effective mass correction δm_{ph} . As we remarked in the last section, the phonon contribution to the electron self-energy is only weakly dependent on momentum. If we consider electron-electron interactions and band effects as included in an energy ϵ_k , the Dyson equation becomes

$$E_k = \epsilon_k + \Sigma^{\text{ph}}(E_k). \quad (29.1)$$

The effective mass ratio can hence be written

$$m^*/m = \epsilon'_k/E'_k = [1 - \partial \Sigma^{\text{ph}}(\omega)/\partial \omega] = 1/Z^{\text{ph}}, \quad (29.2)$$

where Z^{ph} is the renormalization constant.

The first estimate of the effective mass correction seems to have been given by Buckingham and Schafroth,¹²⁶ who obtained the correction factor $1 + 2^{-1/3}F$, where F is the so called "Fröhlich constant",³⁸ which for the alkali metals is about 0.20. Later Ferrell¹²⁷ estimated the correction to be 20–25% for sodium. Quinn¹²⁸ applied the so called jellium model of lattice vibrations together with the free-electron model of the electrons to this problem and calculated the self-energy to the same order as in Eq. (28.1).

The contribution from normal processes is then given in closed form by the expression

$$\delta m_{\text{ph}}/m = F(k_{\text{TF}}/k_{\text{D}})^2 \ln[1 + (k_{\text{D}}/k_{\text{TF}})^2], \quad (29.3)$$

where k_{TF} is the Thomas-Fermi screening parameter and k_{D} is the Debye cut-off wavevector for the phonons. For a monovalent metal $k_{\text{D}} = 2^{1/3}k_{\text{F}}$, and for jellium $F = 0.25$.

¹²⁵ G. Grimvall, *Physik Kondensierter Materie* **9**, 283 (1969).

¹²⁶ M. J. Buckingham and M. R. Schafroth, *Proc. Phys. Soc.* **67**, 828 (1954).

¹²⁷ R. A. Ferrell, *Bull. Am. Phys. Soc.* **1**, 217 (1956).

¹²⁸ J. J. Quinn, "The Fermi Surface" (W. A. Harrison and M. B. Webb, eds.). Wiley, New York, 1960.

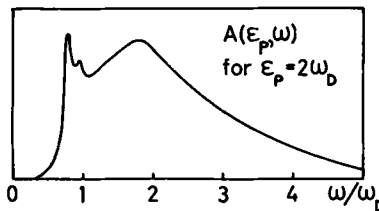


FIG. 29. Spectral function in the Debye model with a coupling constant appropriate to a strong-coupling superconductor after S. Engelsberg and J. R. Schrieffer, *Phys. Rev.* **131**, 993 (1963).

In the limit $k_D/k_{TF} \rightarrow 0$, this expression reduces to the estimate previously given by Ferrell.¹²⁷ Quinn also pointed out the importance of umklapp processes and estimated that they should give a contribution of the same order as the normal processes. His results are summarized in Table VIII together with the results of some more recent calculations. Using a different method to estimate the umklapp contributions, Nakajima and Watabe¹²⁹ obtained the estimate $\delta m_{ph}/m = 0.32$ for Na, to be compared with the value 0.45 given by Quinn.

Under the same conditions as stated before Eq. (29.1), the spectral function becomes

$$A(k, \omega) = \frac{1}{\pi} \frac{|\text{Im } \Sigma^{ph}(\omega)|}{[\omega - \epsilon_k - \text{Re } \Sigma^{ph}(\omega)]^2 + [\text{Im } \Sigma^{ph}(\omega)]^2}. \quad (29.4)$$

Since the momentum dependence of A enters only through the energy ϵ_k , the spectral function is often written as $A(\epsilon_k, \omega)$, with ϵ_k measured from the Fermi energy.

The first comprehensive discussion of the full structure of the electron self-energy and the spectral weight function was given by Engelsberg and Schrieffer.¹³⁰ They rederive in a lucid way and amplify results earlier obtained by Migdal.⁴² Of particular importance are their detailed applications using specific models. They show that the spectral function $A(\epsilon_k, \omega)$ may have a complicated structure for ϵ_k values of the order ω_{max} where ω_{max} is the maximum phonon frequency. The spectral function in this region can thus be far from a Lorentzian and therefore the simple quasi-particle picture may not be directly applicable. For ϵ_k small compared to ω_{max} i.e. for electrons close to the Fermi surface, and for ϵ_k large compared to ω_{max} , the spectral function seems usually to have a sharp quasi-particle peak.

Engelsberg and Schrieffer considered two models. The first one uses an Einstein model for the phonons, i.e. $\omega_{q\lambda} \simeq \omega$ and assumes a constant cou-

¹²⁹ S. Nakajima and M. Watabe, *Progr. Theoret. Phys.* **29**, 341 (1963).

¹³⁰ S. Engelsberg and J. R. Schrieffer, *Phys. Rev.* **131**, 993 (1963).

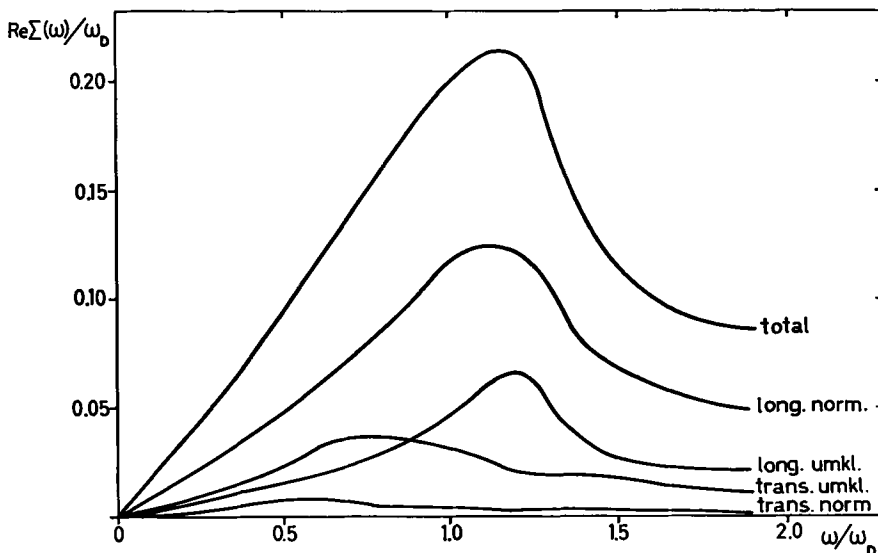


FIG. 30. Contributions to the real part of the self-energy for Na at $T = 0^{\circ}\text{K}$ after G. Grimvall, *Physik Kondensierter Materie* **6**, 15 (1967).

pling g . The second model uses a Debye phonon spectrum, i.e. $\omega_{q\lambda} \simeq |\mathbf{q}|$ and also takes $g(\mathbf{q})$ proportional to $|\mathbf{q}|$ as in the Fröhlich model.³⁸ A typical result is shown in Fig. 29. The coupling constant is chosen to be appropriate to the case of a strong-coupling superconductor. This accentuates the structure very strongly. For metals with intermediate and weak coupling the structure in the spectral function will be less pronounced, but significant deviations from the ideal Lorentzian quasi-particle shape are still expected to occur.

30. CALCULATIONS WITH REALISTIC PHONON SPECTRA AND INCLUDING BAND-STRUCTURE EFFECTS

In recent years more accurate calculations have been made of the effective mass corrections. Ashcroft and Wilkins¹³¹ calculated the corrections for Na, Al, and Pb using the formula

$$\frac{\delta m_{\text{ph}}}{m} = \rho_{\text{bs}} \int \frac{d\Omega_k}{4\pi} \frac{d\Omega_p}{4\pi} \frac{|g_{k-p}|^2}{\hbar\omega_{k-p}}. \quad (30.1)$$

This formula follows directly from writing down the energy in lowest order

¹³¹ N. W. Ashcroft and J. W. Wilkins, *Phys. Letters* **14**, 285 (1965).

in Brillouin-Wigner perturbation theory:

$$E_{\mathbf{k}} = \epsilon_{\mathbf{k}} + \sum_{\mathbf{p}} |g_{\mathbf{k}-\mathbf{p}}|^2 \left\{ \frac{1 - f_{\mathbf{p}}}{E_{\mathbf{k}} - (E_{\mathbf{p}} + \hbar\omega_{\mathbf{k}-\mathbf{p}})} + \frac{f_{\mathbf{p}}}{E_{\mathbf{k}} - (E_{\mathbf{p}} - \hbar\omega_{\mathbf{k}-\mathbf{p}})} \right\}. \quad (30.2)$$

In Eq. (30.1) ρ_{bs} denotes the density of states from the band structure calculation, and the angular integrations extend over the Fermi surface. The electron-phonon matrix $g_{\mathbf{k}-\mathbf{p}}$ is related (via the rigid ion approximation) to the effective potential used in the OPW calculation. The phonon frequencies used in their calculations were taken from experiments and there are no undetermined parameters in the theory. The value for Na was provided by Darby¹³¹; the results are shown in Table VIII.

A similar calculation has been made by Animalu *et al.*¹³² for the alkali metals. They use the Heine-Abarenkov potential for the effective ion potential and the Hubbard modification of the dielectric function. For normal processes they assumed the phonons to be strictly longitudinal or transverse, and for umklapp processes a simplifying assumption about the polarization was made. They estimate that nearly 40% of the contribution comes from umklapp processes. The results are given in Table VIII. Recently a number of calculations of the effective mass for several metals have been made.¹³³

It should be mentioned that the most accurate determination of the effective mass of electrons comes from experimental data from tunneling between superconductors,^{123,124} as was discussed in Section 28, and from analysis of the transition temperature T_c . Some of these values are included in Table VIII.

As already mentioned, the earlier studies of Σ^{ph} have used simple models such as an Einstein or a Debye model. Grimvall^{121,122} has made a more realistic calculation for the case of sodium, in order particularly to study the importance of umklapp processes and the effect of a proper treatment of the polarization of the lattice waves. To study the importance of umklapp it is essential to have a good approximation for the electron-phonon matrix element at large momentum transfers. For this part Grimvall used the nonlocal model by Sham.¹³⁴ The lattice frequencies and polarization vectors were calculated in a network corresponding to 1000 points in the first Brillouin zone using the theoretical model by Krebs.¹³⁵ The direction of

¹³² A. O. E. Animalu, F. Bonsignori, and V. Bortolani, *Nuovo Cimento* **42B**, 83 (1966).

¹³³ E. Pytte, *J. Phys. Chem. Solids* **28**, 93 (1967); J. F. Janak, *Phys. Letters* **27A**, 105 (1968); P. N. Trofimenkoff, J. P. Carbotte, and R. C. Dynes, *ibid.* **27A**, 394 (1968), and others.

¹³⁴ L. J. Sham, *Proc. Roy. Soc. A* **283**, 33 (1965).

¹³⁵ K. Krebs, *Phys. Rev.* **138**, A143 (1965).

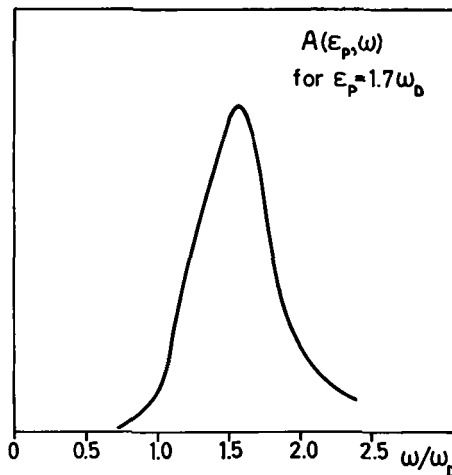


FIG. 31. Spectral function for Na at $T = 0^\circ\text{K}$ calculated with a realistic phonon spectrum after G. Grimvall, *Physik Kondensierten Materie* 6, 15 (1967).

the momentum of the electron was taken along the (100) axis. In Fig. 30 we give $\text{Re } \Sigma^{\text{ph}}$ resolved into four contributing parts: normal processes with "longitudinal" and "transverse" phonons and umklapp processes with "longitudinal" and "transverse" phonons. Grimvall concluded that for $\text{Re } \Sigma^{\text{ph}}$ the use of strictly longitudinal and transverse phonons is a rather good approximation even for the highly anisotropic sodium. The result for $\text{Re } \Sigma^{\text{ph}}$ when the electron momentum p was taken along the (111) axis was practically the same as for p along the (100) axis, so anisotropy in the phonon system does not necessarily give anisotropy in the effective mass. This can be understood from the form of Eq. (28.2) where we integrate over all q vectors up to $2k_F$ and tend to average out details about the lattice vibrations. The imaginary part, however, can be strongly dependent on the direction since the contributions to $\text{Im } \Sigma^{\text{ph}}$ come from a limited region in q space [Eq. (28.2)]. It is also essential to use correct polarization vectors and couple to transverse phonons via $(\hat{\epsilon} \cdot \hat{q})^2$ even for normal processes. $\text{Im } \Sigma^{\text{ph}}$ describes real transitions and is thus dependent on the strength of interaction and on the number of available final states. Even though the coupling to the transverse modes is rather weak, there are so many transverse phonons fulfilling the condition $\omega_T(q) < \omega$ [cf. Eq. (28.2)], that they contribute significantly.

The results for sodium thus show that there is practically no anisotropy in the effective mass. The damping on the other hand is found to be lower by 16% in the (111) direction and by 35% in the (110) direction. A de-

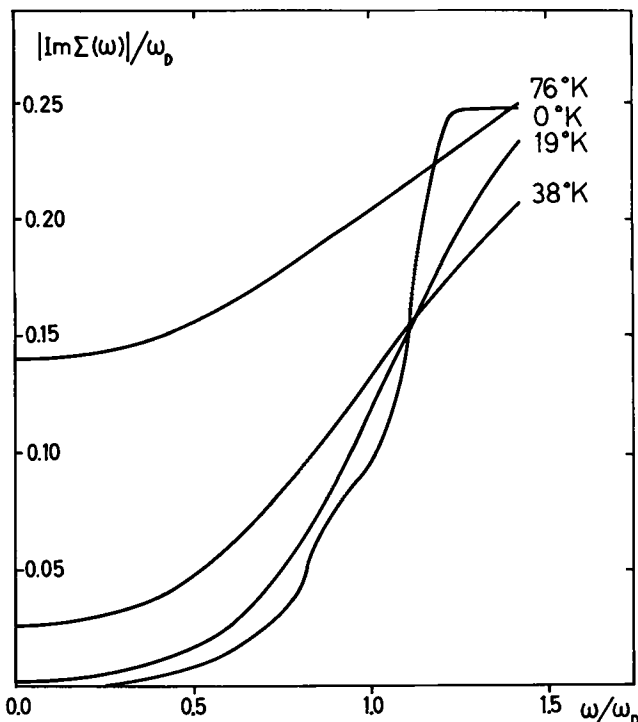


FIG. 32. Imaginary part of the self-energy for Na at different temperatures after G. Grimvall, *Physik Kondensierten Materie* 6, 15 (1967).

tailed study of lattice vibration anisotropy in metals has been made by Grimvall.¹³⁶

A typical example of the spectral function is given in Fig. 31. In the case of Na, the parts of the spectral weight function that cannot be taken into account using a simple Lorentzian do not contribute more than about 20% to the sum rule. Thus, there are no drastic effects for Na of the type illustrated in Fig. 29 by Engelsberg and Schrieffer.¹³⁰ The explanation lies in the weak electron-phonon coupling in Na as compared to the coupling strength considered by Engelsberg and Schrieffer.

The self-energy of an electron depends on both energy and temperature, and as a result, we have, for example, a temperature dependent deviation from the linear specific heat of the electrons. The first discussion of these effects was given in the early paper by Buckingham and Schafroth.¹²⁶ They used a constant electron-phonon coupling and a Debye model for the phonons. They showed that the temperature correction at $T \ll \Theta_D$ to the effective mass followed the law $T^2 \ln T$, a result which was later

¹³⁶ G. Grimvall, *Phys. Status Solidi* 32, 383 (1969).

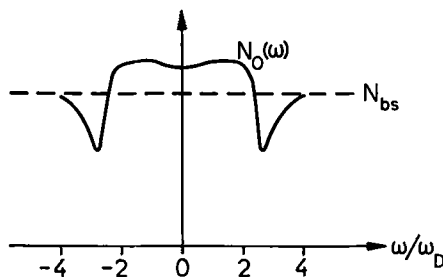


FIG. 33. Density of quasi-particle levels for Na at $T = 0^\circ\text{K}$ after G. Grimvall, *J. Phys. Chem. Solids* **29**, 1221 (1968).

proved in the general case by Eliashberg.¹²⁷ Buckingham and Schafroth obtained a formula for the free energy in terms of integrals, which cannot be evaluated in a closed form. Krebs¹²⁸ has given a plot of a numerical calculation of these integrals.

Much of the structure is smeared out already at very low temperatures, as indicated in Fig. 32, which gives the results for the $\text{Im } \Sigma^{\text{ph}}$ at four different temperatures; similar trends hold also for the real part.

It can easily be shown that the electron-phonon interaction gives no contribution to the density of states obtained by integrating the spectral function $A(p, \omega)$ over all momenta. However, it is well known that for example the electronic specific heat and the cyclotron resonance frequency are affected by the electron-phonon interaction. The result is often stated

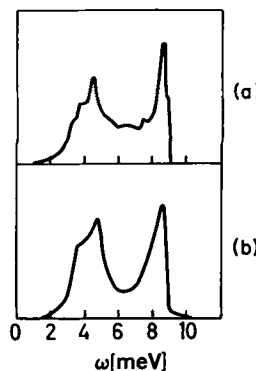


FIG. 34. (a) The density of phonon states $F(\omega)$ [R. Stedman, L. Almqvist, and G. Nilsson, *Phys. Rev.* **162**, 549 (1967)] and (b) the product of the electron-phonon interaction constant $\alpha^2(\omega)$ and $F(\omega)$ [W. L. McMillan and J. M. Rowell, in "Superconductivity" (R. D. Parks, ed.). Marcel Dekker, New York, 1968] for lead.

¹²⁷ G. M. Eliashberg, *Soviet Phys. JETP (English Transl.)* **16**, 780 (1963).

¹²⁸ K. Krebs, *Phys. Letters* **6**, 31 (1963).

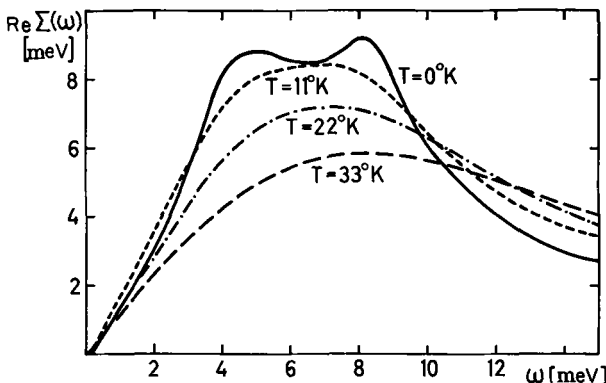


FIG. 35. Real part of the self-energy for lead at different temperatures; after G. Grimvall, *Physik Kondensierten Materie* **9**, 283 (1969).

in the form that the effective mass or the density of states at the Fermi level are enhanced by a factor $1 + \lambda$. To distinguish this concept of density of states from that obtained from the spectral function we call it a *level density* for quasi particles, defined by

$$N_0(\omega) = N_{\text{bs}} \{1 - \partial \Sigma^{\text{ph}}(\omega) / \partial \omega\}. \quad (30.3)$$

A typical plot of the density of levels was given already by Buckingham,¹²⁹ which agrees well with the calculation by Grimvall¹²² for Na, shown in Fig. 33.

31. SELF-ENERGY AND THE SPECTRAL FUNCTION FROM TUNNELING DATA. DENSITY OF LEVELS

A numerical study of the self-energy and spectral properties of Pb and Hg has recently been performed by Grimvall,¹²⁶ using data from superconductor tunneling. The quantity $\alpha^2(\omega)F(\omega)$ [see Eq. (28.4)] has been determined for Pb and Hg by McMillan and Rowell.¹²³ Its shape is not very different from that of the phonon spectrum, indicating that $\alpha^2(\omega)$ does not vary strongly with the energy ω . In Fig. 34 we give $\alpha^2(\omega)F(\omega)$ from McMillan and Rowell,¹²³ and $F(\omega)$ from Stedman *et al.*¹⁴⁰ for Pb. The results for the real and imaginary parts of Σ^{ph} have been calculated using Eq. (28.5). The real part of Σ^{ph} is given for Pb at different temperatures in Fig. 35.

Knowing Σ^{ph} one can easily find the spectral function. From the work by Engelsberg and Schrieffer¹³¹ one expects deviations from quasi-particle

¹²⁹ M. J. Buckingham, *Nature* **168**, 281 (1951).

¹⁴⁰ R. Stedman, L. Almqvist, and G. Nilsson, *Phys. Rev.* **162**, 549 (1967).

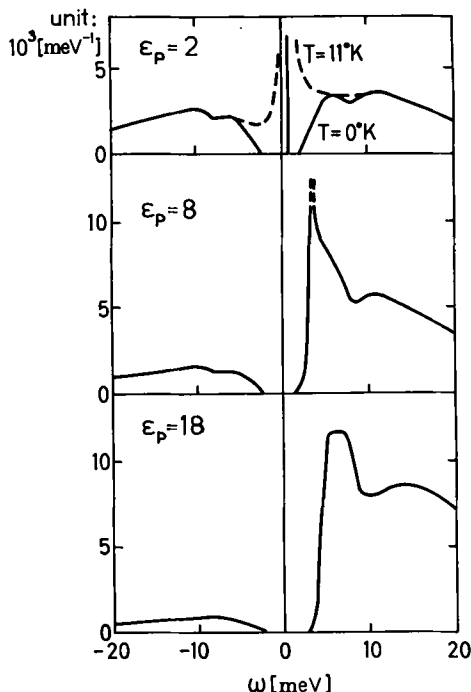


FIG. 36. Spectral function $A(\epsilon_p, \omega)$ for lead at three values of the momentum; after G. Grimvall, *Physik Kondensierter Materie* 9, 283 (1969).

behavior for electron energies $\epsilon(p)$ comparable to phonon energies. Figure 36 shows $A(p, \omega)$ for Pb at three values of $\epsilon(p)$ (i.e. three values of p). The sharp peak for $\epsilon(p) = 2$ meV in Fig. 36 reflects that the electron-phonon interaction causes the system to behave as if the electron had an excitation energy $\epsilon(p)/(1 + \lambda)$, where $1 + \lambda = 1/Z^{ph}$ is the enhancement factor [see Eq. (29.2)]. The broad wing of $A(p, \omega)$ on the upper side of the Fermi level describes the emission of phonons that occurs when the “bare” electron is inserted. The sharp peak contributes $1/(1 + \lambda) = 0.40$ to the sum rule. The system therefore has a well-defined quasiparticle whose strength is only 0.40. At higher energies, $\epsilon(p) = 8$ meV, the electron peak has moved into the upper phonon peak and the system shows no quasi-particle behavior at all. At still higher energies, $\epsilon(p) = 18$ meV, a large portion of the sum rule is filled by the wide Lorentz-like curve centered at an energy roughly equal to that of the inserted “bare” electron; however, the decay rate is now so large that the quasi-particle picture may not be very useful.

32. TEMPERATURE EFFECTS IN SPECIFIC HEAT AND CYCLOTRON RESONANCE

In the limit of low temperatures cyclotron resonance and specific heat, both depend on the same enhancement factor $1 + \lambda = 1 - (\partial \Sigma^{\text{ph}} / \partial \omega)_{\omega=0}$ of the effective electron mass. At finite temperatures we have of course to consider effects of the finite lifetime; however, there are more complications. There will also be excitations to energies, where the self-energy $\Sigma^{\text{ph}}(\omega)$ is no longer linear in ω . The explicit temperature dependence is an additional difficulty. We shall discuss briefly how this may affect the cyclotron resonance frequency and the electronic specific heat. High frequency cyclotron resonance has been treated by Scher and Holstein¹⁴¹ using many-body technique and much of their discussion is relevant also for temperature effects. A general discussion of the specific heat and other properties has been given by Prange and Kadanoff.¹¹⁹ The problem has recently been reconsidered and discussed in lecture notes by Wilkins¹⁴² and in a paper by Grimvall,¹²⁵ with particular emphasis on the experimental verification of the temperature effects.

Let Θ_E be a characteristic temperature for the phonon spectrum, or more appropriately, for the function $\alpha^2(\omega)F(\omega)$, which enters the self-energy formula Eq. (28.5). For monovalent metals the coupling between electrons and longitudinal phonons is dominating and it is reasonable to choose Θ_E as the Debye temperature Θ_D of the metal. For polyvalent metals, however, there is a strong coupling to low energy transverse modes via umklapp processes and Θ_E will be smaller than Θ_D , say, typically $\Theta_E \sim \Theta_D/2$. In Fig. 35 we can notice a strong deviation in $\Sigma^{\text{ph}}(\omega)$ from linearity when $\omega = k_D\Theta_D$ ($= 7.3$ meV). In cyclotron resonance experiments one is always restricted to low temperatures because of the condition $\omega_c\tau \gg 1$, where the lifetime τ is limited by thermal scattering. The electrons taking part in the resonance are located within the energy range of thermal smearing $\sim k_B T$ from the Fermi level. Therefore they will always be on the linear part of $\Sigma^{\text{ph}}(\omega)$. However, the explicit temperature dependence of the self-energy $\Sigma^{\text{ph}}(\omega, T)$ will make the enhancement factor $1 + \lambda(T)$ temperature dependent. This can be interpreted in the form of a temperature dependent effective mass

$$m_e = m_0[1 + \lambda(T)]. \quad (32.1)$$

In Fig. 37 $\lambda(T)/\lambda(0)$ is given for mercury from the calculation by Grimvall.¹²⁵

The electronic specific heat is much more complicated to discuss at

¹⁴¹ H. Scher and T. Holstein, *Phys. Rev.* **148**, 598 (1966).

¹⁴² J. W. Wilkins, Lectures given at NORDITA, Copenhagen, Denmark, 1968.

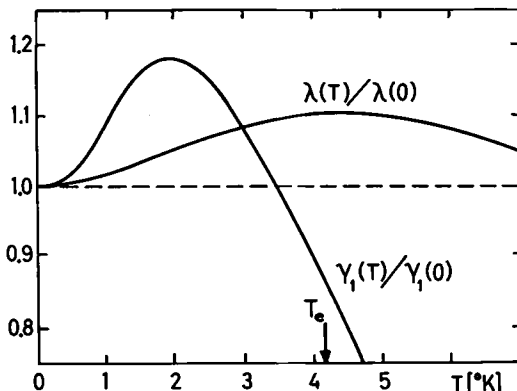


FIG. 37. Temperature dependence of the enhancement factors $\lambda(T)$ for the cyclotron mass in Eq. (32.1) and $\gamma(T)$ for the specific heat in Eq. (32.2); after G. Grimvall, *Physik Kondensierter Materie* 9, 283 (1969).

finite temperatures. From the derivation, in textbooks, of the heat capacity of a degenerate Fermi gas, it is easy to see that the most important excitations are those at 2–3 times $k_B T$ rather than those with energies less than $k_B T$. One therefore expects very strong deviations from the linear temperature dependence of the specific heat when $T \sim \Theta_E/3$. Another question is how the finite lifetime of the excitations will enter the expression for the specific heat. The problem has been treated theoretically by Prange and Kadanoff.¹¹⁹ Let us write for the electronic specific heat C_{el}

$$C_{el} = [\gamma_0 + \gamma_1(T)]T, \quad (32.2)$$

where γ_0 is the result when no electron-phonon effects are included. Thus $\gamma_1(T)$ incorporates all electron-phonon effects. At $T = 0$ we have

$$\gamma_0 + \gamma_1(0) = \gamma_0[1 + \lambda(0)].$$

In Fig. 37 we show $\gamma_1(T)/\gamma_1(0)$ for mercury as calculated by Grimvall¹²⁵ using the expression by Prange and Kadanoff.¹¹⁹ It is seen that the non-linear behavior of the specific heat enters at a low temperature.

The temperature effects in mercury and lead on the cyclotron resonance and the specific heat seem just about large enough to be experimentally accessible. For the interesting structure of the spectral function for a strong-coupling system as illustrated in Section 31, we are not aware of any experimental technique now available to directly study such effects. For de Haas-van Alphen oscillations the temperature effects seem to cancel out.^{142a}

^{142a} S. Engelsberg, private communication.

IX. The One-Electron Spectrum in a Real Solid

33. INTRODUCTORY REMARKS ABOUT THE SELF-ENERGY AND THE ENERGY SPECTRUM

We shall in this part try to present a comprehensive picture of the one-electron spectrum (neglecting phonon effects), over a wide energy range from core electrons to keV electrons injected externally. The emphasis throughout the discussion will be on the effects due to the valence electrons. We will not pay much attention to Fermi surface properties, but will rather concentrate on the interesting effects of the interaction, which occur away from the Fermi surface. For problems related to magnetism, we refer to the recent survey by Herring.¹⁴³

In most regions of the spectrum the quasi particles have an appreciable linewidth, but they are nevertheless physically very well defined excitations. The quasi-particle states are solutions of the single-particle equation

$$[E_k - h(\mathbf{x}) - V(\mathbf{x})] \varphi_k(\mathbf{x}) - \int \Sigma(\mathbf{x}, \mathbf{x}'; E_k) \varphi_k(\mathbf{x}') d\mathbf{x}' = 0, \quad (33.1)$$

where Σ is the self-energy or the exchange-correlation potential. The energy E_k is in general complex; the imaginary part is a measure of the quasi-particle lifetime as described in Part VI.

The structure of the spectrum is conventionally discussed in terms of a *density of states*. This concept is, however, not without ambiguities in an interacting system. When we talk about quasi particles it is natural to introduce a function which describes their distribution in energy, and we define the *quasi-particle density of levels* as

$$N_0(\omega) = \sum_{\mathbf{k}} \delta(\omega - \operatorname{Re} E_k). \quad (33.2)$$

This function gives the distribution of Landau quasi particles, and is therefore associated with the Fermi liquid properties. It is obvious that the results obtained from an energy band calculation, where exchange and correlation is accounted for in an appropriate way, will give $N_0(\omega)$.

We may also define a *density of one-particle states* that takes the width of the quasi particles into account as well as background effects. This density of states, which is pertinent for e.g. soft X-ray spectra and photo-emission, was introduced in Section 10, and is defined as

$$N(\omega) = \operatorname{tr} A(\omega) = \sum_s ||f_s||^2 \delta(\omega - \epsilon_s). \quad (33.3)$$

¹⁴³ C. Herring, in "Magnetism" (G. T. Rado and H. Suhl, eds.), Vol. IV. Academic Press, New York, 1966; see also "Theory of magnetism in transition metals," *Proc. Int. School of Physics* (W. Marshall, ed.). Academic Press, New York, 1967.

In this formula $||f_s||^2$ is an effective "oscillator strength" for adding or removing a particle. The index s refers to exact eigenstates of the whole system.¹⁴⁴ For a noninteracting system N_0 and N are of course the same. They are also for practical purposes the same if the width of the quasi-particle peak is small compared to the bandwidth, and if sideband and background effects can be neglected. In general, $N_0(\omega)$ and $N(\omega)$ are appreciably different.

We shall base our discussion on the same approximation for the self-energy Σ as was defined in Section 14 and discussed in considerable detail in Section 25. Although so-called vertex corrections no doubt are of importance, we believe this approximation to be an essential step beyond the HF theories, and able to give new insight and useful results over the entire spectral region of interest to us.

This approximate formula for the self-energy was first discussed by Quinn and Ferrell⁸⁵ for the electron gas in the small r_s limit. A discussion in relation to valence bands in solids was given by Pratt.¹⁴⁶ A more extensive discussion was presented by Phillips⁷¹ followed by numerical calculations by Cohen and Phillips¹⁴⁶ and by Phillips and Kleinman.¹⁴⁷ The properties of the theory were discussed and analyzed in a fundamental way by Bassani *et al.*,¹⁴⁸ who gave a formulation suitable for application in the OPW method. Quinn¹⁴⁹ discussed the damping of quasi particles in the range from the Fermi surface to the keV range, and Pratt¹⁵⁰ discussed relativistic effects in the valence band. A comprehensive discussion including the effects of core electrons was given by Hedin,¹⁵¹ who also gave numerical results. A careful analysis of correlation for Si was made by Brinkman and Goodman.¹⁵² The first calculations of the spectral function for an electron gas^{88,91,92} and for the core energy region in a metal,¹⁵³ were carried out by Lundqvist. Finally, it should be remarked that extensive discussions of one-electron properties, before the field theory method became fashionable, were given by Nozières and Pines,¹⁵⁴ and we refer to the survey article by Pines²² for a review of the earliest discussions of these problems.

¹⁴⁴ If we sum over the δ functions in Eq. (33.3) without the weight factor f_s , we obtain the spectral density that appears in the sum over states in statistical mechanics.

¹⁴⁵ G. W. Pratt, Jr., *Phys. Rev.* **118**, 462 (1960).

¹⁴⁶ M. H. Cohen and J. C. Phillips, *Phys. Rev.* **124**, 1818 (1961).

¹⁴⁷ J. C. Phillips and L. Kleinman, *Phys. Rev.* **128**, 2098 (1962).

¹⁴⁸ F. Bassani, J. Robinson, B. Goodman, and J. R. Schrieffer, *Phys. Rev.* **127**, 1969 (1962).

¹⁴⁹ J. J. Quinn, *Phys. Rev.* **126**, 1453 (1962).

¹⁵⁰ G. W. Pratt, Jr., *Rev. Mod. Phys.* **35**, 502 (1963).

¹⁵¹ L. Hedin, *Arkiv Fysik* **30**, 231 (1965).

¹⁵² W. Brinkman and B. Goodman, *Phys. Rev.* **149**, 597 (1966).

¹⁵³ B. I. Lundqvist, *Physik Kondensierter Materie* **9**, 236 (1969).

¹⁵⁴ P. Nozières and D. Pines, *Phys. Rev.* **109**, 1062 (1958).

The explicit formula to be used for the self-energy is

$$\begin{aligned}\Sigma(\mathbf{x}, \mathbf{x}'; \omega) &= \frac{i}{(2\pi)} \int W(\mathbf{x}, \mathbf{x}'; \omega') G(\mathbf{x}, \mathbf{x}'; \omega + \omega') e^{i\omega' \delta} d\omega' \\ &= \frac{i}{(2\pi)} \sum_k \int \frac{W(\mathbf{x}, \mathbf{x}'; \omega') \varphi_k^*(\mathbf{x}) \varphi_k(\mathbf{x}')}{\omega' + \omega - \epsilon_k} e^{i\omega' \delta} d\omega',\end{aligned}\quad (33.4)$$

where we have inserted a zero order Green function of the form

$$G_0(\mathbf{x}, \mathbf{x}'; \omega) = \sum_k \varphi_k(\mathbf{x}) \varphi_k^*(\mathbf{x}') (\omega - \epsilon_k)^{-1}.$$

In the screened potential $W = v\epsilon^{-1} = v(1 - Pv)^{-1}$, we calculate the polarization part P using the linearized Hartree theory. The formula for P is given in Eq. (5.21) and also in Eq. (14.5). The sum over occupied states also includes the core levels.

Before going into the more detailed discussions in the following sections, it may be helpful to summarize some important qualitative results. For fast electrons (see Section 14) the real part of Σ is small and the imaginary part gives the now well-known results obtained by Kramers¹⁵⁵ and by Lindhard.²⁰ The core levels are shifted upward relative to their positions in a free atom, and there is a characteristic satellite structure below each level. The effect of Σ on the valence band is essentially a uniform shift to lower energy and in addition the appearance of a low energy satellite from the same physical mechanism, hole-plasmon coupling, as was discussed for the electron gas in Section 25.

After this broad outline we will turn to the more detailed picture in the following sections. We will discuss in turn the polarization propagator and the inversion of the dielectric function, the valence bands, and the core electrons. In the section on the effective crystal potential we discuss primarily the potential from the ion cores.

In the last section of this part we take up the question of local density approaches of the Thomas-Fermi type and in particular the scheme developed by Hohenberg, Kohn, and Sham.¹⁵⁶⁻¹⁵⁸

34. THE DIELECTRIC PROPERTIES

To obtain the screened interaction $W = v\epsilon^{-1} = v(1 - Pv)^{-1}$, we must invert the dielectric function ϵ :

$$\epsilon(\mathbf{r}, \mathbf{r}'; \omega) = \delta(\mathbf{r} - \mathbf{r}') - \int P(\mathbf{r}, \mathbf{r}''; \omega) v(\mathbf{r}'', \mathbf{r}') d\mathbf{r}''. \quad (34.1)$$

¹⁵⁵ H. A. Kramers, *Physica* **13**, 401 (1947).

¹⁵⁶ P. Hohenberg and W. Kohn, *Phys. Rev.* **136**, B864 (1964).

¹⁵⁷ W. Kohn and L. J. Sham, *Phys. Rev.* **140**, A1133 (1965).

¹⁵⁸ L. J. Sham and W. Kohn, *Phys. Rev.* **145**, 561 (1966).

This inversion problem forms the main topic of the present section. For P we use the linearized time-dependent Hartree approximation (LTH),

$$P(\mathbf{r}, \mathbf{r}'; \omega) = - \sum_{\mathbf{k}}^{\text{unocc}} \sum_{\mathbf{l}}^{\text{occ}} \frac{2(\epsilon_{\mathbf{k}} - \epsilon_{\mathbf{l}})}{(\epsilon_{\mathbf{k}} - \epsilon_{\mathbf{l}})^2 - \omega^2} f_{\mathbf{k}\mathbf{l}}(\mathbf{r}) f_{\mathbf{k}\mathbf{l}}^*(\mathbf{r}'), \quad (34.2)$$

where

$$\begin{aligned} f_{\mathbf{k}\mathbf{l}}(\mathbf{r}) &= \int \varphi_{\mathbf{k}}(\mathbf{x}) \varphi_{\mathbf{l}}^*(\mathbf{x}) d\xi = \varphi_{\mathbf{k}}(\mathbf{r}) \varphi_{\mathbf{l}}^*(\mathbf{r}), && \text{same spin} \\ &= 0, && \text{opposite spin.} \end{aligned} \quad (34.3)$$

The LTH approximation for P is probably good enough at present as regards correlation effects on one-electron properties, while for other properties such as pseudopotential screening or lattice vibrations, more elaborate approximations seem to be required.

The explicit inversion of the dielectric function can be done only in extreme limiting cases. The electron gas is such a case. We then transform the equation to momentum space and obtain the scalar formula $\epsilon(q, \omega) = 1 - v(q)P(q, \omega)$ discussed extensively in Section 27. In an electron gas the electrons move freely and do not form localized charges.¹¹⁵ Correspondingly they sample macroscopic regions of the system, so that the effective field acting on each electron is the total macroscopic field. Another limiting case is the idealized van der Waals crystal, with no overlap between atoms. One can also in this case construct explicitly the dielectric tensor and its inverse.²¹ In this case the electrons are well localized and the formulas show that one obtains the full Lorentz local field correction.

Thus the LTH formula does fully include the local corrections to the classical field in the system. The key factor determining the magnitude of the local field correction is the degree of localization of the electron in the initial and final states. There are indications that in real solids the local field corrections are generally quite small.

In a real solid the polarization part is not fully translational invariant but only under the discrete translations of the lattice, and instead of a scalar formula as for an electron gas one obtains a matrix in reciprocal space, $\epsilon_{\mathbf{K}\mathbf{K}'}(q, \omega) = \delta_{\mathbf{K}\mathbf{K}'} - v(q + \mathbf{K})P_{\mathbf{K}\mathbf{K}'}(q, \omega)$. The diagonal element of this matrix was discussed by Ehrenreich and Cohen.²³ Adler¹⁵⁹ showed that the neglect of the nondiagonal terms was equivalent to neglecting local field effects. Wiser¹⁶⁰ found the local field effects to be quite small for Cu and Hedin *et al.*¹⁶¹ obtained the not unexpected result that they seem to be small also in Na.

¹¹⁵ S. L. Adler, *Phys. Rev.* **126**, 413 (1962).

¹⁶⁰ N. Wiser, *Phys. Rev.* **129**, 62 (1963).

¹⁶¹ L. Hedin, A. Johansson, B. I. Lundqvist, S. Lundqvist, and V. Samathiyakanit, *Arkiv Fysik* **39**, 97 (1969).

TABLE IX. ATOMIC POLARIZABILITIES AND RADII IN ATOMIC UNITS

	He	Li^+	Ne	Na^+	Ar	K^+
α_{expt}^a	1.385	0.1934	2.69	1.05	11.0	5.4
α_{HF}^a	1.49	0.205	2.76	1.10	15.7	7.3
r_0^b	1.12	0.73	1.15	1.00	2.03	1.80

^a M. Yoshimine and R. P. Hurst, *Phys. Rev.* **135**, A612 (1964).

^b Last inflection point of outermost HF orbital.

In such cases it seems reasonable to treat the nondiagonal effects as a perturbation. The diagonal elements of the dielectric matrix for a simple metal is expected to have similar general characteristics as for free electrons. Even for valence semiconductors such as Si it has been suggested by Phillips²¹ that the nondiagonal elements are small. Calculations by Penn on Si,¹⁶² using a simple band model, show that the diagonal element is not much different from the electron gas result, except of course for small q values. Brandt and Reinheimer¹⁶³ present extensive numerical results on the influence of a band gap on the dielectric function, using essentially the Penn model. Linderberg¹⁶⁴ has studied the dielectric properties including also the HF exchange terms. He used the Fredholm method to obtain the inverse dielectric function. A recent study of the Penn model has been made by Srinivasan.^{164a}

The sum over occupied states l in Eq. (34.2) includes the core levels. The corresponding energy denominators are large and these terms describe the core polarization. It is convenient to split the polarization propagator P into valence and core parts according to

$$P = \sum_k^{\text{unocc}} \sum_l^{\text{core}} + \sum_k^{\text{unocc}} \sum_l^{\text{occ val}} = P^c + P^v. \quad (34.4)$$

P^c is closely the same as the polarization propagator of a free ion.¹⁵¹ For an ion the polarizability is small and it is meaningful to expand the dielectric function as

$$\epsilon^{-1} = (1 - P^c v)^{-1} = 1 + P^c v + P^c v P^c v + \dots \quad (34.5)$$

The lowest order approximation, $1 + P^c v$, is the so-called uncoupled HF

¹⁶² D. R. Penn, *Phys. Rev.* **128**, 2093 (1962).

¹⁶³ W. Brandt and J. Reinheimer, *Can. J. Phys.* **46**, 607 (1968).

¹⁶⁴ J. Linderberg, *Arkiv Fysik* **26**, 323 (1964).

^{164a} G. Srinivasan, *Phys. Rev.* **178**, 1244 (1969).

approximation,¹⁶⁵ which works fairly well for ions. Some typical values for the polarizability are listed in Table IX. We see that the theoretical values are consistently larger than the experimental ones. The higher order terms in Eq. (34.5) tend to screen the field and will give a reduction of the polarizability, and already the next term $PvPv$ should contain most of the residual effects. A more detailed discussion on dielectric screening in atoms and its effect on atomic polarizabilities has been given by Brandt and Lundqvist.¹⁶⁶

For the case of a metal, where P^c is small compared to P^v , we may expand the screened potential as

$$W = W^v + W^v P^c W^v + W^v P^c W^v P^c W^v + \dots, \quad (34.6)$$

where

$$W^v = v(1 - P^v v)^{-1}. \quad (34.7)$$

Thus we have a clear separation of W in a valence part and a dynamically screened polarization potential from the ion cores. We can also split the reciprocal lattice matrix representation of P into a diagonal and a non-diagonal part $P = P_0 + P_1$, and expand the valence part of W according to

$$W^v = W_0^v + W_0^v P_1^v W_0^v + \dots. \quad (34.8)$$

Alternatively we can expand the full screened potential as

$$W = W_0 + W_0 P_1 W_0 + W_0 P_1 W_0 P_1 W_0 + \dots, \quad (34.9)$$

where

$$W_0 = v(1 - P_0 v)^{-1} \quad (34.10)$$

relates to the diagonal part of P . This expansion is useful if P_1^v and P_1^c are both small compared to P_0^v and P_0^c . This situation may occur e.g. in heavily doped semiconductors where P^c will be the contribution from the valence band and P^v the contribution from the impurity conduction band. If we further neglect the frequency and wave-number dependence in the core part and replace $P_0^c(q, \omega)$ and $P_0^c(0, 0)$ in the expression for W_0 , we obtain the simple and intuitively appealing result¹⁶¹

$$W_0(q, \omega) = [v(q)/\epsilon_s] \{1 - [v(q)/\epsilon_s] P_0^v(q, \omega)\}^{-1}, \quad (34.11)$$

where ϵ_s is the static dielectric constant of the undoped semiconductor. This result was suggested by Wolff¹⁶⁷ and is justified if the energy gap in the semiconductor is large compared with the bandwidth of the impurity band. Normally P_0^c and P_1^c are of comparable magnitude, and Eq. (34.6) then represents the most convenient expansion.

¹⁶⁵ If we use Hartree-Fock rather than Hartree one-electron functions and energies for the core electrons. See Section 37 and also A. Dalgarno, *Advan. Phys.* **11**, 281 (1962).

¹⁶⁶ W. Brandt and S. Lundqvist, *Arkiv Fysik* **28**, 399 (1965).

¹⁶⁷ P. A. Wolff, *Phys. Rev.* **126**, 405 (1962).

For the further discussion of W^* , we transform to wave number space,

$$P^*(\mathbf{q}, \mathbf{q}'; \omega) = \Omega^{-1} \int \exp(i\mathbf{q} \cdot \mathbf{r}) P^*(\mathbf{r}, \mathbf{r}'; \omega) \exp(-i\mathbf{q}' \cdot \mathbf{r}') d\mathbf{r} d\mathbf{r}'. \quad (34.12)$$

P^* is zero unless \mathbf{q} and \mathbf{q}' differ by a reciprocal lattice vector, and one often uses an explicit matrix notation $P(\mathbf{q} + \mathbf{K}, \mathbf{q} + \mathbf{K}'; \omega) = P_{\mathbf{KK}'}(\mathbf{q}, \omega)$, with \mathbf{q} limited to the first Brillouin zone. For the present discussion, however, we prefer the form $P(\mathbf{q}, \mathbf{q}'; \omega)$. Using the extended zone scheme we obtain for the diagonal element $P_0(\mathbf{q}; \omega) \equiv P(\mathbf{q}, \mathbf{q}; \omega)$

$$\begin{aligned} P_0^*(\mathbf{q}, \omega) = & -\Omega^{-1} \sum_{\mathbf{k}}^{\text{unocc}} \sum_{\mathbf{l}}^{\text{occ val}} \frac{2(\epsilon_{\mathbf{k}} - \epsilon_{\mathbf{l}})}{(\epsilon_{\mathbf{k}} - \epsilon_{\mathbf{l}})^2 - \omega^2} \{ \delta_{\mathbf{l}, \mathbf{k}+\mathbf{q}} | 1 + \Delta(\mathbf{k}, \mathbf{q}; 0) |^2 \\ & + \sum_{\mathbf{K} \neq 0} | \Delta(\mathbf{k}, \mathbf{q}; \mathbf{K}) |^2 \delta_{\mathbf{l}, \mathbf{k}+\mathbf{q}+\mathbf{K}} \}. \end{aligned} \quad (34.13)$$

The Bloch functions are written as $\varphi_{\mathbf{k}}(\mathbf{r}) = \Omega^{-1/2} u_{\mathbf{k}}(\mathbf{r}) \exp(i\mathbf{k} \cdot \mathbf{r})$ and

$$\Delta(\mathbf{k}, \mathbf{q}; \mathbf{K}) = \Omega_0^{-1} \int_{\Omega_0} \exp(-i\mathbf{K} \cdot \mathbf{r}) (u_{\mathbf{k}}(\mathbf{r}) u_{\mathbf{k}+\mathbf{q}+\mathbf{K}}^*(\mathbf{r}) - 1) d\mathbf{r} \quad (34.14)$$

is a measure of the deviations of the Bloch functions from plane waves; Ω_0 is the volume of the lattice unit cell. Because of the orthonormality of the Bloch functions, the Δ function vanishes in the important limit $\mathbf{q} \rightarrow 0$:

$$\lim_{\mathbf{q} \rightarrow 0} \Delta(\mathbf{k}, \mathbf{q}; \mathbf{K}) = 0. \quad (34.15)$$

Estimates of Δ have been made by Hedin *et al.*¹⁶¹ for the case of Na using one OPW function. The Δ 's are only a few hundredths large.¹⁶⁸

The nondiagonal term of P^* has the form

$$\begin{aligned} P_1^*(\mathbf{q}, \mathbf{q}'; \omega) = & -\Omega^{-1} \sum_{\mathbf{k}}^{\text{unocc}} \sum_{\mathbf{l}}^{\text{occ val}} \frac{2(\epsilon_{\mathbf{k}} - \epsilon_{\mathbf{l}})}{(\epsilon_{\mathbf{k}} - \epsilon_{\mathbf{l}})^2 - \omega^2} \{ \Delta(\mathbf{k}, \mathbf{q}; \mathbf{q}' - \mathbf{q}) \delta_{\mathbf{l}, \mathbf{k}+\mathbf{q}} \\ & + \Delta^*(\mathbf{k}, \mathbf{q}'; \mathbf{q} - \mathbf{q}') \delta_{\mathbf{l}, \mathbf{k}+\mathbf{q}'} \}, \end{aligned} \quad (34.16)$$

where we have neglected terms quadratic in Δ and where \mathbf{q} and \mathbf{q}' differ by a reciprocal lattice vector. Again the contributions from $\mathbf{k} \sim 1$ are cut down to small values because of the property of Δ expressed in Eq. (34.15).

We have found that, except in special cases, such as heavily doped semi-

¹⁶⁸ With one OPW function only the effects of the core but not of the Brillouin zones are taken into account. Since, however, the Δ 's in P and Σ occur in integrals over \mathbf{k} space, the net effects of the Brillouin zones may not be large. We note that if we neglect the Δ^2 term in P_0^* we have a result which is very similar to the electron gas formula.

conductors, it is suitable to write the screened potential W as $W^* + W^*P^cW^*$ [see Eq. (34.6)]. The second term is a dynamically screened polarization potential from the ion core, and makes only a fairly small contribution. We further conclude that the diagonal part of the valence-electron screened potential W^* is dominating, and that we therefore can regard the second term in Eq. (34.8) as a small correction. The diagonal term W_0^* has a similar structure as in the electron gas case [see Eq. (34.13)]. Since the effects of the lattice enter only in an averaged way, electron gas results should be useful for simple metals, and also to some extent for valence semiconductors.

35. THE VALENCE BANDS

a. Main Features of the Valence Electron Spectrum

We shall first give a discussion of the formula for the self-energy $\Sigma(\omega)$ given in Eq. (33.4). For energies in the valence band region we decompose Σ schematically as

$$\Sigma = GW = G^cW + G^*W^*P^cW^* + G^*W^*, \quad (35.1)$$

where we have written $G = G^c + G^*$. Here G^c contains the contribution from the core states, while G^* includes the summation over valence band states up to infinite energies. Furthermore, we have split G^*W in two terms according to Eq. (34.6). The terms in Eq. (35.1) have the following interpretation:

$G^cW \cong V_{\text{ex}}^c$ exchange potential from the core

$G^*W^*P^cW^* = \Sigma_{\text{pol}}^c$ screened polarization potential from the core (35.2)

$G^*W^* = \Sigma^*$ self-energy of the valence electrons.

We shall next discuss in more detail these various contributions. It was pointed out by Phillips⁷¹ that the screening of the core-valence exchange is ineffective due to the large energy denominators involved, and thus G^cW can be replaced by G^cv , which is exactly the HF exchange potential from the core.^{151,152}

To identify Σ_{pol}^c we make a comparison with the polarization potential from the core of a free ion. In this case we may expand W in powers of the bare potential v , and obtain

$$\Sigma^c = GW = Gv(1 - P^cv)^{-1} = Gv + GvP^cv + \dots$$

The first term is the HF exchange potential, while the second gives the polarization potential. Comparison with Eq. (35.2) shows that Σ_{pol}^c corresponds to a dynamically screened polarization potential. A further discussion will be given in Section 37.

The last term, Σ^v , is the result we obtain by taking only the valence electrons into account. Σ^v is considerably larger than the two other terms, which are of comparable magnitude. In a Bloch function representation we obtain for the diagonal element¹⁵¹ of Σ^v

$$\langle \mathbf{k} | \Sigma^v(\epsilon) | \mathbf{k} \rangle = \frac{i}{(2\pi)^4} \int \frac{W_0^v(\mathbf{q}, \omega)}{\omega + \epsilon - \epsilon_{\mathbf{k}+\mathbf{q}}} | 1 + \Delta(\mathbf{k}, \mathbf{q}; 0) |^2 d\mathbf{q} d\omega, \quad (35.3)$$

and for the nondiagonal element

$$\begin{aligned} \langle \mathbf{k} + \mathbf{K} | \Sigma^v(\epsilon) | \mathbf{k} \rangle &= \frac{i}{(2\pi)^4} \int \left[\frac{W_0^v(\mathbf{q}, \omega) \Delta(\mathbf{k}, \mathbf{q}; \mathbf{K})}{\omega + \epsilon - \epsilon_{\mathbf{k}+\mathbf{q}+\mathbf{K}}} \right. \\ &\quad \left. + \frac{W_0^v(\mathbf{q}, \omega) \Delta^*(\mathbf{k} + \mathbf{K}, \mathbf{q}; -\mathbf{K})}{\omega + \epsilon - \epsilon_{\mathbf{k}+\mathbf{q}}} \right] d\mathbf{q} d\omega. \end{aligned} \quad (35.4)$$

The quantity Δ is a measure of the deviation of the Bloch waves from plane waves defined by Eq. (34.14). We have neglected local field effects by using the diagonal term instead of the full W^v , and we have also dropped some terms of order Δ^2 . The diagonal element $\langle \mathbf{k} | \Sigma^v(\omega) | \mathbf{k} \rangle$ has the same structure as for an electron gas, only that we are using an appropriate energy spectrum and have an effective potential $v | 1 + \Delta |^2$ instead of v .

Equations (35.3) and (35.4) form the basis for the discussion in this section. We shall first comment on how to obtain the spectral function and next on the calculation of the quasi-particle energies E_k . We neglect for simplicity the nondiagonal elements of G and will then obtain

$$G(\mathbf{k}, \omega) = \langle \mathbf{k} | \omega - h - V - \Sigma(\omega) | \mathbf{k} \rangle^{-1}. \quad (35.5)$$

The spectral function now takes the simple form

$$A(\mathbf{x}, \mathbf{x}'; \omega) = \pi^{-1} \sum_{\mathbf{k}} \psi_{\mathbf{k}}(\mathbf{x}) \psi_{\mathbf{k}}^*(\mathbf{x}') | \text{Im } G(\mathbf{k}, \omega) |. \quad (35.6)$$

The main features of the conduction band spectrum for simple metals can now be related to the results for an electron gas. The discussions of the dispersion law, bandwidth, damping, momentum distribution, and density of states given in Sections 25d–25g will all apply.

We should, however, keep in mind that while $G(\mathbf{k}, \omega)$ is by and large the same as for an electron gas, the spectral function is described in terms of the proper Bloch functions, which have all the proper wiggles in the core region and correspond to the correct symmetry combinations of plane waves in the outer parts. This fact is important when we need matrix elements for transitions. We wish to stress that the energy dependence of Σ will give rise to new and important structure like the plasmaron state below the quasi-particle band.

To summarize this discussion we write the effective total "potential" in the form

$$V_n + V_H + V_{ex}^c + \Sigma_{pol}^c(\omega) + \Sigma^*(\omega), \quad (35.7)$$

where V_n is the Coulomb potential of the nuclei and V_H is the total electronic Hartree potential. V_{ex}^c and Σ_{pol}^c are fairly small. For the energy arguments in $\Sigma_{pol}^c(\omega)$ and $\Sigma^*(\omega)$, we may use the unperturbed energy ϵ_k as will be discussed in Section 35d. The nondiagonal elements of Σ^* are fairly small and the diagonal element is often not far from the electron gas results, except possibly in regions close to bandgaps.

The approach developed here is an improved version of earlier work by one of us.¹⁵¹ We shall next review the results by Phillips and co-workers, by Brinkman and Goodman, and by Bassani, Robinson, Goodman, and Schrieffer.

b. The Approach by Phillips and the Work by Brinkman and Goodman

A very direct approach to include dynamical effects in band structure calculations was made by Phillips⁷¹ in 1961. He used the same idea as in Koopmans' theorem and formed the variational derivative of the total energy with respect to the occupation number n_k in order to obtain a single-particle energy. Using the Lindhard dielectric function in the formula for the energy, he concluded that the proper correlation and exchange potential was a dynamically screened exchange potential [cf. Eq. (14.11)] plus a constant contribution that corresponds to the second term in Eq. (14.11), that is, the Coulomb hole term.¹⁵² For an electron gas at small r_s essentially all the \mathbf{k} dependence of the quasi-particle energy comes from the screened exchange term and the Coulomb hole term is essentially constant. It is, however, not at all clear that this term should also remain a constant in a solid. From the discussion in Section 35a it is clear that the dispersion of $\Sigma^*(\mathbf{k}, \epsilon_k)$ has little to do with its influence on band gaps, and we actually may expect the Coulomb hole term to have a more important effect on band structure than the screened exchange one, simply because it is larger.

Cohen and Phillips¹⁴⁶ attempted a self-consistent solution including the exchange potential discussed above for valence semiconductors. They obtained a modified dielectric function; however, the results did not compare favorably with results from the Lindhard dielectric function.

Phillips and Kleinman¹⁴⁷ computed several matrix elements of the screened exchange potential for Si without attempting self-consistency, and made a comparison with the same matrix elements of the HF-exchange potential. They concluded that the HF potential gave results in strong dis-

¹⁵¹ These contributions were denoted by G_{vv} and B_0 , respectively.

TABLE X. MATRIX ELEMENTS IN Ry OF DIFFERENT EXCHANGE POTENTIALS FOR Si

		HF ^a		SX ^b	
		BG ^c	PK ^d	BG	PK
Γ_1	11*	-1.17	-1.10	-0.27	-0.35
$\Gamma_{25'}$	11	-0.73	-0.67	-0.21	-0.25
	12	-0.43	-0.35	-0.08	-0.11
	22	-0.36	-0.38	-0.16	-0.19
Γ_{15}	11	-0.38	-0.35	-0.18	-0.21
	12	-0.06	-0.07	-0.04	-0.05
	22	-0.13	-0.12	-0.10	-0.10
X_1	11	-0.97	-0.86	-0.24	-0.29
	12	-0.24	-0.34	-0.06	-0.11
	22	-0.44	-0.39	-0.18	-0.20

* Hartree-Fock exchange potential.

^b Screened Hartree-Fock exchange potential.

^c W. Brinkman and B. Goodman, *Phys. Rev.* **149**, 597 (1966).

^d J. C. Phillips and L. Kleinman, *Phys. Rev.* **128**, 2098 (1962).

* The numbers 1 and 2 indicate symmetrized plane waves as follows:

$$\begin{array}{llll}
 \Gamma_1 & \Gamma_{25'} & \Gamma_{15} & X_1 \\
 (a/2\pi) \quad \mathbf{k}_1 = & (000) & (111) & (100) \\
 (a/2\pi) \quad \mathbf{k}_2 = & & (200) & (011)
 \end{array}$$

agreement with experiment. They also found that the screened potential gave matrix elements in good agreement with those of the Slater modification of the exchange potential.

Their conclusions were supported by extended and more accurate calculations for Si by Brinkman and Goodman.¹⁵² Results for the matrix elements of the potential using screened and bare exchange are given in Table X. The diagonal elements are consistently smaller for a screened potential except for k large compared to k_F .¹⁷⁰ The nondiagonal elements are in general small, typically ≈ 0.05 Ry. Results for some band gaps are given in Table XI, using different expressions for the potential. The HF results are far away from experimental results, e.g. the direct band gap $\Gamma_{15}-\Gamma_{25'}$ is 9.3 eV compared with the experimental result of 3.5 eV, while the screened exchange potential gives results similar to the Slater exchange potential, which agrees much better with the experiment.

¹⁷⁰ For Γ_{15} (22) we have in units of $2\pi/a$ that $k_2^2 = 8$ while $k_F^2 \cong 3$.

TABLE XI. BAND GAPS FOR Si (IN EV) WITH DIFFERENT APPROXIMATIONS FOR EXCHANGE^a

	$\Gamma_{25'} - \Gamma_1$	$\Gamma_{15} - \Gamma_{25'}$	$\Gamma_2 - \Gamma_{25'}$	$L_1(2) - L_4'$	$L_4 - L_4'$	$X_1(2) - X_4$
HF ^b	14.0	9.3	13.8	11.2	—	11.0
HFS ^c	11.8	2.9	4.5	4.2	4.1	4.1
SX ^d	12.9	2.0	4.0	3.7	4.0	3.5
Expt.	13–16 ^e	3.4 ^f	3.8 ^f	3.2 ^f	5.3 ^f	4.1 ^f

^a W. Brinkman and B. Goodman, *Phys. Rev.* **149**, 597 (1966).

^b Hartree-Fock exchange.

^c Hartree-Fock-Slater exchange.

^d Screened Hartree-Fock exchange.

^e V. A. Fomichev and T. M. Zimkina, *Soviet Phys. JETP (English Transl.)* **9**, 1441 (1967).

^f M. L. Cohen and T. K. Bergstresser, *Phys. Rev.* **141**, 789 (1966).

c. The Projected Wave Field Approach

The projected wave field approach developed by Bassani *et al.*¹⁴⁸ attempts to use the ideas from the OPW method to develop a many-body theory. They define a valence projection of the field operator $\psi(\mathbf{x})$ as $\psi_v(\mathbf{x}) = (1 - \Theta_c)\psi(\mathbf{x})$ where Θ_c is the projection operator for the core states. Assuming the valence electrons to be dynamically independent of the core electrons, one obtains equations of motion involving only ψ_v . In the next step we write $\psi_v(\mathbf{x}) = (1 - \Theta_c)\phi(\mathbf{x})$ where $\phi(\mathbf{x})$ is the “auxiliary wave field” and derive the equations for $\phi(\mathbf{x})$. In this equation a large part of the strong crystal potential is canceled by orthogonality terms by a similar mechanism as in the OPW method. With this procedure the electron gas Green function would be a good zero order approximation for the auxiliary wave field problem in a real metal. The effect of the lattice could, according to Bassini *et al.*, be treated in second order perturbation theory. The exchange-correlation contribution to the quasi-particle energy E_k has a form very similar to that of an electron gas, however, with a modified screened potential

$$v_1(\mathbf{q})[1 - v_2(\mathbf{q})P_0(\mathbf{q}, \omega)]^{-1} \quad (35.8)$$

where

$$v_1(\mathbf{q}) = v(\mathbf{q})\langle \mathbf{p} | (1 - \Theta_c) | \mathbf{p} \rangle \langle \mathbf{p} + \mathbf{q} | (1 - \Theta_c) | \mathbf{p} + \mathbf{q} \rangle$$

and

$$v_2(\mathbf{q}) = v(\mathbf{q})\langle \mathbf{p} | (1 - \Theta_c) | \mathbf{p} \rangle_{av} \langle \mathbf{p} + \mathbf{q} | (1 - \Theta_c) | \mathbf{p} + \mathbf{q} \rangle_{av}.$$

It should be noted that the modification of the screened potential by the

use of v_1 and v_2 is not at all equivalent to the use of the factor $|1 + \Delta|^2$ in Eq. (35.3). In particular, the correction factor comes out different from unity in the important $q \rightarrow 0$ limit, and is always close to unity even in the vicinity of band gaps. Hence, the conclusion of their analysis is essentially that we should just add the free electron self-energy $\Sigma(\mathbf{k}, \epsilon_k)$ to the results of an energy band calculation.

d. Possible Further Improvements

The solution of the Dyson equation for the quasi-particle states requires some care. We should of course formally use the true energy $E_{\mathbf{k}}$ as the argument in $\Sigma^*(\omega)$. However, when calculating Σ^* one usually considers an approximate Green function of the form $(\omega - \epsilon_k)^{-1}$, where ϵ_k is an approximate value, e.g. obtained from a band calculation. In Eq. (35.3) we would then have the difference $E_{\mathbf{k}} - \epsilon_{\mathbf{k}+q}$ whereas in a refined theory we would have $G = (\omega - E_{\mathbf{k}})^{-1}$ and thus the energy difference $E_{\mathbf{k}} - E_{\mathbf{k}+q}$. The limit $E_{\mathbf{k}} - E_{\mathbf{k}+q} = \mathbf{q} \cdot \mathbf{v}$ for small q is quite important; a finite limit would indeed imply an incomplete screening. Since we do not know $E_{\mathbf{k}} - E_{\mathbf{k}+q}$, we may as well use $\epsilon_{\mathbf{k}} - \epsilon_{\mathbf{k}+q}$, which gives the correct type of limit when $q \rightarrow 0$.

There is a variety of procedures to solve Eq. (33.1) for the quasi-particle energy $E_{\mathbf{k}}$. An obvious possibility is to treat Σ^* as a perturbation. The effects of the nondiagonal elements of Σ^* , Eq. (35.4), are likely to be small except in the neighborhood of zone boundaries; their effect may, with a properly chosen basis, be small also at band gaps.

A rather more important effect than that of the nondiagonal elements is the factor $|1 + \Delta(\mathbf{k}, q; 0)|^2$ in Eq. (35.3), which can differ appreciably from unity at band gaps, and will generally have different values on the two sides of the gap. The effect of the same factors in $P_0^*(\mathbf{q}, \omega)$ is certainly of less importance, since we integrate over \mathbf{k} , which averages out most effects due to band gaps.

To handle the $|1 + \Delta|^2$ factor we write Eq. (35.3) as

$$\langle \mathbf{k} | \Sigma^*(\epsilon_k) | \mathbf{k} \rangle = \int F_{\mathbf{k}\mathbf{q}} \left[\int_{\Omega_0} u_{\mathbf{k}}(\mathbf{r}) u_{\mathbf{k}+\mathbf{q}}^*(\mathbf{r}) (d\mathbf{r}/\Omega_0) \right]^2 d\mathbf{q}, \quad (35.9)$$

where

$$F_{\mathbf{k}\mathbf{q}} = \frac{i}{(2\pi)^4} \int \frac{W_0^*(\mathbf{q}, \omega)}{\omega + \epsilon_k - \epsilon_{\mathbf{k}+\mathbf{q}}} d\omega. \quad (35.10)$$

The quantity $F_{\mathbf{k}\mathbf{q}}$ is not difficult to calculate if we use a simplified dielectric function. With the plasmon pole approximation of Eq. (25.11), the ω integration can even be made analytically. It is thus quite possible to in-

clude correlation effects in a band calculation with the approach described here, but it means no doubt a considerable amount of work.

A problem that seems to have more immediate interest is the damping of quasi-particle states which involves a study of the imaginary part of the self-energy. This is a simpler problem than that of estimating corrections to band gaps and has a very direct interest for the understanding of, say, optical spectra, tunneling data, and also electron scattering against surfaces.¹⁷¹

36. THE CORE ELECTRONS

a. Introductory Remarks

The discussion in this section will for simplicity be limited to simple metals with small cores, where the core electrons can be distinguished from the valence electrons, and where we can consider them as well localized to a particular ion. Many of the results, however, can easily be extended to other types of solids. For such metals the core electrons are affected only slightly by the surrounding crystal lattice. In particular, the wave function of a core electron is only very weakly dependent on the state of the outer electrons. The energy levels on the other hand undergo appreciable shifts. These shifts are of the order of 5 to 10 eV, which is large on the scale of valence electron energies but is a small relative change in the core electron energy. The shifts as well as other effects to be discussed in this section are due to the influence of the valence electrons, and this aspect is the justification for discussing core electrons here. The core shifts can be measured to within a few tenths of an electron volt by the method of X-ray photo-emission spectroscopy (XPS), as well as by X-ray absorption.

The shift of the quasi-particle energy of a core electron arises partly from changes in the Coulomb field, and partly from polarization effects. The *Coulomb shift* is due to the change in the valence charge distribution, relative to that in an isolated atom, and generally results in a decrease of the binding energy of the core electron.¹⁷²

¹⁷¹ The calculation of the optical potential for a surface region is of course more complicated than for a perfect crystal. For recent work on this problem see, e.g., J. W. Gadzuk, *Surface Sci.* **11**, 465 (1968).

¹⁷² The definition of the core electron binding energy in a solid requires some care. Experimentally the core energy ϵ_c is measured relative to the chemical potential μ . Theoretically we calculate ϵ_c relative to a zero potential far away from an idealized solid built of an integral number of Wigner-Seitz cells all having zero dipole moment and the same charge distribution as in an infinite solid. The theoretical result for ϵ_c cannot be directly compared with experiment. The difference $\mu - \epsilon_c$, however, can be compared since it does not depend on the state of the surface.

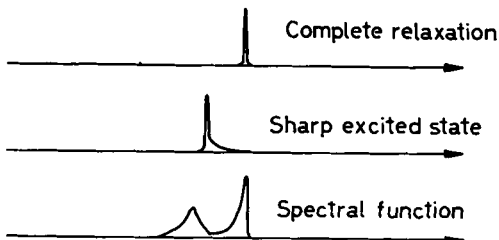


FIG. 38. Qualitative sketch of different conceivable energy distributions of the valence electrons after a core electron has been ejected.

In order to explain the *polarization shift* let us imagine that we can switch off the interaction of the core electron with the valence electrons before we remove the electron. The ionization will then require the same energy as for an isolated core. When the interaction between the core electron under consideration and the valence electrons is turned off, the valence electrons are drawn in toward the positive hole that appears in the ion. This effect decreases the binding energy by half of the change in the valence electron Coulomb potential at the core site, i.e. precisely the amount given by a classical calculation of the self-energy of the hole. Hence both of the contributions to the shifts have a simple physical origin. The shift in core energy thus provides information on the valence charge distribution and polarizability, measured with the core electron as a probe.^{172a}

When a core electron is ejected it can leave the valence electron system not only in the completely relaxed state that we have just discussed, but also in a variety of excited states. Consider the XPS situation when a photon of given energy hits an ion in the solid and an electron races away. The ejected electron has its maximum energy when the valence electron system is left in the completely relaxed state. The observed XPS spectra have sharp peaks corresponding to core energies, and we could conceivably have either of two rather extreme situations illustrated by the first two curves in Fig. 38.

Theoretical calculations give very good agreement for simple metals (Li, Na, K, Al) between the position of the experimentally observed peak and that corresponding to complete relaxation.¹⁶¹ The third curve shows the result obtained by Lundqvist¹⁵³ from an analysis of the one-electron spectral function. The pronounced peak in the satellite can be associated with plasmons coupled to the core hole while the edge of the satellite corresponds to production of free plasmons. This structure should be observable in XPS spectra and possibly also in X-ray absorption spectra. The following

^{172a} L. Hedin and A. Johansson, *J. Phys. B* (to be published).

subsections will give a theoretical discussion of the core electron spectrum. The numerical results for core shifts in simple metals will be reviewed in Section 40.

b. Self-Energy of Core Electrons

The key quantity to study is the expectation value of Σ with regard to the core electron wave function u_c (e.g. the HF function), thus

$$\Sigma_c(\omega) = \langle u_c | \Sigma(\omega) | u_c \rangle. \quad (36.1)$$

The quasi-particle energy is given by the Dyson equation

$$E_c = \epsilon_c + \Sigma_c(E_c), \quad (36.2)$$

and the spectral function in this region by the formula

$$A_c(\omega) = \pi^{-1} \operatorname{Im}[\omega - \epsilon_c - \Sigma_c(\omega)]^{-1}, \quad (36.3)$$

if we neglect nondiagonal elements. We decompose the self-energy as follows:

$$\Sigma_c(\omega) = V_{\text{ex}} + \Sigma_{\text{pol}}^*(\omega) + \Sigma_c^{(2)}(\omega) + \dots, \quad (36.4)$$

where the different terms have the following significance

$$\begin{aligned} V_{\text{ex}} &= \langle u_c | Gv | u_c \rangle && \text{core-core + core-valence exchange} \\ \Sigma_{\text{pol}}^* &= \langle u_c | G(W^* - v) | u_c \rangle && \text{polarization shift} \\ \Sigma_c^{(2)} &= \langle u_c | GW^*P^cW^* | u_c \rangle && \text{second order core term.} \end{aligned} \quad (36.5)$$

The contribution V_{ex} is the total exchange energy. The core-core part of this energy is not small, but contributes almost nothing to the shift and can in the present context be taken as a given constant. The core-valence exchange is small and can be calculated fairly accurately. The second order term is essentially the same as for a free ion core.¹⁵¹ It contributes to the core electron energy but not to the shift and will usually not interfere with the structure in the spectral function that is due to the valence electrons.

The only term of actual interest in this context is the term coupling the valence and core electrons, thus

$$\Sigma_{\text{pol}}^*(\omega) = \frac{i}{2\pi} \sum_k \int u_c^*(\mathbf{x}) u_k(\mathbf{x}) \frac{W_p^*(\mathbf{r}, \mathbf{r}'; \omega')}{\omega' + \omega - \epsilon_k} u_c(\mathbf{x}') u_k^*(\mathbf{x}') d\mathbf{x} d\mathbf{x}' d\omega', \quad (36.6)$$

where W_p^* is the polarization part $W_p^* = W^* - v$. The large contribution comes from the term $k = c$. The magnitude of the terms $k \neq c$ are small because of the large energy denominators and because of the small effective overlap between the wave functions.

c. The Polarization Shift of the Core Levels

We consider only the large term $k = c$ in Eq. (36.6). The contribution $\Sigma_{\text{pol}}^*(\epsilon_c)$ to the quasi-particle energy is proportional to

$$\int d\omega W_p^*(\omega) (\omega - i\delta)^{-1}.$$

Since $W_p^*(\omega)$ is an even function of ω , we have simply

$$\Sigma_{\text{pol}}^*(\epsilon_c) = -\frac{1}{2} \int |u_c(\mathbf{x})|^2 W_p^*(\mathbf{r}, \mathbf{r}'; 0) |u_c(\mathbf{x}')|^2 d\mathbf{x} d\mathbf{x}'. \quad (36.7)$$

This is indeed the classical self-energy contribution. To see this explicitly we can write the integrand schematically as $\rho_c v (\epsilon^{-1} - 1) \rho_c$, with $\rho_c = |u_c|^2$ and $W_p^* = v(\epsilon^{-1} - 1)$. The part $(\epsilon^{-1} - 1) \rho_c$ gives the charge density induced by ρ_c , multiplication with v gives the induced potential, and the final multiplication by ρ_c and integration averages this potential over the density distribution of the core electron.

The factor $\frac{1}{2}$, finally, has to do with the adiabatic process involved in the self-energy calculation. $\Sigma_{\text{pol}}^*(\epsilon_c)$ is a positive quantity, hence the polarization shift will decrease the binding energy.

If we neglect the final extension of the core and thus replace $|u_c(\mathbf{x})|^2$ by a δ function and also neglect the nondiagonal elements of W , we have the very simple result

$$\Sigma_{\text{pol}}^*(\omega) = \frac{i}{(2\pi)^4} \int \frac{W_p^*(\mathbf{q}, \omega')}{\omega' + \omega - \epsilon_c} d\mathbf{q} d\omega'. \quad (36.8)$$

This simple formula is actually a quite adequate approximation for metals with small ion cores.

d. The Core Electron Spectrum

In analogy with the strong effects of the interaction between holes and plasmons in the spectrum of conduction electrons, there is a corresponding coupling between hole states in a core and the density fluctuations of the conduction electrons. This coupling leads to a characteristic structure in the core electron spectrum as was recently shown theoretically by Lundqvist.¹⁵³

The existence of a new structure can easily be seen from Eq. (36.8). Remembering that $W_p^*(\mathbf{q}, \omega')$ has a strong resonance behavior in the plasmon regime, we see that after integration over ω' , the resulting function will show a strong resonance behavior in the frequency region $\omega \simeq \epsilon_c - \omega_p$. The rapid variation in the self-energy will give rise to two solutions of the

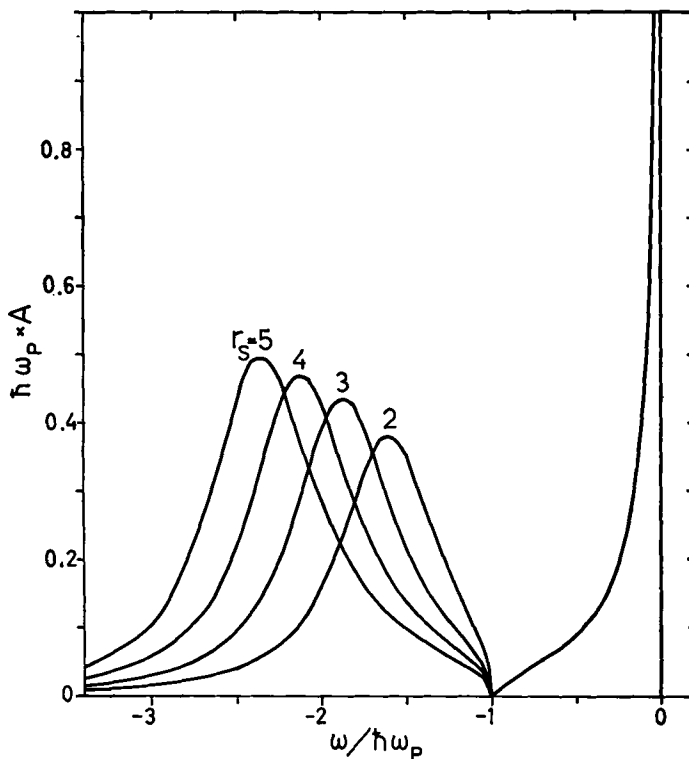


FIG. 39. Quasi-particle peak in the spectral function for a core level and the associated satellite structure for different densities of the conduction electrons; after B. I. Lundqvist, *Physik Kondensierten Materie* **9**, 236 (1969).

Dyson equation. The second solution, however, gives a quite broad peak in the spectral function. If we compare with the narrow plasmaron peak for small \mathbf{k} values (Figs. 16 and 17), the difference can be traced to the lack of momentum conservation in the core case. The broad satellite structure is centered around $\omega/\omega_p = 1.5-2.5$ below the quasi-particle peak. The results are illustrated in Fig. 39, where the full Lindhard formula for the dielectric function has been used in the calculation. The satellite spectrum corresponds to 30–50% of the total spectral strength. Also noteworthy is the strong asymmetry of the peak starting at the quasi-particle energy ϵ_c which corresponds to the adiabatically relaxed valence electron configuration. The fact that experimental results for core levels seem to agree well with those calculated using the adiabatic relaxation is explained in the theory by the strong weight given to states of the system with energies in a close neighborhood of ϵ_c , i.e. states with only a small to moderate excitation

of the conduction electrons. Thus the conclusion is that about half the spectral strength corresponds to excitation close to ϵ_c , and in addition we have a broad satellite structure corresponding to high excitations of the conduction electrons having approximately the same spectral strength.

Since we neglect relaxation effects in the core-electron system, the spectral function has the form

$$A_c(\omega) = \sum_s |\langle N - 1, s | N - 1 \rangle|^2 \delta(\omega - \epsilon_s), \quad (36.9)$$

where $|N - 1\rangle$ is the ground state of the valence electrons *before* the core electron was removed, and $|N - 1, s\rangle$ is an excited valence electron state *with* the core hole present. We note that Eq. (36.9) is the same formula as obtained by using the sudden approximation in perturbation theory.

We shall return to these effects in Sections 39 and 40 and discuss how the structure in the core spectrum can be related to XPS and X-ray spectra.

37. THE EFFECTIVE CRYSTAL POTENTIAL

a. Introduction

A review of the properties of the valence electron system was given in Section 35, in which we discussed both the quasi-particle properties and the structure of the one-electron spectrum. The basic expression for the crystal potential is given in Eq. (35.7). Results of calculations using an approximate formula for the self-energy Σ^* were reviewed in Section 35b and possible improvements were discussed in Section 35d. It was concluded that a refined treatment might lead to more accurate results for the band gaps, and that it would be quite possible to calculate the imaginary part of Σ^* in order to obtain the damping of the quasi particles and the optical potential for scattering of electrons on the surface, and also to calculate the spectral function needed for the interpretation of optical and X-ray data.

We will in this section discuss the real part of the crystal potential. Since we have already discussed the valence electron self-energy, we concentrate on the remaining terms, namely, the effective potential from the ion cores

$$V_c = V_n + V_{H^c} + V_{ex^c} + \Sigma_{pol^c}(E_k), \quad (37.1)$$

and the Hartree potential V_{H^*} from the valence electrons. There is not much to say about the Hartree potential. It would be determined through the self-consistency procedure and can be estimated quite well in advance by just adding the charge densities from the free atoms (as is often done in APW calculations) or from pseudo atoms (i.e. linearly screened ions).

TABLE XII. VALENCE ELECTRON ENERGIES IN RY FOR SODIUM ATOM

	HF	Experiment	$\Delta_{\text{ex}}^{\text{a}}$	$\Delta_{\text{pol}}^{\text{b}}$
3s	-0.36410	-0.37773	-0.03897	-0.01363
4s	-0.14021	-0.14316	-0.00716	-0.00295
5s	-0.07408	-0.07517	-0.00013	-0.00110
3p	-0.21887	-0.22310	-0.01368	-0.00423
4p	-0.10064	-0.10187	-0.00357	-0.00123
5p	-0.05787	-0.05839	-0.00009	-0.00053
3d	-0.11133	-0.11188	-0.00018	-0.00054
4d	-0.06263	-0.06289	-0.00011	-0.00026

^a Exchange part of HF energy.^b Difference between experimental and HF result.

This topic has been discussed by Cohen and Phillips,¹⁴⁶ Ziman,¹⁷³ and others.

The explicit construction of the potential from the ions is often avoided by using pseudopotentials or by using spectral data from free atoms. These methods seem very useful particularly for Fermi surfaces. With the rapid advancement in the technique of doing atomic calculations, there are however no strong reasons not to determine the actual potential. The development of new powerful techniques such as using synchrotron radiation and low energy electrons will open new ways to study the band structure, and these new aspects may require considerably more accurate information about the ion core potential.

b. The Effective Potential of an Ion Core

The effective potential V_e of an ion in a solid is similar to the optical potential of a free ion, except for the screening of the polarization part in the potential. We shall first comment on the free ion potential and thereafter remark on the screening effects in the solid.

The optical potential of the ion determines the energy levels of the valence electron as well as the elastic scattering of electrons on the ion. Some results¹⁶¹ on valence electron energies in the sodium atom are shown in Table XII. The column HF refers to the Koopmans or "frozen core" approximation, obtained when using the HF potential for the closed shell ion. The next column gives experimental values.¹⁷⁴ The quantities Δ_{ex} and Δ_{pol} refer to energy contributions corresponding to V_{ex}^e and Σ_{pol}^e . The exchange contributions are more important than the polarization ones

¹⁷³ J. M. Ziman, *Advan. Phys.* **13**, 89 (1964).

¹⁷⁴ C. E. Moore, "Atomic Energy Levels," *Natl. Bur. Std. Circ.* No. 467, Vol. 1. Washington, D. C., 1949.

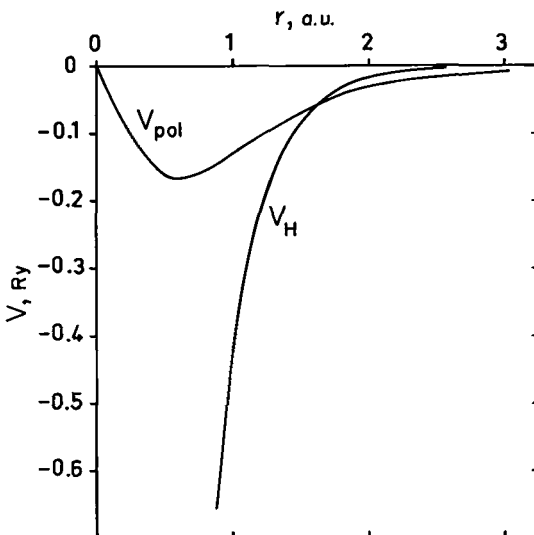


FIG. 40. Polarization potential V_{pol} and Hartree potential V_H for He.

except for rather large quantum numbers, where the “tidal wave” interaction with the ion dominates¹⁷⁶ and the self-energy reduces to

$$\Sigma_{\text{pol}}^c \xrightarrow[r \text{ large}]{} -\alpha e^2 / 2r^4,$$

where α is the dipole polarizability of the ion.

The conclusion from Table XII is that the HF approximation works fairly well for the ions, but that polarization corrections should be included if high accuracy is needed.

Figure 40 shows a plot of the polarization potential for the case of He,¹⁷⁶ together with the Hartree potential. We see that a large part of the polarization comes from the core region. The long range part, going like r^{-4} , is quite weak and will be screened in a solid. The screening in the core part is, however, not very effective. These facts support the idea behind the quantum defect method.^{176a} For some special problems, though, the screening will be of considerable importance, as will be discussed in the end of this section.

More information on the ion potential could in principle be obtained from elastic scattering of electrons. Unfortunately, rather little is known

¹⁷⁶ M. Born and W. Heisenberg, *Z. Physik* **23**, 388 (1924).

¹⁷⁶a H. A. Bethe and E. E. Salpeter, “Handbuch der Physik” (S. Flügge, ed.), Vol. 35. Springer, Berlin, 1957.

^{176a} F. S. Ham, *Solid State Phys.* **1**, 127 (1955).

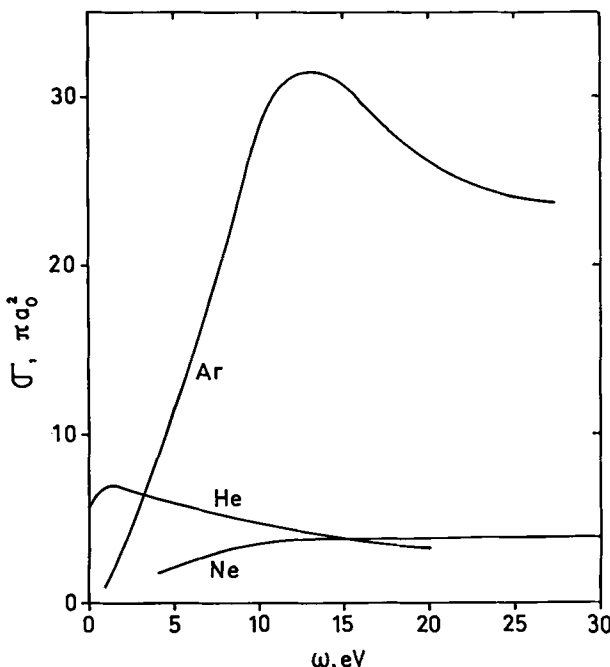


FIG. 41. Experimental results for the total elastic scattering cross sections of some inert gases. He and Ne from C. Ramsauer and R. Kollath, *Ann. Physik* **3**, 536 (1929); **12**, 529 (1932); Ar from W. Aberth, G. Sunshine, and B. Bederson, *Proc. Intern. Conf. Phys. Electronic and At. Collisions* (M. R. C. McDowell, ed.), North-Holland Publ., Amsterdam, 1964.

about the scattering from free ions and the closest source of experimental information is the scattering from inert gases.

The total elastic cross sections for He, Ne, and Ar are shown in Fig. 41 as function of the energy. The curves show considerable structure and the radius of the effective cross-section area (the square root of the ordinate number in the figure) is quite large compared to the extension of the atom (measured, say, by the last inflection point of the outermost orbital function, see Table IX on p. 126).

Figure 42 shows results from calculations of the total cross sections. The Hartree potential V_H (calculated with HF charge densities) gives poor agreement, while the HF potential $V_H + V_{ex}$ reproduces the main features of the experimental curves. Calculations by LaBahn and Callaway¹⁷⁷ and by Pu and Chang¹⁷⁸ for He show that by including polarization effects to

¹⁷⁷ R. W. LaBahn and J. Callaway, *Phys. Rev.* **147**, 28 (1966).

¹⁷⁸ R. T. Pu and E. S. Chang, *Phys. Rev.* **151**, 31 (1966).

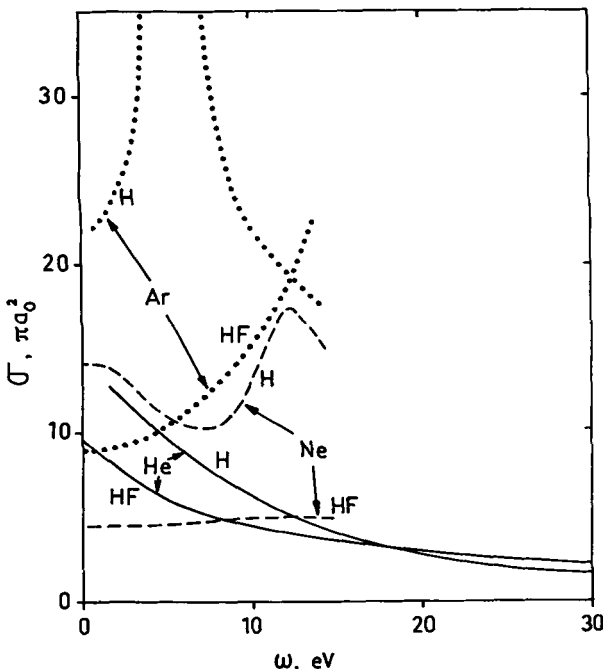


FIG. 42. Calculated cross sections for some inert gases in the Hartree and HF approximations. He from N. F. Mott and H. S. W. Massey, "The Theory of Atomic Collisions." Oxford Univ. Press, London and New York, 1949. Ne and Ar from D. G. Thompson, *Proc. Roy. Soc. A* **294**, 160 (1966).

second order in perturbation theory the experimental cross sections are reproduced much better. Calculations by Kelly¹⁷⁹ on H and by Thompson¹⁸⁰ on Ne and Ar give similar results. Thus the inclusion of effects beyond the one-electron approximation is important to obtain good agreement for the elastic scattering, and is also quite feasible from the calculational point of view.

The preceding remarks seem to be at variance with the picture usually assumed for the scattering of valence electrons by the ion cores in a solid. Many simple metals have a fairly free-electron-like dispersion curve, which implies that the phase shifts produced by the ion core (modulus π) are small and slowly varying.¹⁸¹ The difference between inert gases on one hand, and ions in a solid on the other, can be traced to two main reasons.

¹⁷⁹ H. P. Kelly, *Phys. Rev.* **160**, 44 (1967).

¹⁸⁰ D. G. Thompson, *Proc. Roy. Soc. A* **294**, 160 (1966).

¹⁸¹ See e.g. J. C. Slater, "Quantum Theory of Molecules and Solids," Vol. 2. McGraw-Hill, New York, 1965.

In the first place, the long range parts of the potentials are cut off in the solid, and it is the long range polarization part that is mainly responsible for the structure in the atomic cross sections. Secondly, the ion cores are smaller and have much stronger potentials than the inert gas atoms. This means that the zero energy cross section becomes smaller, and more important, due to the stronger potential, it stays small over a larger energy range.¹⁸² There is no reason, however, that the free-electron-like behavior should remain for all energies, and higher up in the bands we can well encounter deviations corresponding to the cross-section maxima in the curves for the inert gases. Such behavior is indeed indicated by some calculations by Kenney.¹⁸³

The screening of the polarization potential has been extensively discussed in connection with the quantum defect method. Brooks¹⁸⁴ observed that one obtained too strong cohesion if one used an unscreened polarization potential; the same problem was also discussed by Callaway.¹⁸⁵ In a calculation of the g value in the spin resonance of conduction electrons in alkali metals, Bienenstock and Brooks¹⁸⁶ found that the inclusion of an unscreened potential tended to ruin their results. They concluded from physical arguments that the ionic polarization potential should be doubly screened, as indeed also comes out from the analysis in Section 35. Bienenstock and Brooks remarked that the problem was complicated by the fact that the screening radius in a metal is of the same size as the dimension of the ion core itself.

From the analysis in Section 35, we have the explicit formula

$$\Sigma_{\text{pol}}^c(\mathbf{x}, \mathbf{x}'; \omega) = \frac{i}{2\pi} \int \sum_k \frac{W^*(\mathbf{x}, \mathbf{x}_1; \omega') P^c(\mathbf{x}_1, \mathbf{x}_2; \omega') W(\mathbf{x}_2, \mathbf{x}'; \omega')}{\omega + \omega' - \epsilon_k} \\ \times \varphi_k(\mathbf{x}) \varphi_k^*(\mathbf{x}') d\mathbf{x}_1 d\mathbf{x}_2 d\omega'. \quad (37.2)$$

In lowest approximation this reduces to

$$\Sigma_{\text{pol}}^c(\mathbf{x}, \mathbf{x}') \\ = \frac{1}{2} \int \sum_k W^*(\mathbf{x}, \mathbf{x}_1; 0) P^c(\mathbf{x}_1, \mathbf{x}_2; 0) W^*(\mathbf{x}_2, \mathbf{x}'; 0) \varphi_k(\mathbf{x}) \varphi_k^*(\mathbf{x}') d\mathbf{x}_1 d\mathbf{x}_2.$$

This is still a fairly complicated formula, but it can, however, be calculated. We note that it reduces at large ω to the free ion potential.

¹⁸² See e. g. L. I. Schiff, "Quantum Mechanics," p. 112. McGraw-Hill, New York, 1955.

¹⁸³ J. F. Kenney, M. I. T. Solid State and Molecular Theory Group, Quart. Progr. Rept. No. 53, p. 38 (1964).

¹⁸⁴ H. Brooks, *Nuovo Cimento Suppl.* **7**, 165 (1958).

¹⁸⁵ J. Callaway, "Energy Band Theory." Academic Press, New York, 1964.

¹⁸⁶ A. Bienenstock and H. Brooks, *Phys. Rev.* **136**, A784 (1964).

38. LOCAL DENSITY APPROXIMATIONS

a. *Ground State Properties*

We have made extensive use in this review of the progress during the last decade in understanding the nature of a uniform interacting electron gas. In Section 35 we discussed a procedure to use this experience as well as experience from atomic calculations in an analysis of band structure. In this section we shall review another line of approach where we treat the metal as an inhomogeneous electron gas. We then have a different scheme of approximations, where one describes the system by introducing the dependence on the local density and possibly also corrects the results by terms depending on the density gradient and higher derivatives. Such a scheme is basically related to the Thomas-Fermi approach. Indeed, the Thomas-Fermi model was long ago refined by including first the effect of exchange and later, by Gombás¹⁸⁷ in 1943, the effect of correlation. This was done by including in the total energy a term corresponding to the correlation energy and with an energy density depending on the local density. Gombás obtained the correlation energy density from the Wigner interpolation formula. A refinement was later introduced by Lewis¹⁸⁸ using the result of Gell-Mann and Brueckner.²⁶

The same ideas have been used to extend the Hartree and HF methods by including exchange and correlations corrections. One adds to the total energy a term including exchange or correlation, taken as a function of the local density, and then derives the single-particle equation by applying the variational principle to the formula for the total energy. This results in additional potential terms in the equation describing schematically the effects of exchange and correlation. Gáspár¹⁸⁹ used this method to improve the Hartree theory by adding the total exchange energy. In this way he obtained an exchange potential of the form

$$V_{\text{ex}} = - (e^2/\pi) [3\pi^2 \rho(\mathbf{r})]^{1/3}. \quad (38.1)$$

Slightly earlier Slater¹⁹⁰ had suggested a somewhat different approach. Forming the average of the HF exchange over the occupied states, he obtained the following formula for the local exchange potential:

$$V_{\text{ex}} = - (3e^2/2\pi) [3\pi^2 \rho(\mathbf{r})]^{1/3}. \quad (38.2)$$

¹⁸⁷ P. Gombás, *Z. Physik* **121**, 523 (1943).

¹⁸⁸ H. W. Lewis, *Phys. Rev.* **111**, 1554 (1958).

¹⁸⁹ R. Gáspár, *Acta Phys. Hung.* **3**, 263 (1954).

¹⁹⁰ Slater.³ See also J. C. Slater, "Insulators, Semiconductors, and Metals," p. 233. McGraw-Hill, New York, 1967.

It should be added that Gáspár's formula corresponds to taking the exchange contribution due to the electrons at the Fermi level. This is physically appealing because density adjustments come about by redistribution of electrons at the Fermi level. These ideas were extended by Gombás¹⁹¹ and independently by Callaway¹⁹² to include the effects of correlation. Calculations for atoms have been made by Mitler¹⁹³ using such correlation potentials.

The ideas reviewed here were put on a firm ground through the work by Hohenberg and Kohn.¹⁵⁶ They proved that the ground state energy of an inhomogeneous system is a unique functional of the local density $\rho(\mathbf{r})$. This important theorem opens new ways to obtain self-consistent equations for the description of ground state properties. Kohn and Sham¹⁵⁷ have discussed the nature of this functional and to what extent it can and cannot be determined from the properties of a homogeneous electron gas. They rederive the result of Gáspár in Eq. (38.1).¹⁹⁴ They also discuss the effects of density gradients and conclude^{194a} that extensions through a gradient expansion would, in most cases, not lead to improved results. This conclusion is supported by the work of Ma and Brueckner,¹⁹⁵ who calculated the gradient correction to the correlation potential and obtained correlation energies of the inert gas atoms about a factor of 5 in error.

The application of the electron gas result would seem ideal in the high density region near the nuclei. However, the presence of the strong Coulomb potential dominates the behavior in this region. The Coulomb potential from the nucleus not only makes the electron density high but also makes it vary rapidly within the nonlocality length of the electron gas at that density, as has been discussed by Herring.¹⁹⁶ Thus it would not at all be reasonable to treat the atomic electrons as a uniform gas over the diameter of the correlation hole. Use of the free-electron gas value of the correlation energy for the inner electrons of an atom is therefore unjustified; such a procedure clearly overestimates the correlation energy.

b. The Excitation Spectrum

The theorem by Hohenberg and Kohn¹⁵⁶ gives a foundation of Thomas-Fermi-like theories and improvements of self-consistent theories. In the way it was first used by Kohn and Sham,¹⁵⁷ it applies only to ground state

¹⁹¹ P. Gombás, *Acta Phys. Hung.* **4**, 187 (1954).

¹⁹² J. Callaway, *Phys. Rev.* **95**, 656 (1954).

¹⁹³ H. Mitler, *Phys. Rev.* **99**, 1835 (1955).

¹⁹⁴ Equation (38.1) is often referred to as the potential of Kohn and Sham.

^{194a} W. Kohn, in "Many-Body Theory" (R. Kubo, ed.). Benjamin, New York, 1966.

¹⁹⁵ S. K. Ma and K. A. Brueckner, *Phys. Rev.* **165**, 18 (1968).

¹⁹⁶ C. Herring, *Intern. J. Quant. Chem.* **1**, 788 (1967).

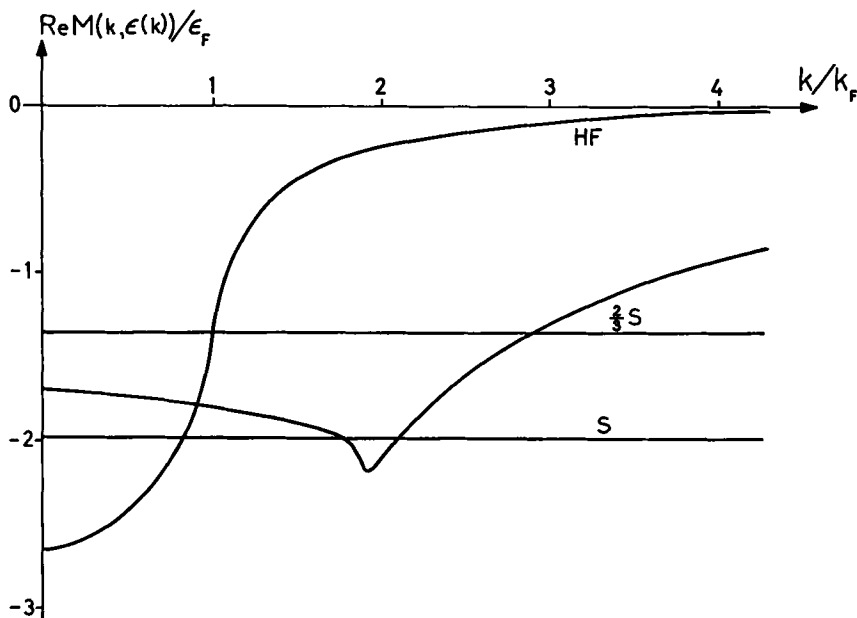


FIG. 43. Exchange-correlation potentials for an electron gas, $\Sigma(\mathbf{k}, E_k)$ after B. I. Lundqvist, *Phys. Stat. Sol.* **32**, 273 (1969). As a comparison the Hartree-Fock, the Slater, and the Gaspar ($\frac{2}{3}$ Slater) approximations are also shown. The density corresponds to that of sodium ($r_s = 4$).

properties. It is intuitively reasonable to interpret the eigenvalues in the one-particle equation as excitation energies, but as pointed out in a later paper by Sham and Kohn,¹⁵⁸ there is no real justification for such an interpretation. However, according to the Hohenberg-Kohn theorem, also the Green function and thus the self-energy are functionals of the density. In this way Sham and Kohn¹⁵⁸ could use the theorem for a discussion of how to calculate the excitation spectrum. They recommended starting from the obvious local density approximation

$$\Sigma(\mathbf{x}, \mathbf{x}'; \omega) \rightarrow \Sigma_0(\mathbf{x} - \mathbf{x}'; \omega - V(\mathbf{r})), \quad (38.3)$$

where Σ_0 is the electron gas self-energy, evaluated for zero Hartree potential, which explains the appearance of the potential $V(\mathbf{r}) = V_n(\mathbf{r}) + V_H(\mathbf{r})$ in the argument.

The potential Σ_0 in Eq. (38.3) is still nonlocal in space. Provided that the density is slowly varying, we can for the quasi-particle description make the replacement

$$\Sigma \rightarrow \Sigma_0(\mathbf{k}, E_k), \quad (38.4)$$

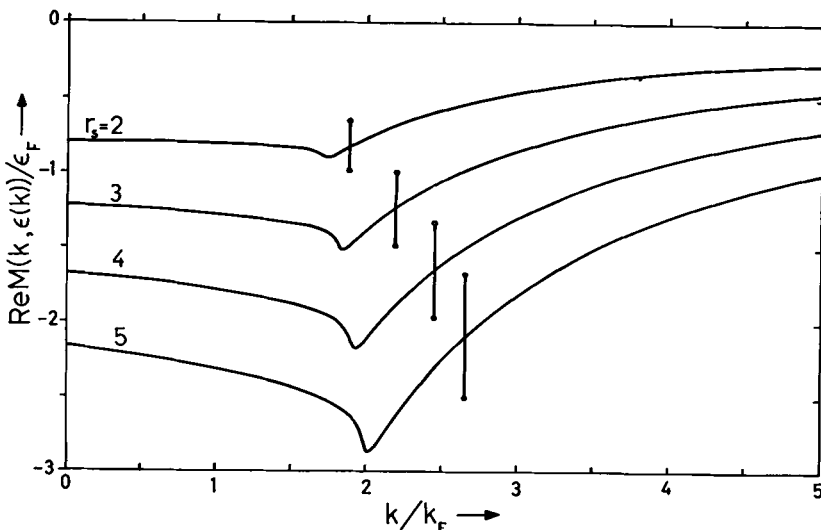


FIG. 44. Exchange-correlation potentials for an electron gas at a range of r_s values; after B. I. Lundqvist, *Phys. Stat. Sol.* **32**, 273 (1969). The rings on the vertical bars indicate the positions of the Slater and $\frac{2}{3}$ Slater approximations.

where the \mathbf{k} dependence, which brings about the nonlocality is determined from the quasi-particle equation (E = quasi-particle energy)

$$E - V(\mathbf{r}) = E_k = \epsilon_k + \Sigma_0(\mathbf{k}, E_k); \quad \epsilon_k = \hbar^2 k^2 / 2m. \quad (38.5)$$

Knowing $\Sigma_0(\mathbf{k}, E_k)$ as a function of \mathbf{k} and r_s one thus obtains from Eqs. (38.4) and (38.5) a local potential which incorporates the effects of exchange and correlation.

It was shown in Section 25 that $\Sigma_0(\mathbf{k}, E_k)$ is only weakly dependent on k in the range $k \lesssim 2k_F$. For not too highly excited states we can therefore use the simple approximation

$$\Sigma \rightarrow \mu_{xc} \quad (38.6)$$

where μ_{xc} is the exchange and correlation part of the chemical potential of an electron gas taken for the r_s value corresponding to the local density.

In Fig. 43 we illustrate different choices of correlation and exchange potentials for an electron gas corresponding to $r_s = 4$, i.e., the density of Na. The flat unlabeled curve gives the result obtained from the approximation discussed at length in Section 25. The Hartree-Fock result, marked HF, has a completely different character. The two horizontal lines give the values of the Slater and the Gáspár (Kohn and Sham) potentials. The latter is sometimes referred to as $2/3$ Slater exchange. Since the cor-

rect potential lies approximately halfway between the two horizontal lines (for moderate \mathbf{k} values), one may rather consider a 5/6 Slater exchange. In Fig. 44 we show curves of $\Sigma_0(\mathbf{k}, E_k)$ for a range of r_s values. Marked on each curve are the positions of the Slater and 2/3 Slater approximations.

We would like to comment on three points regarding the local density approximation defined by Eqs. (38.4) and (38.5):

(i) The large density gradients in the core region will make the local density approach for Σ break down. This can be avoided if only the valence electrons are treated in this approximation. The core exchange and polarization potentials should then be included in the crystal potential.

(ii) For electrons in the bottom of the valence band, Eq. (38.5) may not have solutions for all \mathbf{r} , or expressed in the APW form, the energy may be smaller than the muffin tin constant. In such exceptional cases one may simply choose $\mathbf{k} = 0$.

(iii) For high energies, the variation of $V(\mathbf{r})$ in Eq. (38.5) is unimportant, and we shall have a practically constant local wave number. The potential $\Sigma_0(\mathbf{k}, E_k)$ then depends on $\rho(\mathbf{r})$ only through its r_s dependence.

c. Numerical Calculations

Local density approximations have always had a strong appeal because they are simple to use. When Kohn and Sham revived the suggestion by Gáspár that the numerical factor in the Slater exchange should be modified, the idea was taken up in energy band calculations as well as in atomic calculations. Calculations for atoms have given results which were an improvement of the Hartree-Fock-Slater approach³ but not as good as the HF results.¹⁶⁷ Band calculations were also made with other factors than 2/3, and in some cases 5/6 seemed to give the best agreement with the experiments.¹⁶⁸

All the calculations just referred to were based on the assumption that the first Kohn and Sham¹⁶⁷ approach was applicable to excitation energies, but in reality the approach refers to ground state properties. An early approach which used a local density approximation to the self-energy was applied to the inert gas atoms by Lundqvist and Ufford.¹⁶⁹ Calculations based on Eqs. (38.4) and (38.5) with the HF approximation for Σ_0 have been made by Liberman²⁰⁰ for argon and mercury, using a somewhat different line of reasoning than Sham and Kohn.¹⁶⁸ His results are quite close to the full HF solution.

¹⁶⁷ B. Y. Tong and L. J. Sham, *Phys. Rev.* **144**, 1 (1966); R. D. Cowan, A. C. Larson, D. Liberman, J. B. Mann, and J. Waber, *Phys. Rev.* **144**, 5 (1966).

¹⁶⁸ J. W. D. Connolly, *Phys. Rev.* **159**, 415 (1967); E. C. Snow, *ibid.* **171**, 785 (1968); **172**, 708 (1968).

¹⁶⁹ S. Lundqvist and C. W. Ufford, *Phys. Rev.* **139**, A1 (1965).

²⁰⁰ D. A. Liberman, *Phys. Rev.* **171**, 1 (1968).

d. Concluding Remarks and Recommendations

A local density approximation for exchange and correlation is convenient for calculational purposes. The best available such potential seems to be the one defined by Eqs. (38.4) and (38.5). This potential should be no more difficult to use in actual calculations than the Slater or Gáspár approximations, if use is made of the numerical data tabulated for this purpose by Hedin *et al.*²⁰¹ The core electrons should not be included in the charge density, only the valence electrons. Instead, the exchange and if possible the polarization potential from the core electrons should be included in the crystal potential (cf. Section 37).

Alternative procedures to local density approximations were discussed in Section 35. These methods seem better founded on theory but are also in general more difficult to apply. If, however, the corrections at band gaps are small, which may be true in many cases, the calculations can be made without any valence exchange-correlation potential at all, and the diagonal term $\Sigma^*(\mathbf{k}, E_k)$ may be just added on afterward.

X. Discussion of Various Metallic Properties

39. SOFT X-RAY EMISSION SPECTRA

We shall discuss only the simplest possible situation where we can assume complete relaxation toward the core hole before the emission takes place; we shall further neglect the width of the hole state. These conditions make the discussion applicable only to light metallic elements such as Li, Be, Na, Mg, Al, and K and excludes explicitly e.g. all transition metals.

In one-electron theory the intensity is given by

$$I(\omega) = C\omega \sum_k^{occ} |p_{ck}|^2 \delta(\omega + \epsilon_c - \epsilon_k), \quad (39.1)$$

where C is a constant and p_{ck} is the matrix element for the transition, ϵ_c and ϵ_k denote the core and valence electron energies. The intensity can also be written in either of the forms $I(\omega) = C\omega |p|^2 N(\omega) = C\omega^3 |r|^2 N(\omega)$, where $N(\omega)$ is the density of states, and the matrix elements depend on the frequency. If we take the matrix element to be constant, then the intensity directly reflects the shape of the density of states for the valence band. The experimental curves for simple metals do indeed have an approximately parabolic shape with a sharp Fermi edge and a width not far from the Fermi gas value. As an example we show in Fig. 45 the L spectrum for Al. The structure at the Fermi edge is due to Brillouin zone effects.

²⁰¹ L. Hedin, B. I. Lundqvist, and S. Lundqvist (to be published).

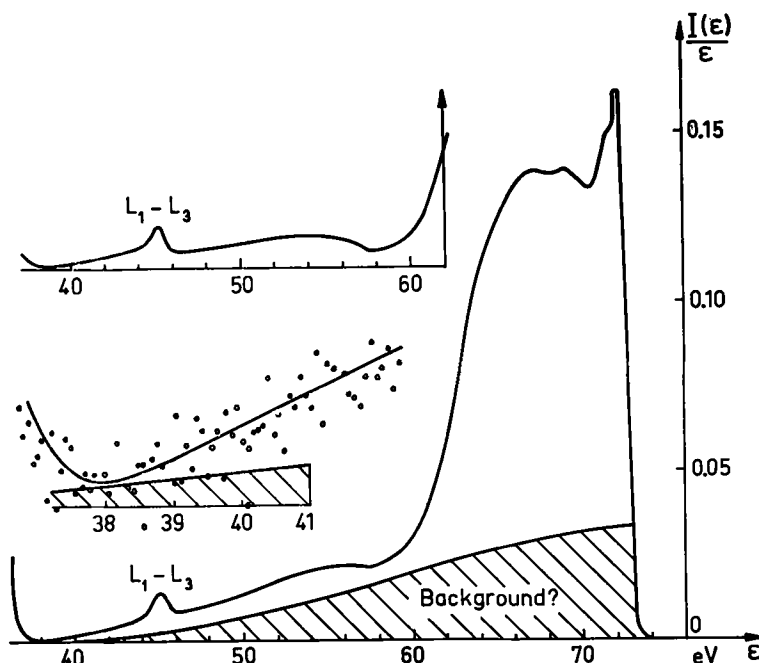


FIG. 45. Soft X-ray emission spectrum for Al from R. K. Dimond (private communication). $I(\epsilon)$ is intensity per energy unit. The inset with experimental points is a blowup of the lower part of the curve with a factor of 10. The other inset shows the satellite with "background?" subtracted. The background is discussed by L. Hedin, in "Soft X-Ray Band Spectra and the Electronic Structure of Metals and Materials" (D. Fabian, ed.). Academic Press, New York, 1968.

The experimental curve has a tail at the low energy end which is not predicted by one-electron theory. To discuss this tail it is convenient to turn the level diagram upside down.²⁰² Figure 46a shows the one-electron levels, Fig. 46b shows the corresponding levels of the total system, and Fig. 46c gives the one-electron density of states for an interacting system; thus

$$N(\omega) = \sum_s |f_s|^2 \delta(\omega - \epsilon_s), \quad (39.2)$$

where

$$\epsilon_s = E(N) - E(N-1, s), \quad (39.3)$$

and f_s is an "oscillator strength" for removing an electron leaving the system behind in a state s with energy $E(N-1, s)$. The $N(\omega)$ curve has a tail on the main band due to the finite lifetime of the quasi particles and a satellite structure caused by the plasmarons (see Sections 25 and 35).

²⁰² L. G. Parrat, *Rev. Mod. Phys.* **31**, 616 (1959).

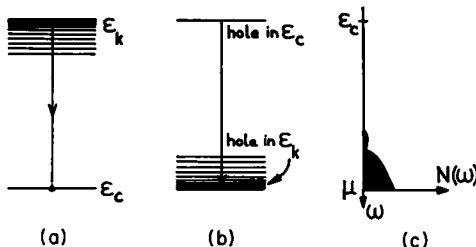


FIG. 46. Qualitative sketch of different representations for the energy spectrum involved in soft X-ray emission. Independent particle model: (a) one-particle levels, (b) levels for the total system, (c) one-particle density of states for an interacting system.

We would like to point out that several of the features coming from many-body theory have been discussed earlier in a direct physical language, and we refer to discussions of lifetimes, Auger processes, and plasmon effects by Landsberg,²⁰³ Ferrell,²⁰⁴ Pirenne and Longe,²⁰⁵ and others.

To show the relation between the one-particle density of states and the experimental results, one starts from the golden rule. The initial state has a hole in one of the ion cores, which causes the valence electrons to screen the unbalanced charge. Thus we can write the initial state as $|i\rangle = a_c |N^*\rangle$, where N^* indicates that the valence electron cloud is relaxed toward the hole in the core. Thus the golden rule gives²⁰⁶

$$I(\omega) = C\omega \sum_s |\langle N - 1, s | \sum_k p_{ck} a_k | N^* \rangle|^2 \delta(\omega + \epsilon_c - \epsilon_s). \quad (39.4)$$

The core electrons are now explicitly eliminated from the picture. Neglecting coupling between different valence bands we obtain the further reduction

$$I(\omega) = C\omega \sum_k |p_{ck}|^2 \sum_s |\langle N - 1, s | a_k | N^* \rangle|^2 \delta(\omega + \epsilon_c - \epsilon_s). \quad (39.5)$$

If we neglect the relaxation of the valence electrons and replace $|N^*\rangle$ by $|N\rangle$, the sum over s gives the spectral function $A(k, \omega)$ [see Eq. (10.1)]. Hence we obtain

$$I(\omega) = C\omega \sum_k |p_{ck}|^2 A(k, \omega + \epsilon_c) \quad (39.6)$$

which reduces to Eq. (39.1) for independent particles.

For free-electron-like metals the spectral function is quite similar to

²⁰³ P. T. Landsberg, *Proc. Phys. Soc. A* **62**, 806 (1949).

²⁰⁴ R. A. Ferrell, *Rev. Mod. Phys.* **28**, 308 (1956).

²⁰⁵ J. Pirenne and P. Longe, *Physica* **30**, 277 (1964).

²⁰⁶ L. Hedin, *Solid State Comm.* **5**, 451 (1967).

the electron gas spectrum. The matrix elements for transitions to p levels are not expected to show strong variations, and thus the intensity should have about the same shape as the density of states for an electron gas as shown in Fig. 25. The tailing of the main band and the existence of a plasmon edge at $\hbar\omega_p$, below the Fermi edge agree with experiments.²⁰⁷ There are also recent experimental indications, although marginal, of the plasmaron edge.²⁰⁸ The density of states curve is, however, much larger in the satellite region than the corresponding portions of the experimental curves.

The possibility of plasmon emission was first discussed by Ferrell²⁰⁴ and a theoretical explanation of the low intensity of the plasmon satellite was later given by Brouers.²⁰⁹ Brouers used the method of Bohm and Pines with canonical transformations to describe quasi particles as bare electrons surrounded by virtual plasmons. Similarly, the initial state $|N^*\rangle$ was chosen as a superposition of the ground state $|N\rangle$ and virtual plasmon excitations. The coefficients for the virtual plasmons are appreciable since the energy of relaxation is indeed a substantial fraction of the plasmon energy. Thus one would expect a large probability for plasmon excitation in the emission. The satellite intensity is, however, drastically cut down by a destructive interference between the two virtual plasmon fields that are associated with the hole in the core and that of the electron, making the transition to the core level.²⁰⁹ While Brouers' explanation seems qualitatively correct, the numerical results for the satellite intensity are smaller than the experimental by about the same factor as the electron gas density of states results are larger.²¹⁰

A straightforward diagrammatic analysis was given by Glick and Longe.²¹¹ They use the van Hove method to transform the golden rule formula into one involving a correlation function, and obtain

$$I(\omega) = C\omega \operatorname{Re} \int_0^\infty e^{-i\omega t} \langle i | p(t)p(0) | i \rangle dt, \quad (39.7)$$

where $p(t)$ is the momentum in the Heisenberg picture. Like Brouers they find large cancellation effects in the satellite region due to the core hole. In the main band, however, their expansion diverged. The calculations

²⁰⁷ G. A. Rooke, *Phys. Letters* **3**, 234 (1963).

²⁰⁸ J. R. Cuthill, R. C. Dobbyn, A. J. McAlister, and M. L. Williams, *Phys. Rev.* **174**, 515 (1968).

²⁰⁹ F. Brouers, *Phys. Letters* **11**, 297 (1964); *Phys. Status Solidi* **11**, K25 (1965); **22**, 213 (1967); F. Brouers and P. Longe, in "Soft X-Ray Spectra and the Electronic Structure of Metals and Materials" (D. Fabian, ed.). Academic Press, New York, 1968.

²¹⁰ L. Hedin, in "Soft X-Ray Spectra and the Electronic Structure of Metals and Materials" (D. Fabian, ed.). Academic Press, New York, 1968.

²¹¹ A. J. Glick and P. Longe, *Phys. Rev. Letters* **15**, 589 (1965); see also P. Longe and A. J. Glick, *Phys. Rev.* **177**, 526 (1969).

were extended by Bose,²¹² who avoided the divergencies by performing an infinite summation.

A particular difficulty in the approach of Glick and Longe is how to handle the perturbation expansion for a highly excited state, like the initial state $|i\rangle$ with its core hole. For such situations the standard many-body techniques do not apply. An attempt to avoid this difficulty is made by Rystephanick and Carbotte,²¹³ who introduce a three-particle Green function, and try to project out the expectation value in Eq. (39.7). This approach has, however, not yet been carried far enough to yield explicit new results.

Although ultimately one may have to use the more general methods just discussed, it seems that much of the basic physics can be discussed in terms of a simple elaboration of Eq. (39.5).²¹⁰ The initial state is taken as

$$|N^*\rangle = \alpha_0 |N\rangle + \sum_{p,q} \alpha_q^p a_p^+ a_q |N\rangle, \quad (39.8)$$

which as a special case contains the ansatz by Brouers. The emission intensity will now involve matrix elements of triple products such as a^+aa . From the equation of motion for a_k follows a relation between matrix elements of triple products $\langle N - 1, s | a^+aa | N \rangle$ and the simple operator $\langle N - 1, s | a_k | N \rangle$. By use of this relation the triple products can be approximately replaced by the simple operator in the expression for the emission intensity. One then has the same relation to the spectral function as in Eq. (39.6) with, however, an effective matrix element p_{ck}^{eff} , which contains the effects of interferences discussed earlier. The effective dipole matrix element should have the form

$$p_{ck}^{\text{eff}} = p_{ck} + p_{ck}^{(+)} + (\omega + \epsilon_c - \epsilon_k^{\text{HF}}) p_{ck}^{(-)}. \quad (39.9)$$

The quantities $p_{ck}^{(\pm)}$ involves the coefficients α_q^p of Eq. (39.8) and couple to Bloch states above (+) and below (-) the Fermi level. For ω in the main band, the coefficient of $p_{ck}^{(-)}$ is small and the expression for p_{ck}^{eff} is similar to the result obtained by Shuey²¹⁴ in an independent particle approach, treating the relaxation toward the hole in an approximately self-consistent way. In the plasmon satellite, on the other hand, there is a cancellation between the $p_{ck}^{(-)}$ term and the two others which cuts down the intensity relative to the density of states results in Fig. 25.

Many-body effects sometimes manifest themselves not only in the satellite structure but also as a spike in the emission spectrum at the Fermi edge.^{214a} For polyvalent metals such as Mg and Al, the spike is interpreted

²¹² S. M. Bose, Ph.D. Thesis, Univ. of Maryland, 1967.

²¹³ R. G. Rystephanick and J. P. Carbotte, *Phys. Rev.* **166**, 607 (1968).

²¹⁴ R. T. Shuey, *Physik Kondensierter Materie*. **5**, 192 (1966).

^{214a} J. Friedel, *Comments Sol. Stat. Phys.* **2**, 21 (1969).

in a natural way as a Brillouin zone effect.²¹⁵ However, the spike also appears for Na where this explanation does not work. We note in passing that the formula in Eq. (39.9) for the effective matrix element predicts such a spike through the singular behavior of ϵ_k^{HF} at the Fermi level. The problem of the spike at the Fermi surface has recently been attacked from a fundamental point of view by several people. The problem does not yet seem completely solved. Recent work by Bergersen and Brouers²¹⁶ indicates that the effect is associated with the Anderson orthogonality paradox.²¹⁷ Mahan²¹⁸ pointed out that the final-state Coulomb interactions between the electron and the hole would lead to exciton resonances, which would give rise to a power law singularity at the threshold energy. The many-body theory of these ideas has recently been developed in a series of papers by Nozières and collaborators²¹⁹ who developed new theoretical techniques to handle this type of problems. In the paper by Nozières and de Dominicis, a simple description of the edge problem is given by means of a *transient* one-electron Green function. Recent work on this problem has also been made by several other authors.^{219a}

The relaxed initial state can be considered as the result of scattering of itinerant electrons on the core hole. This scattering may be of resonance character as discussed by Allotey.²²⁰ By calculating the resonance scattering, Allotey explained the peculiar shape of the Fermi edge in Li and the absence of the corresponding effect in Na. An alternative explanation of the Li edge in terms of the dipole matrix element has been given by Stott and March.^{220a}

We finally remind the reader that the discussion in this section has been confined to the simplest possible case; that of complete relaxation in the initial state. Problems where this does not apply require a complete reconsideration of the approach where the excitation of the core electron and the subsequent emission of the soft X-ray is treated as one single dynamical

²¹⁵ G. A. Rooke, *J. Phys.* [2] **C1**, 767, 776 (1968).

²¹⁶ B. Bergersen and F. Brouers, *J. Phys. C*, **2**, 651 (1969).

²¹⁷ P. W. Anderson, *Phys. Rev. Letters* **18**, 1049 (1967).

²¹⁸ G. D. Mahan, *Phys. Rev.* **163**, 612 (1967).

²¹⁹ B. Roulet, J. Gavoret, and P. Nozières *Phys. Rev.* **178**, 1072 (1969); P. Nozières, J. Gavoret, and B. Roulet, *ibid.* **178**, 1084 (1969); P. Nozières and C. T. De Dominicis, *ibid.* **178**, 1097 (1969).

^{219a} Y. Mizuno and K. Ishikawa, *J. Phys. Soc. Japan* **25**, 627 (1968); A. Morita and M. Watabe, *ibid.* **25**, 1060 (1968); D. C. Langreth, *Phys. Rev. Comments and Addenda* (to be published); G. A. Ausmann, Jr., and A. J. Glick, Techn. Rep., Univ. of Maryland, 1969.

²²⁰ F. K. Allotey, *Phys. Rev.* **157**, 467 (1967).

^{220a} M. J. Stott and N. H. March, in "Soft X-Ray Band Spectra and the Electronic Structure of Metals and Materials" (D. Fabian, ed.). Academic Press, New York, 1968.

process. Study of such processes are likely to open up new aspects on the dynamical interactions in solids.

40. PHOTOEMISSION AND PHOTOABSORPTION SPECTRA

a. *Introductory Remarks*

A complete discussion of photoabsorption and photoemission would require an analysis of the two-particle and three-particle Green functions and would hence fall outside the scope of this review. Some aspects of the problem can be discussed in terms of the one-electron spectrum, the condition being that "final state" or "particle-hole" interactions can be neglected. To be specific, let us consider a transition out of the ground state $|N\rangle$ into an excited state of the form $a_{\kappa}^+ |N - 1, s\rangle$, in which we treat the photoelectron in state κ as dynamically decoupled but retain the full many-body interactions between the other ($N - 1$) electrons. This approximation applies in the case of X-ray radiation when the photoelectron acquires a high energy (XPS). In cases where the photoelectron has an energy comparable to that of the conduction electrons, the photoelectron may interact strongly with the hole left behind. A decoupling of the electron is then no longer justifiable, and the problem is intrinsically a two- or three-particle problem.

We would like to point out that a complete many-body theory for these problems has not yet been worked out, and that the independent particle theory has been applied with success to a number of cases. We refer to the results obtained by Brust^{220b} and by Dresselhaus and Dresselhaus²²¹ for valence semiconductors. The optical properties of the polyvalent simple metals seem also to be fairly well understood using first order theory. However, in none of these calculations were the dipole matrix elements properly evaluated. Such calculation will with certainty be available in a near future, and one can then easier assess the limitations of the simple theory. For a recent review of these problems we refer to Abelès.²²²

We shall next derive the relation to the one-electron spectral function which follows when final state interactions are neglected. The structure in the spectral function discussed in Sections 35 and 36 should give rise to observable effects in XPS and perhaps also in uv photoemission spectra. We shall also discuss some features in the soft X-ray absorption spectrum

^{220b} D. Brust, *Phys. Rev.* **134**, A1337 (1964).

²²¹ G. Dresselhaus and M. S. Dresselhaus, *Phys. Rev.* **160**, 649 (1967).

²²² F. Abelès, in "Soft X-Ray Spectra and the Electronic Structure of Metals and Materials" (D. Fabian, ed.). Academic Press, New York, 1968.

of Al, which may be tentatively explained in terms of the one-electron spectrum. Some final remarks about recent work on excitation effects and further refinements will conclude this section.

b. Photoemission and Photoabsorption Discussed in Terms of the One-Electron Spectrum

We consider the probability of absorption of an energetic photon having frequency ω . Neglecting final state interactions, i.e. assuming that a decoupled electron leaves the system in the state $a_{\mathbf{k}}^+ | N - 1, s \rangle$, we obtain

$$w \sim \sum_{\mathbf{k}, s} | \langle N - 1, s | a_{\mathbf{k}} \sum_{\mathbf{k}, \mathbf{k}'} p_{\mathbf{k}' \mathbf{k}} a_{\mathbf{k}'}^+ a_{\mathbf{k}} | N \rangle |^2 \\ \times \delta[\epsilon_{\mathbf{k}} + E(N - 1, s) - E(N) - \omega]. \quad (40.1)$$

For large enough energies $E_{\mathbf{k}}$ we have that $a_{\mathbf{k}} | N \rangle \approx 0$, and hence we obtain

$$w \sim \sum_{\mathbf{k}, s} | \sum_{\mathbf{k}} p_{\mathbf{k} \mathbf{k}} \langle N - 1, s | a_{\mathbf{k}} | N \rangle |^2 \delta(\epsilon_{\mathbf{k}} - \omega - \epsilon_s) \quad (40.2)$$

or, neglecting nondiagonal elements of the spectral function A ,

$$w \sim \sum_{\mathbf{k}, \mathbf{k}} | p_{\mathbf{k} \mathbf{k}} |^2 A(\mathbf{k}, \epsilon_{\mathbf{k}} - \omega); \quad \epsilon_{\mathbf{k}} - \omega < \mu. \quad (40.3)$$

The energy distribution of the photoelectrons is hence given by, taking $\epsilon = \epsilon_{\mathbf{k}} \sim k^2$,

$$I(\epsilon) \sim \epsilon^{1/2} \sum_{\mathbf{k}} | p_{\mathbf{k}, \mathbf{k}} |^2 A(\mathbf{k}, \epsilon - \omega); \quad \epsilon - \omega < \mu. \quad (40.4)$$

As a further simplification we introduce an average dipole matrix element p_{eff} , thus

$$I(\epsilon) \sim \epsilon^{1/2} p_{\text{eff}}^2 N(\epsilon - \omega); \quad \epsilon - \omega < \mu, \quad (40.5)$$

where $N(\omega) = \sum_{\mathbf{k}} A(\mathbf{k}, \omega)$ is the one-particle density of states.

With X-ray radiation (XPS) the outgoing electrons obtain a high energy, which however can be measured to within a few tenths of an electron volt.²²³ The energy distribution of the photoelectrons will, according to Eq. (40.5), give the density of states in the solid.²²⁴

According to the discussion in Section 35 the theory predicts that in

²²³ K. Siegbahn *et al.* "ESCA, Atomic, Molecular and Solid State Structure Studied by Means of Electron Spectroscopy." Almqvist and Wiksell, Uppsala, 1967; J. A. Bearden and A. F. Burr. *Rev. Mod. Phys.* **39**, 125 (1967).

²²⁴ The raw experimental data are of course somewhat distorted from a number of secondary effects, such as the scattering of the outgoing electron, background radiation, and the widths of the X-ray line used for the excitation. These effects can, however, be corrected for to some extent.

TABLE XIII. ENERGIES OF CORE ELECTRONS IN RY

	$r_s:$	Li, 1s 3.25	Na, 2s 3.93	K, 3s 4.86	Al, 2s 2.07
Contributions to chemical potential	μ_{bs}^*	-0.429	-0.365	-0.320	-1.663
	$V_{H^+}^{\circ f}$	0.743	0.615	0.497	+2.418
	$\Sigma^{\circ g}$	-0.471	-0.398	-0.330	-0.706
	μ	-0.157	-0.148	-0.153	+0.049
Contributions to core level	$\epsilon_{ion}(\text{expt})^h$	-5.560	-5.887	-3.529	-12.089
	$V_{H^+}^{\circ i}$	0.924	0.763	0.617	3.010
	$V_{ex}^{\circ j}$	-0.037	-0.014	-0.010	-0.052
	$\Sigma_{pol}^{\circ k}$	0.541	0.474	0.408	0.734
	$\Delta \Sigma_{pol}^{\circ l}$	-0.056	-0.064	-0.094	-0.021
	ϵ_c	-4.188	-4.728	-2.608	-8.416
$\mu - \epsilon_c$ (theory)		4.03	4.58	2.46	8.47
$\mu - \epsilon_c$ (experiment) ^m		4.03	4.67	2.51	8.48

^a F. S. Ham, *Phys. Rev.* **128**, 82 (1962).^b B. Segall, *Phys. Rev.* **124**, 1797 (1961).^c L. Hedin, *Arkiv Fysik* **30**, 231 (1965).^d L. Hedin, *Phys. Rev.* **139**, A796 (1965).

^e Fermi level from band-structure calculation for Li, Na, and K by Ham^a and for Al by Segall.^b Segall's value for μ_{bs} included the contribution V_{H^+} , which has been given separately in the table. For the definition of μ and ϵ_c see footnote 172.

^f Coulomb potential from the valence electrons, $V_{H^+} = 2.417 \cdot Z/r_s$ Ry according to footnote c. Here Z is the number of valence electrons per unit cell of volume $4\pi r_s^3/3$

^g Electron gas result for valence electron self-energy.

^h C. E. Moore, "Atomic Energy Levels," *Natl. Bur. Std. Circ.* No. 467, Vol. 1, Washington, D.C., 1949.

ⁱ Coulomb potential from the valence electrons assuming a uniform charge distribution, $V_{H^+} = 3Z/r_s$ Ry.

^j Estimated exchange potential from the valence electrons.^k Polarization potential according to Eq. (36.8).^l Correction for finite extention of core wave function, see footnote c.^m J. A. Bearden and A. F. Burr, *Rev. Mod. Phys.* **39**, 125 (1967).

simple metals there should be a fairly flat conduction band satellite starting at $\hbar\omega_p$ below the Fermi edge and ending at somewhat more than two times $\hbar\omega_p$ below. Similarly, the theory predicts that all core quasi-particle levels (see Section 36) should be accompanied by a broad satellite with its maximum at $(1.6-2.3) \times \hbar\omega_p$, the actual value dependent on the density of conduction electrons. Today very few complete X-ray photoemission spectra for metals are found in the literature. There are none on the satellite structure in simple metals. Experimental data for noble metals by Siegbahn

*et al.*²²³ show some structure in the region of interest, but due to unknown effects of the *d* electrons, the interpretation of this structure as due to plasmaron effects is only tentative. X-ray photoemission spectroscopy seems to be a useful tool to study the plasmaron effects associated with both valence bands and with core levels.

The published data obtained by XPS for free-electron-like metals concern only accurately determined core quasi-particle levels.²²³ The core levels have been calculated by Hedin¹⁵¹ using the methods discussed in Sections 35 and 36. They are in good agreement with the experimental values as shown in Table XIII.

When the energy of the photoelectron is of the same order as the energies of plasmon states or typical virtual one-particle states, which mix into the many-particle ground state, a number of complications will disturb the simple picture just given. First, we cannot use the free electron formula for ϵ_k but have to use the proper dispersion law from an energy band calculation. Secondly, we should have to consider the finite lifetime of the electron and also the structure in the spectral function above the Fermi edge (see Section 25).²²⁵ Thirdly, we have the particle-hole interactions which require the use of spectral functions for two or more particles. The many-body theory for these processes has, however, not yet been fully worked out and applied to these problems. We shall here take a simple point of view and treat the new structure of conduction and core-electron spectra as additional levels or groups of levels in a simple one-electron scheme. Such a simplified discussion of plasmon effects in X-ray absorption in simple metals was given by Ferrell.²⁰⁴ Due to the presence of satellite structure in both core and conduction bands there should be a characteristic structure above the threshold as discussed by Lundqvist.¹⁵³ This is illustrated in Fig. 47.

In principle there should be four kinds of absorption processes: (1) from core quasi particle to quasi particle in the conduction band, (2) from core quasi particle to unoccupied satellite, (3) from core satellite to quasi particle in the conduction band, (4) from satellite to satellite. The values of the characteristic energies depend on the density of conduction electrons and we give the values for Al as an example. Just above the threshold only process 1 is effective. Process 2 and 3 both start at $\hbar\omega_p$, (15 eV for Al) above the threshold energy. The maximum strength of the core satellite is at 24 eV for Al. Process 4 starts at $2 \times \hbar\omega_p$, (30 eV) with a maximum at 39 eV. The fine structure of the $L_{2,3}$ absorption spectrum of Al is experimentally

²²⁵ The finite lifetime is generally poorly represented by a simple Lorentzian broadening of the quasi-particle level and the true spectral function is often strongly asymmetric. In particular, the damping is zero at the absorption threshold for semiconductors (neglecting phonon effects).

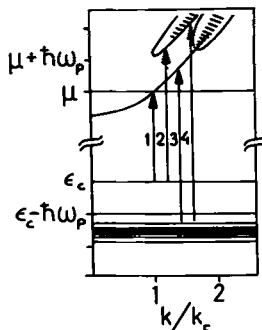


FIG. 47. Level structure in the one-electron spectrum of a metal; after B. I. Lundqvist, Thesis, Chalmers Univ. of Technol., 1969.

well established, both in soft X-ray absorption²²⁶ and by inelastic scattering of electrons.²²⁷ The experimental L_{23} absorption spectrum for Al contains knees at 7, 15, and 30 eV above threshold and maxima at 23 and 38 eV. Thus there is a close correspondence in the location of the structure between the predicted and observed absorption (except for the knee at 7 eV).^{227a}

By the same mechanism there should also be additional absorption in the uv spectrum of simple metals. Due to the broadening of the quasi-particle peak there is a tail in the absorption below the threshold, which besides the phonon effects should contribute to the experimentally observed tail. The plasmon contribution to the absorption in alkali metals has recently been discussed by Esposito *et al.*²²⁸

Similar considerations will also apply to photoemission, where in particular the experimental work by Spicer *et al.*²²⁹ is attracting much attention. With uv radiation the valence plasmaron band would give structure in the low-energy region of the energy distribution, provided that photons of sufficiently high energy are used. The photon energy must be larger than $W + \hbar\omega_p$, where W is the work function. In this region there is also a large

²²⁶ V. A. Fomichev and A. P. Lukirskii, *Soviet Phys.-Solid State (English Transl.)* **8**, 1674 (1967); T. Sagawa *et al.*, *J. Phys. Soc. Japan* **21**, 2602 (1966); K. Codling and R. P. Madden, *Phys. Rev.* **167**, 587 (1968).

²²⁷ H. Watanabe, *J. Appl. Phys.* **3**, 804 (1964); N. Swanson and C. J. Powell, *Phys. Rev.* **167**, 592 (1968).

^{227a} Recent measurements for other metals do not show such a good agreement as for Al and the detailed interpretation of such data is still an open question (R. Haensel and C. Kunz, private communication).

²²⁸ R. J. Esposito, L. Meldawer, and P. E. Bloomfield, *Phys. Rev.* **168**, 744 (1968).

²²⁹ W. E. Spicer, *Phys. Rev.* **154**, 385 (1967).

contribution from scattered electrons, which complicates the interpretation of the experimental data.

c. *Exciton Effects and Related Recent Work*

The simple discussion just given applies only to the location of possible structure in the spectrum. A quantitative treatment of photoabsorption and photoemission requires a substantial step further in developing new theoretical techniques and workable approximation schemes. The need for including particle hole interactions has recently been discussed by several authors. We would particularly like to mention the work by Hopfield,²³⁰ who also discussed the influence of a dynamically screened interaction in photoemission.

Of particular relevance is the recent work by Mahan,²¹⁸ who has shown that exciton resonances in metals may occur near the interband threshold in optical absorption and substantially alter the shape and strength of the absorption edge. In the language of the many-body theory such effects are due to important vertex effects, which we have neglected. Watabe and Yasuhara²³¹ have recently calculated the vertex corrections to the optical conductivity for direct interband absorption in alkali metals to first order in the dynamical screened interaction and have shown that they are very important. Much progress in this field is expected to occur over the next few years.

41. POSITRON ANNIHILATION IN METALS

Positron annihilation is an interesting case from the theoretical point of view as an example where the approximations discussed in most of this review are insufficient and where calculations have been and are being performed using more sophisticated theoretical assumptions. This need for a more refined theory means on one hand that the relation between experiments and the properties of the system become quite complex, but may also give important clues how to treat the electron-electron interaction more accurately.

In the experiments, fast positrons are shot into the material and are slowed down to thermal or near-thermal velocities before annihilation. The predominant mode of annihilation in metals is the decay into two photons, which come out at almost opposite angles. One measures

- (i) *the positron lifetime* (the mean lifetime for metals lies between 0.1 and 0.5 nsec), and

²³⁰ J. J. Hopfield, *Phys. Rev.* **139**, A419 (1965); Elastic scattering at inelastic thresholds—Application to solids," *Proc. Tokyo Summer Inst. Theor. Phys.*, **1965**. *Comments Sol. State Phys.* **1**, 198 (1969).

²³¹ M. Watabe and H. Yasuhara, *Phys. Letters* **28A**, 329 (1968).

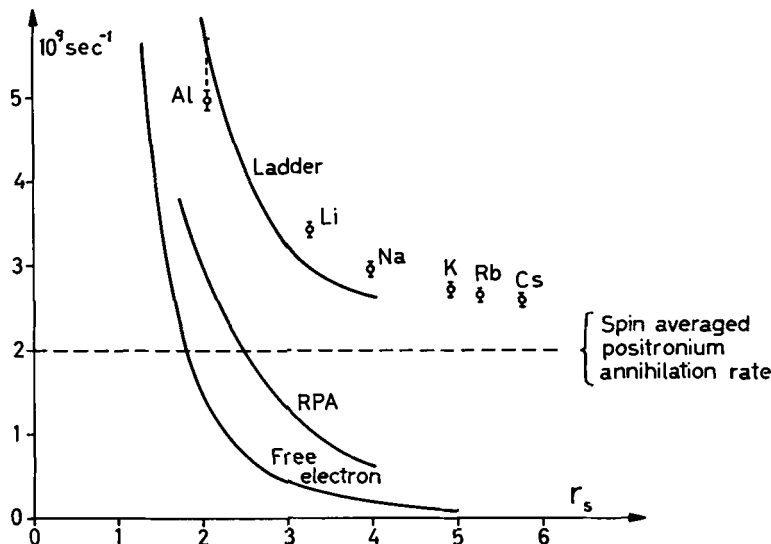


FIG. 48. Experimental and theoretical results for positron annihilation rates in metals. Experimental values from H. L. Weisberg and S. Berko, *Phys. Rev.* **154**, 249 (1967); "free electron" from Eq. (41.6); "RPA" from B. Bergersen, Ph.D. Thesis, Brandeis Univ., 1964; "Ladder" from S. Kahana, *Phys. Rev.* **129**, 1622 (1963).

(ii) *the angular correlation* (the angle between the two photons differs from π by a few milliradians).

The *annihilation rate* λ (inverse mean lifetime) can be taken as proportional to the electron density at the position of the positron, provided all particles have nonrelativistic velocities. One obtains²³²

$$\lambda = \pi \alpha^4 a_0^2 c \sum_{\sigma} \int d^3r \langle N | \phi^+(\mathbf{r}) \phi(\mathbf{r}) \psi_{\sigma}^+(\mathbf{r}) \psi_{\sigma}(\mathbf{r}) | N \rangle, \quad (41.1)$$

where α is the fine structure constant ($\sim 1/137$), a_0 is the Bohr radius, and c is the velocity of light. The operators $\phi^+(\mathbf{x})$ and $\phi(\mathbf{x})$ are the positron creation and annihilation operators.²³³

²³² See e. g. J. M. Jauch and F. Rohrlich, "The Theory of Photons and Electrons," p. 263. Addison-Wesley, Reading, Massachusetts, 1958.

²³³ It has recently been pointed out by Mogensen²³⁴ that the derivation of Eq. (41.1) is not free from problems, because of the difficulty in taking the nonrelativistic limit for the fully interacting system. Criticism questioning the validity of Eq. (41.1) has also been raised by Sedov²³⁵; however, it seems to us that his correction terms are indeed already taken into account by Eq. (41.1).

²³⁴ O. E. Mogensen, Thesis, Tech. Univ. of Denmark, Lyngby, 1968.

²³⁵ V. L. Sedov, *Soviet Phys.-Solid State (English Transl.)* **9**, 1540 (1968).

Two-photon annihilation is associated with a singlet alignment of the spins of the annihilating particles, and is forbidden from the triplet state; therefore only one of four spin states will contribute, as will be taken into account in the equations to follow. It is convenient to work in momentum space and we obtain

$$\lambda = (3\alpha^4 c / 4a_0) r_s^{-3} N^{-1} \sum_{\mathbf{k}} P(\mathbf{k}) \quad (41.2)$$

with

$$P(\mathbf{k}) = P^d(\mathbf{k}) + P^{n.d.}(\mathbf{k})$$

where

$$\begin{aligned} P^d(\mathbf{k}) &= \sum_{\mathbf{p}, \sigma} \langle N | d_{\mathbf{p}}^+ d_{\mathbf{p}} a_{\mathbf{k}-\mathbf{p}, \sigma}^+ a_{\mathbf{k}-\mathbf{p}, \sigma} | N \rangle \\ P^{n.d.}(\mathbf{k}) &= \sum_{\mathbf{p}, \sigma, q \neq 0} \langle N | d_{\mathbf{p}+\mathbf{q}}^+ d_{\mathbf{p}} a_{\mathbf{k}-\mathbf{p}-\mathbf{q}, \sigma}^+ a_{\mathbf{k}-\mathbf{p}, \sigma} | N \rangle. \end{aligned} \quad (41.3)$$

\mathbf{k} is the center of mass momentum of the annihilating pair. Angular correlation experiments are usually made with a parallel slit geometry,²³⁶ and the angular distribution is given by

$$N(\theta) = \frac{A}{\pi} \int_{-\infty}^{\infty} dk_x \int_{-\infty}^{\infty} dk_y P(k_x, k_y, k_z = mc\theta), \quad (41.4)$$

where A is a constant.

In the simplest approximation one considers the positron as a non-interacting test particle which is completely thermalized before it annihilates in a noninteracting electron gas at zero temperature. We obtain in this case

$$P_0(\mathbf{k}) = P_0^d(\mathbf{k}) = 2\Theta(p_F - |\mathbf{k}|) \quad (41.5)$$

$$\lambda_0 = (3\alpha^4 c / 4a_0) r_s^{-3} \quad (41.6)$$

$$N_0(\theta) = A[p_F^2 - (mc\theta)^2]\Theta(p_F - mc\theta). \quad (41.7)$$

The experimental curves for sodium²³⁷ agree qualitatively quite well with Eq. (41.7). However, two differences should be observed:

(i) The experiments show a high momentum tail, which is due to core annihilation.²³⁸

(ii) There is an enhancement of the annihilation probability near the angle which corresponds to the Fermi momentum. This effect is due to the electron-positron interaction and has been explained by Carbotte and Kahana.²³⁹

²³⁶ The experimental setup is discussed in many places, e.g., in "Positron Annihilation" (A. T. Stewart and L. O. Roellig, eds.). Academic Press, New York, 1967.

²³⁷ J. J. Donaghy and A. T. Stewart, *Phys. Rev.* **164**, 396 (1967).

²³⁸ J. P. Carbotte and A. Salvadori, *Phys. Rev.* **162**, 290 (1967).

²³⁹ J. P. Carbotte and S. Kahana, *Phys. Rev.* **139**, A213 (1965).

The experimental annihilation rates for Al and the alkali metals²⁴⁰ are given in Fig. 48 together with some theoretical curves.

Comparison between the noninteracting model with λ_0 calculated from Eq. (41.6) shows the complete failure to account for the observed annihilation rate. The discrepancy must be sought in the electron-positron interaction.

A plausible approximation would be to account for the enhancement by calculating the linear response of the medium regarding the positron as a test charge,²⁴¹ i.e. using the dielectric theory discussed extensively in this review. The result of this approximation is given by the curve RPA in Fig. 48. The failure of this approximation to account for the experimental annihilation rates even qualitatively indicates the urgent need to go beyond linear response theory. It does not, however, necessarily show that the Lindhard (or RPA) dielectric function is much in error.²⁴² One such approach is the so-called ladder approximation. This corresponds to solving a two-body problem describing the dynamics of the positron-electron system. The basic equation of the ladder approximation is the Bethe-Goldstone equation:

$$[(\mathbf{k} + \mathbf{q})^2 + \mathbf{q}^2 - \mathbf{k}^2][\varphi_{\mathbf{k}}(\mathbf{q}) - \delta_{\mathbf{q},0}] = (8\pi/a_0^2\Omega) \sum_{\mathbf{p}} \Theta(|\mathbf{k} + \mathbf{p}| - \mathbf{p}_F) v(\mathbf{q} - \mathbf{p}) \varphi_{\mathbf{k}}(\mathbf{p}). \quad (41.8)$$

This equation looks very much like the Schrödinger equation for an electron with initial momentum \mathbf{k} interacting with a positron having zero initial momentum. Because of the exclusion principle, only scattering into states outside the Fermi sea is allowed.

The ladder approximation was first applied to the problem by Kahana.²⁴³ The results are in good qualitative agreement with the experimental rates as shown by the curve in Fig. 48. Several people²⁴⁴ have redone the calculation using somewhat different effective interactions or summing up a more general subset of diagrams in perturbation theory.²⁴⁵ The results obtained were not much different from those of Kahana.²⁴⁶

²⁴⁰ H. L. Weisberg and S. Berko, *Phys. Rev.* **154**, 249 (1967).

²⁴¹ B. Bergersen, Ph.D. Thesis, Brandeis Univ., 1964.

²⁴² The perturbation is much too strong for linear response theory to apply. If one would consider a negative unit charge instead of a positive, one would obtain a negative number density at the position of the test charge.

²⁴³ S. Kahana, *Phys. Rev.* **117**, 123 (1960); **129**, 1622 (1963).

²⁴⁴ J. Arponen and P. Jauho, *Phys. Rev.* **167**, 239 (1968); J. Crowell, V. E. Anderson, and R. H. Ritchie, *ibid.* **150**, 243 (1966); A. J. Zuchelli and T. G. Hickman, *ibid.* **136**, A1728 (1964).

²⁴⁵ H. Kanazawa, Y. Ohtsuki, and S. Yanagawa, *Progr. Theoret. Phys.* **33**, 1010 (1965).

²⁴⁶ It should be remembered that since the experimental data include core annihilation and band structure effects, the electron gas results can only give a qualitative agreement.

The ladder approximation provides a simple example of a two-body equation for a many-body system, and because of the simple structure one may check whether it satisfies different consistency requirements. Two such requirements are²⁴⁷:

(i) The positron should be completely screened, i.e. the total polarization charge around the positron should be equal in magnitude to the positron charge. This requirement is not satisfied in the ladder approximation,²⁴¹ but it has been shown how corrections to the ladder approximation could be introduced so that the requirement is satisfied. The numerical effect of such corrections was shown by Carbotte²⁴⁸ to be fairly small.

(ii) For a sufficiently small density a positronium-like state should form. This is indicated by the experimental data and is intuitively reasonable. It has been shown by Bergersen²⁴⁹ that one can introduce a bound state by making an ansatz $|\phi\rangle$ for the polarization charge around the positron. This procedure gives an annihilation rate which agrees with the positronium rate for low densities, but gives a rate which is too low at high densities.²⁵⁰

We shall next turn to the question of angular correlation. The ladder approximation gives

$$P(\mathbf{k}) = 2\Theta(p_F - |\mathbf{k}|) \left| \sum_{\mathbf{q}} \varphi_{\mathbf{k}}(\mathbf{q}) \right|^2. \quad (41.9)$$

The electron-positron interaction does not contribute to the tail above the angle corresponding to the Fermi momentum in the angular correlation. The only difference compared to the noninteracting case is an enhancement of the annihilation rate from states with c.m. momenta near the Fermi momentum. The agreement with experiment in this picture is somewhat fortuitous and depends strongly on the fact that a static interaction was used instead of the full dynamical interaction.

Carbotte and Kahana²³⁹ calculated the angular correlation including

²⁴⁷ A third requirement has been discussed by B. Bergersen and J. H. Terrell, in "Soft X-Ray Spectra and the Electronic Structure of Metals and Materials" (D. Fabian, ed.). Academic Press, New York, 1968.

²⁴⁸ J. P. Carbotte, *Phys. Rev.* **155**, 197 (1967).

²⁴⁹ B. Bergersen, *Phys. Rev.* **181**, 499 (1969).

²⁵⁰ At sufficiently low densities, the homogeneous equation associated with Eq. (41.8) has a solution, which many authors have associated with the formation of a bound state. The physical nature of such a solution has in our opinion not been convincingly clarified. It may even be that such bound state solutions represent unphysical modes and arise because the ladder approximation only imperfectly takes into account screening and the exclusion principle for states outside the Fermi sea. At high densities the ladder approximation seems well established whereas further development of the theory seems necessary at low densities.

self-energy effects and using a dynamical screened interaction. An important aspect of their work seems to be a strong cancellation effect. The angular correlation contains two types of terms, one arising from the dielectric screening and another due to self-energy corrections for both electrons and the positron. Both terms give rather large contributions, both in the main band and to the tail above the Fermi momentum and they have opposite sign. Above the Fermi momentum the cancellation is almost complete while below there is an enhancement near the Fermi surface. The calculated angular correlation curves are in excellent agreement with recent experimental results by Donaghy and Stewart.²³⁷

It has been shown by Majumdar²⁵¹ that when full account is taken of electron-positron correlations in perturbation theory, a discontinuity in $P(\mathbf{k})$ at the Fermi momentum will exist in all orders at zero temperature. This shows up as a discontinuity in the derivative of the angular distribution at $\theta = p_F/mc$. Kim *et al.*²⁵² have studied experimentally the angular correlation at low temperatures and find results in disagreement with the theory. This has been interpreted as due to incomplete thermalization of the incoming fast positron. One has estimated an "effective temperature" of 160°K for Na,²⁵² below which the positron cannot be thermalized. A theoretical calculation of the thermalization time which results in qualitative agreement with the conclusions by Kim *et al.* has been given by Carbotte and Arora.²⁵³

The thermal motion of positrons is of interest also at temperatures above the minimum thermalization temperature. In free electron theory the thermal smearing of the Fermi momentum would be simply related to $k_B T$ and the kinetic energy of the positron would be given by

$$k_+^2/2m^* = \frac{3}{2}k_B T. \quad (41.10)$$

The effect of both terms on the angular correlation is small, but the effective mass term is the more important effect and is detectable. Stewart and Shand²⁵⁴ have obtained results for the smearing of the Fermi surface of Na, which are compatible with an effective positron mass according to Eq. (41.10) of the magnitude

$$m^* = 1.8 \pm 0.2. \quad (41.11)$$

Hamann²⁵⁵ has calculated the self-energy, neglecting vertex corrections, and obtains a dynamical mass correction much smaller than in Eq. (41.11).

²⁵¹ C. K. Majumdar, *Phys. Rev.* **140**, A227 (1965).

²⁵² S. M. Kim, A. T. Stewart, and J. P. Carbotte, *Phys. Rev. Letters* **18**, 385 (1967).

²⁵³ J. P. Carbotte and H. L. Arora, *Can. J. Phys.* **45**, 387 (1967).

²⁵⁴ A. T. Stewart and J. B. Shand, *Phys. Rev. Letters* **16**, 261 (1966); *Proc. Phys. Soc.* **88**, 1001 (1966).

²⁵⁵ D. R. Hamann, *Phys. Rev.* **146**, 277 (1966).

Mikeska²⁵⁶ suggested that this may be explained by lattice effects. The question of how to interprete these experimental data must still be considered as wide open.

Very little work has been done to study the effects on the positron of the lattice structure in real solids. In early work one assumed the positron wave function to be constant, whereby the angular correlation would measure the momentum distribution. In recent years, however, several calculations of the positron wave function have been made using conventional schemes for band calculations, or, as done by Stroud and Ehrenreich²⁵⁷ by using the experimental X-ray form factors. The corresponding calculations of the angular correlation show good agreement with experiments, which indicates that the effect of many-body interactions on angular distribution is small, or rather limited to special features near the Fermi edge. The effect on annihilation rates is important; however, the only attempts to estimate lifetimes seem to have been made simply by grafting on the results for the electron gas to the formulas obtained in an independent particle approximation.

This section has served to illustrate a case in which one needs to go beyond the approximations discussed in most of this review. The ladder approximation describes the annihilation rate quite well at high densities, but it remains still much work to be done to extend the theory down to the low-density end with formation of positronium. The angular distribution near the Fermi edge has a structure which can be explained only by including properly dynamical interactions as well as self-energy corrections to both electrons and positrons. Finally, we mention the puzzling question about the effective mass as determined by thermal smearing, which is as yet unexplained.

42. COHESIVE ENERGY

a. *Introduction*

We have in this review been largely concerned with the one-electron spectral function of the solid and the information it contains about the excitation spectrum. The total energy can also be calculated from the spectral function by using the formula of Galitskii and Migdal.²⁴ One may question how the satellite structure below the valence band and below each core level can be compatible with important aspects on cohesion. Work by Lundqvist and Samathiyakanit²⁵⁸ and by Lundqvist¹⁵³ shows that the satel-

²⁵⁶ H. J. Mikeska, *Phys. Letters* **24A**, 402 (1967).

²⁵⁷ D. Stroud and H. Ehrenreich, *Phys. Rev.* **171**, 399 (1968).

²⁵⁸ B. I. Lundqvist and V. Samathiyakanit, *Physik Kondensierten Materie* **9**, 231 (1969).

lite structure is essential in a discussion of cohesion using the spectral function.

Actually the spectral function seems to be a practical tool for studying cohesion, since it permits a fairly clean cut separation of valence and core contributions to the total energy.²⁵⁹ However, this separation requires considerable care. One would like to treat the ions just as an external potential and calculate the energy of the valence electrons in the field of the ions. It might *a priori* seem natural to choose the optical potential of a free ion, but, as shown by Brooks,¹⁸⁴ Callaway,¹⁸⁵ and others, the long range polarization potential gives too much binding. Another try would be the doubly screened polarization potential which appears in the crystal potential (see Section 37). Also this choice seems, however, to be improper. The analysis of the problem is simple but long and detailed and we defer further discussion until Section 42c.

b. The Role of the Satellite Structure

The total energy is calculated from the Galitskii-Migdal formula [see Eq. (12.6)]

$$E = \frac{1}{2} \operatorname{tr} \int_{-\infty}^{\mu} (\omega + h) A(\omega) d\omega + V_{\text{nuc}}. \quad (42.1)$$

One should observe that this formula applied to an independent particle model does not reduce to the sum of one-particle energies but will properly include the average interaction energy [cf. also Eq. (12.9)].

We first discuss the electron gas. The term of the form hA gives the expectation value of h , which then equals the kinetic energy $\sum_k \epsilon_k n_k$. This term increases only slightly if the interactions are taken into account, and we may therefore focus attention on the term $\omega A(\omega)$, which is determined by the energy distribution (density of states). Clearly, if we were including only the quasi-particle peak contribution to $A(\omega)$, we would obtain an energy higher than in the HF approximation.²⁶⁰ However, the plasmaron contribution corresponds to much lower energies and there is a substantial oscillator strength in this part, which gives rise to a lowering of the total energy. Calculations for the electron gas using Eq. (42.1) indeed give good results for the total energy.²⁵⁸ Thus the satellite structure in the spectral function accounts for most of the exchange and correlation effects and is hence of vital importance for cohesive properties. We further remark that the HF theory aims at giving the best energy under the given constraints

²⁵⁹ L. Hedin, B. I. Lundqvist, and V. Samathiyakanit (to be published).

²⁶⁰ This can be seen from Fig. 43. The average exchange energy, corresponding to the Slater curve, lies lower than the quasi-particle curve $\Sigma(k, E_k)$.

TABLE XIV. VALUES FOR THE SPIN SUSCEPTIBILITY RATIO

	Na	K
Experiment ^a	1.74 ± 0.1	1.58 ± 0.1
Experiment ^b	1.51 ± 0.06	1.68 ± 0.25
Theory ^c	1.48	1.55
Theory ^d	1.47	1.55

^a Na, R. T. Schumacher and W. E. Vehse, *J. Phys. Chem. Solids* **24**, 297 (1963); K, J. A. Kaeck, *Phys. Rev.* **175**, 897 (1968).

^b From spin wave data and effective mass.^e

^c Expansion method, see E in Table VII.

^d The Hubbard approximation, see R in Table VII.

^e T. M. Rice, *Phys. Rev.* **175**, 858 (1968).

on the wave function. The way this is achieved can be seen to be a compromise: The total energy is reasonably good and so is the average excitation energy, but at the expense of an unsatisfactory dispersion law.

For the core electrons the interaction with the valence electrons give a large polarization shift of the quasi particles toward higher energies. In addition, a pronounced satellite structure appears below the quasi-particle peak. Intuitively we do not expect core electrons to contribute to the cohesion, and hence the polarization shift must be compensated by other effects. Indeed, it turns out that the shift of the core levels is perfectly balanced by the accompanying satellite structure, in the sense that the average core electron energy, or the center of gravity of the core spectrum, is almost exactly unchanged.¹⁵³

Thus we conclude that the satellite structure in the valence band describe important exchange and correlation contributions to the cohesive energy. In the core spectrum the satellite structure is equally important by balancing the core electron shifts so that the net contribution from the core electrons to the binding becomes effectively zero.

c. Separation of Valence and Core Parts in the Total Energy

Neglecting the core electrons, one should be able to write the valence electron contribution in the form

$$E^v = \frac{1}{2} \operatorname{tr} \int_{\mu_c}^{\infty} [\omega + h + V_H^c + \Sigma^c(\omega)] A(\omega) d\omega + V_{\text{ion}}, \quad (42.2)$$

where V_{ion} is the mutual interaction between the ions and μ_c is an energy slightly above all core electron energies. The problem is how to choose the effective exchange-correlation potential from the ions. If we assume that

the density matrix associated with the core is the same in the metal as in a free ion, it can be shown that $\Sigma^c(\omega)$ should be taken as the *singly screened* polarization potential plus the HF exchange potential V_{ex} . Thus, while the positions of the quasi-particle levels are determined by the doubly screened polarization potential, which contributes to the cohesion through the term $\omega A(\omega)$, the contribution from the effective core potential $V_n + V_H^c + \Sigma^c(\omega)$ involves the singly screened polarization potential. This seems to be a diplomatic resolution of the arguments about doubly versus singly screened potentials which have been taken up by Bienenstock and Brooks¹⁸⁶ and others.

43. FERMI LIQUID PARAMETERS

The application of the Landau Fermi liquid theory to the properties of real metals is a lengthy and technically complicated affair. Out of this complex we chose some particular aspects for discussion in Sections 18 and 19 from a general point of view. We discussed the calculation of the parameters of the theory for an interacting electron gas in Section 26 and touched briefly on some aspects of the electron-phonon interaction in Part VIII.

We shall here state a few results from experiments involving wavelike excitations: magnetoplasma waves and spin waves. These questions have recently been treated in a paper by Rice¹¹² and we shall essentially quote his results. We shall also put together results for the plasmon dispersion relation as predicted by the Landau theory and compare with other theoretical and experimental results. In all three cases much more accurate experimental results may be available in the near future and would then constitute useful checks on the theoretical calculations.

Until recently only two independent experimental quantities were available for determination of the Landau parameters, namely, the effective mass m^* and the spin susceptibility χ . The latter quantity is given by

$$\chi_F/\chi = (m/m^*)(1 + B_0), \quad (43.1)$$

where the electron-phonon effects cancel in the ratio of Eq. (43.1). Measurement of the spin susceptibility would thus provide an ideal way of testing theories for electron-electron interactions. Unfortunately, the method developed by Schumacher and Slichter²⁶¹ has not yet given accurate enough results to provide an effective test on theory. Recently, however, two new types of experiments have been carried out which seem capable of giving very detailed information on several of the Landau parameters (see Section 19). In Table XIV we give theoretical and experimental results for the

²⁶¹ R. T. Schumacher and C. P. Slichter, *Phys. Rev.* **101**, 58 (1956).

TABLE XV. VALUES OF THE LANDAU PARAMETERS FOR SODIUM

	Experiment ^a	Theory ^b	Theory ^c
A_0		-0.62	-0.64
A_1		+0.12	0.07
A_2	-0.05 ± 0.01	-0.03	
A_3	0.0 ± 0.005	+0.004	
B_0	-0.21 ± 0.05	-0.14	-0.19
B_1	0.01 ± 0.03	+0.01	-0.03
B_2	0.0 ± 0.05	-0.01	0.01
B_3		+0.000	-0.005
m^*/m	1.24 ± 0.02	1.26	1.21

^a See T. M. Rice, *Phys. Rev.* **175**, 858 (1968).

^b See footnote *a*. Electron-electron part from Hubbard's approximation, see R in Table VII. Electron-phonon contribution calculated with several plane waves and Ashcroft's pseudopotential.

^c Electron-electron part from expansion method, see E in Table VII. The electron-phonon part is the same as in footnote *b*.

TABLE XVI. VALUES FOR THE PLASMON DISPERSION COEFFICIENT α

Z	r_s	ω_p (eV)		Dispersion coefficient α^*					
		El. gas	Expt.	LTH	NP	FL	S	Expt.	
Be	2	1.87	18.5	18.9	0.47	0.42	0.39	0.31	0.42 ^d
Al	3	2.07	15.8	15.0	0.44	0.39	0.36	0.27	0.40 ^e
Sb	5	2.14	15.1	15.2	0.43	0.38	0.35	0.27	0.37 ^f
Ga	3	2.19	14.5	13.75	0.43	0.38	0.34	0.26	0.45 ^g
Mg	2	2.66	10.9	10.5	0.39	0.33	0.30	0.20	0.39 ^h
Li	1	3.26	8.0	—	0.35	0.29	0.25	0.14	0.26 ⁱ
Na	1	4.00	5.9	5.7	0.32	0.25	0.20	0.09	0.29 ^j

*LTH: Lindhard dielectric function, $\alpha_0 = 0.636r_s^{-1/2}$.

NP: Nozières and Pines,^a $\alpha = \alpha_0(1 - \gamma(\alpha r_s/3\pi))$; $\gamma = 1$.

FL: Fermi liquid theory,^b $\gamma = 1.7$.

S: Singwi *et al.*,^c $\gamma = 3.3$.

^a P. Nozières and D. Pines, *Phys. Rev.* **111**, 442 (1958).

^b V. P. Silin, *JETP Soviet Phys. (English Transl.)* **7**, 538 (1958).

^c K. S. Singwi, M. P. Tosi, R. H. Land, and A. Sjölander, *Phys. Rev.* **176**, 589 (1968).

^d H. Watanabe, *J. Phys. Soc. Japan* **11**, 112 (1956).

^e P. Schmüser, *Z. Physik* **180**, 105 (1964).

^f J. Geiger, *Z. Naturforsch.* **17a**, 696 (1962).

^g C. Kunz, *Phys. Letters* **15**, 312 (1965).

^h K. Zeppenfeld *Z. Physik* **223**, 32 (1969).

spin susceptibility. The agreement between the theoretical values and the spin wave results is quite good in this case. We should also note that the theoretical electron gas results for B_0 are remarkably consistent in different approximations. In Table XV we present experimental and theoretical results for several Landau parameters for Na. There is in general no detailed agreement between theory and experiments, but there is enough correlation between the data to encourage further work on both fronts.

The plasmon dispersion relation provides a way to test theories of electron-electron interactions since the oscillations are so rapid that no phonon effects could be important. The Landau theory is, however, strictly speaking not applicable to plasma oscillations because of the high excitation energy. As we remarked in Section 19, the present status of dielectric theory on the other hand is not more advanced than it seems legitimate to stretch the Landau theory to deal with the plasma problem as well. In Table XVI we give results for the plasmon dispersion coefficients of several metals as calculated from Eq. (19.21) with the appropriate electron gas parameters. We have also considered the Lindhard results, the Pines-Nozières formula, and the theory of Singwi *et al.* (cf. Section 27). The experimental results are obtained from the review by Raether,²⁶² but there are also some later results included.²⁶³ We see that there is an overall correlation between experimental and theoretical values but no detailed agreement.

The conclusion of the comparisons given in this section is that accurate experimental determination of the interaction parameters would be a valuable guidance for further theoretical work. At the present stage, however, both experimental and theoretical data are not accurate enough to draw any detailed conclusions.

Appendix A: Linear Response Theory

The purpose of these appendices is to exhibit key ideas rather than being very detailed. The material in Appendices A and C can be found in a number of places, while that of Appendix B is more difficult to extract from the literature and is even partly new. We only discuss the zero temperature case, and we neglect spin.

In linear response theory the coupling between an external probe and the system is treated linearly, while all interactions within the system are treated exactly. The external probe may be e.g. an electromagnetic field, or a beam of charged particles or neutrons. For a large class of applications it is quite sufficient to treat the response linearly.

²⁶² H. Raether, *Springer Tracts Mod. Phys.* **38**, 84 (1965); Springer, Berlin 1965.

²⁶³ We are indebted to Professor H. Raether for communicating some unpublished material.

As an example, which trivially can be extended to other situations, we derive the induced charge density caused by an external potential, cf. Eq. (5.7),

$$\rho_{\text{ind}}(\mathbf{r}, t) = \int_{-\infty}^{\infty} dt' \int d\mathbf{r}' R(\mathbf{r}, \mathbf{r}'; t - t') \phi(\mathbf{r}', t'). \quad (\text{A.1})$$

The probe in this case is the potential ϕ , and the corresponding term in the Hamiltonian is

$$H_1(t) = \int \rho(\mathbf{r}) \phi(\mathbf{r}, t) d\mathbf{r}. \quad (\text{A.2})$$

Here $\rho(\mathbf{r}) = \psi^\dagger(\mathbf{r})\psi(\mathbf{r})$ is the operator for the charge density, while $\phi(\mathbf{r}, t)$ is a scalar function.

We will derive an expression for the linear response function in terms of ground state properties. It is convenient to work in the interaction picture with H_1 as the interaction, and the full Hamiltonian H_0 of the interacting system as the unperturbed part. The state vector then satisfies the equation of motion

$$i(\partial/\partial t) |t\rangle = H_1^I(t) |t\rangle, \quad (\text{A.3})$$

where

$$H_1^I(t) = \exp(iH_0t) H_1(t) \exp(-iH_0t) = \int \rho(\mathbf{r}, t) \phi(\mathbf{r}, t) d\mathbf{r}. \quad (\text{A.4})$$

The density operator $\rho(\mathbf{r}, t)$ is given in the Heisenberg representation corresponding to $\phi = 0$. Keeping only terms linear in ϕ , we obtain from Eq. (A.3)

$$|t\rangle = \left(1 - i \int_{t_0}^t H_1^I(t') dt' \right) |\Phi_0\rangle, \quad (\text{A.5})$$

where we have taken t_0 as some early time when ϕ was zero and the system was in its ground state $|\Phi_0\rangle$. The charge density at time t is

$$\begin{aligned} \rho(\mathbf{r}, t) &= \langle t | \rho(\mathbf{r}, t) | t \rangle \\ &= \langle \Phi_0 | \left(1 + i \int_{t_0}^t H_1^I(t') dt' \right) \rho(\mathbf{r}, t) \left(1 - i \int_{t_0}^t H_1^I(t') dt' \right) | \Phi_0 \rangle. \end{aligned} \quad (\text{A.6})$$

Separating out the charge density in the ground state $\langle \Phi_0 | \rho(\mathbf{r}, t) | \Phi_0 \rangle = \langle \Phi_0 | \rho(\mathbf{r}) | \Phi_0 \rangle$, we have for the induced charge density, taking $t_0 = -\infty$,

$$\rho_{\text{ind}}(\mathbf{r}, t) = i \langle \Phi_0 | \int_{-\infty}^t [H_1^I(t') \rho(\mathbf{r}, t) - \rho(\mathbf{r}, t) H_1^I(t')] dt' | \Phi_0 \rangle. \quad (\text{A.7})$$

Comparison with Eqs. (A.1) and (A.4) gives the result

$$R(\mathbf{r}, \mathbf{r}'; t - t') = (-i) \langle \Phi_0 | [\rho(\mathbf{r}, t), \rho(\mathbf{r}', t')] | \Phi_0 \rangle \Theta(t - t'). \quad (\text{A.8})$$

The linear response function R is thus given by the expectation value with respect to the ground state of the commutator of the density operator taken at different times. We note that the causality property follows directly from the derivation; $R(t - t')$ is zero unless $t > t'$. The response functions are closely related to the Green functions, as will be shown from the spectral resolutions in Appendix C.

The result in Eq. (A.8) is easily extended to other situations. As an additional example, consider the coupling to an electromagnetic field,

$$H_1(t) = \int \mathbf{j}(\mathbf{r}) \mathbf{A}(\mathbf{r}, t) d\mathbf{r}, \quad (\text{A.9})$$

where $\mathbf{A}(\mathbf{r}, t)$ is the vector potential and \mathbf{j} the current density operator. The response function for the induced current density is then given by a $[\mathbf{j}, \mathbf{j}]$ commutator.

Appendix B: Equations of Motion for Green Functions

In this appendix we supplement the discussion in Sections 13 and 15 by deriving Eqs. (13.19) and (15.19), and the equation of motion for the phonon Green function. As a preparation for this we first derive, by elementary methods, a basic functional derivative expression.²⁷ The resulting equation (B.8) can also be obtained directly from Schwinger's dynamical principle.²⁸⁴

a. A Functional Derivative Expression

We consider a Hamiltonian $H(t) = H_0 + H_1(t)$, where H_1 is given in Eq. (A.2) and H_0 describes the interacting system. The solution of the Schrödinger equation

$$i(\partial/\partial t) |t\rangle = H |t\rangle \quad (\text{B.1})$$

can be written in terms of a time evolution operator

$$|t\rangle = V(tt') |t'\rangle, \quad (\text{B.2})$$

which satisfies the equation

$$i(\partial/\partial t) V(tt') = H(t) V(tt'); \quad V(tt) = 1. \quad (\text{B.3})$$

²⁷ See, e.g., T. Kato, T. Kobayashi and M. Namiki, *Progr. Theor. Phys. Suppl.* **15**, 3 (1960) or G. Baym, *Ann. of Physics (N.Y.)* **14**, 1 (1961).

This differential equation can be transformed to an integral equation

$$V(tt') = U(tt') - i \int_{t'}^t U(tt'') H_1(t'') V(t''t') dt'', \quad (\text{B.4})$$

where U is the time evolution operator for H_0 , $U(tt') = \exp[-iH_0(t-t')]$. From Eq. (B.4) we have

$$\delta V(tt')/\delta\phi(\mathbf{r}'', t'') = -iV(tt'')\rho(\mathbf{r}'')V(t''t'), \quad (\text{B.5})$$

when $t > t'' > t'$; for t'' outside this interval the functional derivative is zero.

We define the Heisenberg representation of an operator Θ as

$$\Theta(t) = V(-T_0, t)\Theta V(t, -T_0), \quad (\text{B.6})$$

where T_0 tends toward $+\infty$. We further define expectation values of time-ordered products as

$$\langle T(\Theta_1(t_1)\Theta_2(t_2)\cdots) \rangle$$

$$= \frac{\langle N | U(-T_0, T_0)V(T_0, -T_0)T[\Theta_1(t_1)\Theta_2(t_2)\cdots] | N \rangle}{\langle N | U(-T_0, T_0)V(T_0, -T_0) | N \rangle}. \quad (\text{B.7})$$

In the final formulas we let ϕ approach zero. V then approaches U , and Eq. (B.7) reduces to the usual type of expectation value. From Eq. (B.5) we have for the functional derivative of an expectation value

$$\delta\langle T[\Theta_1(t_1)\Theta_2(t_2)\cdots]\rangle/\delta\phi(\mathbf{r}, t) = (-i)\langle T[\rho'(\mathbf{r}, t)\Theta_1(t_1)\Theta_2(t_2)\cdots]\rangle, \quad (\text{B.8})$$

where $\rho'(\mathbf{r}, t) = \rho(\mathbf{r}, t) - \langle\rho(\mathbf{r}, t)\rangle$. The fact that ρ' rather than ρ appears in Eq. (B.8) is due to the denominator in Eq. (B.7).

b. The Electron Green Function

We first discuss the case of a rigid lattice. The Green function and all other expectation values used in Section 13 are now considered to be defined as in Eq. (B.7). From its derivation it is clear that Eq. (13.3) still holds. The term with four field operators can be generated by functional differentiation, and we have

$$[i(\partial/\partial t_1) - h(1) - V(1)]G(12) - i \int v(1+3) \delta G(12)/\delta\phi(3) d(3) = \delta(12). \quad (\text{B.9})$$

Here V is the total average potential given in Eq. (13.5), and we have used

the notation of Eq. (13.13). By 1^+ we understand $(\mathbf{r}, t^+) = (\mathbf{r}, t + \delta)$ [cf. Eq. (12.2)]. We insert the identity

$$\delta G(12)/\delta\phi(3) = - \int G(14)[\delta G^{-1}(45)/\delta\phi(3)]G(52) d(45) \quad (\text{B.10})$$

into Eq. (B.9), and compare with Eq. (13.4) to obtain

$$\Sigma(12) = -i \int v(1+3)G(14)[\delta G^{-1}(42)/\delta\phi(3)]d(34). \quad (\text{B.11})$$

This expression for Σ can be rewritten on the form in Eq. (13.19a) by use of the chain rule for functional differentiation and the definition of the screened potential

$$W(12) = \int v(13) \delta V(2)/\delta\phi(3) d(3). \quad (\text{B.12})$$

The remaining parts of Eq. (13.19) are easily verified along similar lines.

In the case of a vibrating lattice, the derivation of the expression for Σ in Eq. (15.19) is almost identical to the one given for a rigid lattice. Thus Eq. (15.7) can be written in terms of a functional derivative on the form in Eq. (B.9), with V defined in Eq. (15.9), ρ in Eq. (15.5), and ϕ in Eq. (15.4). By use of the identity in Eq. (B.10) and the definition of the screened potential in Eq. (15.10), the expression for Σ follows.

The remaining nontrivial part to prove in Eq. (15.19) is the second relation, involving D , the density-density correlation function for the nuclei, which is defined in Eq. (15.14). We start from the definition of W in Eq. (15.10):

$$W(12) = v(12) + \int v(13)[\delta\langle\rho(4)\rangle/\delta\phi(3)]v(42) d(34). \quad (\text{B.13})$$

Separating ρ as $\rho_e + \rho_n$, we have

$$\begin{aligned} W(12) &= v(12) + \int W(13)[\delta\langle\rho_e(4)\rangle/\delta V(3)]v(42) d(34) \\ &\quad + \int v(13)[\delta\langle\rho_n(4)\rangle/\delta\phi(3)]v(42) d(34), \end{aligned} \quad (\text{B.14})$$

where according to the definition in Eq. (15.11), $\delta\langle\rho_e(1)\rangle/\delta V(2) = P_e(12) = P_e(21)$. Thus if the last term in Eq. (B.14) is neglected, W reduces to W_e . To treat the effect of the nuclei, we follow Baym,²⁶⁴ and introduce an extra term in the Hamiltonian,

$$H_2 = \int \rho_n(\mathbf{r})J(\mathbf{r}, t) d\mathbf{r}, \quad (\text{B.15})$$

to obtain

$$\begin{aligned}\delta\langle\rho_n(1)\rangle/\delta\phi(2) &= (-i)\langle T(\rho_n'(1)\rho_e'(2))\rangle - i\langle T(\rho_n'(1)\rho_n'(2))\rangle \\ &= \delta\langle\rho(2)\rangle/\delta J(1).\end{aligned}\quad (\text{B.16})$$

We can now eliminate the mixed term $\langle\rho_n'\rho_e'\rangle$ in Eq. (B.16) by writing

$$\delta\langle\rho(1)\rangle/\delta J(2) = D(12)$$

$$+ \int [\delta\langle\rho_e(1)\rangle/\delta V(3)]v(34)[\delta\langle\rho(4)\rangle/\delta J(2)]d(34) \quad (\text{B.17})$$

to obtain

$$\delta\langle\rho(1)\rangle/\delta J(2) = [(1 - P_e v)^{-1}D]_{12}. \quad (\text{B.18})$$

Collecting our results, we have $W = v + WP_e v + v(1 - P_e v)^{-1}Dv$, which, solving for W , yields the relation

$$W = W_e + W_e DW_e, \quad (\text{B.19})$$

which we set out to prove.

c. The Phonon Green Function

To calculate phonon effects on the electron self-energy Σ in the harmonic approximation, we do not need D but only the phonon Green function $D_{\mu\nu}$ defined in Eq. (16.8). Introducing a source term

$$H_2 = \sum_{\mu} \mathbf{u}_{\mu} \mathbf{J}_{\mu}(t), \quad (\text{B.20})$$

instead of the one defined in Eq. (B.15), we have the simple representation

$$D_{\mu\nu}(tt') = \delta\langle\mathbf{u}_{\mu}(t)\rangle/\delta\mathbf{J}_{\nu}(t'). \quad (\text{B.21})$$

To obtain the equation of motion for $D_{\mu\nu}$, we start from the equation of motion for \mathbf{u}_{μ} . The first time derivative gives $M(\partial/\partial t)\mathbf{u}_{\mu} = \mathbf{p}_{\mu}$, and from the $[\mathbf{p}_{\mu}, H]$ commutator we obtain

$$M(\partial^2/\partial t^2)\mathbf{u}_{\mu}(t) = Z(\partial/\partial R_{\mu}) \int v[R_{\mu}(t) - \mathbf{r}] \rho(\mathbf{r}, t) d\mathbf{r} - \mathbf{J}_{\mu}(t). \quad (\text{B.22})$$

We take the functional derivative of the expectation value of this equation and have

$$\begin{aligned}M(\partial^2/\partial t^2)D_{\mu\nu}(tt') &= -\delta_{\mu\nu}\delta(t - t') + Z(\partial/\partial R_{\mu}) \int v(R_{\mu}^{(0)} - \mathbf{r}) \\ &\quad \times \delta\langle\rho(\mathbf{r}, t)\rangle/\delta\mathbf{J}_{\nu}(t') d\mathbf{r},\end{aligned}\quad (\text{B.23})$$

where we have provisionally replaced $\mathbf{R}_\mu(t)$ in the argument of v by the equilibrium value $\mathbf{R}_\mu^{(0)}$. To evaluate $\delta\langle\rho\rangle/\delta J$ we proceed as in Eqs. (B.17) and (B.18) to obtain

$$\delta\langle\rho(1)\rangle/\delta J_\nu(t') = \int (1 - P_\nu v)_{12}^{-1} \delta\langle\rho_n(2)\rangle/\delta J_\nu(t') d(2). \quad (\text{B.24})$$

The last term in Eq. (B.23) now becomes, using Eq. (B.24) and the definition of ρ_n in Eq. (15.5),

$$-Z^2(\partial/\partial\mathbf{R}_\mu)[\delta/\delta\mathbf{J}_\nu(t')] \sum_{\nu'} \int W_e(\mathbf{R}_\mu^{(0)}, \mathbf{R}_{\nu'}(t_2); t - t_2) dt_2. \quad (\text{B.25})$$

Expanding $\mathbf{R}_{\nu'}(t_2)$ in $\mathbf{u}_{\nu'}(t_2)$ we can write Eq. (B.25) in the form

$$\int \sum_{\nu'} \pi_{\mu\nu'}(tt_2) D_{\nu'\nu}(t_2t') dt_2, \quad (\text{B.26})$$

where the phonon self-energy is given by

$$\pi_{\mu\nu}(tt') = -Z^2(\partial/\partial\mathbf{R}_\mu)(\partial/\partial\mathbf{R}_\nu) W_e(R_\mu^{(0)}, R_\nu^{(0)}; t - t'). \quad (\text{B.27})$$

Going through the derivation again, we see that the replacement of $\mathbf{R}_\mu(t)$ by $\mathbf{R}_\mu^{(0)}$ in Eq. (B.23) affects the diagonal element $\pi_{\mu\mu}$. This contribution can easily be evaluated; it involves the average charge density $\langle\rho(\mathbf{r})\rangle$. The zero frequency component of the diagonal element is determined by the force constant sum rule²⁶⁵:

$$\sum_\nu \pi_{\mu\nu}(\omega = 0) = 0 \quad (\text{B.28})$$

To keep the derivation simple, we have used a potential W_e that is screened both by core and valence electrons. In most applications we can, however, work with the ions as basic units. To lowest approximation we then have to replace Eq. (B.26) by

$$\begin{aligned} \pi_{\mu\nu}(tt') &= -(\partial/\partial\mathbf{R}_\mu)(\partial/\partial\mathbf{R}_\nu) \\ &\times \int \rho_{\text{ion}}(\mathbf{R}_\mu^{(0)} - \mathbf{r}) d\mathbf{r} W_e(\mathbf{r}, \mathbf{r}'; t - t') d\mathbf{r}' \rho_{\text{ion}}(\mathbf{r}' - \mathbf{R}_\nu^{(0)}), \end{aligned} \quad (\text{B.29})$$

where $\rho_{\text{ion}}(\mathbf{r})$ is the charge density of an ion core, and W_e is screened only by the valence electrons. We also have to add some type of Born-Mayer core repulsion term.

The derivation of $\pi_{\mu\nu}$ given here is a simplified zero temperature version of that given by Baym.²⁶⁴ Related types of derivations have been given by Engelsberg and Schrieffer,¹³¹ Sjölander and Johnson,²⁶⁵ and by Garland.²⁶⁶

²⁶⁵ A. Sjölander and R. Johnson, *Proc. Intern. Conf. on Inelastic Scattering of Neutrons, Bombay, 1964* (IAEA Proceedings series) 1, 61 (1965).

²⁶⁶ J. W. Garland, *Phys. Rev.* **153**, 460 (1967).

Appendix C: Spectral Resolutions

We will here derive the spectral resolutions for the response-function

$$R_r(\mathbf{r}, \mathbf{r}'; t - t') = -i\langle N | [\rho(\mathbf{r}, t), \rho(\mathbf{r}', t')] | N \rangle \Theta(t - t'), \quad (\text{C.1})$$

and the time-ordered function

$$R_t(\mathbf{r}, \mathbf{r}'; t - t') = -i\langle N | T(\rho'(\mathbf{r}t)\rho'(\mathbf{r}'t')) | N \rangle, \quad (\text{C.2})$$

where $\rho'(\mathbf{r}t) = \rho(\mathbf{r}t) - \langle \rho(\mathbf{r}t) \rangle$. The derivation is very similar to that for the spectral resolution of the one-electron Green function in Sections 9, and 10. We have

$$\begin{aligned} R(\mathbf{r}, \mathbf{r}'; \tau) &= -i \sum_s [\rho_s(\mathbf{r})\rho_s^*(\mathbf{r}') \exp(-i\epsilon_s \tau) \Theta(\tau) \\ &\quad \mp \rho_s(\mathbf{r}')\rho_s^*(\mathbf{r}) \exp(i\epsilon_s \tau) \Theta(\pm\tau)]. \end{aligned} \quad (\text{C.3})$$

The upper sign refers to R_r , and the lower to R_t , and

$$\rho_s(\mathbf{r}) = \langle N | \rho(\mathbf{r}) | N, s \rangle, \quad \epsilon_s = E_s - E_0 \geq 0. \quad (\text{C.4})$$

The Fourier transform is, taking $\rho_s(\mathbf{r})$ to be real,²⁶⁷

$$\begin{aligned} R(\mathbf{r}, \mathbf{r}'; \omega) &= \int_{-\infty}^{\infty} \exp(i\omega\tau) R(\mathbf{r}, \mathbf{r}'; \tau) d\tau \\ &= \sum_s \rho_s(\mathbf{r})\rho_s(\mathbf{r}') [(\omega - \epsilon_s + i\delta)^{-1} - (\omega + \epsilon_s \pm i\delta)^{-1}]. \end{aligned} \quad (\text{C.5})$$

We see that the real parts of R_r and R_t are equal for all ω , while the imaginary parts

$$\text{Im } R(\mathbf{r}, \mathbf{r}'; \omega) = -\pi \sum_s \rho_s(\mathbf{r})\rho_s(\mathbf{r}') [\delta(\omega - \epsilon_s) \mp \delta(\omega + \epsilon_s)], \quad (\text{C.6})$$

are equal only for $\omega > 0$. These results verify the statements at the end of Section 12.

Since the energy levels ϵ_s form a continuous set in a solid, the spectral resolution is often written as an integral, e.g.

$$R_t(\mathbf{r}, \mathbf{r}'; \omega) = \int_0^{\infty} \frac{2\omega' B(\mathbf{r}, \mathbf{r}'; \omega')}{\omega^2 - \omega'^2} d\omega' \quad (\text{C.7})$$

where ω' has a slightly negative imaginary part.

²⁶⁷ If no magnetic fields are present we can consider $\rho_s(\mathbf{r})$ as a real function. For metals where we like to work with Blochfunctions, $\rho_s(\mathbf{r})$ is generally not real, but $\sum_s \rho_s(\mathbf{r})\rho_s^*(\mathbf{r}') \delta(\epsilon_s - \epsilon)$ is.

ACKNOWLEDGMENTS

We would like to thank Drs. A. Bienenstock, J. A. Krumhansl, B. I. Lundqvist, and J. W. Wilkins for many valuable and clarifying discussions and comments which have been very helpful in improving the manuscript. Dr. B. Bergersen's and G. Grimvall's cooperation in preparing Section 41 and Part VIII, respectively, has been most valuable for us. We would also like to thank Drs. N. Ashcroft, T. Claeson, and P. O. Nilsson for critical reading of parts of the manuscript. Finally, the authors wish to thank the Swedish Natural Science Research Council for financial support.